

University of Southampton Research Repository ePrints Soton

Copyright © and Moral Rights for this thesis are retained by the author and/or other copyright owners. A copy can be downloaded for personal non-commercial research or study, without prior permission or charge. This thesis cannot be reproduced or quoted extensively from without first obtaining permission in writing from the copyright holder/s. The content must not be changed in any way or sold commercially in any format or medium without the formal permission of the copyright holders.

When referring to this work, full bibliographic details including the author, title, awarding institution and date of the thesis must be given e.g.

AUTHOR (year of submission) "Full thesis title", University of Southampton, name of the University School or Department, PhD Thesis, pagination

UNIVERSITY OF SOUTHAMPTON

FACULTY OF ENGINEERING AND ENVIRONMENT
INSTITUTE OF SOUND AND VIBRATION RESEARCH

**MEASURING AND PREDICTING THE TRANSMISSION OF VIBRATION
THROUGH GLOVES TO THE HAND**

by

Khairil Anas bin Md Rezali

Thesis for the degree of Doctor of Philosophy

MAY 2015

UNIVERSITY OF SOUTHAMPTON

ABSTRACT

FACULTY OF ENGINEERING AND THE ENVIRONMENT

INSTITUTE OF SOUND AND VIBRATION RESEARCH

Doctor of Philosophy in Sound and Vibration

**MEASURING AND PREDICTING THE TRANSMISSION OF VIBRATION THROUGH
GLOVES TO THE HAND**

by Khairil Anas Md Rezali

The main objective of this research was to advance understanding of factors influencing the transmission of vibration through glove materials to the hand and to the fingers. The transmissibility of a glove to the hand depends on two primary factors: the biodynamic response of the hand and the dynamic characteristics of the glove material. Although some of the factors affecting the biodynamic response of the hand and the dynamic characteristics of glove materials have been investigated previously, there is insufficient understanding to be able to predict glove transmissibilities. The apparent mass of the hand, the dynamic stiffness of three glove materials (Foam A, Foam B, and Gel A), and their transmissibilities to the hand were measured with five variables: (a) material thickness (6.4, 12.8, and 19.2 mm), (b) push force (10, 15, and 20 N), (c) contact area (with diameters 12.5, 25.0, and 37.5 mm), (d) vibration magnitude (1, 2, and 4 m/s² r.m.s.), (e) with and without arm support, and (f) different frequency ranges (10 to 300 Hz and 2 to 50 Hz). With the hand pushing down on a flat surface and vertical vibration, measurements were obtained at the palm of the hand, the thenar eminence, and the index finger.

It is concluded that the apparent mass of the hand and the dynamic stiffnesses of the glove materials at high frequencies are predominantly affected by contact area and contact force. A change in contact area or contact force can therefore increase or decrease glove transmissibility. At frequencies greater than 20 Hz, the apparent mass at the palm and the transmissibilities of the glove materials to the palm were similar with and without arm support. At frequencies between 20 and 100 Hz, as the dynamic stiffness of the material decreased, the transmissibility of the material to the palm decreased whereas the transmissibility to the index finger increased. Changes in the vibration magnitude will not have a large effect on glove transmissibility.

Using the measured apparent mass of the hand and the measured dynamic stiffnesses of the glove materials, the transmissibility of the materials to the hand were predicted using an impedance model. The predicted transmissibilities were similar to, and showed similar trends to, the measured transmissibilities. The predicted transmissibilities seemed to reflect individual changes in the dynamic response of the hand, suggesting a method of predicting inter-subject variability in glove transmissibility.

Simple lumped parameter models of the hand were developed (with two and four degrees-of-freedom) and combined with the dynamic characteristics of glove material (represented by a standard linear viscoelastic model) to predict glove transmissibility to the palm of the hand. The two degree-of-freedom model (representing the material and the hand) consistently provided a prediction of glove transmissibility to the palm that was inferior to the predictions of the four degree-of-freedom model (representing the material, the hand, and the arm), suggesting the exclusion of the dynamic response of the arm affects the ability of a model to predict glove transmissibility to the palm.

The research shows that the transmission of vibration through a glove to the palm of the hand or to the finger can be predicted from the dynamic stiffness of the glove material and the apparent mass of the hand. Such predictions will assist the optimisation of glove dynamics, reduce the time to assess the performance of a glove, and reduce the need for testing with human subjects.

Table of Contents

ABSTRACT	i
Table of Contents	iii
List of tables	xi
List of figures	xiii
DECLARATION OF AUTHORSHIP	xxv
Acknowledgements	xxvii
Chapter 1: Introduction	29
1.1 Thesis outline.....	29
Chapter 2: Literature Review	31
2.1 Introduction.....	31
2.1.1 Factors influencing the biodynamic response of the hand and the fingers	33
2.2 The dynamic characteristics of glove materials.....	43
2.2.1 Axial stiffness of a glove material.....	43
2.2.2 Dynamic stiffness of glove material	44
2.3 The transmissibility of a glove to the hand.....	45
2.3.1 Factors affecting glove transmissibility.....	45
2.4 International Standards.....	52
2.4.1 ISO 5349-1:2001 and ISO 5349-2:2002.....	52
2.4.2 ISO 10819:2013, Method for the measurement and evaluation of the vibration transmissibility of gloves at the palm of the hand.....	53
2.4.3 ISO 13753:2008, Method for measuring the vibration transmissibility of resilient materials when loaded by hand- arm system	56
2.4.4 ISO 10068:2012, Mechanical impedance of the human hand-arm system at the driving point.....	58
2.5 Vibration emitted by powered tools.....	58
2.6 Biodynamic modelling of the hand and the fingers to predict glove transmissibility to the hand and to the fingers	61
2.6.1 Mechanical impedance model of the hand	61
2.6.2 Lumped parameter models of the hand.....	63
2.7 Discussion and Conclusions.....	66
2.7.1 Apparent mass of the hand and the fingers	67
2.7.2 Dynamic stiffness of the material of a glove	68
2.7.3 Transmissibility of a glove to the hand.....	68

2.7.4	Improving the method to predict the transmissibility of a glove to the hand and to the fingers.....	69
2.7.5	The objective of the research.....	70
Chapter 3:	Methodology	73
3.1	Introduction.....	73
3.2	Measuring the apparent mass of the hand.....	74
3.3	Measuring the transmissibility of the material to the hand	76
3.4	Measuring the dynamic stiffness of the material	76
3.5	Sample preparation	77
3.6	Safety and ethics.....	78
3.7	Signal generation and data acquisition.....	78
3.7.1	Derritron VP4.....	79
3.7.2	Derritron VP30.....	79
3.7.3	Accelerometers.....	80
3.7.4	Force transducer	80
3.7.5	Impedance head.....	81
3.8	Analysis for the measurement of apparent mass of the hand, material transmissibility, and dynamic stiffness of the material.....	83
3.8.1	Transmissibility of the glove material to the hand and the finger	83
3.8.2	Apparent mass of the hand and the finger.....	83
3.8.3	Dynamic stiffness of the glove material.....	84
3.8.4	Statistical analysis	85
3.9	Predicting the transmissibility of the glove material using mechanical impedance model.....	85
3.10	Accuracy and precision of the measuring equipment used in Experiments 1, 2, and 3.	85
3.10.1	Apparent mass of a rigid body at frequencies between 5 and 500 Hz	86
3.10.2	Transmissibility between input and output accelerometer	88
3.10.3	Dynamic stiffness of a glove material	90
Chapter 4:	Transmission of vibration through gloves: Effects of material thickness	93
4.1	Introduction.....	93
4.2	Methods	94
4.2.1	Glove materials.....	94
4.2.2	Subjects.....	94

4.2.3	Measuring the apparent mass of the hand	94
4.2.4	Measuring the transmissibility of the glove material to the hand and finger	95
4.2.5	Measuring the dynamic stiffnesses of the materials	95
4.2.6	Analysis	95
4.2.7	Impedance model for predicting material transmissibility to the hand and finger.....	96
4.3	Results.....	96
4.3.1	Dynamic stiffness and viscous damping of the glove material	96
4.3.2	Apparent mass at the palm and the index finger	96
4.3.3	Transmissibility of the glove material to the palm of the hand and to the finger.....	97
4.3.4	Predicted transmissibility of the glove material to the palm and to the index finger	99
4.4	Discussion	100
4.4.1	Apparent mass at the palm and at the finger.....	100
4.4.2	Transmissibility of the glove material to the palm and to the index finger.....	102
4.4.3	Effects of dynamic stiffness of glove material.....	103
4.4.4	Inter-subject variability in the measured and predicted material transmissibility.....	104
4.4.5	Predicted transmissibility of the glove material to the palm and to the index finger	105
4.5	Conclusions	106
Chapter 5: Transmission of vibration through gloves: Effects of area of contact with a glove		107
5.1	Introduction.....	107
5.2	Methods	108
5.2.1	Materials and contact area.....	108
5.2.2	Subjects	108
5.2.3	Measuring apparent mass at the palm and at the thenar eminence.....	109
5.2.4	Measuring the transmissibility of the material to the palm and to the thenar eminence.....	109
5.2.5	Determining the dynamic stiffness of the material	110
5.2.6	Analysis	110
5.2.7	Predicting the transmissibility of material to the palm and to the thenar eminence	111

5.3	Results.....	112
5.3.1	Dynamic stiffnesses of the materials	112
5.3.2	Apparent mass at the palm and at the thenar eminence	112
5.3.3	Transmissibility of glove materials to the palm and the thenar eminence	114
5.3.4	Predicted material transmissibilities to the palm and to the thenar eminence	118
5.4	Discussion	119
5.4.1	Apparent mass at the palm and at the thenar eminence	119
5.4.2	Effect of apparent mass and dynamic stiffness on material transmissibility.....	122
5.4.3	Predicting the effects of contact area on glove transmissibility.....	123
5.4.4	Inter-subject variability.....	125
5.5	Conclusions	125
Chapter 6: Transmission of vibration through gloves: Effects of contact force		127
6.1	Introduction.....	127
6.2	Methods	128
6.2.1	Glove materials.....	128
6.2.2	Subjects.....	128
6.2.3	Measuring the apparent mass of the hand and the material transmissibility to the hand.....	129
6.2.4	Measuring the material dynamic stiffness	130
6.2.5	Analysis	130
6.2.6	Impedance model for predicting material transmissibility to the hand and finger	130
6.3	Results.....	131
6.3.1	Dynamic stiffness and viscous damping of the glove material.....	131
6.3.2	Apparent mass at the palm and at the index finger.....	132
6.3.3	Transmissibility of glove material to the palm and to the index finger	133
6.3.4	Predicted transmissibility of the glove material to the palm and to the index finger	136
6.4	Discussion	138
6.4.1	Dynamic stiffness of the glove materials.....	138
6.4.2	Apparent mass at the palm and at the finger	138

6.4.3	Effect of contact force on the transmissibility of the glove materials to the palm and to the fingers	140
6.4.4	Predicting the effects of contact force on glove transmissibility	141
6.5	Conclusions	142
Chapter 7: Transmission of vibration through gloves: Effects of vibration magnitude and arm support.....		145
7.1	Introduction.....	145
7.2	Method.....	147
7.2.1	Glove materials.....	147
7.2.2	Subjects	147
7.2.3	Measuring hand apparent mass and material transmissibility to the hand	147
7.2.4	Measuring the dynamic stiffnesses of the glove materials	149
7.2.5	Analysis	149
7.2.6	Predicting the apparent mass at the palm of the hand ..	149
7.3	Results.....	150
7.3.1	Dynamic stiffness of the glove materials	150
7.3.2	Apparent mass at the palm of hand	150
7.3.3	Glove transmissibility to the palm of the hand	152
7.3.4	Predicting the transmissibility of material to the palm using an impedance model	153
7.4	Discussions.....	156
7.4.1	Apparent mass at the palm of the hand.....	156
7.4.2	Effects of vibration magnitude and arm support on glove transmissibility	158
7.4.3	Predicting the apparent mass at the palm using the measured glove transmissibility	159
7.5	Conclusions	160
Chapter 8: Low frequency measurement of the apparent mass at the palm of the hand.....		161
8.1	Introduction.....	161
8.2	Method	162
8.2.1	Subjects	162
8.2.2	Measuring apparent mass at the palm of the hand	162
8.2.3	Analysis	163
8.3	Results.....	163
8.3.1	Apparent mass at the palm of the hand.....	163

8.4 Discussion	164
8.5 Conclusions	166
Chapter 9: Predicting the transmissibility of gloves to the hand using lumped parameter models of the hand	167
9.1 Introduction.....	167
9.2 Biodynamic models of the arm, the hand, and the fingers	169
9.2.1 Four degree-of-freedom multi-body biodynamic model of the hand (Model A)	169
9.2.2 Two degree-of-freedom multi-body biodynamic model of the hand	183
9.3 Lumped parameter model of glove material	189
9.3.1 Model description	189
9.3.2 Measuring the material dynamic stiffness	190
9.3.3 Calibrating the model of the glove material.....	190
9.3.4 Identification of the model parameters.....	190
9.3.5 Measured and fitted material dynamic stiffness	191
9.4 Predicting the transmissibility of glove material to the palm of the hand	194
9.4.1 Model description	194
9.4.2 Equations of motion	195
9.4.3 Measuring the material transmissibility to the palm of the hand.....	196
9.4.4 Predicted and measured glove transmissibility.....	197
9.5 Discussion	198
9.5.1 Proposed model of biodynamic response of the hand and the arm.....	198
9.5.2 Parameter sensitivity, modal analysis, and effects of contact area and push force on the apparent mass at the palm.....	199
9.5.3 Predicting transmissibility of a glove material to the hand	201
9.6 Conclusions	202
Chapter 10: General discussions	205
10.1 Apparent mass of the hand.....	205
10.2 Dynamic characteristics of the glove materials	206
10.3 Transmission of vibration through gloves to the hand	206
10.4 Repeatability and reproducibility of the measurement in this research	209

10.5 Predicting glove transmissibility using a mechanical impedance model of the hand and the glove.....	209
10.6 Transmissibility of Foam A to the palm of the hand assessed according to ISO 10819:2013	210
10.7 Improving methods of assessing glove transmissibility to the palm of the hand	211
10.7.1 Effects of contact area and contact force on the glove transmissibility	212
10.7.2 Measuring glove transmissibility to the fingers	212
10.7.3 Rank ordering gloves in terms of effectiveness in reducing vibration	213
Chapter 11: Conclusions and recommendations	215
11.1 Conclusions	215
11.2 Recommendations	217
Appendices	219
Appendix A: Procedures to calibrate transducers	221
Appendix B: Individual calculated and optimized parameters for Model A and Model B, individual predicted resonance frequency for Model A and Model B, and individual modal analysis for Model A and Model B.	223
Appendix C: Individual calibrated apparent mass at the palm for Model A and Model B, and individual predicted glove transmissibilities for Model A and Model B	228
Appendix D: Load deflection curves of the glove materials	233
List of References	235

List of tables

Table 2-1 Several flaws of the standard as discussed by Griffin (1998)	56
Table 3-1 Experiments conducted in this research	73
Table 3-2 Details of the independent variables for each of the experiments...	75
Table 3-3 Ethics number for each experiment.....	78
Table 3-4 Accelerometers and force transducers used in this experiment with its sensitivity and range of measurements.	82
Table 5-1 Physical characteristics of the materials used in the experiment...	108
Table 5-2 Characteristics of the subjects in the experiment.....	108
Table 5-3 Overall transmissibility of the three glove materials to the hand. Means and strandard deviations for 10 subjects.	118
Table 6-1 Characteristics of the subjects in the experiment.....	128
Table 7-1 Characteristics of the subjects in the experiment.....	147
Table 8-1 Characteristics of the subjects in the experiment.....	162
Table 9-1 Dimensions and masses of the body segments for Model A (Dempster and Gaughran, 1967; Adewusi <i>et al.</i> , 2012)	170
Table 9-2 Median optimized and calculated model parameters: Model A.	177
Table 9-3 Median undamped natural frequencies and mode shapes, Model A.	180
Table 9-4 Dimension and mass of the hand segments, Model B.....	184
Table 9-5 Optimized and calculated model parameters, Model B.	185
Table 9-6 Undamped natural frequencies and mode shapes, Model B.	187
Table 9-7 Optimized model parameters for Foam A, Foam B, and Gel A.....	192
Table 9-8 Predicted resonance frequencies of the apparent mass of the hand.....	200

List of figures

Figure 2-1 Diagrammatic presentation of the direction of the dynamic force and acceleration for the calculation of the apparent mass of the hand to vibration (ISO 5349-1:2001) 32

Figure 2-2 Median measured apparent mass of the hand (— — — Palm pushing a cylindrical handle with adapter at 50 N, horizontal direction, Dong *et al.* (2005), — — — Full-hand pushing on flat surface, horizontal direction, Xu *et al.* (2011), — Hand on a handle in horizontal direction, Reynolds (1977), and ----: Palm pushing a flat surface at 10N on a 25-mm diameter plate, vertical direction (O'Boyle and Griffin ,2004)..... 34

Figure 2-3 Apparent masses of the hand in the horizontal vibration direction with a bent-arm posture for ten subjects at a 15-N push force, together with the corresponding mean for the subjects (Xu *et al.*, 2011)..... 35

Figure 2-4 Influence of vibration magnitude on the mechanical impedance (——, 30mm handle, $a_{h_w}=2.5 \text{ m/s}^2$, 30mm handle, $a_{h_w}=5.0 \text{ m/s}^2$; — · — · — 40mm handle, $a_{h_w}=2.5 \text{ m/s}^2$, — — — 40mm handle, $a_{h_w}=5.0 \text{ m/s}^2$, ——— 50mm handle, 36

Figure 2-5 Apparent mass of the hand in three axes calculated from dynamic compliance curves presented by Reynolds (1977). This figure was taken from the Handbook of Human Vibration (Griffin, 1990) page 543. 36

Figure 2-6 Magnitude and phase of the mechanical impedance of the hand for different vibration directions (Burström, 1997). 37

Figure 2-7 The effect of increasing the size of the cylindrical handle on the mechanical impedance of the hand (——: 30 mm, ——— 40 mm and ——— 50 mm diameter of handle; Marcotte *et al.*, 2005). 38

Figure 2-8 Effect of push force on the median apparent mass at the palm of the hand for 12 subjects (O'Boyle and Griffin, 2004)..... 39

Figure 2-9 Influence of the grip force on the mechanical impedance of the hand (—, 10N grip;- - -, 30N grip;- -, 50N grip; Marcotte *et al.*, 2005). 39

Figure 2-10 Influence of the push force on the mechanical impedance of the hand (—, 25N push;- - -, 50N push;- · -, 75N push; Marcotte <i>et al.</i> , 2005).....	39
Figure 2-11 Comparison of mean moduli of driving point apparent mass (———— condition 1, - - - - condition 2, - · - · condition 3, · · · · condition 4, - · - · condition 5, · - · - condition 6, — condition 7; Concettoni and Griffin 2009), see Figure 2-12 for the condition of the hand.....	40
Figure 2-12 Condition of the hand during the measurements reported by Concettoni and Griffin, 2009).....	41
Figure 2-13 The apparent mass of the hand measured in two postures (P1 bent-arm, P2 extended-arm; Aldien <i>et al.</i> , 2006).	42
Figure 2-14 The apparent mass of the hand measured with different angle between the upper and the lower arm (Burström, 1997)	42
Figure 2-15 The apparent mass of the hand measured with different angles of the upper arm and the body (Burström, 1997).....	42
Figure 2-16 Diagrammatic representation of the indenter rig that is used to determine dynamic stiffness of glove material.....	44
Figure 2-17 Transmissibility of several gloves to the palm of the hand (Laszlo and Griffin, 2011).	46
Figure 2-18 Effect of vibration magnitude on the transmissibility of the gloves to the hand (— 0.25 ms ⁻² r.m.s.; · · · · 0.5 ms ⁻² r.m.s.; - - - - 1 ms ⁻² r.m.s.; · · · · 2 ms ⁻² r.m.s.; - - - - 4 ms ⁻² r.m.s.; — 8 ms ⁻² r.m.s.; Laszlo and Griffin, 2011).....	47
Figure 2-19 Overall mean transmissibility of two gloves at the tip of two fingers (index and middle fingers; Welcome <i>et al.</i> , 2014).	48
Figure 2-20 Effect of arm angle on the transmission of vibration through gloves to the hand: from handle to knuckle (Wu and Griffin, 1989). ...	49
Figure 2-21 Transmissibility of three materials to the palm of the hand with different contact force (O’Boyle and Griffin, 2004).....	50
Figure 2-22 Effect of push force on the transmissibility of four gloves as a function of frequency with 2.0 ms ⁻² r.m.s. vibration (means for 12 subjects: — 5 N; · · · · 10 N; - - - - 20 N; · · · · 40 N; — — — 50 N; — — — 80 N; Laszlo and Griffin, 2011).....	51
Figure 2-23 Effect of material thickness of a glove on the transmissibility of the glove to the hand (Wu and Griffin, 1989).....	52

Figure 2-24 Average glove isolation effectiveness of 10 gloves used with a nutrunner (Griffin, 2010).	53
Figure 2-25 Frequency weighting W_h with band-limiting (ISO 5349-1:2001)....	54
Figure 2-26 The position of the hand and the adapter during the measurement of the glove transmissibility according to the standard ISO 10819:2013 (upper figure). Picture of a wooden adapter with accelerometer embedded in it used in the standard ISO 10819:2013 (lower figure).	55
Figure 2-27 Equipment setup for the measurement of the glove transmissibility as specified in International Standard ISO 10819 (2013).	55
Figure 2-28 Measurement setup as specified in the ISO 13753:2008.	57
Figure 2-29 Model of the hand-arm impedance (ISO 13753:2008).	58
Figure 2-30 Basicentric coordinate system of the hand (ISO 10068:2012).	59
Figure 2-31 Examples of vibration magnitudes for common tools (Griffin <i>et al.</i> , 2006).	60
Figure 2-32 One-third octave band spectra of 20 powered hand tools (solid lines: un-weighted, dotted lines: weighted; Griffin 1997).....	61
Figure 2-33 The impedance model of the hand and material (O'Boyle and Griffin, 2004).	62
Figure 2-34 Predicted and measured transmissibility of a material to the palm of the hand with different push forces (O'Boyle and Griffin, 2004).	63
Figure 2-35 A seven degree-of-freedom biodynamic model of the hand and the glove (Dong <i>et al.</i> , 2009).	64
Figure 2-36 Comparisons of fitted glove transmissibility (magnitude) with the experimental data (—: fitted transmissibility using palm direct method, ◆: fitted transmissibility using on-the-wrist method, x x x: measured transmissibility using biodynamic method, ■: measured transmissibility using palm adapter method – ISO 10819:1996; Dong <i>et al.</i> , 2009).....	64
Figure 2-37 A seven degree-of-freedom model of the hand in bent arm posture (Adewusi <i>et al.</i> , 2012).	65
Figure 2-38 A seven degree-of-freedom model of the hand in extended arm posture (Adewusi <i>et al.</i> , 2012).	65
Figure 2-39 Comparisons of the measured responses with the responses of models derived from combined impedance and transmissibility	

responses: (a) impedance response in the bent-arm posture; (b) transmissibility responses in the bent-arm posture; (c) impedance response in the extended arm postures; (d) transmissibility responses in the extended arm postures; (Adewusi <i>et al.</i> , 2012).	66
Figure 3-1 Measuring the apparent mass of the hand.....	74
Figure 3-2 Equipment setup for the measurement of the apparent mass of the hand; Left: equipment used in Experiment 1, Right: equipment used in Experiment 2 and 3.	75
Figure 3-3 Indenter rig used in the first experiment.....	77
Figure 3-4 Indenter rig used in the second and the third experiment.	77
Figure 3-5 Samples of glove material used in this research; black: Foam A, orange: Gel A, and blue: Foam B.....	78
Figure 3-6 Left: Derritron VP4, Right: Derritron VP30.	79
Figure 3-7 Accelerometer embedded in a wooden adapter.	80
Figure 3-8 Force transducer Kistler 4576A.	81
Figure 3-9 Impedance head B&K 8001.	81
Figure 3-10 Apparent mass (modulus and phase) of a 3-gram rigid body measured with equipment used in Experiment 1. Coherency of the measurement of the rigid body apparent mass was calculated before mass cancellation.	87
Figure 3-11 Apparent mass (modulus, phase and coherency) of a 12-gram rigid body measured with equipment used in Experiments 2 and 3.	88
Figure 3-12 Transmissibility between the input and the output accelerometer (— for the measurement using Equipment 1, --- for the measurement using Equipment 2 and 3).	89
Figure 3-13 Dynamic stiffness (modulus, phase, and coherency) of Foam A. ...	90
Figure 4-1 The arrangement for the measurement of the apparent mass of the hand and the index finger.	94
Figure 4-2 Left: posture of the hand for the measurement of the apparent mass at the index finger. Right: arrangement for the measurement of the apparent mass at the palm of the hand. The downward force is indicated on the oscilloscope.....	95
Figure 4-3 Stiffness and damping of the glove material (--- 6.4 mm, --- 12.8 mm, and — 19.2 mm) according to Kelvin Voigt viscoelastic model (see Section 3.8.3).	97

Figure 4-4 Apparent mass of the hand of all 14 male subjects. Left: palm; Right: index finger. (Thicker black lines: Median apparent mass)..... 97

Figure 4-5 Transmissibility of the glove material with thickness of 6.4, 12.8, and 19.2 mm to the palm (upper graphs) and index finger (lower graphs) with 14 male subjects. Thicker lines: median transmissibility. 98

Figure 4-6 Median transmissibility (modulus and phase) of the glove material to the palm of the hand (left graphs) and to the index finger (right graphs) with three thicknesses of glove material:: 6.4 mm, ---: 12.8 mm, and —: 19.2 mm. Medians for 14 subjects. 99

Figure 4-7 Predicted and measured individual transmissibility of the glove material to the index finger with material thickness of 6.4, 12.8, and 19.2 mm (---: measured, and —: predicted). 100

Figure 4-8 Predicted and measured transmissibility to the palm (upper graphs) and the index finger (lower graphs) with glove material of thickness 6.4, 12.8, and 19.2 mm (---: measured, and —: predicted). Medians for 14 subjects. 101

Figure 4-9 Apparent mass of the hand (— palm pushing down on a flat surface at 10 N on a 25-mm diameter plate, vibration in vertical direction; — index finger pushing down a flat surface at 10 N on a 25-mm diameter plate, vibration in vertical direction; — — vertical palm pushing horizontally on a cylindrical handle with adapter at 50 N, vibration in horizontal direction (from Dong *et al.*, 2005); — — full hand pushing on horizontally on a flat surface, vibration in horizontal direction (from Xu *et al.*, 2011); palm pushing down on a flat surface at 10 N on a 25-mm diameter plate, vibration in vertical direction (from O'Boyle and Griffin, 2004)..... 102

Figure 4-10 Transmissibility of a gel material to the palm of the hand (left graphs) and to the index finger (right graphs):: 6.4 mm, ---: 12.8 mm, and —: 19.2 mm. Modulus (upper graphs) and phase (lower graphs). Medians for 14 subjects..... 104

Figure 4-11 Comparison of predicted transmissibility to the palm (upper graphs) and to the index finger (lower graphs) with and without

the wooden adapter: --- with adapter, — without adapter).	
Medians for 14 subjects.	105
Figure 5-1 Posture of the hand for the measurement of the apparent mass at the thenar eminence.	109
Figure 5-2 Acceleration power spectral densities of the stimuli: --- for the measurement of apparent mass and material transmissibility, — for the measurement of dynamic stiffness. Spectra with 2-Hz resolution.	110
Figure 5-3 Left: posture of the hand for the measurement of the transmissibility of the material to the palm of the hand. Right: arrangement for the measurement of the apparent mass and the material transmissibility. The downward force is indicated on the oscilloscope.	111
Figure 5-4 Stiffness and damping of the material according to the diameter of the contact area (— 12.5-mm, --- 25.0-mm, 37.5-mm; based on Kelvin Voigt viscoelastic model: see Section 3.8.3).	112
Figure 5-5 Individual apparent mass (modulus and phase) at the palm of the hand and at the thenar eminence according to its diameter of contact area. 10 Subjects.	113
Figure 5-6 Apparent mass (modulus and phase) at the palm of the hand and at the thenar eminence according to the diameter of the contact area (— 12.5-mm, --- 25.0-mm, 37.5-mm). Medians of 10 subjects.	114
Figure 5-7 Median transmissibilities (modulus and phase) of the three materials to the palm and to the thenar eminence according to the diameter of the contact area (— 12.5 mm, --- 25.0 mm, 37.5 mm). Median values from 10 subjects.	115
Figure 5-8 Individual transmissibilities (predicted and measured) for Foam A to the palm (upper figures) and to the thenar eminence (lower figures) according to the diameter of the contact area (— 12.5-mm, — 25.0-mm, — 37.5-mm; — measured, --- predicted).	116
Figure 5-9 Individual transmissibility (predicted and measured) of Foam B to the palm (upper figures) and the thenar eminence (lower figures) according to the diameter of contact area (— 12.5-mm,	

<p>———— 25.0-mm, ——— 37.5-mm; ——— measured, ---- predicted).....</p>	117
<p>Figure 5-10 Individual transmissibility (predicted and measured) of Gel A to the palm (upper figures) and the thenar eminence (lower figures) according to the diameter of contact area (———— 12.5-mm, ——— 25.0-mm, ——— 37.5-mm; ——— measured, ---- predicted).....</p>	120
<p>Figure 5-11 Median transmissibility (predicted and measured) with Foam A, Foam B, and Gel A to the palm and to the thenar eminence according to the diameter of the contact area (———— measured thenar eminence, predicted thenar eminence, ——— measured palm, predicted palm). Median values from 10 subjects.....</p>	121
<p>Figure 5-12 Median measured apparent mass at the palm of the hand with a force of 10 N, in the vertical direction. This study (———— 12.5-mm, ---- 25.0-mm, 37.5-mm); ——— palm pushing a flat surface at 10 N on a 25-mm diameter plate, vertical direction, Rezali and Griffin (2014); ——— index finger pushing a flat surface at 10 N on a 25-mm diameter plate, vertical direction, Rezali and Griffin (2014); ---- palm pushing a cylindrical handle with adapter at 50 N, horizontal direction, Dong <i>et al.</i> (200); and --- full-hand pushing on flat surface, horizontal direction, Xu <i>et al.</i> (2011).....</p>	122
<p>Figure 5-13 The predicted transmissibility (modulus and phase) of the three materials to the palm of the hand for three cases: (i) the dynamic stiffness unaffected by the area of contact, (ii) the apparent mass unaffected by the area of contact, (iii) both apparent mass and dynamic stiffness affected by the area of contact area, as in this study, Diameter of the contact area: ——— 12.5 mm, ---- 25.0 mm, 37.5 mm. Median values from 10 subjects.</p>	124
<p>Figure 6-1 Acceleration power spectral densities of the stimuli: --- for the measurement of apparent mass and transmissibility, ——— for dynamic stiffness measurement. Spectra with 10-Hz resolution.....</p>	129

Figure 6-2 Stiffness and damping of the three materials as a function of the preload force in logarithmic scale (· · · · · 10 N, ---- 15 N, ——— 20 N; based on Kelvin Voigt viscoelastic model: see Section 3.8.3)..... 131

Figure 6-3 Apparent mass (modulus and phase; modulus in logarithmic scale) at the palm of the hand and at the tip of the index finger as a function of frequency and contact force. (Individual data for 10 subjects). 132

Figure 6-4 Apparent mass at the palm and at the index finger with contact force of 10, 15, and 20 N (———: Palm, ———: Index finger, · · · · · 10 N, ---- 15 N, ——— 20 N,)..... 133

Figure 6-5 Transmissibilities of all materials to the palm and to the index finger (———: Palm, ———: Index finger, · · · · · 10 N, ---- 15 N, ——— 20 N,)..... 134

Figure 6-6 Individual transmissibility (predicted and measured) of Foam A to the palm and the index finger according to its contact force (——— 10 N, ——— 15 N, ——— 20 N; ——— measured, ---- predicted). 135

Figure 6-7 Individual transmissibility (predicted and measured) of Foam B to the palm and the index finger according to its contact force (——— 10 N, ——— 15 N, ——— 20 N; ——— measured, ---- predicted). 136

Figure 6-8 Individual transmissibility (predicted and measured) of Gel A to the palm and the index finger according to its contact force (——— 10 N, ——— 15 N, ——— 20 N; ——— measured, ---- predicted). 137

Figure 6-9 Transmissibility (predicted and measured) for Foam A, Foam B, and Gel A to the palm and to the index finger according to contact force (———: Palm, ———: Index finger, ---- predicted, ——— measured) Median values from 10 subjects. 139

Figure 6-10 Median measured apparent mass at the palm of the hand, z direction, this study (——— 20 N, ---- 15 N, · · · · · 10 N); median measured apparent mass at the index finger, z direction, this study (——— 20 N, ---- 15 N, · · · · · 10 N), Palm pushing a flat surface at 10 N on a 25-mm diameter plate (———), z-direction, Rezali and Griffin (2014), Index Finger pushing a flat

surface at 10N on a 25-mm diameter plate (----), z-direction, Rezali and Griffin (2014), and Palm pushing a cylindrical handle with adapter at 50 N (· · · · ·), x-direction, Dong et all (2005).	141
Figure 6-11 The predicted transmissibility (modulus) of Foam A to the palm of the hand for three cases: (case i) the dynamic stiffness unaffected by the contact force, (case ii) the apparent mass unaffected by the contact force, (case iii) both apparent mass and dynamic stiffness affected by the area of contact area, as in this study, according to the contact force conditions (· · · · · 10 N, ---- 15 N, ——— 20 N). Median values from 10 subjects.	143
Figure 7-1 Acceleration power spectral densities of the stimuli: · · · · · 1 ms ⁻² , ---- 2 ms ⁻² , ——— 4 ms ⁻² , for the measurement of apparent mass and transmissibility, ——— for dynamic stiffness measurement. Spectra with 2-Hz resolution.	148
Figure 7-2 Dynamic stiffness of the glove materials (· · · · · Foam A, ---- Foam B, ——— Gel A; based on Kelvin Voigt viscoelastic model: see Section 3.8.3).	151
Figure 7-3 Individual apparent mass (modulus and phase) at the palm of the hand according to their vibration magnitude and arm condition. Median of 12 subjects.....	151
Figure 7-4 Apparent mass at the palm at the palm of the hand according to the vibration magnitude and arm condition (Left: ———: 1 ms ⁻² , ---- 2 ms ⁻² , · · · · · 4 ms ⁻² , Right: ———: without arm support, · · · · · with arm support). Median of 12 subjects.	152
Figure 7-5 Individual transmissibility (modulus) of Foam A, Foam B, and Gel A to the palm of the hand according to their vibration magnitude and arm condition.	153
Figure 7-6 Transmissibilities of the materials to the palm of the hand according the glove materials (———: 1 ms ⁻² , ---- 2 ms ⁻² , · · · · · 4 ms ⁻²). Median of 12 subjects.....	154
Figure 7-7 Transmissibilities of the materials to the palm of the hand according to the glove materials (———: without arm support, ----: with arm support). Median of 12 subjects.....	155
Figure 7-8 Predicted transmissibility of the glove materials to the palm of the hand (modulus and phase) according to the vibration magnitude	

and arm condition (———: measured, ---- predicted). Median of 12 subjects.	157
Figure 7-9 Predicted transmissibility of the glove materials to the palm of the hand (modulus) according to the vibration magnitude (top row; ——: 1 ms ⁻² , ---- 2 ms ⁻² , 4 ms ⁻²) and arm condition (lower row; ——: without arm support, ---- with arm support). Median of 12 subjects.	158
Figure 7-10 Predicted apparent mass at the palm (modulus and phase) without arm support using mechanical impedance model according to the glove materials (vibration magnitude 2m/s ⁻² ; ——: measured, predicted). Median of 12 subjects.	160
Figure 8-1 Acceleration power spectral density of the stimulus for measuring the apparent mass at the palm. Spectrum with 1-Hz frequency resolution.	163
Figure 8-2 Inter-subject variability in apparent mass (modulus and phase) at the palm of the hand.	164
Figure 8-3 Apparent mass (modulus and phase) at the palm of the hand. Median of 12 subjects.	165
Figure 8-4 Apparent mass (modulus and phase) at the palm of the hand (—— measured in this chapter, ---- measured in Chapter 7). Medians of 12 subjects.	166
Figure 9-1 Multi-body biodynamic model of the hand and the arm, Model A	170
Figure 9-2 Locations of the measured dimensions of the fingers, the hand, the lower-arm, and the upper-arm.	171
Figure 9-3 Angles of the fingers, the lower arm, and the upper arm.	171
Figure 9-4 Fitted and measured apparent mass (modulus and phase) at the palm of the hand (— — — fitted, —— measured). Frequency resolution: Stage 1: 1 Hz Stage 2: 2 Hz). Median of 12 subjects.	179
Figure 9-5 Transmissibility responses of the hand (— — — predicted, —— measured). Frequency resolution: 2 Hz. Median of 12 subjects.	180
Figure 9-6 Illustration of the mode shapes for Model A (—— initial condition of the hand and the arm, — — — predicted condition of the hand and the arm during resonance).	181
Figure 9-7 Simple biodynamic model of the hand, Model B	183

Figure 9-8 Measured and fitted apparent mass (modulus and phase) at the palm of the hand (— — — Fitted, ——— Measured) . Median of 12 subjects.....	186
Figure 9-9 Transmission of vibration to the palm and to the fingers (Modulus). (— — — predicted, ——— measured; Concettoni and Griffin, 2009) . Median of 12 subjects.....	187
Figure 9-10 Illustration of the mode shapes for Model B (——— initial condition of the hand and the arm, — — — predicted condition of the hand and the arm during resonance)	188
Figure 9-11 Viscoelastic models of the glove material (Jones, 2001).	189
Figure 9-12 Measured and fitted dynamic stiffness (modulus and phase) of Foam A, Gel A, and Foam B (— — — fitted, ——— measured)	193
Figure 9-13 Model for predicting the transmissibility of a glove material to the palm of the hand: Model A.....	194
Figure 9-14 Model for predicting the transmissibility of a glove material to the palm of the hand: Model B.	194
Figure 9-15 Maxwell component in Standard Linear Solid model.....	196
Figure 9-16 Predicted and measured transmissibility of glove materials to the palm of the hand (——— measured, Model A, — — — Model B). Median of 12 subjects.	197
Figure 9-17 Operating deflection shapes in condition 7: a. 22 Hz, b. 46 Hz (——— deflection, — — — initial condition; Concettoni and Griffin, 2009).....	200
Figure 9-18 Predicted transmissibility for three prediction methods (— — — predicted, ——— measured).	202
Figure 10-1 The effects of vibration magnitude, arm support, contact area, contact force and material thickness on the apparent mass at the palm, the dynamic stiffness of Foam A, and the transmissibility of Foam A to the palm. Median data.	208
Figure 10-2 Apparent mass at the palm measured in similar conditions but with different sets of subjects (——— Boyle and Griffin, 2004, ---- Experiment 2, Experiment 1).....	209
Figure 10-3 Transmissibility of Foam A to the palm of the hand. (——— measured on a 37.5-mm diameter flat plate at 10 N push force in Chapter 5, ---- ISO 10819:2013 Condition 1 The grip force	

and feed force were maintained at about 30 N and 50 N, respectively, ---- ISO 10819:2013 Condition 2 Only the feed force was applied to the handle and maintained at about 25 N).
Subject 1 of Chapter 5. 213

DECLARATION OF AUTHORSHIP

I, KHAIRIL ANAS MD REZALI

declare that this thesis and the work presented in it are my own and has been generated by me as the result of my own original research.

MEASURING AND PREDICTING THE TRANSMISSION OF VIBRATION THROUGH GLOVES TO THE HAND

I confirm that:

1. This work was done wholly or mainly while in candidature for a research degree at this University;
2. Where any part of this thesis has previously been submitted for a degree or any other qualification at this University or any other institution, this has been clearly stated;
3. Where I have consulted the published work of others, this is always clearly attributed;
4. Where I have quoted from the work of others, the source is always given. With the exception of such quotations, this thesis is entirely my own work;
5. I have acknowledged all main sources of help;
6. Where the thesis is based on work done by myself jointly with others, I have made clear exactly what was done by others and what I have contributed myself;
7. Parts of this work have been published as:
Rezali KAM and Griffin MJ (2014) Transmission of vibration through gloves: effects of material thickness. Submitted to Ergonomics
Rezali KAM and Griffin MJ (2014) The transmission of vibration through gloves to the hand and to the fingers: effects of material dynamic stiffness. Applied Mechanics and Materials, Vol. 564, pp 149-154

Signed:.....

Date:.....

Acknowledgements

In the name of God, the Beneficent, the Merciful.

This research work has been given a huge support from many parties and individuals. Thank you for the financial support given by the Ministry of Higher Education of Malaysia, and the Universiti Putra Malaysia (UPM).

I am honoured to have been given the opportunity to work at the Human Factors Research Unit (HFRU) of the Institute of Sound and Vibration Research (ISVR). I would like to express my sincerest thanks to my main supervisor, Professor Michael J Griffin, for his words of wisdom that have helped to motivate and inspire me throughout this journey. I am thankful to Dr. Yi Qiu for his generous time in providing support during the course of the work.

I am grateful to Dr. Neil Ferguson and Dr. Emiliano Rustighi for their constructive comments and suggestions during the reviewing processes.

Special thanks to Dr. Weidong Gong, Dr. Henrietta Howarth, Mr Peter Russell, and Mr Gary Parker for providing technical support. Thank you to all members of HFRU especially Mingming Yang and Chi Liu and all my friends who have made my journey a learning and research experience at the University of Southampton.

This thesis is specially dedicated to my parents, Aishah, and Aqil.

Chapter 1: Introduction

Long exposure to vibration emitted by powered tools can cause serious injuries to the tool operators (Griffin, 1990), known as the hand-arm vibration syndrome. Anti-vibration gloves have been suggested as a method to reduce vibration transmitted to the hand.

Studies have shown that vibrations emitted by vibrating tools transmitted to the hand of the tool operators can be attenuated or amplified by using anti-vibration gloves (Wu and Griffin, 1989; Paddan and Griffin, 1999; Laszlo and Griffin, 2011). In 1996, the first International Standard that defined the method for assessing the effectiveness of a glove to reduce vibration transmitted to the palm of the hand was published (International Standard ISO 10819, 1996). The standard sets the minimum requirements for a glove to be considered as an anti-vibration glove. However, the effectiveness of an anti-vibration glove in reducing vibration transmitted to the hand depends on many factors.

The transmission of vibration through a glove to the hand principally depends on the biodynamic response of the hand and the dynamic stiffness of the material in the glove. The biodynamic response of the hand can be affected by the contact area, contact force, vibration magnitude, posture of the hand and the arm, vibration direction, and vibration frequency. On the other hand, contact area, contact force, and material thickness can also affect the dynamic stiffness of the glove material. Factors that affect the biodynamic response of the hand or the dynamic stiffness of the glove material will also affect the glove transmissibility to the hand. Previous studies have investigated how these factors affect glove transmissibility but the mechanisms of how these factors affect the glove transmissibility to the hand are still not clear.

The main objective of this research was to advance understanding of factors influencing the transmission of vibration through gloves to the hand and to the fingers. This was achieved by measuring and modelling the biodynamic response of the hand and the fingers, the dynamic stiffness of the material in a glove, and the transmissibility of a glove to the hand and to the fingers.

1.1 Thesis outline

Previous studies of the biodynamic response of the hand, the dynamic stiffness of the material in a glove, and the transmissibility of gloves to the hand were reviewed and are presented in Chapter 2. This chapter also discusses the information that the previous studies have given to the understanding of the mechanisms of factors influencing glove

transmissibility. The problem statements and the objectives of this research are also presented in this chapter of the thesis.

Chapter 3 aims to provide information related to the methods used in this research and the impedance model of the hand that is considered in Chapters 4 to 7. The chapter also includes discussion of the limitations of the equipment (i.e., precision and accuracy of the equipment in acquiring data), and the methods of analysis of the results.

Chapters 4, 5, 6, and 7 discuss the effects of material thickness, contact area, contact force, vibration magnitude, and arm support on the transmissibility of a glove to the palm of the hand, and to the fingers. The dynamic response of the hand, the dynamic stiffness of glove materials and the transmissibility of glove materials to the hand were acquired and analysed. Using the dynamic response of the hand and the dynamic stiffness of the glove materials, the transmissibilities of the glove materials to the hand were predicted using a mechanical impedance model.

Chapter 8 investigates the apparent mass of the hand at frequencies less than 10 Hz. This measurement was performed to provide data for the calibration of alternative lumped parameter models of the hand presented in Chapter 9

Chapter 9 proposes lumped parameter models of the biodynamic response of the hand and lumped parameter models of the dynamic stiffness of glove materials. The models were used to predict glove transmissibility. The predictions of glove transmissibility using the models were compared with glove transmissibility predicted using a mechanical impedance model and the glove transmissibility measured experimentally.

Chapter 9 presents a general discussions of the main findings reported in this thesis.

Chapter 10 concludes the main findings of the research, along with recommendations for future research.

Chapter 2: Literature Review

2.1 Introduction

Vibration exposures in working environments are common everywhere in the world. Efforts in reducing vibration transmitted to the human have been done by many engineers and researchers in order to have a better working environment. The reason is pretty simple, biological entities such as human react differently to vibration compared to other elements on earth.

Powered tools such as needle guns, impact wrenches, chain saws, and power drills are used in many industries. These tools emitted vibration that can cause serious injuries to the tool operator (e.g., Griffin, 1990). Among listed disorders associated with hand-transmitted vibration are vascular disorders, muscle disorders, neurological disorders, and bone and joint disorders (Griffin, 1990). It has been reported that exposing the hand to vibration at frequencies in the range 8 to 250 Hz decreases finger blood flow (Ye and Griffin, 2014). Epidemiological studies have shown that the prevalence of vibration injuries in industries is above 40% in many cases (Hamilton, 1918; Seyring, 1930; McLaughlin *et al.*, 1945; Grounds, 1964; Starck *et al.*, 1994; Chetter *et al.*, 1997). Prevention and improvements in working conditions can reduce the number of cases of hand-arm vibration diseases (Starck *et al.*, 1994).

In an attempt to control the hand-arm vibration syndrome, 'anti-vibration gloves' have been developed. Anti-vibration gloves might reduce vibration by acting as a medium that isolates the hand from the vibration at some frequency of vibration (Wu and Griffin, 1989; Chang *et al.*, 1999). Anti-vibration gloves are usually made of foam or gel and these materials are sometimes wrapped in a thin layer of material that contacts with the vibrating surface. There are also gloves made of rubber with dimpled surfaces.

In European countries, a glove that passes a test specified in International Standard ISO 10819:2013 can be considered an 'anti-vibration glove'. In the standard, the glove is required to attenuate vibration by at least 10% at frequencies between 25 and 200 Hz and by least 40% at frequencies between 200 and 1250 Hz. Assessing a glove for its ability to reduce vibration can be difficult because a lot of factors can affect glove performance.

The transmissibility of a glove to the hand primarily depends on two factors, the biodynamic response of the hand and the dynamic stiffness of the material in the glove. Biodynamic response of the hand and the fingers

The biodynamic response of the hand describes the way the hand responds to a vibration. It provides useful information for the evaluation of the mechanisms of how the hand responds to vibration. It is divided into two categories, transmissibility responses (e.g., hand to upper-arm transmissibility), and the driving-point response of the hand (i.e., the mechanical impedance of the hand or the apparent mass of the hand).

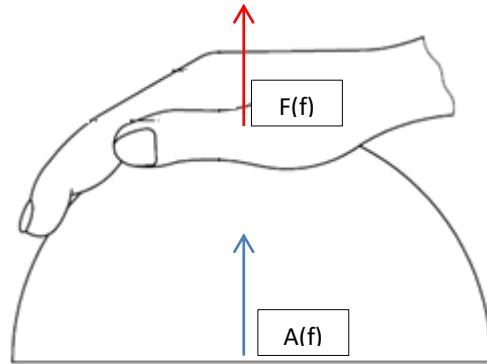


Figure 2-1 Diagrammatic presentation of the direction of the dynamic force and acceleration for the calculation of the apparent mass of the hand to vibration (ISO 5349-1:2001)

The apparent mass of the hand, $M(f)$, can be determined from the ratio of the cross-spectral density of the input acceleration, $A_{ii}(f)$, and the output dynamic force, $F_{io}(f)$, to the power spectral density of the input acceleration, $A_{ii}(f)$, at the same location in the same direction:

$$M(f) = \frac{F_{io}(f)}{A_{ii}(f)} \quad (2.1)$$

The mechanical impedance of the hand is the ratio of the cross-spectral density of the input velocity, $v_{ii}(f)$, and the output dynamic force, $F_{io}(f)$, to the power spectral density of the input velocity, $v_{ii}(f)$, at the same location in the same direction:

$$Z(f) = \frac{F_{io}(f)}{v_{ii}(f)} \quad (2.2)$$

The apparent mass of the hand can be measured at any location on the hand in contact with the vibrating surface (i.e., if the measurement is obtained at the palm of the hand, the apparent mass is called the apparent mass at the palm and if the measurement is obtained at the index finger, the apparent mass is called the apparent mass at the index finger).

Vibration that is transmitted from the handle to other locations of the hand (i.e., to the lower-arm or the upper-arm) is described using transmissibility. For example, the handle to forearm transmissibility is the ratio of the cross-spectral density of the acceleration at the handle and the acceleration at the forearm, $A_{hf}(f)$, to the power spectral density of the acceleration at the handle, $A_{hh}(f)$:

$$T(f) = \frac{A_{hf}(f)}{A_{hh}(f)} \quad (2.3)$$

2.1.1 Factors influencing the biodynamic response of the hand and the fingers

The biodynamic response of the hand has been widely studied. The response of the hand to vibration depends on the frequency of the vibration, magnitude of vibration, contact area, contact force, posture of the hand and the arm, vibration direction, and location of measurement.

2.1.1.1 Frequency of vibration

The apparent mass of the hand is greatest at low frequencies and decreases as the frequency of vibration increases (Figure 2-2, 2-3; Reynolds and Angevine, 1977; O'Boyle and Griffin, 2004; Dong *et al.*, 2005). The impedance of the hand can increase, decrease, or remain unchanged as the frequency vibration increases (Reynolds and Soedel, 1972; Suggs and Mishoe, 1977). A principal resonance in the apparent mass at the palm has been observed at about 15 Hz (O'Boyle and Griffin, 2004) or 30 Hz (Marcotte *et al.*, 2005). The apparent mass of the hand can be small at high frequencies: less than 100 grams at frequencies greater than 250 Hz (Xu *et al.*, 2011) and less than 20 grams at frequencies greater than 350 Hz (O'Boyle and Griffin, 2004). The apparent mass of the full-hand pushing on a vibrating surface in the horizontal direction (Xu *et al.*, 2011) is greater than the apparent mass of the hand pushing on a 25-mm diameter vibrating plate in the vertical direction (O'Boyle and Griffin, 2004; Figure 2-2).

2.1.1.2 Magnitude of the vibration

A change in vibration magnitude has a small influence on the mechanical impedance of the hand (Figure 2-4; Marcotte *et al.*, 2005). Increasing the magnitude of vibration will increase the mechanical impedance of the hand at frequencies greater than 500 Hz and decrease the mechanical impedance of the hand at frequencies less than about 100 Hz (Lundström *et al.*, 1989). The increase in the mechanical impedance of the hand when

the magnitude of vibration is decreased is significant at frequencies greater than 150 Hz (Burström, 1997). However, it has also been reported that the effect of vibration magnitude on the dynamic response of the hand is negligible at frequencies greater than 100 Hz (Marcotte *et al.*, 2005). The mechanical impedance of the hand decreases as the vibration magnitude increases at frequencies between 30 and 100 Hz (Marcotte *et al.*, 2005). These contradictory findings indicate that these studies cannot provide clear understanding of the effects of vibration magnitude. It is not evident whether the effects of vibration magnitude in those studies resulted from the shear vibration of the hand (i.e., the hand was in a gripping posture), or from the vibration normal to the hand. It is also not apparent which part of the hand influenced by the changes in vibration magnitude.

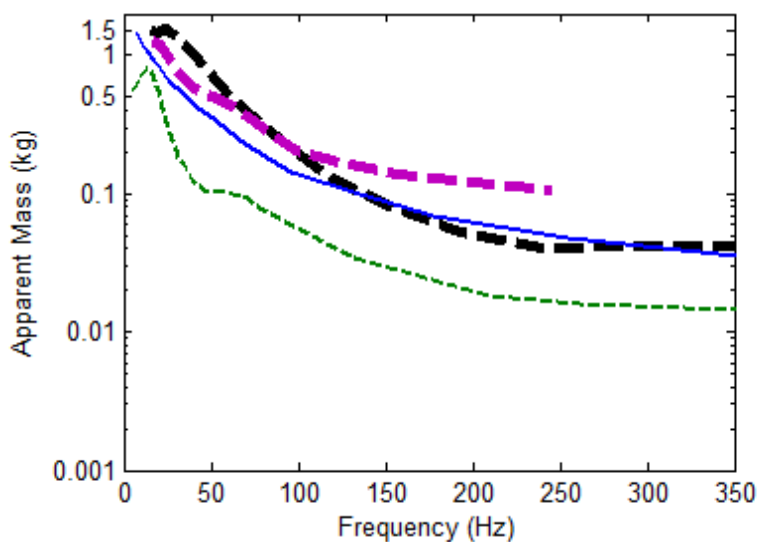


Figure 2-2 Median measured apparent mass of the hand (— — — Palm pushing a cylindrical handle with adapter at 50 N, horizontal direction, Dong *et al.* (2005), — — — Full-hand pushing on flat surface, horizontal direction, Xu *et al.* (2011), — Hand on a handle in horizontal direction, Reynolds (1977), and - - - : Palm pushing a flat surface at 10N on a 25-mm diameter plate, vertical direction (O'Boyle and Griffin, 2004).

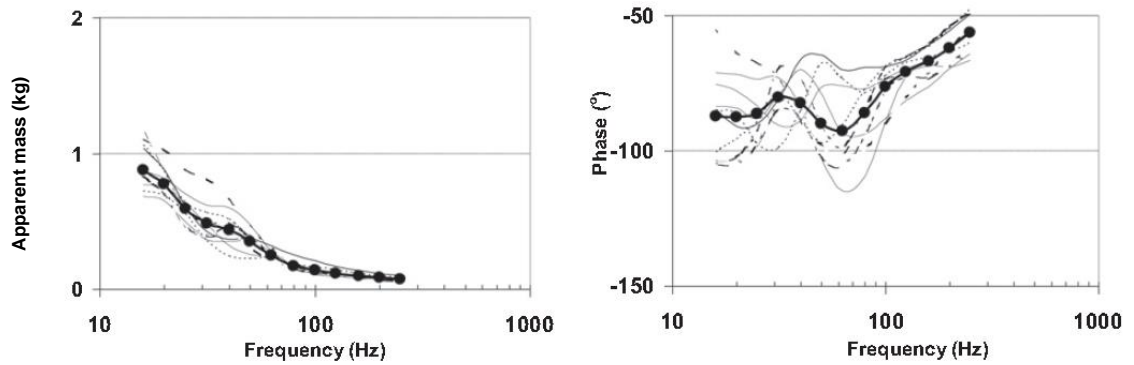


Figure 2-3 Apparent masses of the hand in the horizontal vibration direction with a bent-arm posture for ten subjects at a 15-N push force, together with the corresponding mean for the subjects (Xu *et al.*, 2011).

2.1.1.3 Vibration direction

The effects of vibration direction on the apparent mass of the hand are shown in Figure 2-5 and 2-6. The apparent mass of the hand in the horizontal direction is greater than the apparent mass of the hand in the vertical and the axial directions at frequencies less than about 80 Hz (Figure 2-5; Reynolds, 1977). However, in a separate study, it has been found that the mechanical impedance of the hand in the vertical direction is greater than the mechanical impedance of the hand in the horizontal and the axial directions at frequencies less than about 80 Hz (Figure 2-6; Burström 1997). The apparent mass in the axial direction is similar to the apparent mass in the vertical direction at frequencies less than about 40 Hz (Reynolds, 1977). At frequencies greater than 100 Hz, the apparent mass of the hand in the horizontal direction is comparable with the apparent mass of the hand in the vertical direction (Reynolds, 1977).

The apparent mass of the hand presented in Figures 2-5 and 2-6 can provide a general indication of how vibration direction can affect the dynamic response of the hand. The difference in the apparent mass of the hand may significantly affect the transmissibility of a glove to the hand. Previous studies have not shown which parts of the hand (i.e., lower arm or upper arm) contribute to the change in the dynamic response of the hand when the vibration direction is changed. This may be important so that the study of the mechanisms of the effects of vibration direction does not have to focus on all parts of the hand and the arm.

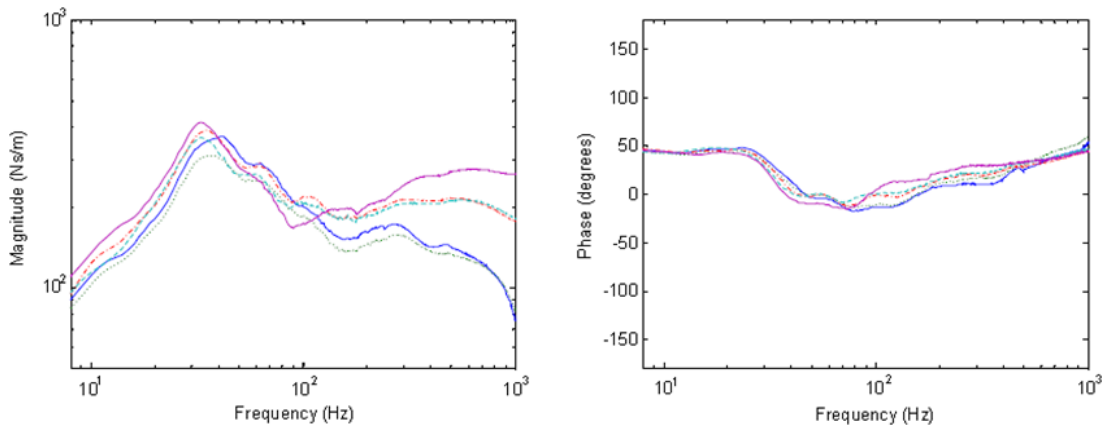


Figure 2-4 Influence of vibration magnitude on the mechanical impedance (—, 30mm handle, $a_{h,w}=2.5 \text{ m/s}^2$, 30mm handle, $a_{h,w}=5.0 \text{ m/s}^2$; - · - · - 40mm handle, $a_{h,w}=2.5 \text{ m/s}^2$, - - - 40mm handle, $a_{h,w}=5.0 \text{ m/s}^2$, ——— 50mm handle, $a_{h,w}=2.5 \text{ m/s}^2$, ——— 50mm handle, $a_{h,w}=5.0 \text{ m/s}^2$; Marcotte *et al.*, 2005).

2.1.1.4 Contact area

The mechanical impedance of a finger increases with increasing area of contact at frequencies greater than 400 Hz (Mann and Griffin, 1996). The driving-point mechanical response of the hand measured on a cylindrical handle increases with increasing diameter of the cylindrical handle, especially at frequencies greater than 125 Hz (Figure 2-7; Marcotte *et al.*, 2005). The increase in the area of contact also influences the phase (i.e., the phase increases with increasing diameter of the cylindrical handle) especially at frequencies between 100 and 600 Hz.

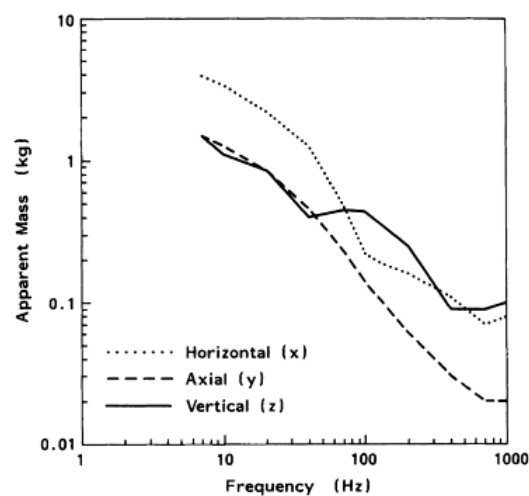


Figure 2-5 Apparent mass of the hand in three axes calculated from dynamic compliance curves presented by Reynolds (1977). This figure was taken from the Handbook of Human Vibration (Griffin, 1990) page 543.

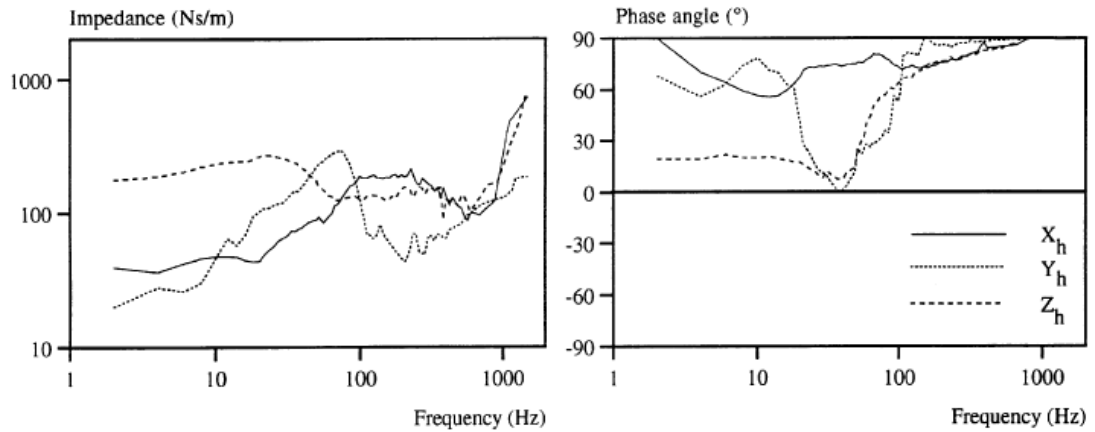


Figure 2-6 Magnitude and phase of the mechanical impedance of the hand for different vibration directions (Burström, 1997).

The impedance of a flat hand pushing on a plate (i.e., Miwa, 1964a, 1964b) is different than the impedance of the hand gripping handles of different diameters (i.e., the area of contact of a flat hand pushing on a plate is larger than the area of contact of a hand gripping a handle provided that the vibration is generated in one direction (Reynolds and Falkenberg, 1984). At frequencies greater than 100 Hz and with the same vibration direction, the apparent mass of the hand on a cylindrical handle is less than the apparent mass of the hand on a flat surface consistent with the larger contact area of the flat surface than with the cylindrical handle (Figure 2-2; Dong *et al.*, 2005, Xu *et al.*, 2011).

An increase in the area of contact will increase the hand tissues in contact with the vibrating surface: this will only affect the apparent mass of the hand at high frequencies because at high frequencies, the components that are close to the vibration driving-point will dominate the motion of the dynamic system (i.e., hand and arm). Based on the previous studies showed in this section, it is not clear whether the increase in the apparent mass of the hand when the area of contact increases is due to the increase in the mass of the hand tissues close of the vibration driving-point (i.e., it may be due to changes in the other parts of the hand or the arm).

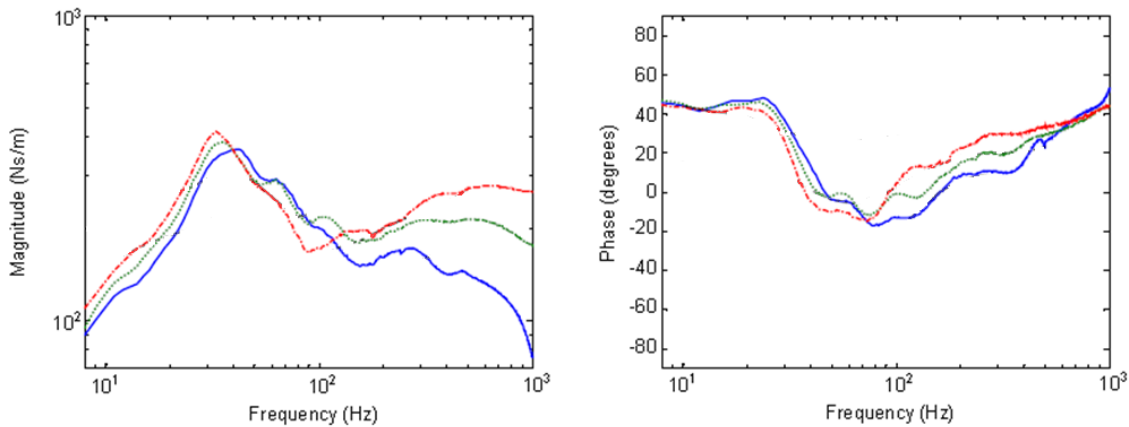


Figure 2-7 The effect of increasing the size of the cylindrical handle on the mechanical impedance of the hand (—: 30 mm, — 40 mm and — 50 mm diameter of handle; Marcotte *et al.*, 2005).

2.1.1.5 Contact force

The effects of contact force on the mechanical impedance of the hand have been studied previously by several researchers (Mann and Griffin, 1996; O'Boyle and Griffin, 2004; Marcotte *et al.*, 2005; Xu *et al.*, 2011).

It has been reported that increasing the contact force increases the resonance frequency in the apparent mass at the palm (Figure 2-8; O'Boyle and Griffin, 2004; Marcotte *et al.*, 2005). The apparent mass at the palm at frequencies greater than about 20 Hz increases with increasing contact force (Figure 2-8, 2-9, and 2-10; O'Boyle and Griffin, 2004; Riedel, 1995; Burström, 1997; Marcotte *et al.*, 2005; Xu *et al.*, 2011). The peak in the magnitudes of the mechanical impedance of the hand tends to be greater with greater grip and push forces (Marcotte *et al.*, 2005). The influence of grip and push force is negligible at frequencies less than 20 Hz (Marcotte *et al.*, 2005). The mechanical impedance of the index finger increases with increasing contact force from 0.25 to 8 N at frequencies greater than 60 Hz (Mann and Griffin, 1996)

The increase in the resonance frequency when the contact force is increased could be due to an increase in the stiffness and the damping of the hand and the arm. However, it is not clearly evidenced which parts of the hand or the arm predominantly influence the apparent mass of the hand at the increased resonance frequency.

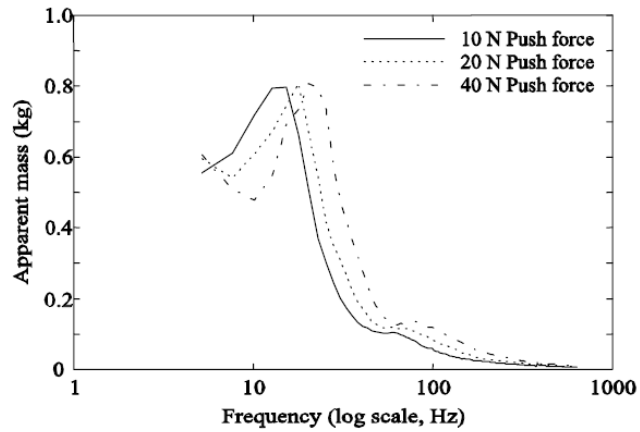


Figure 2-8 Effect of push force on the median apparent mass at the palm of the hand for 12 subjects (O'Boyle and Griffin, 2004)

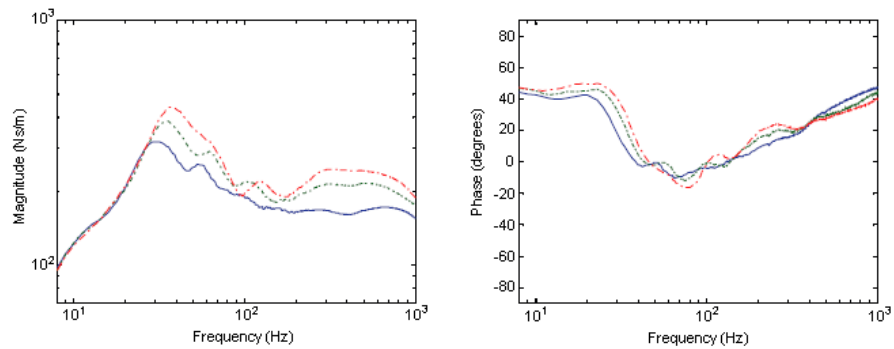


Figure 2-9 Influence of the grip force on the mechanical impedance of the hand (—, 10N grip; - - -, 30N grip; - · -, 50N grip; Marcotte *et al.*, 2005).

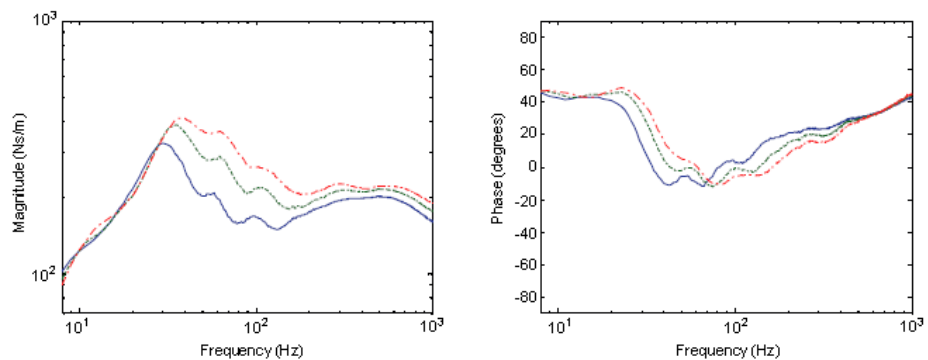


Figure 2-10 Influence of the push force on the mechanical impedance of the hand (—, 25N push; - - -, 50N push; - · -, 75N push; Marcotte *et al.*, 2005).

2.1.1.6 Location of measurement

The apparent mass of the hand is usually measured at the palm of the hand (e.g., ISO 10819:2013; O'Boyle and Griffin, 2004; Dong *et al.*, 2006; Xu *et al.*, 2011). In some

cases, the apparent mass of the hand is measured at different locations of the hand in contact with the vibrating surface (e.g., at the fingers, at the thenar eminence).

It has been reported that the apparent mass at the fingers is considerably less than the apparent mass at the palm (Figure 2-11; Concettoni and Griffin, 2009): the mass of the fingers is less than the mass of the palm. The apparent mass of the hand decreases when the hand in contact with the vibrating surface decreases from full hand to the tip of the index finger (i.e., conditions 1 to 4; Figure 2-12). The apparent mass of the hand does not greatly influence by the apparent mass of the fingertips (i.e., condition 5, 6, and 7; Figure 2-11): the mass of the fingertips is small compared to the rest of the hand-arm system.

It is expected that if the area of the hand in contact with the vibrating surface reduces, as observed in a previous study (Concettoni and Griffin, 2009), the glove transmissibility to the hand may be altered and may provide poor vibration reduction (i.e., the apparent mass of the hand reduces as the area of the hand in contact with vibrating surface reduces. Reduced apparent mass of the hand is expected to increase the glove transmissibility to the hand at frequencies greater than the resonance, assuming that the motion of the hand and the arm is similar to a single degree-of-freedom system).

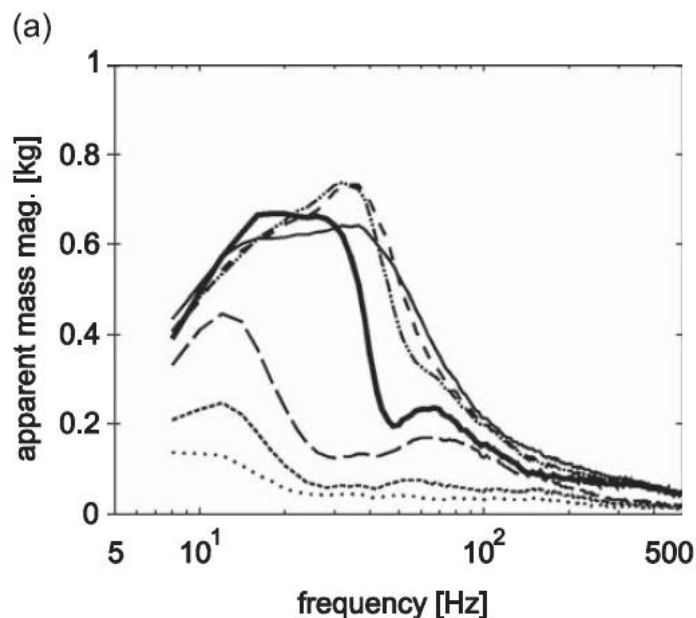


Figure 2-11 Comparison of mean moduli of driving point apparent mass (— condition 1, — — — condition 2, - - - - condition 3, ····· condition 4, — · — condition 5, — · — condition 6, ——— condition 7; Concettoni and Griffin 2009), see Figure 2-12 for the condition of the hand.

2.1.1.7 Arm posture

The effect of arm posture on the dynamic response of the hand has been previously investigated (Burström, 1997; Besa *et al.*, 2007; Aldien *et al.*, 2006; Adewusi *et al.*, 2010, 2012).

The mechanical impedance of the hand decreases with decreasing angle between the upper and the lower arm at frequencies less than about 30 Hz (Figure 2-13 and 2-14; Burström, 1997; Aldien *et al.*, 2006; Besa *et al.*, 2007; Adewusi *et al.*, 2010). At about 8 Hz, the apparent mass with an extended-arm posture is about three times greater than with a bent-arm posture (Aldien *et al.*, 2006). Increasing the angle between the upper-arm and the body increases the impedance of the hand at frequencies less than 20 Hz (Figure 2-15; Burström, 1997).

It may be concluded that the change in the upper-arm greatly influences the hand's dynamic response at frequencies less than 30 Hz. However, this does not explain how the lower-arm influences the hand's dynamic response when its posture is changed. If the effects of both lower-arm and upper-arm on the dynamic response of the hand are clear (i.e., frequency range), it may help in indicating how the dynamic response of the hand changes when the arm posture is varied.

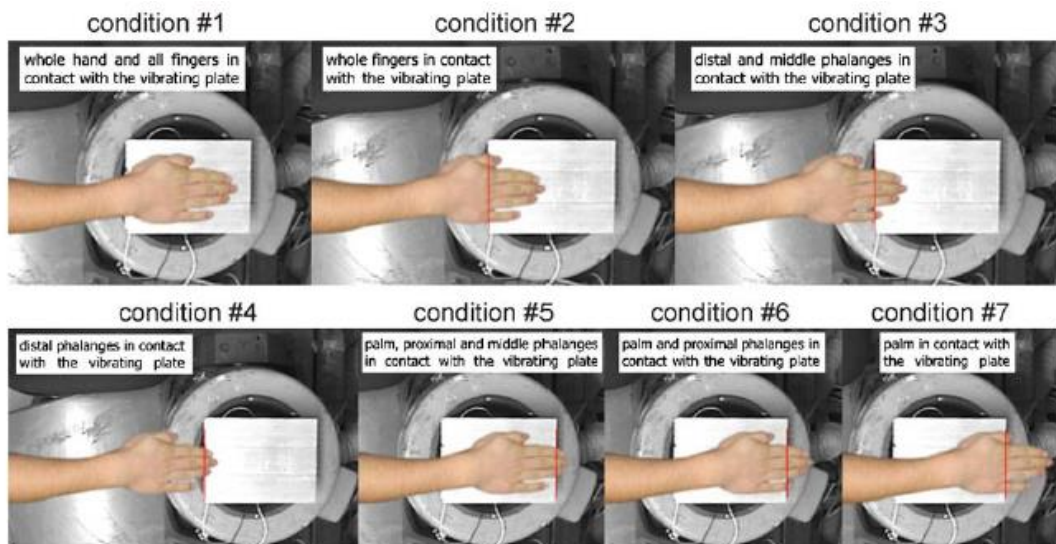


Figure 2-12 Condition of the hand during the measurements reported by Concettoni and Griffin, (2009)

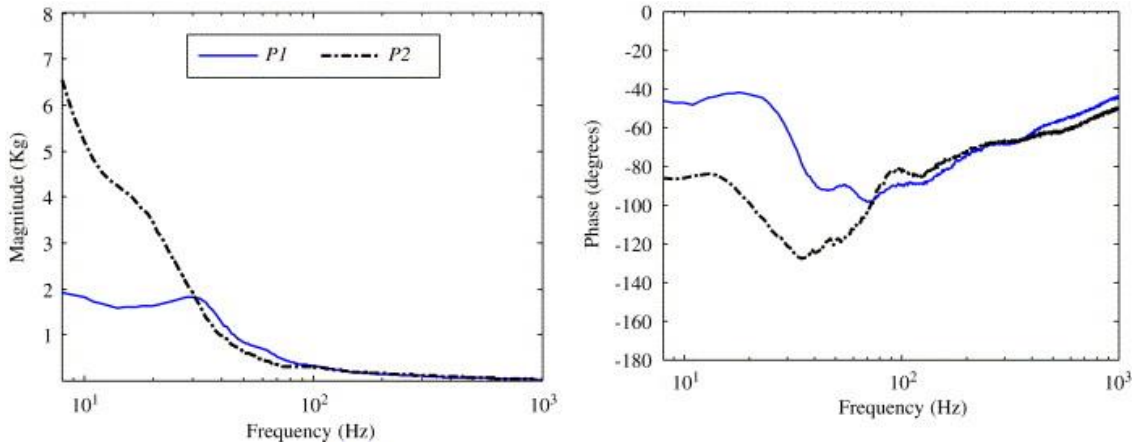


Figure 2-13 The apparent mass of the hand measured in two postures (P1 bent-arm, P2 extended-arm; Aldien *et al.*, 2006).

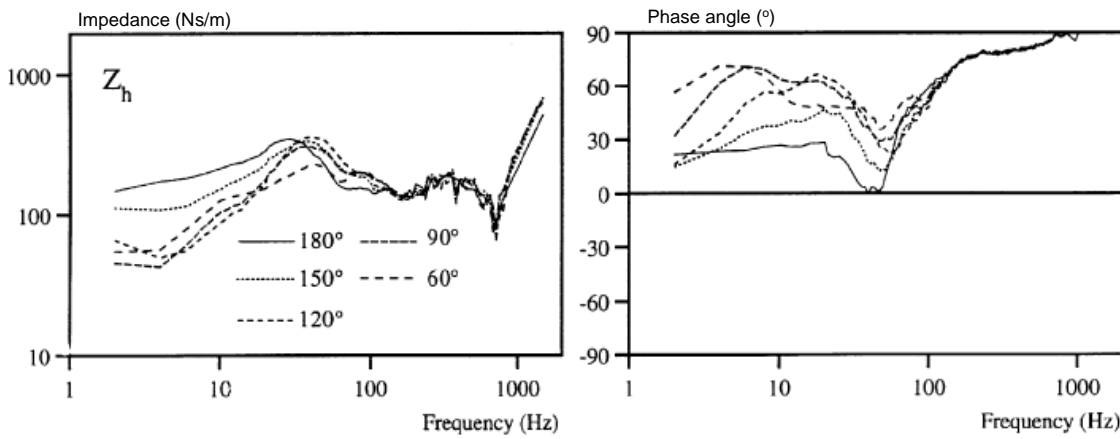


Figure 2-14 The apparent mass of the hand measured with different angle between the upper and the lower arm (Burström, 1997)

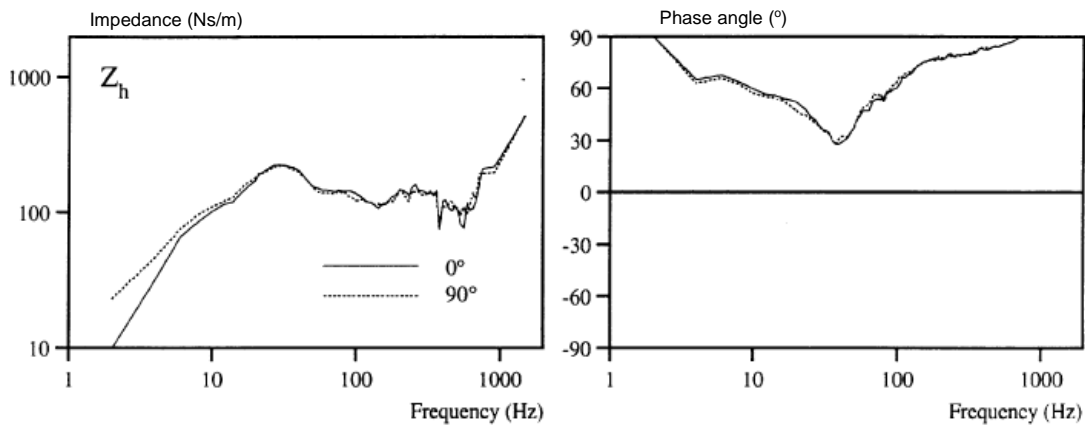


Figure 2-15 The apparent mass of the hand measured with different angles of the upper arm and the body (Burström, 1997)

2.2 The dynamic characteristics of glove materials

Anti-vibration gloves are usually made of viscoelastic materials such as foam and gel. These materials are complex and non-linear. The dynamic characteristics of a glove material can be represented by its dynamic stiffness. The dynamic stiffness of a viscoelastic material depends on many factors (e.g., chemical composition, density) and so predicting the dynamic stiffness of a material is almost impossible and measurement is required.

2.2.1 Axial stiffness of a glove material

If the glove material is assumed to be a linear elastic material, the axial stiffness of the glove material can be represented by Equation 2.4.

$$k = \frac{AE}{t} \quad (2.4)$$

where A is the cross-sectional area, E is the elastic modulus or young's modulus of the material and t is the thickness of the material.

International Standard ISO 10819:2013 states that the vibration-reducing material in a glove should cover the complete palm area of the hand and the three phalanges of each finger and the two phalanges of the thumb (International Standard ISO 10819:2013). On the other hand, the area of contact with a vibrating tool varies from one tool to another. Based on Equation 2.4, increasing the area of contact of a glove material will increase the stiffness of the glove material and may thus affect glove transmissibility, although this assumes the static stiffness of a glove material is the same as the dynamic stiffness of the glove material. A measurement to investigate the effects of contact area on the glove dynamic stiffness is needed to better understand glove characteristics when contact area is varied.

Another variable that can be expected to alter the properties and may be changed easily is the material thickness. Such changes should have predictable effects on dynamic properties. It is expected that for a linear material, increasing the thickness of the glove material will decrease the stiffness of the glove material. It should be noted that the thickness of the material in a glove varies from the palm to the tip of the fingers. International Standard 10819:2013 specifies that the thickness of the material should be equal or greater than 0.58 times of the thickness of the material on the palm (International Standard ISO 10819:2013). The thickness of the material should not exceed 8 mm.

2.2.2 Dynamic stiffness of glove material

The dynamic stiffness of a glove material is a ratio of the cross-spectral density of the input displacement and the output dynamic force transmitted by the material, $F_{io}(f)$, to the power spectral density of the input displacement, $X_{ii}(f)$, measured in the same direction as the applied force .

$$S(f) = \frac{F_{io}(f)}{-\omega^2 A_{ii}(f)} \quad (2.5)$$

where $A_{ii}(f)$ is the input acceleration, ω is the angular frequency ($\omega=2\pi f$), $-\omega^2 A_{ii}(f)$ is the input displacement, $X_{ii}(f)$.

The dynamic stiffness of a viscoelastic glove material varies according to the vibration frequency and contact force (e.g., O'Boyle and Griffin, 2004). The dynamic stiffness of a material can be measured using an indenter rig (Figure 2-16). The material is placed on a plate secured to a lower plate attached to the vibrator platform. In the upper part of the indenter rig, a force transducer with a plate is suspended through a bearing so that a downward force can be applied to the material by turning the preload screw. Vertical acceleration is measured using an accelerometer secured on the plate attached to the table of the vibrator. The dynamic stiffness is calculated based on the Equation 2.5.

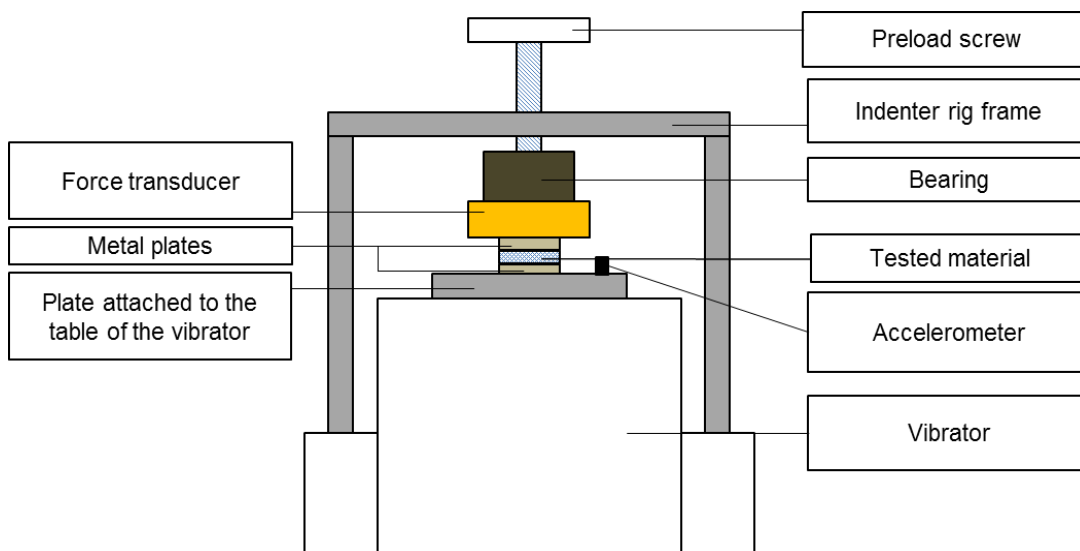


Figure 2-16 Diagrammatic representation of the indenter rig that is used to determine dynamic stiffness of glove material.

2.3 The transmissibility of a glove to the hand

The transmissibility of a glove material to the hand, $T(f)$, is the ratio of the cross-spectral density of the input acceleration and the output acceleration, $A_{io}(f)$, to the power spectral density of the input acceleration, $A_{ii}(f)$:

$$T(f) = \frac{A_{io}(f)}{A_{ii}(f)} \quad (2.6)$$

A glove that attenuates vibration to the hand can also amplify the vibration. Measuring glove transmissibility to the hand provides information on the glove performance in reducing or amplifying vibration to the hand. However, to optimize the glove to reduce vibration in a specific condition in a range vibration frequency will require understanding of the mechanisms of the glove in reducing vibration (i.e., the behaviour of both the dynamic response of the hand and the dynamic stiffness of the glove material when factors such as area of contact or contact force are varied).

2.3.1 Factors affecting glove transmissibility

The transmissibility of a glove material to the hand depends on two primary factors, the dynamic response of the hand, and the dynamic stiffness of the material. Factors affecting the dynamic response of the hand and the dynamic stiffness of the glove material will also affect the transmissibility of the glove to the hand.

2.3.1.1 Frequency of vibration

The transmissibility of a glove material to the hand is frequency-dependent. The difficulty in understanding the behaviour of a glove in attenuating or amplifying vibration increases because the biodynamic response of the hand and the dynamic stiffness of the material in the glove also vary according to the frequency of vibration as discussed previously.

Previous studies have investigated the transmissibility of several anti-vibration gloves to the hand (e.g., Rens *et al.*, 1987; Wu and Griffin, 1989; Hewitt, 1998; Paddan and Griffin, 1999; Lazlo and Griffin, 2011). The transmissibility of a glove to the hand is high at low frequencies and gradually decreases as the frequency of the vibration increases (Figure 2-17; Laszlo and Griffin). It is not clear how different gloves can be if they are only compared based on their transmissibilities. Increasing glove dynamic stiffness will increase the glove transmissibility to the hand (e.g., O'Boyle and Griffin, 2004), so it is expected that at frequencies greater than the resonance, a glove with greater transmissibility than another glove would have greater dynamic stiffness than the other

glove, assuming the dynamic response of the hand remains unchanged when the glove changes.

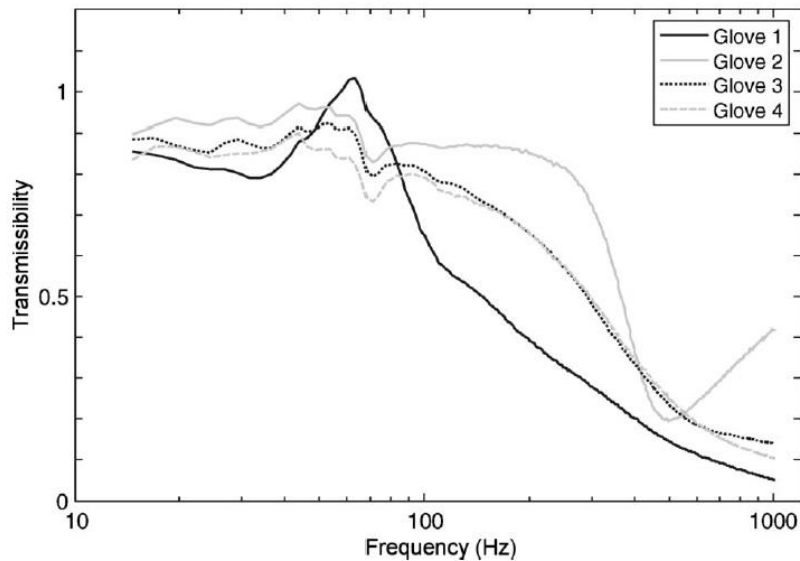


Figure 2-17 Transmissibility of several gloves to the palm of the hand (Laszlo and Griffin, 2011).

2.3.1.2 Magnitude of vibration

The transmissibility of a glove to the hand can be influenced by the magnitude of vibration (Figure 2-18; Wu and Griffin, 1989; Laszlo and Griffin, 2011). It was suggested that the effects of the vibration magnitude are small and mostly apparent at low frequencies (Laszlo and Griffin, 2011). If the effects of vibration magnitude on glove transmissibility are observed as in Glove 4 in Figure 2-18, it is expected to be predominantly caused by the changes in dynamic response of the glove material when the vibration magnitude is varied: the effect of vibration magnitude on the dynamic response of the hand is small and can be ignored at frequencies greater than 100 Hz (Marcotte *et al.*, 2005).

2.3.1.3 Direction of vibration

There are studies that investigated how vibration is transmitted to the hand in three vibration directions (e.g., Welcome *et al.*, 2015) but there is no systematic study that investigated the effects of vibration direction on glove transmissibility to the hand (i.e., measuring apparent mass of the hand, glove dynamic stiffness, and glove transmissibility).

Using previously measured impedance of the hand, the effects of vibration direction can be indicated (i.e., from the understanding of a single degree-of-freedom model) and be

assessed (i.e., this is assuming that the material dynamic stiffness remains unchanged when the vibration direction is varied; see Section 2.2.1.3 for the impedance of the hand in different vibration direction). Previously, there are contradictory findings of the effects of vibration direction on the dynamic response of the hand at low frequencies.

- If changes in the apparent mass of the hand when changing the vibration direction are similar to those shown in Figure 2-5 (Reynolds, 1977), the transmissibility of a glove material to the hand is expected to be lower in the horizontal direction than in the vertical direction at low frequencies: for a single degree-of-freedom system, the greater the mass, the lower the glove transmissibility at frequencies greater than the resonance frequency. Similarly, the dynamic response of the hand in the horizontal direction is similar with the dynamic response of the hand in vertical direction at high frequencies (Figure 2-8), so the transmissibilities in the horizontal and in the vertical direction are expected to be similar at high frequencies.
- If changes in the apparent mass of the hand when changing the vibration direction are similar to those reported in Figure 2-6 (Burström, 1997), the transmissibility of the glove material to the hand is expected to be lower in the vertical direction than in the horizontal direction at low frequencies but similar at high frequencies.

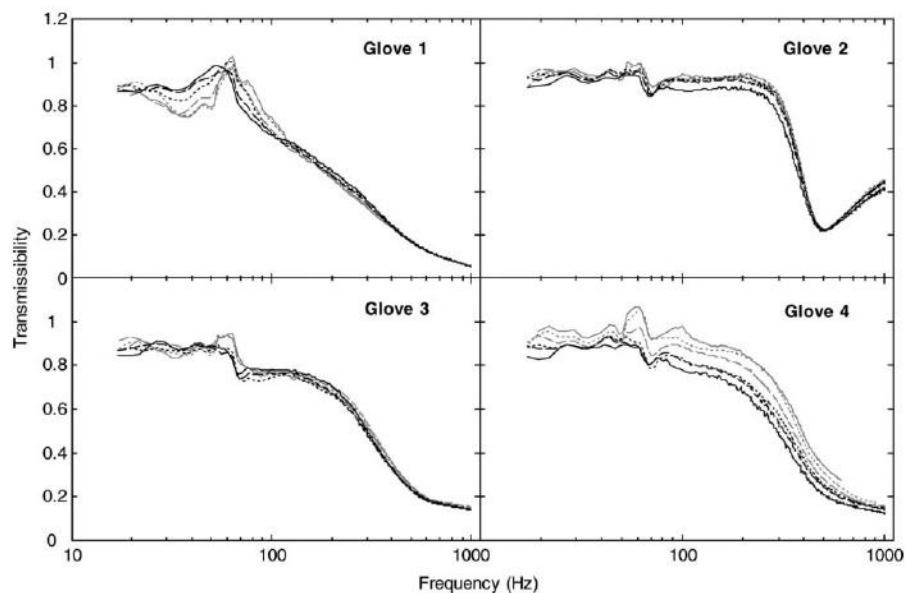


Figure 2-18 Effect of vibration magnitude on the transmissibility of the gloves to the hand (— 0.25 ms^{-2} r.m.s.; . . . 0.5 ms^{-2} r.m.s.; - - - 1 ms^{-2} r.m.s.; . . . 2 ms^{-2} r.m.s.; - - - 4 ms^{-2} r.m.s.; — 8 ms^{-2} r.m.s.; Laszlo and Griffin, 2011).

2.3.1.4 Location of measurement

Glove transmissibility to the fingers at frequencies less than 100 Hz is near to unity (Welcome *et al.*, 2014). Glove transmissibility to the fingers increases with increasing frequency of vibration at frequencies greater than 100 Hz (Figure 2-19; Welcome *et al.*, 2014). It is expected that the transmissibility of a glove to the palm of the hand is less than the transmissibility to the finger at frequencies greater than the resonance, considering the greater apparent mass at the palm than at the fingers (Concettoni and Griffin, 2009).

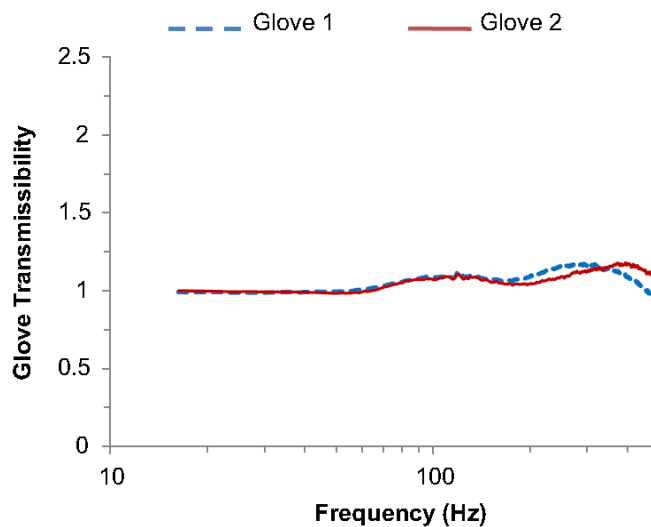


Figure 2-19 Overall mean transmissibility of two gloves at the tip of two fingers (index and middle fingers; Welcome *et al.*, 2014).

2.3.1.5 Arm posture

If material dynamic stiffness remains unchanged when the posture of the arm is changed, glove transmissibility will only be affected by a change in the dynamic response of the hand due to the change in arm posture. The dynamic response of the hand is influenced by the posture of the arm at frequencies less than 30 Hz (Burström, 1997, Aldien *et al.*, 2006, Adewusi *et al.*, 2012). It is therefore expected that if the posture of the arm is changed, glove transmissibility will change at frequencies less than about 30 Hz. However, the transmissibility of gloves to the hand was found to be changed at all frequencies of vibration from 10 to 210 Hz when arm posture was varied (Wu and Griffin, 1989; Figure 2-20) although that it was measured at the knuckle. The frequency of the resonance in the glove transmissibility increases as the arm angle increases from 0° to 30° and from 60° to 90° and decreases as the arm angle increases from 30° to 60° (i.e.,

the resonance frequencies occurred at 100 Hz, 122 Hz, 98 Hz and 135 Hz for the 0°, 30°, 60°, 90° arm angle, respectively; Wu and Griffin, 1989).

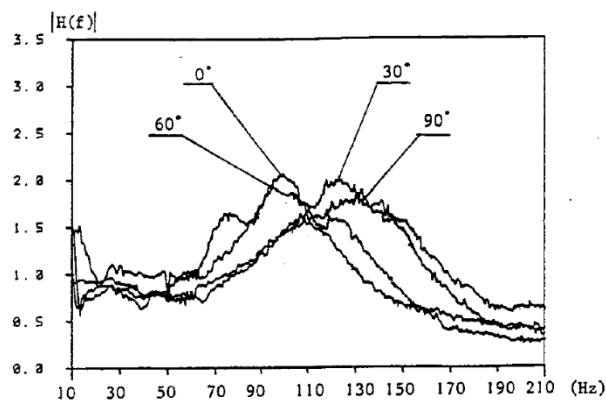


Figure 2-20 Effect of arm angle on the transmission of vibration through gloves to the hand: from handle to knuckle (Wu and Griffin, 1989).

Using an arm support can be appropriate for providing support around the strained area. However, it was previously reported that the use of wrist support (forearm support) can increase the transmission of vibration through gloves to the hand (Chang *et al.*, 1999). It is expected that the use of wrist support will reduce the influence of the forearm and the upper-arm on the driving-point response of the hand thus, increasing the vibration transmission through gloves to the hand (i.e., if the dynamic system of the hand and the glove is assumed to be similar to a single degree-of-freedom system).

2.3.1.6 Contact force

In a systematic study, the apparent mass at the palm and the dynamic stiffness of several glove materials were found to increase with increasing contact force (O'Boyle and Griffin, 2004). The increases in the apparent mass at the palm and in the material dynamic stiffness resulted in a slight increase in the transmissibility of the glove material as the contact force increased (Figure 2-21; O'Boyle and Griffin, 2004).

In a separate study, increasing the contact force increased glove transmissibilities to the hand at all frequencies from 20 to 1000 Hz (Figure 2-22; Laszlo and Griffin, 2011). It has been observed previously that the dynamic response of the hand and the dynamic stiffness of glove material are expected to increase with increasing contact force (O'Boyle and Griffin, 2004). Increasing the apparent mass of the hand will reduce glove transmissibility at frequencies greater than the resonance whilst increasing the dynamic stiffness of glove material will increase glove transmissibility at frequencies greater than the resonance. Therefore, it is expected that the effect of contact force on glove

transmissibility as observed in Figure 2-22 is predominantly due to changes in the dynamic stiffness of the glove material rather than the dynamic response of the hand.

2.3.1.7 Contact area

The effects of contact area on the biodynamic response of the hand and on the dynamic stiffness of glove material have been discussed previously (see Section 2.2.1.4 and 2.3.1). The greater the area of contact, the greater the apparent mass of the hand at high frequencies. Similarly, the greater the area of contact, the greater the glove dynamic stiffness (i.e., assuming the glove material is linear). An increase in contact area may increase glove transmissibility at frequencies greater than the resonance (i.e., due to the increase in dynamic stiffness) or decrease glove transmissibility at frequencies greater than the resonance (i.e., due to the increase in the apparent mass of the hand). However, there is no systematic study investigating the effects of contact area on glove transmissibility.

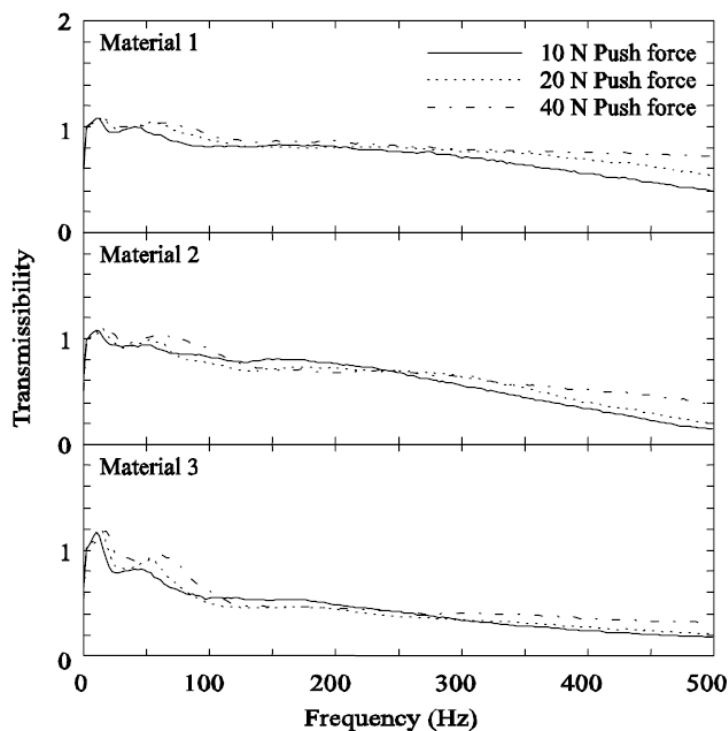


Figure 2-21 Transmissibility of three materials to the palm of the hand with different contact force (O'Boyle and Griffin, 2004).

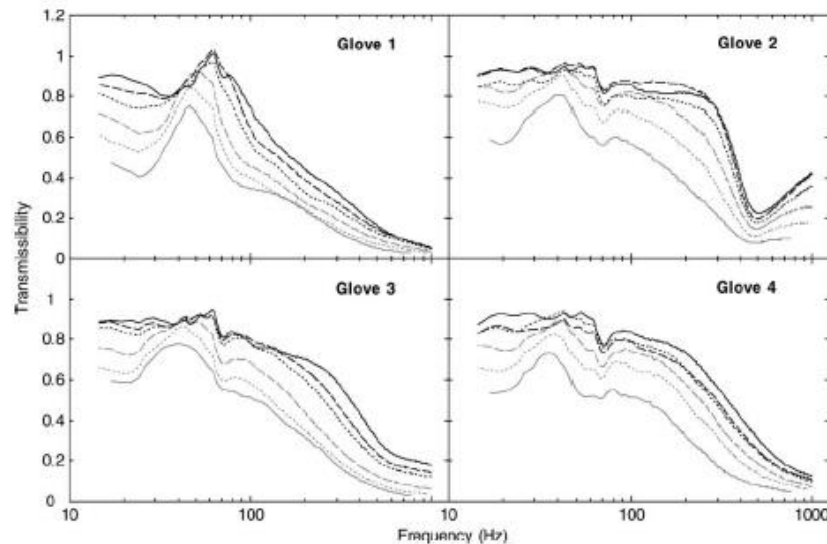


Figure 2-22 Effect of push force on the transmissibility of four gloves as a function of frequency with 2.0 ms⁷² r.m.s. vibration (means for 12 subjects: — 5 N; 10 N; - - - - 20 N; · · · · · 40 N; — — — 50 N; — 80 N; Laszlo and Griffin, 2011).

2.3.1.8 Material thickness

It is expected that increasing the material thickness will reduce its dynamic stiffness (i.e., assuming that the material behaviour is similar to the Kelvin Voigt viscoelastic model, the effects of doubling the thickness of a glove material can be represented by adding a damper and a spring on top of the original single spring and damper, causing the effective stiffness and damping to be reduced). If the material dynamic stiffness is decreased, the resonance frequency in the glove transmissibility is expected to decrease. This will also reduce the transmissibility at frequencies greater than the resonance. It was indicated from previous study that the transmissibility of a glove to the hand at frequencies greater than the resonance decreases with increasing material thickness, although the measurement was obtained at the knuckle (Figure 2.23; Wu and Griffin, 1989).

2.3.1.9 Frequency weighting

International Standards ISO 5349-1:2001 and ISO 5349-2:2002 suggest the use of frequency weighting, W_h , when assessing vibration transmitted to the hand (see Section 2.5.1 for details of the standard). The frequency weighting can affect the glove isolation effectiveness (i.e., the glove isolation effectiveness is calculated based on the r.m.s. acceleration). With frequency weighting, the effectiveness of a glove in isolating the vibration of 10 gloves was about the same (Figure 2-24; Griffin, 2010). Without the

frequency weighting, the glove isolation effectiveness varied across the same 10 gloves (Figure 2-24; Griffin, 2010).

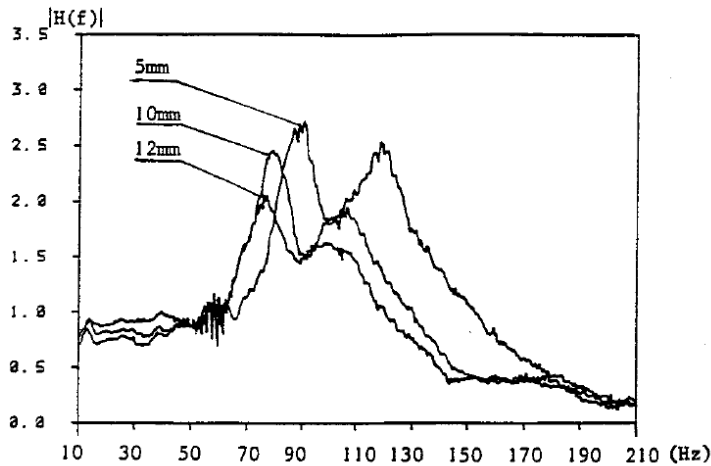


Figure 2-23 Effect of material thickness of a glove on the transmissibility of the glove to the hand (Wu and Griffin, 1989)

2.4 International Standards

2.4.1 ISO 5349-1:2001 and ISO 5349-2:2002

International Standard ISO 5349 specifies general requirements for measuring and reporting hand-transmitted vibration exposures (ISO 5349-1:2001) and practical guidance for measuring hand-transmitted vibration at the workplace (ISO 5349-2:2002). In order to characterize an exposure to vibration, the standard requires consideration of factors that can influence the effects of vibration transmitted to the hand:

- frequency spectrum of the vibration,
- magnitude of the vibration,
- duration of exposure, and
- cumulative exposure

The severity of a vibration stimulus is quantified through the vibration daily exposure. In assessing vibration transmitted to the hand and the fingers, the ISO 5349:2001 suggests the use of weighting, W_h (Figure 2-25). Using the frequency weighting W_h in assessing the magnitude of a vibration, the daily vibration exposure to a hand can be calculated as 8-hour energy equivalent acceleration using Equation 2.7.

$$a_{hv(eq,8h)} = A(8) = a_{hv} \sqrt{\frac{T}{T_0}} \quad (2.7)$$

where a_{hv} is the frequency-weighted r.m.s. acceleration, T is daily duration of exposure and $T_0 = 8$ hours.

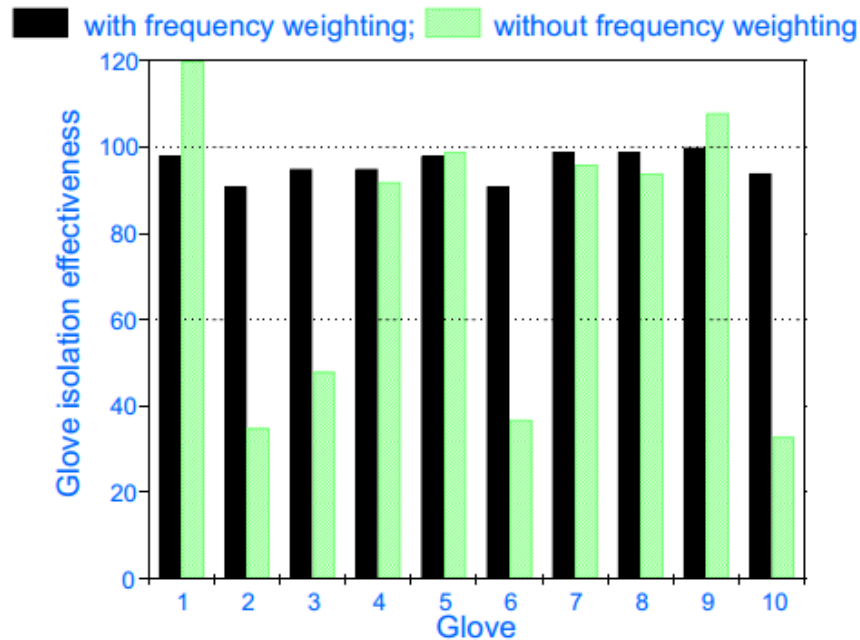


Figure 2-24 Average glove isolation effectiveness of 10 gloves used with a nutrunner (Griffin, 2010).

Vibration exposures with an $A(8)$ greater than 5.0 ms^{-2} r.m.s. should be avoided as stated in the European Union Physical Agents (vibration) Directive on handling vibration at the workplace (EU Directive, 2002).

2.4.2 ISO 10819:2013, Method for the measurement and evaluation of the vibration transmissibility of gloves at the palm of the hand

International Standard 10819 specifies methods for measuring and evaluating the performance of a glove in reducing vibration to the hand. It was first published in 1996 and revised in 2013 to address several of its flaws. The standard is used as the method to assess glove effectiveness in isolating vibration before it can be considered an anti-vibration glove.

The standard requires a specifically built cylindrical handle with two force transducers attached to it to measure the grip force and the feed force. An accelerometer is attached inside the handle to measure the input vibration. The vibration at the hand-glove interface

is measured using a miniature accelerometer embedded in a wooden palm adapter that is placed at the palm interface as shown in Figure 2-26. The mass of the wooden adapter including the mass of the accelerometer shall not exceed 15 grams.

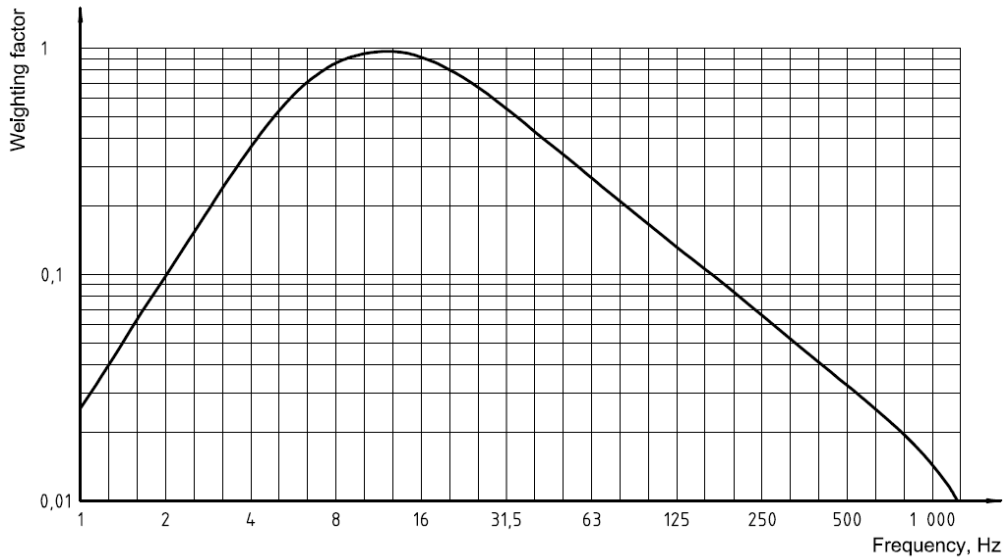


Figure 2-25 Frequency weighting W_h with band-limiting (ISO 5349-1:2001).

Five subjects are required with hand sizes between 7 and 10 (i.e., according to the EN 420). Subjects stand upright and grip the handle with a push force of 50 N and a grip force of 30 N with his or her forearm directed to the axis of the vibration (Figure 2-27). The palm adapter is placed at the palm interface. Vibration is generated at a magnitude of 4.9 ms^{-2} r.m.s. weighted (W_h) acceleration. The vibration is directed to the subject's hand horizontally. The transmissibility of the glove is calculated as the complex ratio of the output acceleration measured in the palm adapter, to the input acceleration measured on the cylindrical handle. A glove can be considered as an anti-vibration glove if it has a transmissibility less than 0.9 at frequencies between 25 and 200 Hz and transmissibility of less than 0.6 at frequencies between 200 and 1250 Hz. However, the glove that passes the test specified in ISO 10819 may not be beneficial to the person who wears the glove because the standard has several flaws: the glove transmissibility measured according to the standard may not indicate the actual performance of the glove in working conditions (Table 2-1; Griffin, 1998).

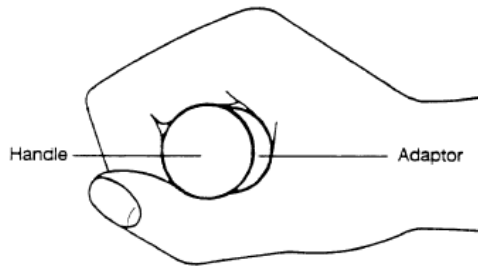


Figure 2-26 The position of the hand and the adapter during the measurement of the glove transmissibility according to the standard ISO 10819:2013 (upper figure). Picture of a wooden adapter with accelerometer embedded in it used in the standard ISO 10819:2013 (lower figure).

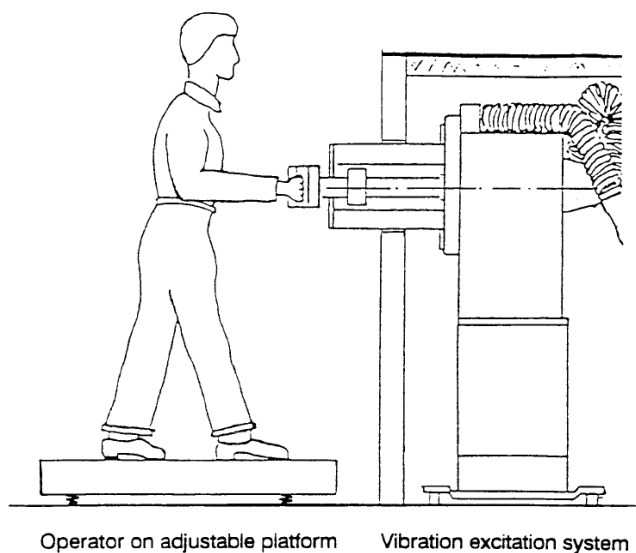


Figure 2-27 Equipment setup for the measurement of the glove transmissibility as specified in International Standard ISO 10819 (2013).

Table 2-1 Several flaws of the standard as discussed by Griffin (1998)

General	Vibration spectra on tools vary greatly, hence using one spectra cannot represent spectra for all tools.
	It may possible that the glove that fails the test provide better attenuation than the glove that passes the test on a particular tool at a particular frequency of vibration.
	Subject variability may influence the measurements especially at high frequencies of vibration.
	The repeatability of tests performed in different laboratory is not known.
	No measurement at the fingers is required.
Assumptions	It is assumed that the palm adapter will not alter the glove-hand dynamics.
	It is assumed that the hand and arm posture do not sufficiently change hand impedance and thus the transmissibility to the palm of the hand.

2.4.3 ISO 13753:2008, Method for measuring the vibration transmissibility of resilient materials when loaded by hand-arm system

International standard ISO 13753:2008 was published as a guide for assessing vibration transmissibility of a material when it is loaded with the hand-arm system. Instead of requiring a human subject, the standard predicts the transmissibility of the material to the hand using the measured material impedance and provided mechanical impedance of the hand. In the standard, the material that is considered to be used in a glove is laid on a flat plate on a shaker with a mass (i.e., 2.5 kg) placed on top of the material (Figure 2-28). The output acceleration measured on the mass and the input acceleration measured on the input plate are recorded during a vibration exposure and the transmissibility of the material is determined as the complex ratio of the output acceleration to the input acceleration.

Assuming that the material has negligible mass, the impedance of the material is given by:

$$m\ddot{x}_2 = -z_M(\dot{x}_2 - \dot{x}_1) \quad (2.8)$$

$$Z_M = \frac{j\omega m}{\frac{a_1}{a_2} - 1} \quad (2.9)$$

where z_m is the impedance of the material, ω is angular speed, m is the mass of about 2.5 kg, a_1 is the input acceleration and a_2 is the output acceleration.

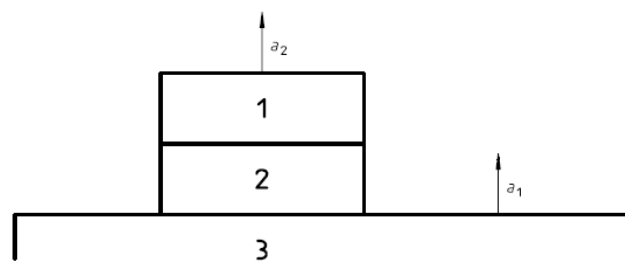
The transmissibility of the material to the hand will then be predicted using a hand-arm impedance model (Figure 2-29).

$$z_H \dot{x}_2 = -z_M (\dot{x}_2 - \dot{x}_1) \quad (2.10)$$

$$T(f) = \left| \frac{\dot{x}_2}{\dot{x}_1} \right| = \left| \frac{z_M}{z_H + z_M} \right| \quad (2.11)$$

where $T(f)$ is the transmissibility of the material to the hand, z_H is the impedance of the hand, \dot{x}_1 is the input acceleration and \dot{x}_2 is the output acceleration.

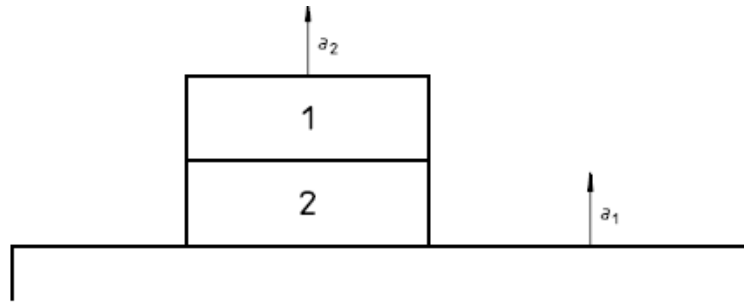
The lower the predicted material transmissibility to the hand, the better the material is in providing vibration attenuation when it is used in a glove. It is claimed that this method will enable rank ordering materials for gloves in terms of their effectiveness in reducing vibration to the hand, but it will not necessarily predict glove transmissibility fabricated from these materials (ISO 13753:2008). A study that investigated the effectiveness of the rank ordering materials' for gloves using ISO 13753 has found that a glove that predicted greater vibration attenuation than the other gloves may not provide better attenuation than the other gloves when tested according to the ISO 10819:1996 (Koton *et al.*, 1998).



Key

- 1 Mass m
- 2 Resilient material
- 3 Shaker

Figure 2-28 Measurement setup as specified in the ISO 13753:2008.



Key

- 1 Hand-arm impedance Z_H
- 2 Resilient material of impedance Z_M

Figure 2-29 Model of the hand-arm impedance (ISO 13753:2008).

2.4.4 ISO 10068:2012, Mechanical impedance of the human hand-arm system at the driving point

The mechanical impedance of the human hand-arm system can provide information of the overall motion at a location in contact with the vibrating surface. International Standard 10068:2012 provides data of the measured mechanical impedance of the hand at the driving point in the x-, y-, and z-axis directions of a basicentric coordinate system for the hand (Figure 2-30).

The mechanical impedance of the hand is suggested to be used together with the impedance model specified in ISO 13753:2008 to predict the transmissibility of a glove to the hand. The standard also provides several proposed lumped parameter models of the hand and the arm to be used to study the motion of the hand and the arm. Some of the models are presented in Section 2.7.2.

2.5 Vibration emitted by powered tools

There are many types of powered tool available in the market. Each of the powered tools vibrates differently (Figure 2-31 and 2-32). It may not be possible to have a single spectrum to represent vibration emitted by all vibrating tools. It is also not possible to have a single set of hand-arm postures to represent the way a person handles the many types of vibrating tools. Although the effects of vibration magnitude are small and may only be apparent at low frequencies (Laszlo and Griffin, 2011), it does not mean that this factor can be excluded when assessing the performance of a glove in attenuating vibration. Vibration emitted by powered tools contains frequency components that may differ from one tool to another. Some gloves may provide better vibration attenuation

than other gloves at low frequencies compared to high frequencies. Analysing the frequency component of vibration emitted by a tool can provide information to assist in the development of better anti-vibration gloves (i.e., develop a glove that can reduce vibration at a specific range of vibration frequencies).

Figure 2-32 shows one-third octave band spectra of 20 powered tools. The un-weighted spectra show vibration emitted by powered tools is generally at high frequencies (i.e., at frequencies greater than 100 Hz). The weighted spectra, on the other hand, show the importance of the vibration at low frequencies: vibration emitted by powered tools is generally at frequencies between 25 and 250 Hz. The weighted vibration has reduced the importance of measuring vibration transmission to the hand at frequencies greater than 250 Hz. An anti-vibration glove should be able to attenuate vibration at frequencies between 25 and 250 Hz in order to benefit the person who is wearing the glove.

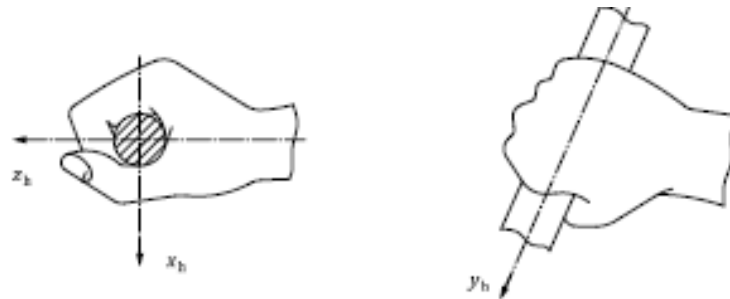


Figure 2-30 Basicentric coordinate system of the hand (ISO 10068:2012).

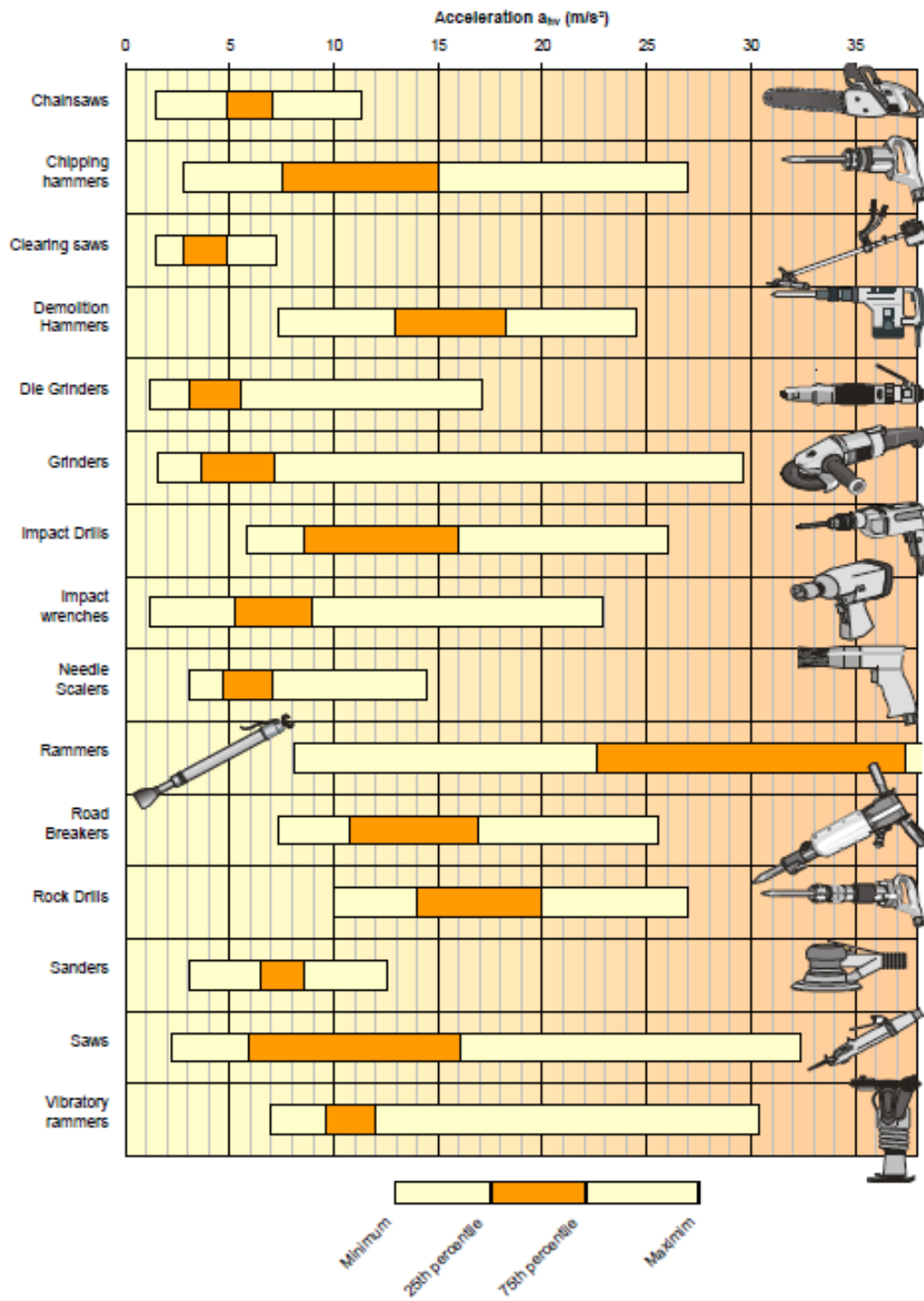


Figure 2-31 Examples of vibration magnitudes for common tools (Griffin *et al.*, 2006).

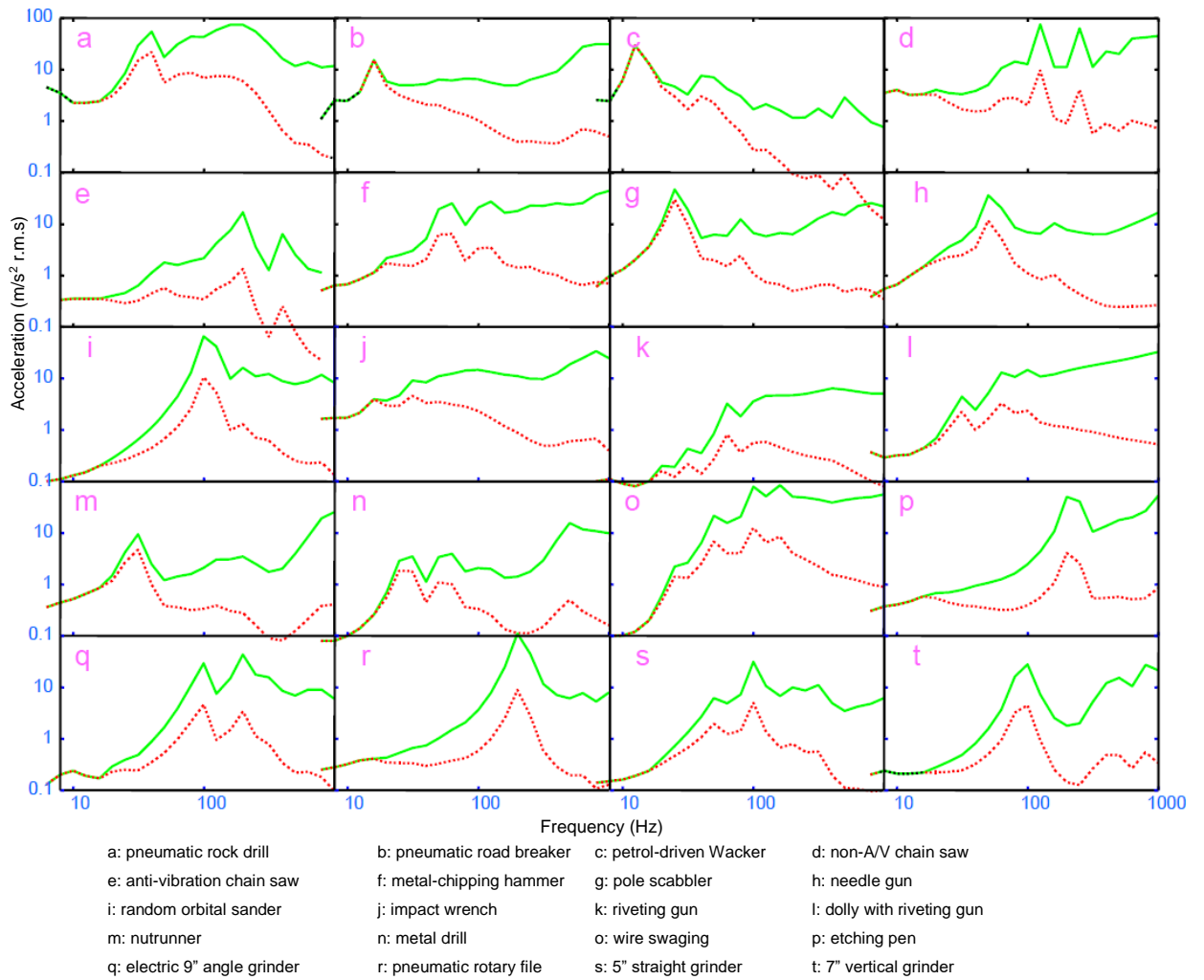


Figure 2-32 One-third octave band spectra of 20 powered hand tools (solid lines: un-weighted, dotted lines: weighted; Griffin 1997).

2.6 Biodynamic modelling of the hand and the fingers to predict glove transmissibility to the hand and to the fingers

2.6.1 Mechanical impedance model of the hand

A mechanical impedance model of the human body was first used by Fairley and Griffin in 1986 to predict the transmissibility of a seat. It was later adopted to be used to predict glove transmissibility to the hand (O'Boyle and Griffin, 2004). The impedance model used to calculate the transmissibility of glove material to the hand is shown in Figure 2-33.

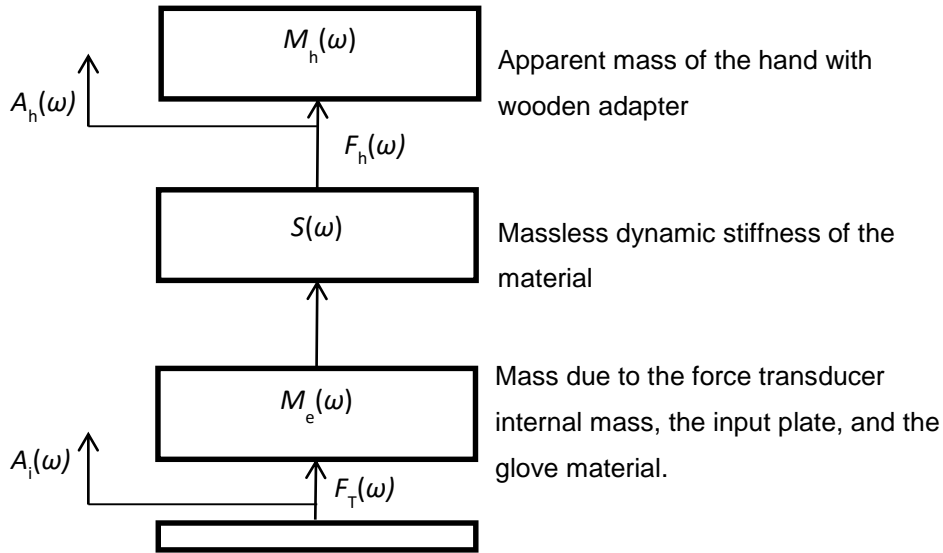


Figure 2-33 The impedance model of the hand and material (O'Boyle and Griffin, 2004).

During the measurement of glove material transmissibility, the apparent mass of the hand or the finger and the dynamic stiffness of the material are:

$$\text{Apparent mass of the hand} = M_h(f) = F_h(f)/A_h(f) \quad (2.12)$$

$$\text{Dynamic stiffness of material} = S(f) = F_h(f)/(\omega^2(A_h(f) - A_i(f))) \quad (2.13)$$

where $F_h(f)$ is the force transmitted to the hand or by the material, $A_h(f)$ is the acceleration at the hand, $A_i(f)$ is the acceleration measured at the input plate, and $\omega^2(A_h(f) - A_i(f))$ is the relative displacement of the material.

Equations 2.12 and 2.13 can be expressed in terms of the force transmitted by the material to the hand:

$$M_h(f)A_h(f) = \omega^2 S(f)(A_h(f) - A_i(f)) \quad (2.14)$$

Thus, the predicted transmissibility of the material to the hand is:

$$\frac{A_h(f)}{A_i(f)} = \frac{\omega^2 S(f)}{\omega^2 S(f) - M_h(f)} = T_h(f) \quad (2.15)$$

The mechanical impedance method uses the measured apparent mass of the hand and the measured dynamic stiffness of the glove material to predict the transmissibility of the glove material to the hand. The model may not be able to explain the mechanisms involved in the hand response to vibration or how a glove transmissibility is influence by

a factor, but it is expected to be able to predict the transmissibility of the glove material better than using lumped parameter models of the hand and the glove.

A study was conducted to predict the effect of contact force using the mechanical impedance model (O'Boyle and Griffin 2004). The predicted transmissibilities of several materials to the hand using the mechanical impedance model were similar to the transmissibility measured experimentally (Figure 2-34). However, any limitations of the method were not explored and it requires further investigations before it is suggested for use widely as a method to assess glove transmissibility.

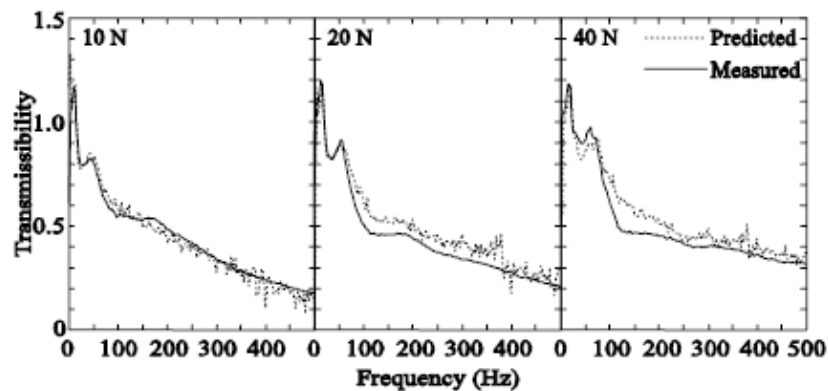


Figure 2-34 Predicted and measured transmissibility of a material to the palm of the hand with different push forces (O'Boyle and Griffin, 2004).

2.6.2 Lumped parameter models of the hand

Lumped parameter models are being used widely to develop hand models and understand the motion of the hand exposed to vibration. This method uses masses to represent the hand and the arm, connected by translational or rotational springs and dampers. These masses are not necessarily anatomically representative.

Figure 2-35 shows a 7 degree-of-freedom model of the hand and the glove (Dong *et al.*, 2009), developed with masses that correspond to several parts of the human body and a glove (i.e., fingers, finger tissues, palm, palm tissues, upper-arm, mass of the glove at the fingers interface and at the palm interface). The model has the posture of the hand similar to that employed in International standard ISO 10819:1996 (i.e., posture of the hand in ISO 10819:1996 is similar with posture of the hand in ISO10819:2013). The fitted transmissibility using the 7 degree-of-freedom model was similar to the measured transmissibility at low frequencies but underestimated the measured transmissibility at frequencies greater than about 200 Hz (Figure 2-36).

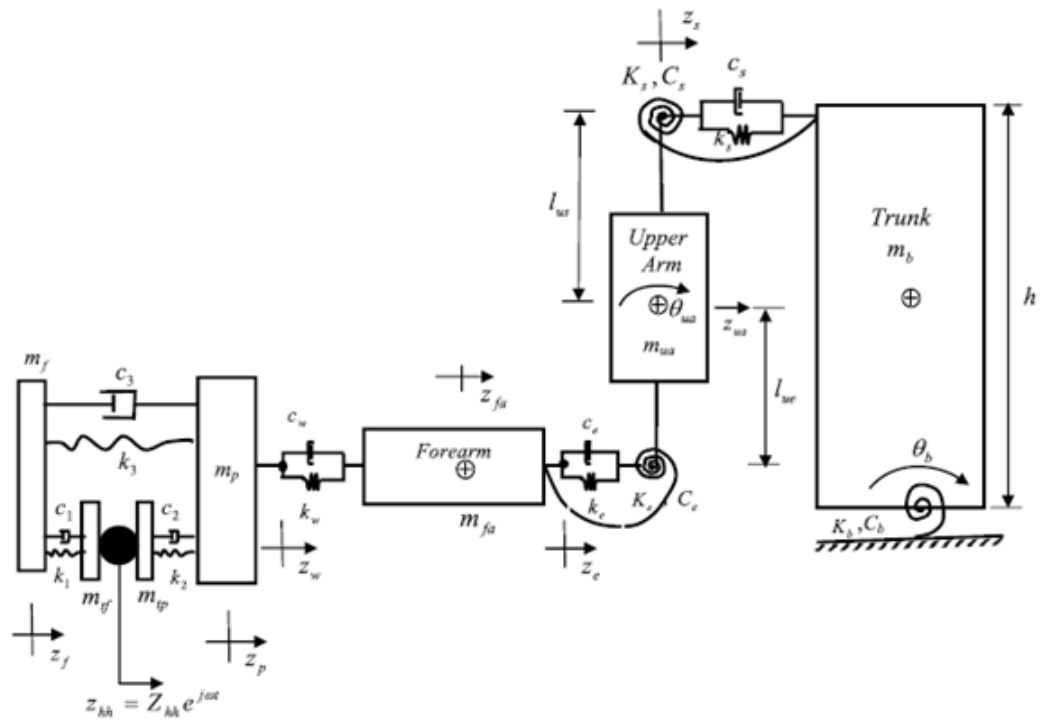


Figure 2-37 A seven degree-of-freedom model of the hand in bent arm posture (Adewusi *et al.*, 2012).

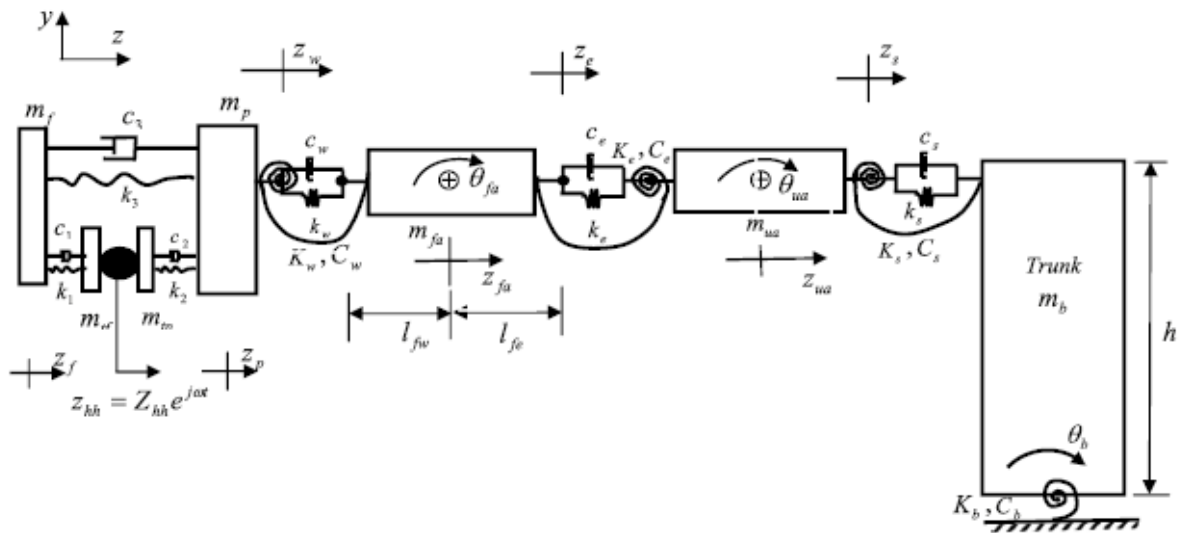


Figure 2-38 A seven degree-of-freedom model of the hand in extended arm posture (Adewusi *et al.*, 2012).

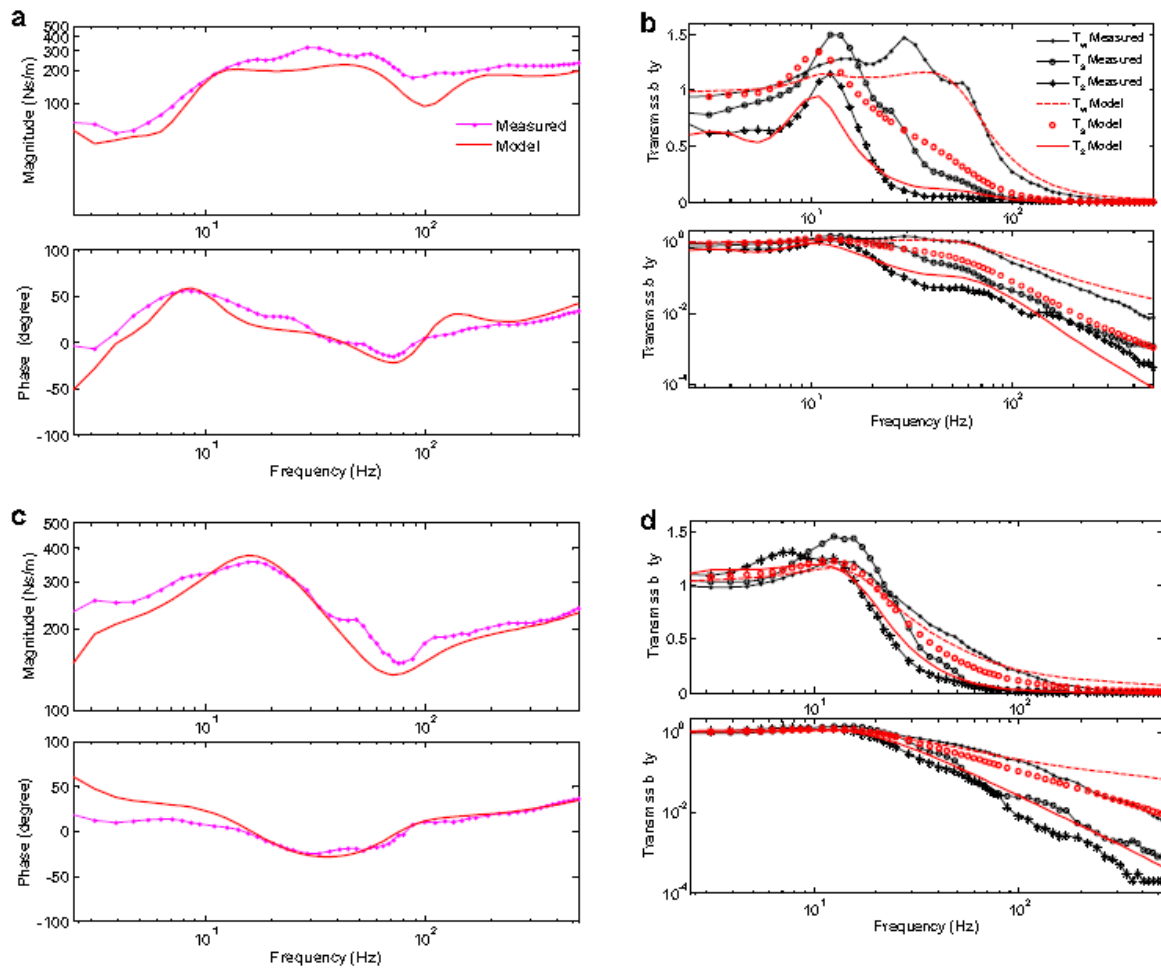


Figure 2-39 Comparisons of the measured responses with the responses of models derived from combined impedance and transmissibility responses: (a) impedance response in the bent-arm posture; (b) transmissibility responses in the bent-arm posture; (c) impedance response in the extended arm postures; (d) transmissibility responses in the extended arm postures; (Adewusi *et al.*, 2012).

2.7 Discussion and Conclusions

Previous sections of this chapter have discussed and shown that the transmission of vibration through gloves to the hand can be influenced by many factors (i.e., contact area, contact force, vibration magnitude, vibration direction, hand-arm posture, frequency of vibration). There are grey areas (i.e., gaps) in the understanding of how these factors affect glove transmissibility to the hand, even though they have been investigated in many studies.

2.7.1 Apparent mass of the hand and the fingers

Studies have shown how factors (e.g., contact area, push force) can influence the dynamic response of the hand (i.e., apparent mass of the hand). There is still no clear evidence of the mechanisms of how those factors affect the dynamic response of the hand.

- i. It was suggested that at high frequencies, the apparent mass of the hand predominantly depends on the mass close to the vibration driving-point (i.e., mass of the hand tissues; e.g., Dong *et al.*, 2009). If increasing the area of contact increases the mass of the hand tissues in contact with the vibrating surface, increasing the area of contact will increase the apparent mass of the hand at high frequencies. Although the effects of contact area on the dynamic response of the hand are shown in previous studies (see Section 2.2.1.4), it is not clear whether it is due to the increase in the mass of the hand tissues.
- ii. There are contradictory findings of the effects of vibration magnitude on the dynamic response of the hand, as discussed in Section 2.4.1.2. In those studies, the effects of vibration magnitude were investigated in a complex condition of the hand and the arm (e.g., hand gripping cylindrical handle: the effects of shear vibration on material dynamic stiffness and on the dynamic response of the hand are not clearly understood). Measurement in this condition of the hand and the arm may not provide clear understanding of the effects of vibration magnitude on the dynamic response of the hand.
- iii. Although there are studies that investigated the effects of arm posture, there is no systematic study that investigated the effects of arm support on the hand's dynamic response. With different arm posture (i.e., bent-arm and extended-arm posture), the apparent mass of the hand reduces at frequencies less than 30 Hz (e.g., Besa *et al.*, 2007; Adewusi *et al.*, 2012). With arm support, the influence of the lower-arm and the upper-arm on the apparent mass of the hand is expected to be reduced because the lower and the upper arm are now supported by the arm support. The influence of lower and upper arm cannot be clearly seen when changing the arm angle as studied previously (i.e., there is a possibility that the lower-arm can still affect vibration at frequencies greater than 30 Hz). Investigating the effects of arm support will also provide indication of the influence of the hand and the fingers on hand dynamic response that will help in the development of a better lumped parameter model of the hand and the arm.

- iv. There are few systematic studies that investigated the apparent mass of the hand at frequencies less than 10 Hz (e.g., Adewusi *et al.*, 2012). It has been reported that the posture of the arm affects the apparent mass at frequencies less than 30 Hz (see Section 2.2.1.7), indicating the influence of the lower and the upper arm on the apparent mass is at frequencies less than 10 Hz. Study of the dynamic response of the hand at frequencies less than 10 Hz is needed to provide data for modelling of the biodynamic response of the hand.
- v. It is difficult to investigate the dynamic response of the fingers because of the complexity of the method of measurement. Each of the fingers could have a different response to vibration. There are a few systematic studies that investigated the effects of contact area (e.g., Mann and Griffin, 1996), and contact force (e.g., Mann and Griffin, 1996) on the dynamic response of the fingers.

2.7.2 Dynamic stiffness of the material of a glove

Viscoelastic materials such as those used in glove materials are non-linear and may be too complex to be predicted. Generally, increasing the dynamic stiffness of the material will increase the glove transmissibility at frequencies greater than the resonance (e.g., O'Boyle and Griffin, 2004). Some materials possess relaxation behaviour (i.e., shape memory foam) and the effects of this behaviour on the glove transmissibility when contact area, contact force, and material thickness are varied are not clearly evidenced.

2.7.3 Transmissibility of a glove to the hand

The transmissibility of a glove to the hand depends on two main factors, the dynamic response of the hand, and the dynamic stiffness of the glove materials. Without measuring both the dynamic response of the hand and the dynamic stiffness of the glove materials, the reason for changes in the glove transmissibility to the hand when factors (e.g., contact area, contact force) are varied may not be clear.

- i. Gloves have been investigated as a means of controlling the risks associated with the hand-arm vibration syndrome. In some countries a glove must conform to the requirements of International Standard ISO 10819 (2013) before it can be sold as an 'anti-vibration glove'. A glove that conforms to the standard is not necessarily beneficial and a glove that fails the standard might be beneficial. One of the limitations is that there is no method of measuring

- the transmission of vibration to the fingers, even though the principal disorders caused by hand-transmitted vibration are observed in the fingers.
- ii. Increasing the contact force increases the apparent mass of the hand at frequencies greater than the resonance frequency but the increase in the apparent mass may be small and not greatly affect the transmissibility of gloves (O'Boyle and Griffin, 2004). In a separate study, increasing the contact force significantly increases the glove transmissibility (Laszlo and Griffin, 2011). These contradictory findings do not mean that they have provided wrong conclusions, they may indicate that the reasons for the findings have yet to be explained.
 - iii. International Standard ISO 10819:2013 specifies that the thickness of the material can be equal or greater than 0.58 times of the thickness of the material on the palm. Increasing the thickness of the material will reduce the material stiffness and damping, thus tending to reduce the resonance frequency in the glove transmissibility. Decreasing the thickness of the material will increase the dynamic stiffness of the glove material; thus increasing the resonance frequency of the glove transmissibility. The effect of material thickness on the transmissibility of a glove material to the palm or to the fingers however is yet to be investigated systematically.
 - iv. The dynamic response of the hand increases with increasing contact area (Mann and Griffin, 1996, Marcotte *et al.*, 2005), and so if a material did not change its dynamic stiffness with area, the transmissibility would be expected to decrease with increasing area. In reality, however, increasing the contact area of the glove material will increase the glove dynamic stiffness. This is yet to be investigated systematically.
 - v. It is not clear which of the factors (e.g., contact area, contact force, vibration magnitude, and arm posture) is the predominant factor that affects glove transmissibility to the hand.

2.7.4 Improving the method to predict the transmissibility of a glove to the hand and to the fingers

The currently standardised method for measuring glove transmissibility has many flaws, as discussed in Section 2.5.2. In order to improve the test, it is necessary to address several main flaws. This can be done effectively if the mechanisms of factors influencing the transmission of vibration through gloves to the hand are understood. On the other hand, there are many advantages if the glove transmissibility to the hand can be

predicted (e.g., glove tests may not require human subjects, reducing time for a glove test, improving reliability of the test).

- i. Mechanical impedance methods (see Section 2.7.1) seem to be able to produce reasonable predictions of glove transmissibility to the hand at frequencies from 10 to 500 Hz (O'Boyle and Griffin, 2004). However, there are no studies investigated whether the mechanical impedance model is able to predict glove transmissibility and subject variability in different conditions (e.g., contact area, vibration magnitude, arm posture, location of measurement).
- ii. If the mechanical impedance model of the hand can be used to predict glove transmissibility using the measured apparent mass of the hand and the measured glove dynamic stiffness, it can also be used to predict apparent mass of the hand using the measured glove transmissibility and the measured glove dynamic stiffness.
- iii. Lumped parameter models can provide indications and representations of the motion of the hand and the arm when exposed to vibration. It can also provide understanding of the mechanisms of how factors as discussed in this chapter influence the glove transmissibility. Several models have been developed and proposed to represent the motion of the hand with and without a glove. None of the models is able to provide indications or predictions of the effects of factors (i.e., as discussed in this chapter) on glove transmissibility to the hand. The ability of the proposed models in predicting individual or subject variability is also not known.

2.7.5 The objective of the research

The main objective of this research was to advance understanding of factors influencing the transmission of vibration through gloves to the hand and to the fingers. This was performed by measuring and modelling the biodynamic response of the hand and the fingers, the dynamic stiffness of the material in a glove, and the transmissibility of the glove material to the hand and to the fingers. This research emphasised the effects of contact area, contact force, vibration magnitude, wooden adapter, and arm support. These factors contribute most to the variability in the assessment of an anti-vibration glove.

Other objectives of the research are:

- To develop a model that can predict the transmissibility of a glove to the hand and to the fingers.
- To quantify which factors predominantly influence the transmissibility of a glove to the hand and to the fingers.
- To provide guidance on how to optimize and minimize the transmission of vibration through gloves to the hand and to the fingers.
- To devise methods for improving ISO 10819:2013 and ISO 13753:2008 in their applicability to identification of the effects of gloves.

The main contributions to the new knowledge of this research are:

- This research has shown that the predominant factors that affect the performance of a glove in reducing vibration to the hand are the area of contact and the force applied on the glove material. Several combinations of contact area and contact force are required in order to obtain reliable measures of the performance of a glove in attenuating vibration.
- This research has shown that glove transmissibility to the hand can be predicted using a mechanical impedance model of the hand and the glove. The model can be used to assist the optimisation of glove dynamic response, reduce the time used to assess the performance of a glove, and reduce the need for testing with human subjects.

Chapter 3: Methodology

3.1 Introduction

Glove transmissibility to the hand, the apparent mass of the hand, and the dynamic stiffness of glove materials were measured and analysed to study the effects of material thickness, contact area, contact force, vibration magnitude, and arm condition (i.e., with and without arm support) on glove transmissibility. Glove transmissibility was predicted using a mechanical impedance model and a lumped parameter model (see Chapter 9 for the methods of predicting glove transmissibility using lumped parameter model). Three experiments were conducted in this research as summarized in Table 3-1.

Table 3-1 Experiments conducted in this research

Experiment number	Title of the experiment	Independent variables	Dependent variables
1	Effects of material dynamic stiffness	Material thickness, location of measurement	Apparent mass of the hand, material dynamic stiffness, material transmissibility
2	Effects of contact area and contact force	Contact area, contact force	Apparent mass of the hand, material dynamic stiffness, material transmissibility
3	Effects of vibration magnitude and arm support. Low frequency measurement of hand apparent mass	Vibration magnitude, arm condition, vibration frequency	Apparent mass of the hand, material transmissibility

All experiments were conducted in Laboratory 4 of Human Factors Research Unit, Institute of Sound and Vibration Research, University of Southampton.

3.2 Measuring the apparent mass of the hand

Subjects sat with their arms not otherwise supported and placed the hand (see Table 3-2 for the location of measurement for each experiment), on a wooden adapter (Figure 3-1 and Figure 3-2). The wooden adapter was located on top of an input plate (see Table 3-2 for the size of the input plate). The wooden adapter had the same diameter as the input plate. Subjects were required to push down the wooden adapter with a certain amount of force (see Table 3-2 for the push force). An oscilloscope was located in front of the subjects to provide feedback so that they could monitor the force applied to the input plate. Random vibration (see Table 3-2 for the magnitude of the vibration; frequency-weighted using W_h according to ISO 5349-1:2001) was generated using MATLAB (R2011b) and *HVLab* toolbox (version 1.0 and 2.0).

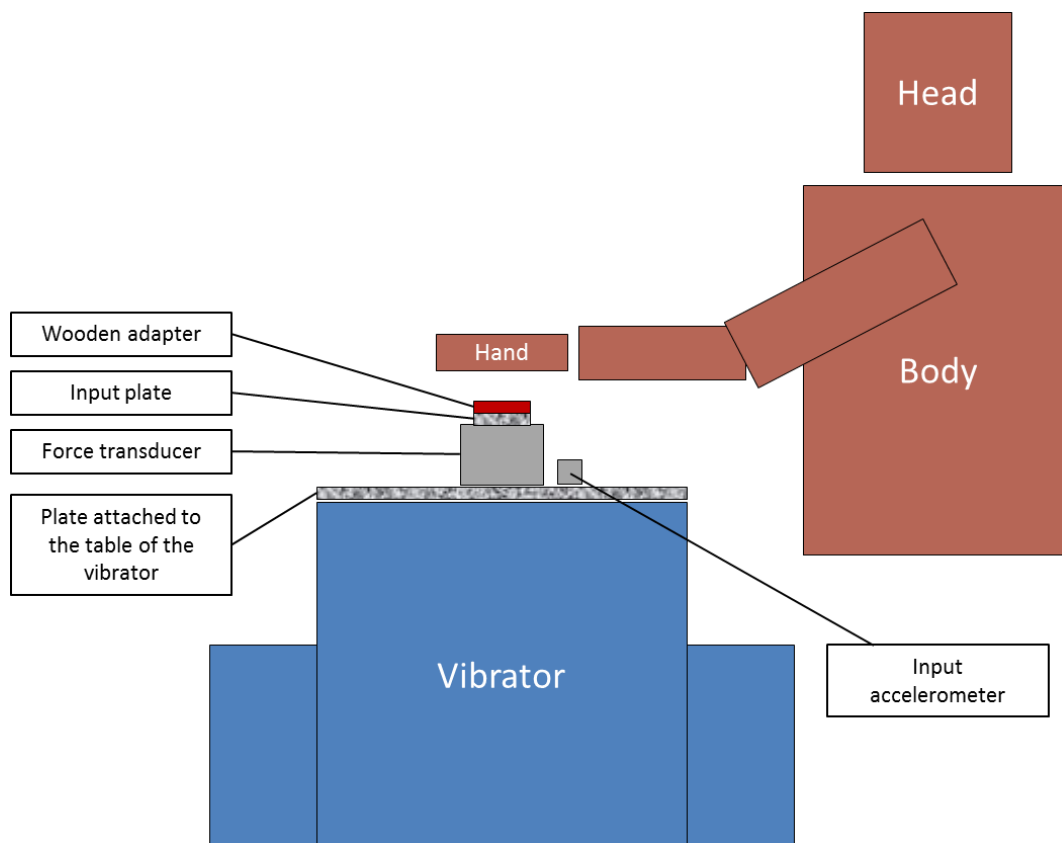


Figure 3-1 Measuring the apparent mass of the hand.

In the first experiment (Equipment 1), the input acceleration was measured using a piezo-electric accelerometer (B&K 4371) secured to a plate attached to the table of a vibrator (i.e., lower plate; Derritron VP4; Figure 3-2). The output dynamic force was measured using a piezo-resistive force transducer (Kulite TC2000 500) secured to the lower plate. The force applied on the input plate was monitored through an oscilloscope connected to the force transducer.

Table 3-2 Details of the independent variables for each of the experiments.

Exp.	Input plate (i.e., contact area)		Wooden adapter		Contact force (N)	Location of measurement	Vibration magnitude (m/s ² r.m.s.)
	Diameter (mm)	Weight (grams)	Diameter (mm)	Weight (grams)			
1	25.0	12	25.0	3	10	Palm of the hand, tip of the index finger	3.24
2	12.5, 25.0, 37.5	1, 12, 20	12.5, 25.0, 37.5	1, 3, 5	10, 15, 20	Palm of the hand, thenar eminence, tip of the index finger	2.00
3	25.0	12	25.0	3	20	Palm of the hand	1, 2, 4

In the second and the third experiment (Equipment 2), the input acceleration and the output dynamic force were measured using a piezo-electric impedance head (B&K 8001) attached to a piezo-resistive force transducer (Kistler 4576A; Figure 3.2). The piezo-resistive force transducer (Kistler 4576A) used to measure static force was connected to an oscilloscope to allow subjects to monitor the force applied to the input plate, similar to the first experiment. The force transducer (Kistler 4576A) was secured to a lower plate attached to the table of a vibrator (Derritron VP30)

The output acceleration in all three experiments (i.e., vibration at the hand interface) was measured using a miniature accelerometer (B&K 8307 used in Experiment 1, and B&K 4374 used in Experiments 2 and 3) embedded in a wooden adapter. The wooden adapter was placed on top of the input plate.

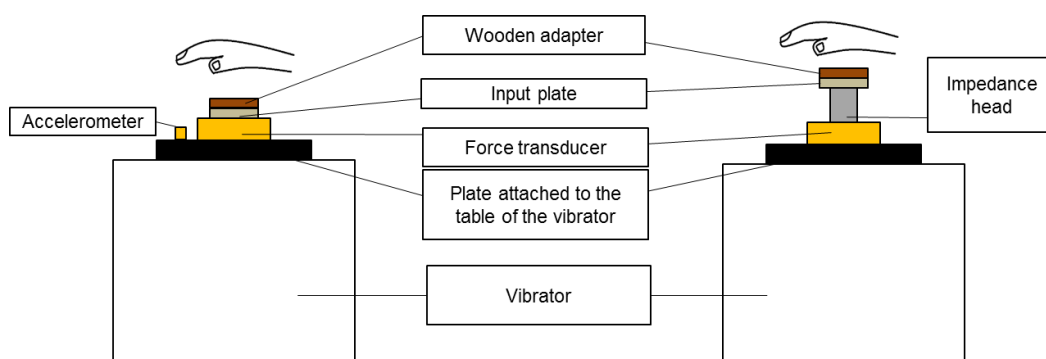


Figure 3-2 Equipment setup for the measurement of the apparent mass of the hand; Left: equipment used in Experiment 1, Right: equipment used in Experiment 2 and 3.

The signals from the input acceleration, output dynamic force and output acceleration were transferred to a computer via a data acquisition device (i.e., National Instrument NI-USB 6211 16bit).

3.3 Measuring the transmissibility of the material to the hand

Procedures similar to those used to measure hand apparent mass were repeated to measure the transmissibility of glove materials to the hand. The samples of glove materials were placed on the input plate and below the wooden adapter of the same diameter, with the hand placed on the wooden adapter exerting a downward force.

The material transmissibility was measured using the same random vertical vibration used to measure the apparent mass of the hand.

The order of measuring apparent mass and material transmissibility of all sizes of contact area, contact force, location of measurements and the three materials was randomised.

3.4 Measuring the dynamic stiffness of the material

An 'indenter rig' was used to determine the dynamic stiffness of the glove material.

In the first experiment, a piezo-resistive force transducer (Kistler 4576A) with a plate was attached to a bearing located at the upper part of the rig (Figure 3-3). Another plate of the same size was secured to the vibrator platform. The samples of glove materials were placed between the two plates. The plates and the glove materials had the same diameter (i.e., the diameter of the plates were the same as the diameter of the input plate in the measurement of hand apparent mass). The materials were subjected to a preload force (i.e., the preload force was similar to the force used when measuring the hand apparent mass) by turning the preload screw. An accelerometer (B&K 4371) was attached to the lower plate to measure the input vibration generated by a vibrator (Derritron VP4).

The equipment setup for the second and the third experiment was similar to the first experiment except that the dynamic force transmitted by the material to the upper part of the indenter rig was measured using an impedance head (Figure 3-4; B&K 8001). The impedance head with an input plate was secured to the force transducer. The static force was measured using the force transducer (Kistler 4576A).

A 10-s period of random vertical vibration (5 to 500 Hz) was generated using MATLAB (R2011b) and *HVLab* toolbox (version 1.0 and 2.0). The vibration was presented at a

magnitude of 3.5 ms^{-2} r.m.s. (for Experiment 1) or 0.75 ms^{-2} r.m.s. (for Experiment 2 and 3; weighted using W_h according to ISO 5349-1:2001).

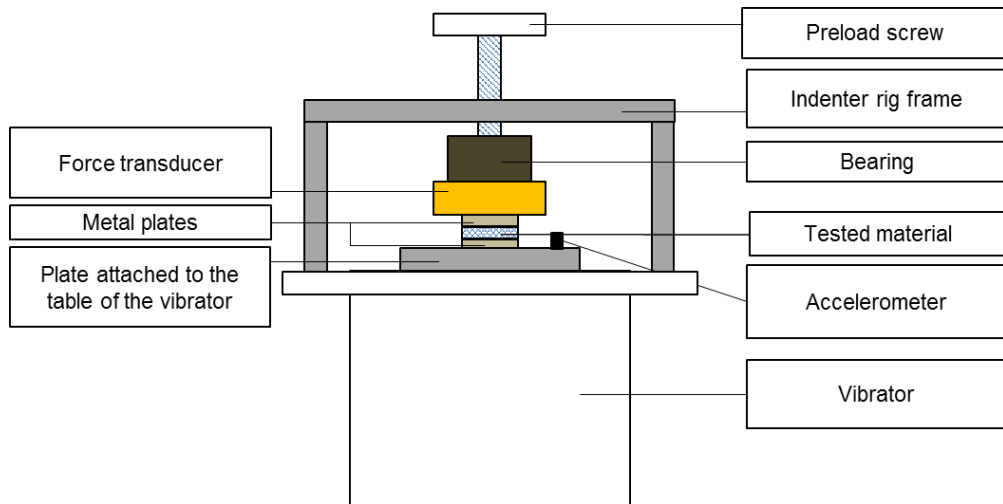


Figure 3-3 Indenter rig used in the first experiment.

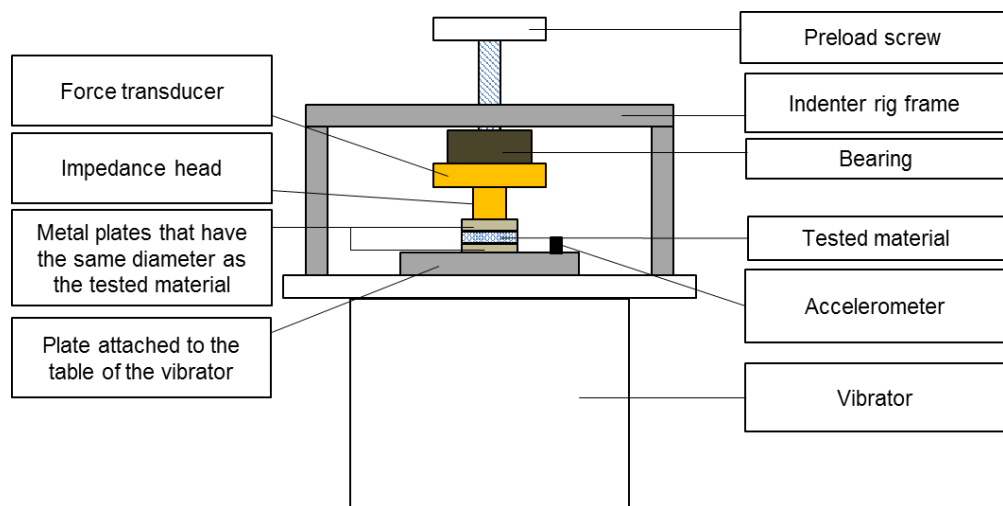


Figure 3-4 Indenter rig used in the second and the third experiment.

3.5 Sample preparation

There were three materials used in this research.

The first material was a foam (referred to as Foam A) cut from a glove that passed ISO 10819:1996. The material was taken from inside the glove. It had a thickness of 6.4 mm. The foam material was perforated. The foam was a closed-cell foam.

The second material was a gel (referred to as Gel A) cut from a glove that failed ISO10819:1996. The material was taken from inside the glove. It had a thickness of 5.0 mm. The gel material was sticky when it was first taken out of the glove.

The third material was a foam (referred to as Foam B) that can be used as a material that isolates vibration in a glove. It had a thickness of 6.0 mm. The foam was a closed-cell foam.

In this research, these materials are referred to as glove materials. All three glove materials were prepared with three diameters, 12.5, 25.0, and 37.5 mm.



Figure 3-5 Samples of glove material used in this research; black: Foam A, orange: Gel A, and blue: Foam B

3.6 Safety and ethics

All experiments were approved by the Ethics Committee of the Faculty of Engineering and the Environment at the University of Southampton (Table 3-3). Informed consent to participate the experiment was given by all subjects.

Table 3-3 Ethics number for each experiment

Experiment	Ethics number
1	2300
2	8824
3	12038

3.7 Signal generation and data acquisition

Vertical input vibration was generated using MATLAB (R2011b) with *HVLab* toolbox (version 1.0 and 2.0). All signals were generated and acquired at 4096 samples/second

after low-pass filtering at 1000 Hz. For the low frequency measurement (i.e., experiment 3, Chapter 8), the signals were generated and acquired at 2048 samples/second after low-pass filtering at 1000 Hz. The input and output signals were acquired and controlled via data acquisition box, NI-USB6211 16bit.

The maximum frequency component in the signal should be no more than half of the sampling rate to avoid aliasing. The maximum frequency component of interest in all experiments was no more than 500 Hz. For the low frequency measurements in Experiment 3, the maximum frequency of interest was 50 Hz.

3.7.1 Derritron VP4

The Derritron VP4 vibrator was capable of producing accelerations up to 250 ms^{-2} peak with a frequency range 1 to 10,000 Hz. A first major resonance is quoted at 8,900 Hz. The maximum displacement of the vibrator was $\pm 3 \text{ mm}$. The vibrator had a weight of 56 kg. The maximum unsupported load on the vibrator was 1.8 kg. An aluminium alloy plate was secured on top of the vibrator so that transducers could easily be mounted on top of the vibrator.



Figure 3-6 Left: Derritron VP4, Right: Derritron VP30.

3.7.2 Derritron VP30

The Derritron VP30 vibrator was capable of producing acceleration up to 400 ms^{-2} peak with a frequency range 1 to 4,500 Hz. The maximum displacement of the vibrator was about $\pm 5.7 \text{ mm}$. The weight of the vibrator was 240 kg and it used forced air for cooling.

The maximum unsupported weight was 23 kg. A steel plate was secured on top of the vibrator so that transducers can easily be mounted.

3.7.3 Accelerometers

A miniature piezo-electric accelerometer was used to measure vibration at the hand interface. This accelerometer was embedded in a wooden adapter (Figure 3-7). There were two miniature accelerometers used in the experiments conducted in this research, B&K 8307 and B&K 4374. The B&K 4374 had a weight of 0.65 gram with a resonance frequency of 85 kHz, capable of measuring vibration up to 26,000 Hz. The B&K 8307 had a weight of 0.4 grams and capable of measuring vibration up to 25,000 Hz.



Figure 3-7 Accelerometer embedded in a wooden adapter.

Another piezo-electric accelerometer, B&K 4371 was used to measure input vibration at the lower plate attached to the table of the vibrator (i.e., Experiment 1). The first resonance frequency occurred at frequency greater than 12,600 Hz.

All accelerometers were connected to a Flyde 128CA charge amplifier in the first experiment and B&K Type 2635 charge amplifier in the second and in the third experiment. All accelerometers were calibrated using calibrators (see Appendix A for the method of calibrating accelerometers using calibrators; B&K 4294). The range of magnitude of acceleration for each of the accelerometers depends on the spectra used in the experiment (see Table 3-4).

3.7.4 Force transducer

Force transducers were used to measure the static and dynamic force. The static force was measured for easy monitoring of the force applied on the input plate before and during the vibration exposure.

In the first experiment, the dynamic force and the static force were measured using a piezo-resistive force transducer (Kulite TC2000 500). This force transducer is capable of

measuring up to 100 kN. The force transducer was calibrated using a static mass (see Appendix A for the calibration of force transducer using static mass).

In the second and the third experiment, the static force was measured using a piezo-resistive force transducer (Kistler 4576A; Figure 3-8). This force transducer is capable of measuring up to 500 N. It had a weight of 0.25 kg. The first resonance frequency of the unloaded transducer occurred at a frequency greater than 2 kHz. The force transducer was calibrated using a static mass.



Figure 3-8 Force transducer Kistler 4576A.

3.7.5 Impedance head

In the second and the third experiment, a piezo-electric impedance head (B&K 8001) capable of measuring acceleration and dynamic force was used to measure the input acceleration and the output dynamic force (Figure 3.9).



Figure 3-9 Impedance head B&K 8001.

The maximum compression load of the impedance head was 2,000 N while the maximum tension load was 300 N. The force cell in the impedance head was calibrated

dynamically using a rigid mass (see Appendix A for the calibration of the force cell in the impedance head).

The accelerometer in the impedance head was calibrated using a calibrator (B&K 4294). The first resonance frequency quoted by the manufacturer of the impedance head was at frequency greater than 10,000 kHz.

The impedance head was connected to two B&K Type 2635 charge amplifiers.

Table 3-4 Accelerometers and force transducers used in this experiment with its sensitivity and range of measurements.

Accelerometers / Force cell	Sensitivity after calibration	Range after calibration	Method of calibration	Charge amplifier
Experiment 1: Biodynamic response of the hand				
B&K 4371	0.067 V/ ms ⁻²	±150	Calibrator	Flyde 128CA
B&K 8307	0.019 V/ ms ⁻²	±520	Calibrator	Flyde 128CA
Kulite TC2000 500	0.4 V/N	±25	Static mass	Flyde 359TA
Experiment 1: Dynamic stiffness of the material				
B&K 4371	0.037 V/ ms ⁻²	±272	Calibrator	Flyde 128CA
Kistler Type 4576A	0.02 V/N	±483	Static mass	Flyde 359TA
Experiment 2				
B&K 4374	0.059 V/ ms ⁻²	±170	Calibrator	B&K Type 2635
B&K 8001 (Accelerometer)	0.043 V/ ms ⁻²	±230	Calibrator	B&K Type 2635
B&K 8001 (Force transducer)	0.125 V/N	±80	Dynamically using a rigid mass	B&K Type 2635

Kistler Type 4576A	0.01 V/N	±1000	Static mass	Flyde 359TA
Experiment 3				
B&K 4374	0.059 V/ ms ⁻²	±170	Calibrator	B&K Type 2635
B&K 8001 (Accelerometer)	0.043 V/ ms ⁻²	±230	Calibrator	B&K Type 2635
B&K 8001 (Force transducer)	0.125 V/N	±80	Dynamically using a rigid mass	B&K Type 2635
Kistler Type 4576A	0.01 V/N	±1000	Static mass	Flyde 359TA

3.8 Analysis for the measurement of apparent mass of the hand, material transmissibility, and dynamic stiffness of the material

3.8.1 Transmissibility of the glove material to the hand and the finger

The material transmissibility transfer function, $T(f)$, was determined from the ratio of the cross-spectral density of the input and output acceleration, $A_{io}(f)$, to the power spectral density of the input acceleration, $A_{ii}(f)$:

$$T(f) = A_{io}(f)/A_{ii}(f) \quad (3.1)$$

The coherency, $\gamma^2(f)$, was calculated using:

$$\gamma^2_{io}(f) = \frac{|A_{io}(f)|^2}{A_{ii}(f) A_{oo}(f)} \quad (3.2)$$

where $A_{oo}(f)$ is the power spectral density of the output acceleration.

3.8.2 Apparent mass of the hand and the finger

The apparent mass at the palm or the index finger, $M_h(f)$, was determined from the ratio of the cross-spectral density of the input acceleration and output force, $F_o(f)$, to the power spectral density of the input acceleration, $G_{ii}(f)$:

$$M_h(f) = F_{io}(f)/G_{ii}(f) \quad (3.3)$$

The coherency, $\gamma^2(f)$, was calculated using:

$$\gamma^2_{io}(f) = \frac{|F_{io}(f)|^2}{G_{ii}(f)F_{oo}(f)} \quad (3.4)$$

where $F_{oo}(f)$ is the power spectral density of the force.

When measuring the apparent mass of the hand, the masses of the force transducer, the input plate, and the wooden adapter all contributed to the measured dynamic force (Figure 3-2). The influence of this force was subtracted from the total force using mass cancellation in the frequency domain or in the time domain. The mass to be cancelled was determined using the method in Section 3.2, so as to measure the dynamic force and the acceleration without either the hand or the finger.

- Mass cancellation in the frequency domain;

$$\text{Apparent mass of the hand or finger, } M_h(f) = M_T(f) - M_s(f) \quad (3.5)$$

where $M_T(f)$ is the apparent mass of the hand or finger including the mass of the moving system, and $M_s(f)$ is the apparent mass of the moving system other than the hand or finger. All values are complex quantities.

- Mass cancellation in time domain;

The apparent mass of the hand was calculated using:

$$M(f) = \frac{F_h(f)}{G_{ii}(f)} \quad (3.6)$$

where $F_h(t)$ is the force exerted by the hand and was given by:

$$F_h(t) = F_{io}(t) - M_s(t)G_{ii}(t) \quad (3.7)$$

where $M_s(t)$ is the apparent mass of the moving system other than the hand or finger.

3.8.3 Dynamic stiffness of the glove material

The dynamic stiffness of the material, $S(f)$, was determined from the ratio of the cross-spectral density of the input acceleration and the output force, $F_{mio}(f)$, to the power spectral density of the input displacement $-\omega^2 A_{mii}(f)$:

$$S(f) = F_{mio}(f)/(-\omega^2(A_{mi}(f))) \quad (3.8)$$

where $F_{mio}(f)$ is the dynamic force transmitted by the material, $A_{mi}(f)$ is the input acceleration, and ω is the angular frequency ($\omega = 2\pi f$).

Based on the Kelvin Voigt viscoelastic model, the dynamic stiffness of the material can be assumed to be represented by $S(f) = k + ic\omega$, where k is the equivalent stiffness of the material and c is the equivalent viscous damping of the material.

3.8.4 Statistical analysis

Non-parametric statistical analysis were used to interpret a collection of data to avoid making assumption of the distribution of the population. In this study, Friedman test and Wilcoxon Signed Rank test with statistical significant of $p < 0.05$ were used in Experiment 2 and 3 to provide indication of the difference between numbers of related samples.

3.9 Predicting the transmissibility of the glove material using mechanical impedance model

A mechanical impedance model, as discussed in Chapter 2, was used to predict the transmissibilities of glove materials to the hand.

The predicted transmissibility of the material to the hand or to the finger is given by:

$$T_h(f) = \frac{A_h(f)}{A_i(f)} = \frac{\omega^{-2}S(f)}{\omega^{-2}S(f) - M_h(f)} \quad (3.9)$$

where $A_h(f)$ is the acceleration at the hand, $A_i(f)$ is the acceleration measured at the input plate, $M_h(f)$ is the apparent mass of the hand, and $S(f)$ is the dynamic stiffness of the glove material.

The apparent mass of the hand, $M_h(f)$, was calculated with mass cancellation as explained in Section 3.8.2. However, the mass of the wooden adapter was not cancelled so it can be included as part of the mass of the hand to predict the glove transmissibility.

3.10 Accuracy and precision of the measuring equipment used in Experiments 1, 2, and 3.

It was anticipated that there would be noise (e.g., generated by the amplifiers or transferred from the floor to the transducers) at certain frequencies that would limit the

accuracy and the precision of the measurements. A study was conducted to determine the reasonable frequency range to get accurate and precise measurements using sets of equipment as shown previously (see Sections 3.2, 3.3 and 3.4 for the equipment used for the hand apparent mass, glove transmissibility, and material dynamic stiffness measurements, respectively).

3.10.1 Apparent mass of a rigid body at frequencies between 5 and 500 Hz

The reasonable frequency range to get accurate and precise measurement for the equipment used to measure hand apparent mass was determined based on the measurement of the apparent mass of a rigid body. It was expected that if a rigid body is exposed to a random vibration at frequencies from 5 to 500 Hz, the modulus of the measured apparent mass of the rigid body at those frequencies would be the static mass of the rigid body and the phase would be zero.

3.10.1.1 Apparent mass of a rigid body using equipment in Experiment 1

The apparent mass of a 3-gram rigid body was measured using equipment in Experiment 1 at frequencies from 5 to 500 Hz using procedures similar to Section 3.2 but with the rigid body attached on top of the force transducer (Kulite TC 2000 500; Figure 3-2, left). The rigid body was exposed to a random vibration over the frequency range 5 to 500 Hz at 3.24 m/s^2 r.m.s. (frequency-weighted W_h according to the ISO 5349-1:2001). Mass cancellation of the apparent mass was performed in the frequency domain (see Section 3.8.2) due to the varied apparent mass across the frequency of vibration produced by the masses other than the rigid body (i.e., see Section 3.8.2 for the explanation of the masses other than the rigid body).

It was observed that the mass of the rigid body was about 3 grams at 20 Hz and remained almost unchanged as the frequency of vibration increased at frequencies from 20 to 500 Hz (Figure 3-10). There is phase lag at frequencies from 5 to about 200 Hz and phase lead at frequencies from 200 to 500 Hz. The phase lead was expected to be due to the different time constants between amplifiers: in the second experiment, a similar setup was used to compare between setups using the same amplifiers and setup using different types of amplifiers and it was observed that measurements with the same amplifiers did not have phase lead as seen in this study. It is not clear the reason of the phase lag at low frequencies but it was suspected that this was due to the amplifier for the accelerometer: in the second experiment, the amplifier for the input accelerometer

was changed and the phase lag was not observed. At frequencies less than 20 Hz, the apparent mass of the rigid body increased with decreasing frequency of vibration from 20 to 5 Hz.

It was concluded that the reasonable frequency range to get accurate and precise measurement of hand apparent mass using equipment in Experiment 1 was from 20 to 350 Hz. The effect of the phase lead at frequencies greater than 200 Hz is small: the phase is close to zero. However, it was expected that there will be incorrect phase (i.e., phase lag) at low frequencies especially at frequencies less than about 70 Hz. The equipment setup for experiment 1 was improved for the second and the third experiment to address the problems mentioned in this section (i.e., phase lag at low frequencies and phase lead at high frequencies).

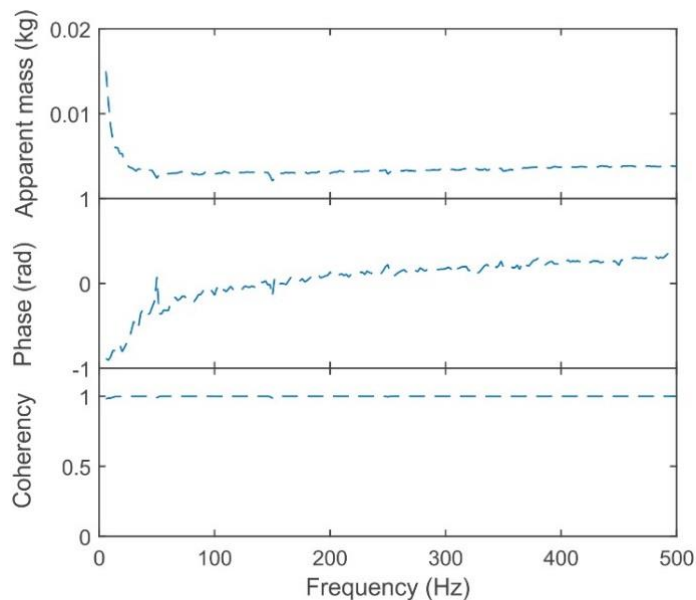


Figure 3-10 Apparent mass (modulus and phase) of a 3-gram rigid body measured with equipment used in Experiment 1. Coherency of the measurement of the rigid body apparent mass was calculated before mass cancellation.

3.10.1.2 Apparent mass of a rigid body using equipment in Experiment 2 and 3

Similar procedures to those for the equipment employed in Experiment 1 were repeated but with equipment used in Experiments 2 and 3 with a 12-gram rigid body placed on top of the impedance head (B&K 8001; Figure 3-2, right). The rigid body was exposed to a random vibration over the frequency range 5 to 500 Hz at 2.0 m/s² r.m.s. (frequency-weighted W_h according to the ISO 5349-1:2001). The mass cancellation was performed

in the time domain (see Section 3.8.2). The moving mass other than the added rigid body was about 29.8 grams.

It was observed that the mass of the rigid body was about 12 grams at 5 Hz and remained almost unchanged as the frequency of vibration increased from 5 to 500 Hz (Figure 3-11) although there was evidence of resonances or mass other than the rigid body that affected the measured apparent mass at frequencies from 70 to 150 Hz: the apparent mass of the hand (i.e., about 0.025 kg) was expected to be much greater than this mass (i.e., mass other than the rigid body) at those frequencies, so, it was expected that they (i.e., resonances or mass other than the rigid body) may not affect the measurement of hand apparent mass. The phase was close to zero at all frequencies from 5 to 500 Hz.

It was concluded that the reasonable frequency range to get accurate and precise measurement for the measurement of hand apparent mass using equipment in Experiment 2 and 3 was from 5 to 500 Hz.

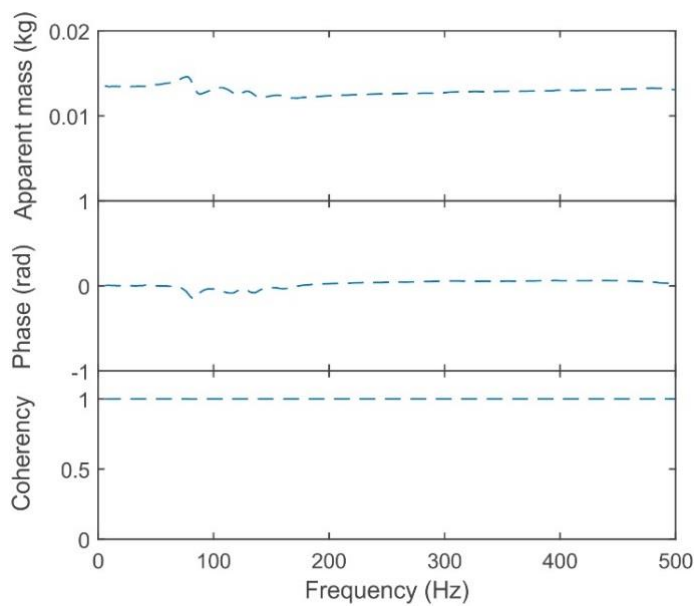


Figure 3-11 Apparent mass (modulus, phase and coherency) of a 12-gram rigid body measured with equipment used in Experiments 2 and 3.

3.10.2 Transmissibility between input and output accelerometer

If acceleration on a vibrating surface is measured using two accelerometers at the same location, the accelerations measured by both accelerometers are expected to be similar. The accuracy of the measurement of glove transmissibility can be determined by measuring the transmissibility between the input acceleration accelerometer (i.e., located inside the impedance head or on the lower plate attached to the table of the

vibrator) and the output acceleration accelerometer (i.e., located inside the wooden adapter placed on-top of the input plate, see Sections 3.2 and 3.3 for the location of the input and output acceleration accelerometers).

Using procedures similar to Section 3.3 but without the glove material, the transmissibility between the input and the output accelerometer was measured. Random vibration was generated over the frequency range 5 to 500 Hz at both 3.24 m/s² r.m.s. and 2.0 m/s² r.m.s. (frequency-weighted by W_h according to the ISO 5349-1:2001) for the equipment in Experiment 1, and the equipment in Experiments 2 and 3, respectively. Figure 3-12 shows the transmissibility between the input and the output accelerometer used in both setups.

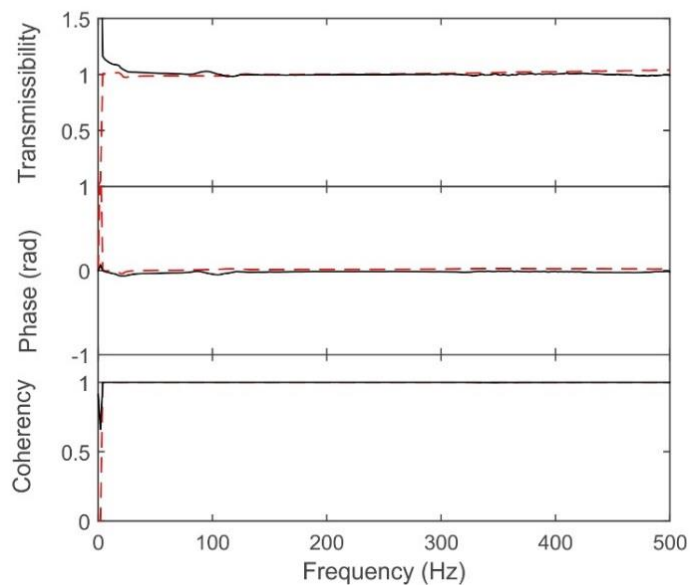


Figure 3-12 Transmissibility between the input and the output accelerometer (— for the measurement using Equipment 1, - - - for the measurement using Equipment 2 and 3).

The transmissibilities between the input and the output accelerometers were close to unity (e.g., 1.0) in both of the setups (i.e., the differences between the input and the output accelerometers were about 5% for Experiment 1 from 20 to 500 Hz and about 4% for Experiment 2 and 3 from 5 to 500 Hz). It was concluded that both setups will provide reasonably accurate (i.e., errors of less than 5%) material transmissibility at frequencies from 20 to 500 for Experiment 1 and at frequencies from 5 to 500 Hz for Experiment 2 and 3.

3.10.3 Dynamic stiffness of a glove material

Vibrations could be transmitted through the indenter rig frame from the floor and may affect the accuracy in the measurement of dynamic force (see Section 3.4). The frequency range for measurements using the indenter rig (see Section 3.4) was determined based on the measurement and the analysis of a material dynamic stiffness. It was expected that the coherency for the dynamic stiffness measurement would be close to unity (i.e., 1.0) if there is no noise affecting the measurement.

The dynamic stiffness of Foam A was measured using procedures similar to Section 3.4 with a diameter of the contact area of 25 mm and a preload force of 20 N. The material was exposed to a random vibration over the frequency range 5 to 500 Hz at 0.75 m/s² r.m.s. (frequency-weighted by W_h according to ISO 5349-1:2001). The dynamic stiffness of Foam A and its measurement coherency are shown in Figure 3-13.

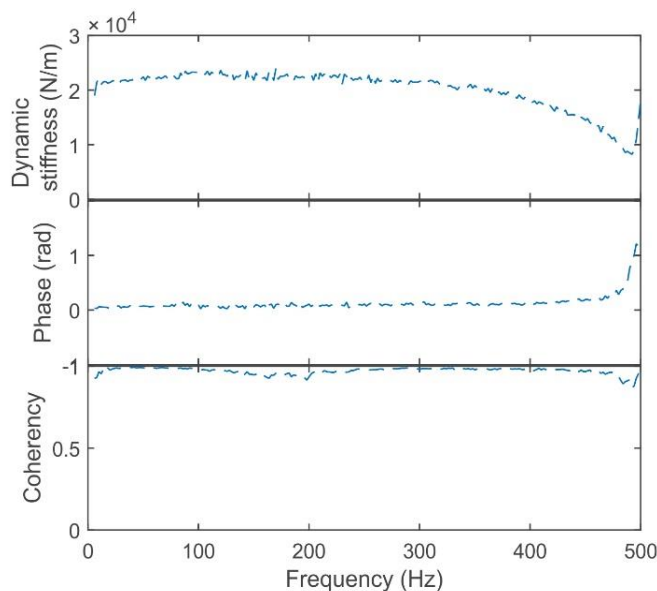


Figure 3-13 Dynamic stiffness (modulus, phase, and coherency) of Foam A.

There was evidence of noise in the measurement at around 180 Hz and 480 Hz: the coherency of the measurement was slightly decreased at these frequencies. The noise at 180 Hz slightly affected the measured dynamic stiffness as seen in Figure 3-13. The noise at about 480 Hz affected the material dynamic stiffness: the material dynamic stiffness decreased with increasing vibration frequency from 350 to 480 Hz. A second indenter rig was built with improved structural rigidity but it had almost the same noise characteristics as the previously tested indenter rig (i.e., in this section) at similar frequencies.

It was concluded that the reasonable frequency range for the measurement of material dynamic stiffness using the indenter rig for this research was from 10 to 350 Hz. However, it was expected that the measured material dynamic stiffness using the indenter rig may slightly be affected by noise at frequencies around 180 Hz.

Chapter 4: Transmission of vibration through gloves: Effects of material thickness

4.1 Introduction

The transmission of vibration through a dynamic system (e.g., vibration isolator) depends on the dynamic loading on the system (e.g., mechanical impedance or apparent mass of the device supported by the isolator), so the transmissibility of a glove depends on the apparent mass of the hand in contact with the glove and not only on the dynamic properties of the glove.

The biodynamic responses of the hand depend on the frequency of the vibration (e.g., Miwa, 1964a) and the direction of the vibration (e.g., Reynolds, 1977). The apparent mass of the hand is high at lower frequencies but decreases considerably as the frequency of vibration increases (Reynolds, 1977; O'Boyle and Griffin, 2004; Xu *et al.*, 2011). The resonance frequency in the apparent mass of the hand depends on the part of the hand contacting a vibrating surface (Concettoni and Griffin, 2009). At frequencies less than about 50 Hz the apparent mass at the fingers is considerably less than the apparent mass at the palm (Concettoni and Griffin, 2009). The transmission of vibration through a material to the fingers will therefore differ from the transmission of vibration through the same material to the palm of the hand, because the dynamic properties of the fingers differ from the dynamic properties of the hand.

When optimising the transmission characteristics of a glove, some control over the dynamic properties of the material is required, but this is difficult because the prediction of the dynamic properties from the physical and chemical characteristics of glove material is not usually possible. A variable that can be expected to alter the dynamic properties, and that may be changed easily, is the material thickness. There are no reported systematic studies of the effect of material thickness on the transmissibility of gloves to either the palm of the hand or to the fingers.

The objective this study was to measure the transmission of vibration to the palm of the hand and to the tip of the index finger with a resilient material having three different thicknesses. The apparent mass at the palm and at the finger, and the dynamic stiffnesses of the material, were also measured. It was hypothesised that the thickness of the material would alter both the dynamic stiffness and the transmissibility of the glove material, and that the measured transmissibility could be predicted from the measured apparent mass of the hand or finger and the measured dynamic stiffness of the material.

4.2 Methods

4.2.1 Glove materials

Three samples of foam material (Foam A) were cut from a glove classed as an anti-vibration glove according to ISO 10819:1996. All samples were 25-mm in diameter with an uncompressed thickness of 6.4 mm and weight of 0.34 grams. The samples were stacked together to produce three thicknesses: 6.4 mm, 12.8 mm, or 19.2 mm.

4.2.2 Subjects

Fourteen male subjects participated in the study: median age 27 years (range 23 to 33), stature 171 cm (165 – 196), weight 65 kg (40 – 110), hand circumference 200 mm (192 – 255), and hand length 200 mm (180 – 220).

The experiment was approved by the Ethics Committee of the Faculty of Engineering and the Environment at the University of Southampton.

4.2.3 Measuring the apparent mass of the hand

Subjects sat with their arms not otherwise supported and placed the palm of their hand, or the tip of their index finger, on the wooden adapter and pushed down with a force of 10 N (Figure 4-1 and 4-2). Random vibration (10 s over the frequency range 5 to 500 Hz at 3.24 ms^{-2} r.m.s., frequency-weighted with W_h according to ISO 5349-1:2001) was generated using MATLAB (R2011b) and *HVLab* toolbox (version 1.0). Please see Section 3.2 for the equipment setup used to measure the apparent mass of the hand.

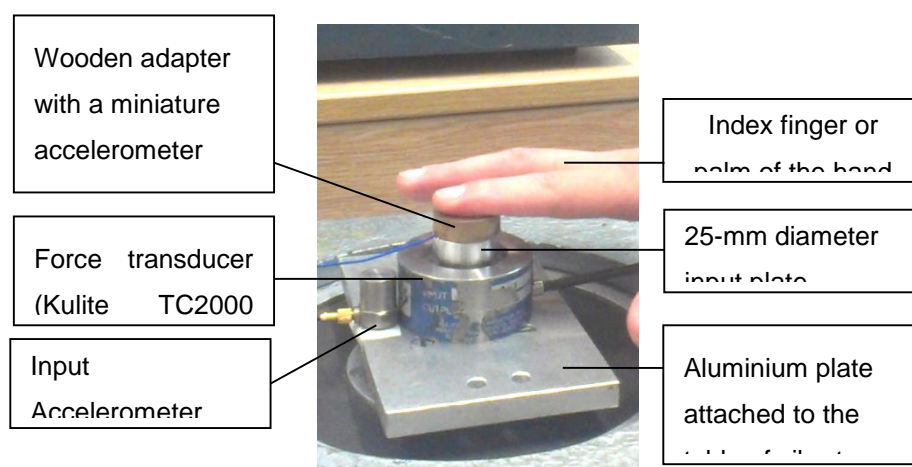


Figure 4-1 The arrangement for the measurement of the apparent mass of the hand and the index finger.

4.2.4 Measuring the transmissibility of the glove material to the hand and finger

The material samples were placed on the 25-mm diameter input plate secured to the top of the force transducer to measure the transmissibility of the material to the palm or to the index finger. The 25-mm diameter wooden adapter was placed on top of the material, with the palm or tip of the index finger placed on the wooden adapter exerting a downward force of 10 N. Other conditions of the test were the same as when measuring the apparent mass of the hand and the finger. The order of measuring the material transmissibilities and the apparent mass of the hand was randomised.

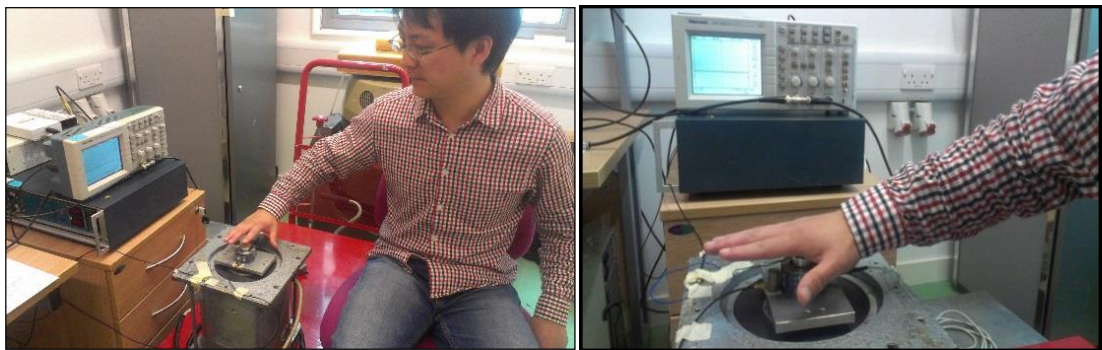


Figure 4-2 Left: posture of the hand for the measurement of the apparent mass at the index finger. Right: arrangement for the measurement of the apparent mass at the palm of the hand. The downward force is indicated on the oscilloscope.

4.2.5 Measuring the dynamic stiffnesses of the materials

An 'indenter rig' was used to determine the dynamic stiffness of the glove material (see Section 3.4 for the equipment setup and the procedures used to measure material dynamic stiffness). The samples of glove material were placed between the two 25-mm plates. The materials were subjected to a preload force of 10 N. A 10-s period of random vertical vibration (5 to 500 Hz) was generated using MATLAB (R2011b) and *HVLab* toolbox (version 1.0). The vibration was presented at a magnitude of 3.5 ms^{-2} r.m.s. (weighted using W_h according to ISO 5349-1:2001).

4.2.6 Analysis

Constant bandwidth frequency analysis was performed across the frequency range 20 to 350 Hz with a frequency resolution of 2 Hz and 84 degrees of freedom.

Procedures for the analysis of hand apparent mass, glove transmissibility to the hand and material dynamic stiffness can be found in Section 3.8.

The apparent mass of the hand was calculated with mass cancellation in frequency domain (see Section 3.8.2).

4.2.7 Impedance model for predicting material transmissibility to the hand and finger

The transmissibility of the material to the hand or finger, $T_h(f)$, was predicted using Equation 3.9.

The apparent mass of the hand, $M_h(f)$ was calculated with mass cancellation in frequency domain (as explained in Section 3.8.2). For the calculation of the predicted transmissibilities, the mass of the wooden adapter was not included in the mass cancellation. The wooden adapter with accelerometer had a mass of 5.06 g that added to the apparent mass of the hand or finger and would have influenced the transmissibility of the material, especially the finger that had a lower apparent mass.

4.3 Results

4.3.1 Dynamic stiffness and viscous damping of the glove material

The stiffness and damping of the glove material decreased as the material thickness increased (Figure 4-3). The viscous damping of the material was high at lower frequencies but decreased as the frequency of vibration increased.

4.3.2 Apparent mass at the palm and the index finger

Inter-subject variability in the apparent mass at the palm and at the index finger is shown in Figure 4-4. The median apparent masses at the palm and at the index finger of the subjects were high at lower frequencies but decreased considerably with increasing frequency of vibration. At all frequencies, the apparent mass at the palm was greater than the apparent mass at the index finger (Figure 4-4).

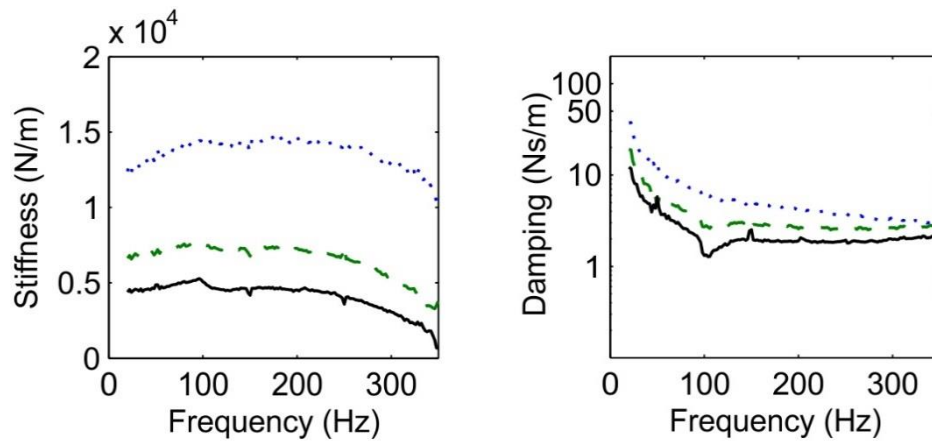


Figure 4-3 Stiffness and damping of the glove material (· · · 6.4 mm, - - - 12.8 mm, and — 19.2 mm) according to Kelvin Voigt viscoelastic model (see Section 3.8.3).

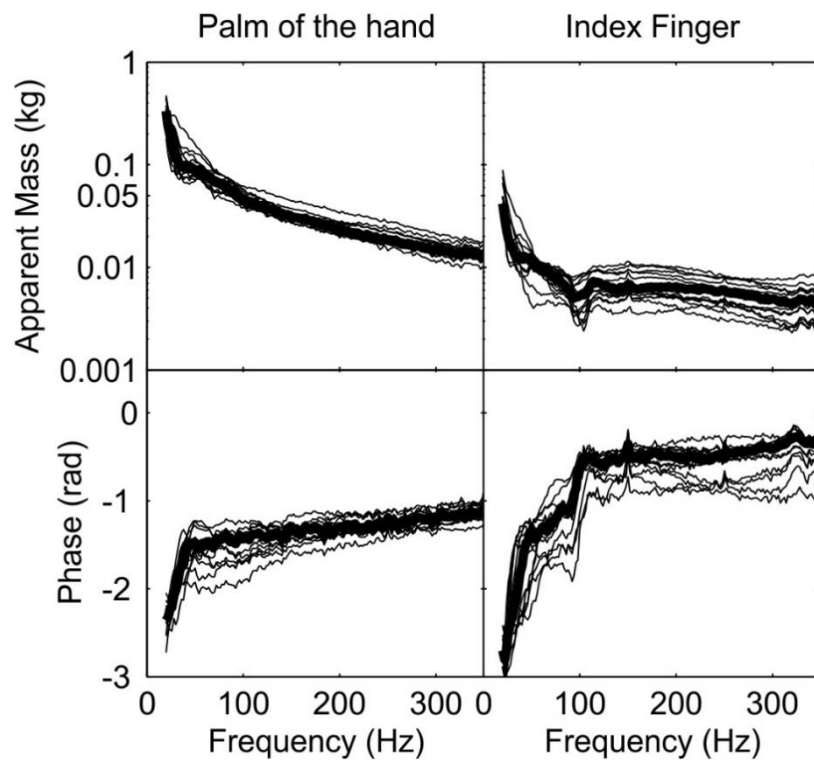


Figure 4-4 Apparent mass of the hand of all 14 male subjects. Left: palm; Right: index finger. (Thicker black lines: Median apparent mass).

4.3.3 Transmissibility of the glove material to the palm of the hand and to the finger

Inter-subject variability in the transmissibility of the glove material to the palm and to the index finger is shown for each material thickness in Figure 4-5. Some subjects showed two resonances while most showed only one resonance.

The median transmissibility of the glove material to the palm of the hand varied according to the material thickness (Figure 4-6, left). One resonance frequency, between 30 and 40 Hz, decreased as the thickness of the material increased. The glove material attenuated vibration at frequencies greater than about 40 Hz, with the attenuation increasing with increasing material thickness.

The median transmissibility of the glove material to the index finger shows the material appreciably amplified vibration at lower frequencies but attenuated the vibration at higher frequencies. The first resonance frequency in the transmissibility of the glove material to the finger reduced from about 166 Hz with a thickness of 6.4 mm to about 100 Hz with a thickness of 19.2 mm (Figure 4-6, right).

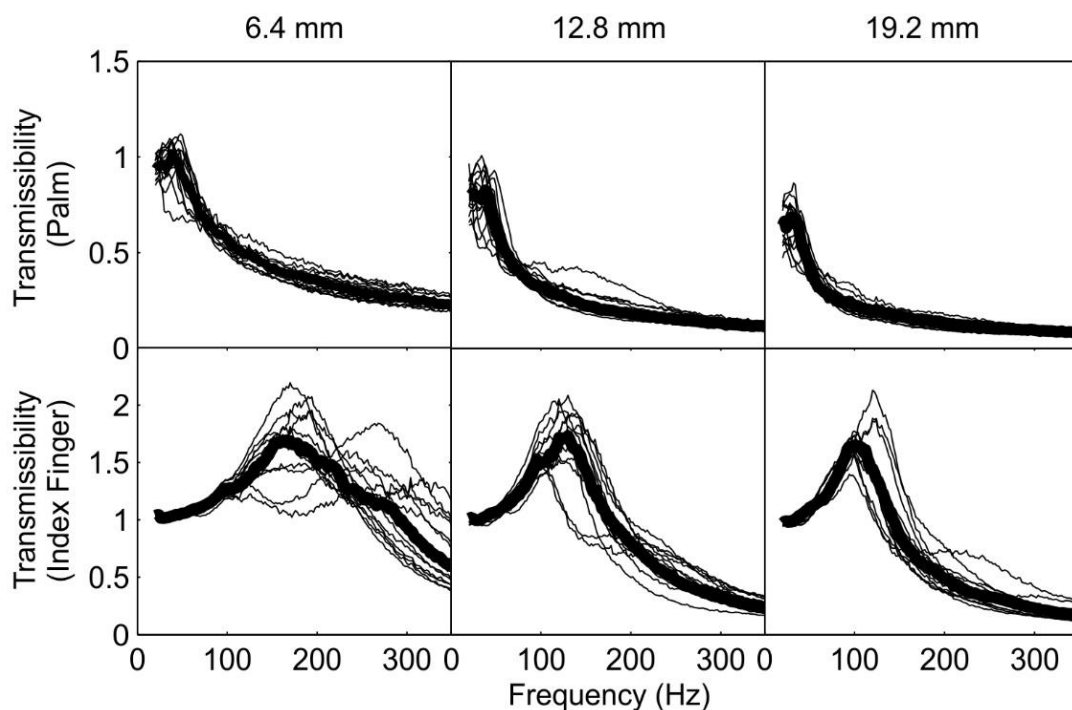


Figure 4-5 Transmissibility of the glove material with thickness of 6.4, 12.8, and 19.2 mm to the palm (upper graphs) and index finger (lower graphs) with 14 male subjects. Thicker lines: median transmissibility.

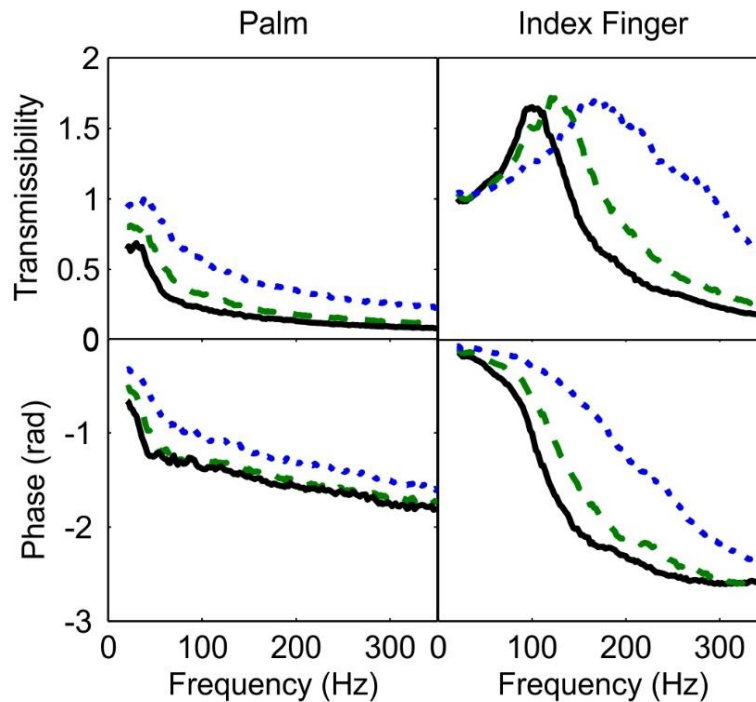


Figure 4-6 Median transmissibility (modulus and phase) of the glove material to the palm of the hand (left graphs) and to the index finger (right graphs) with three thicknesses of glove material:: 6.4 mm, ---: 12.8 mm, and —: 19.2 mm. Medians for 14 subjects.

4.3.4 Predicted transmissibility of the glove material to the palm and to the index finger

The predicted transmissibilities varied between subjects, because they depend on the apparent mass at the palm and at the finger which differs between people (Equation 4.1). Predictions of the glove material transmissibility are shown for all subjects and all three thickness of the glove material at the index finger in Figure 4-7. The individual predicted transmissibilities of the glove material are generally similar to the individual measured transmissibilities.

Notwithstanding the individual variability, with all three material thicknesses, the median predicted transmissibility to the palm of the hand and to the index finger was similar to the median measured transmissibility over the range 20 Hz to 350 Hz (Figure 4-8). The greatest percentage difference between the median measured and the median predicted transmissibility was 28%, which occurred with 19.2-mm thickness at the palm at 350 Hz, although not visible in Figure 4-8 because the transmissibility is very low (around 0.081) at this frequency.

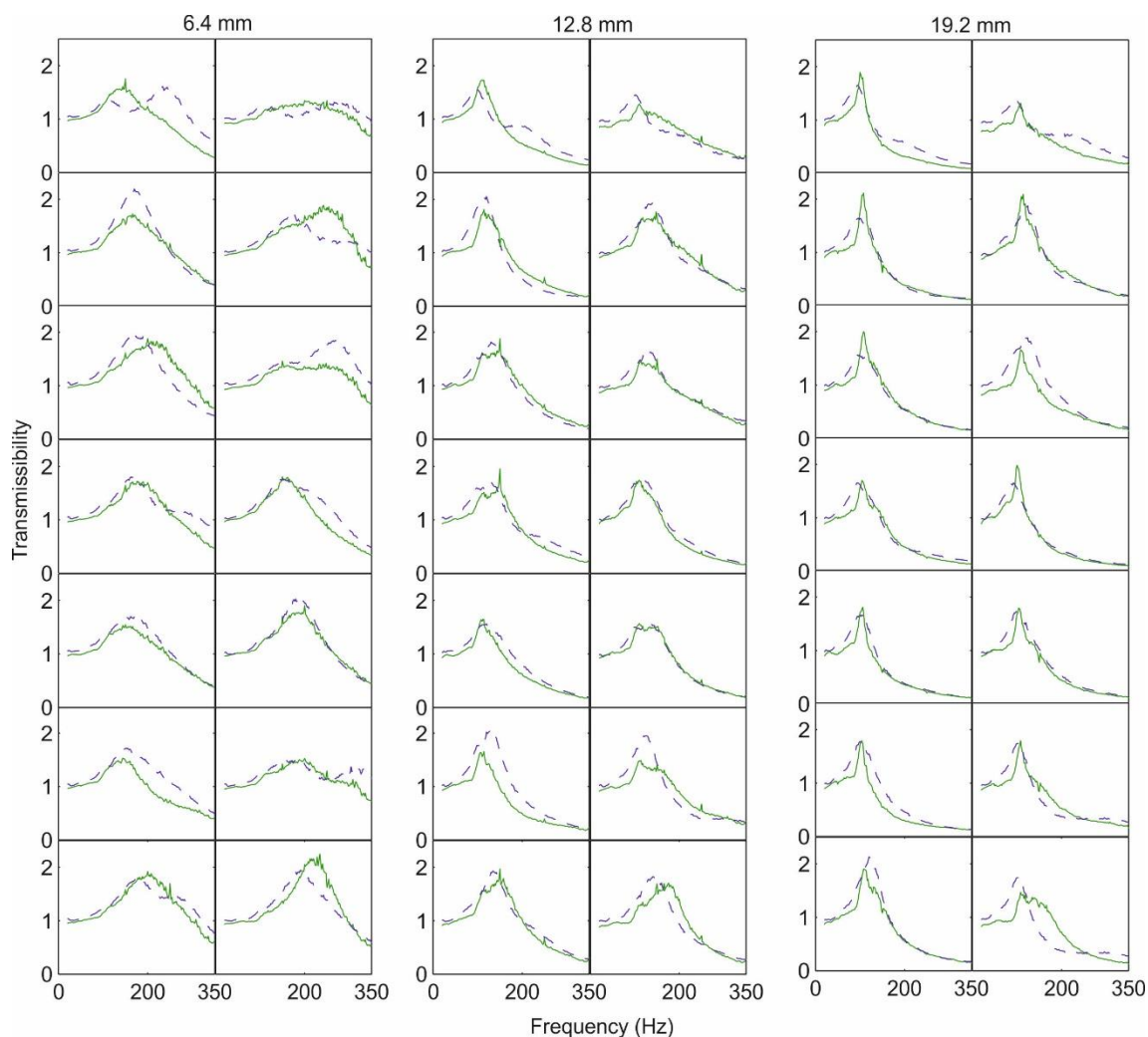


Figure 4-7 Predicted and measured individual transmissibility of the glove material to the index finger with material thickness of 6.4, 12.8, and 19.2 mm (---: measured, and —: predicted).

4.4 Discussion

4.4.1 Apparent mass at the palm and at the finger

At all frequencies of vibration, the palm of the hand had greater apparent mass than the index finger (Figure 4-4). However, the relative difference between the apparent masses at both locations decreased as the frequency of vibration increased. This is consistent with the apparent mass at higher frequencies at both locations being controlled by the soft tissues, whereas at lower frequencies the apparent mass is more dependent on the mass of the upper limb, as suggested by Reynolds and Angevine (1977) and Dong *et al.* (2005).

The apparent masses at the palm and at the index finger measured in this study have been compared with those reported previously (Figure 4-9). The apparent mass of the hand reported by Dong *et al.* (2005) and Xu *et al.* (2011) is greater than the apparent mass found here, possibly because they measured the apparent mass with a vertical palm pushing horizontally and with a greater surface of the hand in contact with the input plate or handle. The apparent mass of a full-hand will be greater than the apparent mass measured with a 25-mm diameter contactor, as in this study.

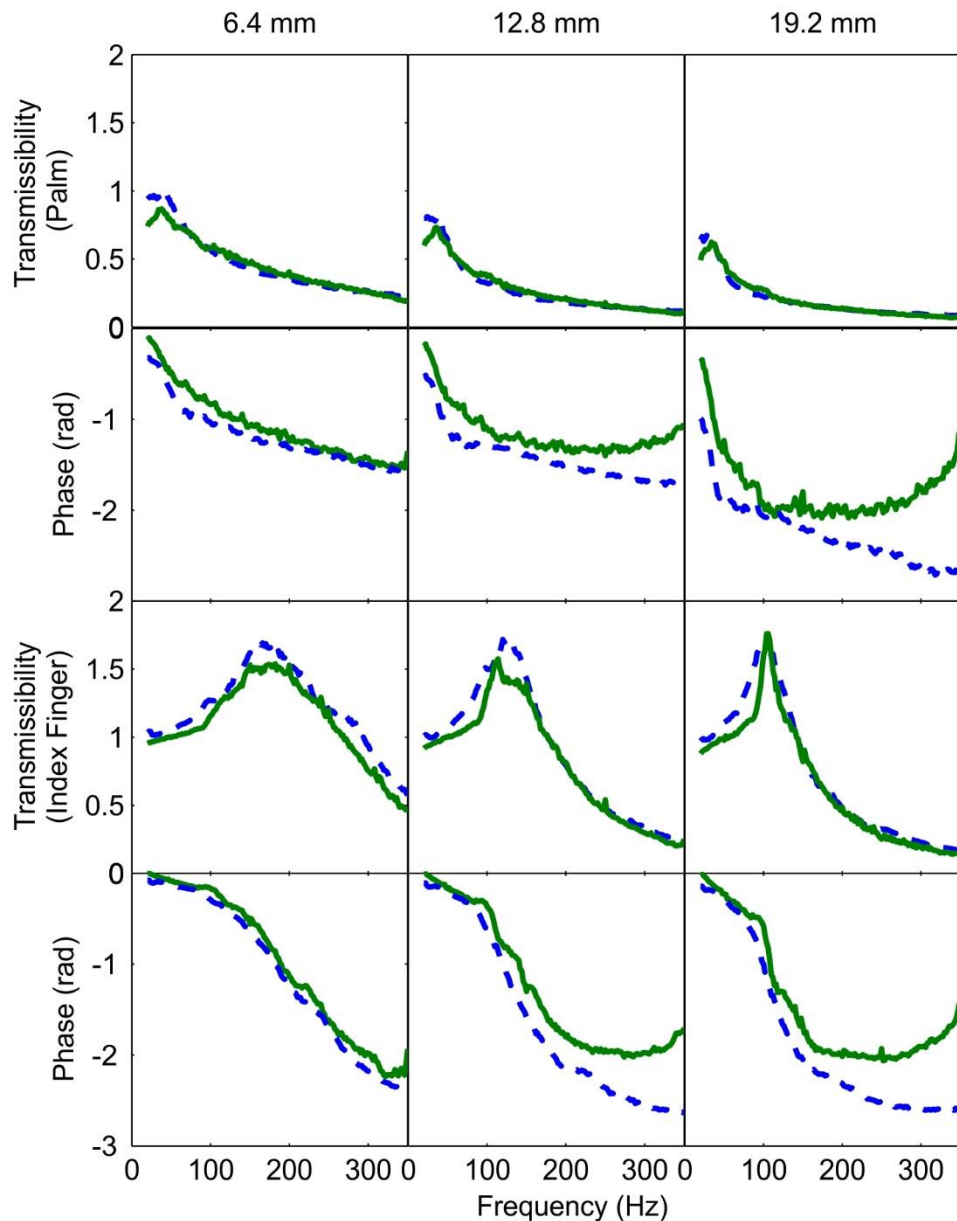


Figure 4-8 Predicted and measured transmissibility to the palm (upper graphs) and the index finger (lower graphs) with glove material of thickness 6.4, 12.8, and 19.2 mm (---: measured, and —: predicted). Medians for 14 subjects.

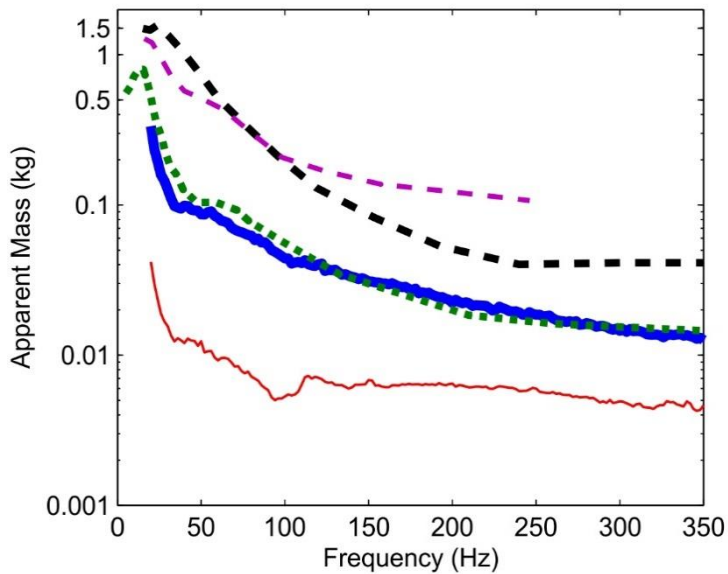


Figure 4-9 Apparent mass of the hand (— palm pushing down on a flat surface at 10 N on a 25-mm diameter plate, vibration in vertical direction; — index finger pushing down a flat surface at 10 N on a 25-mm diameter plate, vibration in vertical direction; — vertical palm pushing horizontally on a cylindrical handle with adapter at 50 N, vibration in horizontal direction (from Dong *et al.*, 2005); — full hand pushing on horizontally on a flat surface, vibration in horizontal direction (from Xu *et al.*, 2011); palm pushing down on a flat surface at 10 N on a 25-mm diameter plate, vibration in vertical direction (from O'Boyle and Griffin, 2004).

The apparent mass at the palm measured in this study is similar to the apparent mass at the palm reported by O'Boyle and Griffin (2004), who measured with similar conditions (i.e., size of contact area, contact force, hand posture, the palm of the hand, vertical vibration) but with different subjects.

4.4.2 Transmissibility of the glove material to the palm and to the index finger

The transmissibility to the palm was considerably less than the transmissibility to the index finger at all frequencies from 20 to 350 Hz, when the comparison is made with the same material thickness (Figure 4-6). With the thinnest material, the median transmissibility to the palm was around unity at frequencies less than 50 Hz. At higher frequencies, and at all frequencies with the two thicker materials, there was attenuation in the transmission of vibration to the palm.

The resonance frequency in the transmissibility to the finger was at a higher frequency than the resonance in the transmissibility to the palm of the hand. This resulted in the glove material amplifying the transmission of vibration to the finger at all frequencies up to 272 Hz with the thinnest material, and at all frequencies up to 140 Hz with the thickest material.

The greater transmissibility of the glove material to the finger than to the palm of the hand has been reported previously (Paddan and Griffin, 1999). The difference is large and casts doubt on the value of a standardised glove test that does not yield understanding of the influence of a glove on the transmission of vibration to the fingers (Griffin, 1998). The findings of this study suggest that measuring the transmission of vibration to the palm of the hand is not sufficient to assess the value of an 'anti-vibration' glove.

4.4.3 Effects of dynamic stiffness of glove material

The dynamic stiffnesses of the material varied with the thickness of the material. If the material behaved linearly, it would be expected that as the thickness doubled the stiffness would halve and the damping would halve. Although this makes assumptions that will not be valid for all materials, the measured stiffness and the measured damping were approximately half when the thickness doubled from 6.4 to 12.8 mm (Figure 4-3).

The reduction in dynamic stiffness with increase in material thickness affected the transmission of vibration to the palm of the hand and to the index finger (Figure 4-6). At frequencies lower than about 100 Hz, the transmissibility to the palm of the hand decreased as the thickness of the material increased whilst the transmissibility to the finger increased with increasing material thickness.

The same trends reported in this paper were found when performing the same measurements with three thicknesses of a gel material taken from a glove that did not pass the test for an anti-vibration glove in ISO 10819 (1996) (Figure 4-10). The gel material attenuated the vibration transmitted to the palm of the hand but amplified the transmission of vibration to the index finger (except for the higher frequencies with the thicker material). The resonance frequency in the transmissibilities to the index finger decreased as the thickness of the material decreased. Similar to the foam glove material, whereas the transmissibility of the gel material to the palm tended to reduce with increasing thickness, the transmissibility to the index finger increased with increasing thickness at frequencies less than about 200 Hz.

Reducing the dynamic stiffness of the material in a glove can reduce the transmission of vibration to the palm of the hand but increase the transmission of vibration to the fingers at some frequencies. The requirement in ISO 10819:2013 for an anti-vibration glove to have the part covering the fingers the same properties as the part covering the palm, and with a thickness equal to, or greater than, 0.55 times the thickness at the palm needs reconsideration.

4.4.4 Inter-subject variability in the measured and predicted material transmissibility

Across the 14 subjects, inter-subject variability in transmissibilities to the palm of the hand was less than for the index finger (Figure 4-5). The large variability in transmissibility to the finger is similar to the findings of Paddan and Griffin (1999). The variability may have primarily arisen from differences in the mechanical impedance of the fingers, but also from small difference in the preload force influencing the dynamic stiffness of the material (e.g., O'Boyle and Griffin, 2004). There can also be large inter-subject variability in the measures obtained using the method of assessing whether a glove can be classed as an anti-vibration glove in ISO10819:1996 and ISO 10819:2013 (e.g., O'Boyle and Griffin, 2001; Laszlo and Griffin, 2011).

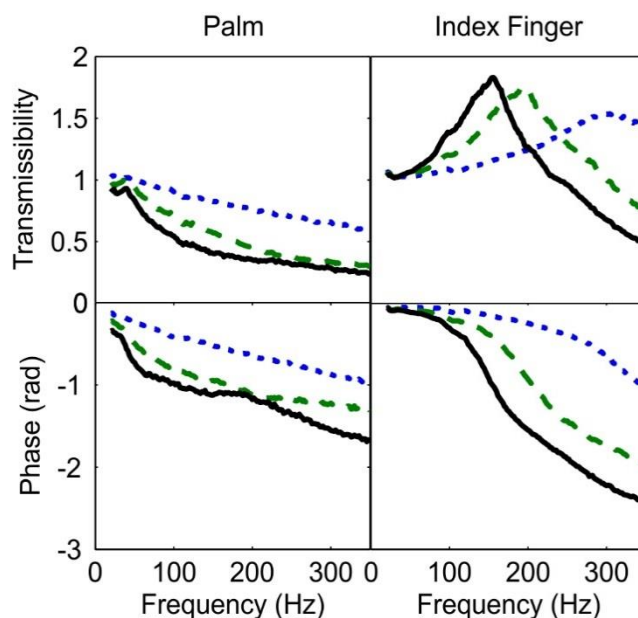


Figure 4-10 Transmissibility of a gel material to the palm of the hand (left graphs) and to the index finger (right graphs):: 6.4 mm, ---: 12.8 mm, and —: 19.2 mm. Modulus (upper graphs) and phase (lower graphs). Medians for 14 subjects.

4.4.5 Predicted transmissibility of the glove material to the palm and to the index finger

The predicted and the measured transmissibilities show good agreement for individual subjects as well as in the median data, notwithstanding differences in apparent mass between subjects and between the palm and the finger. This suggests it might be possible to predict the benefits of wearing a particular glove for an individual worker.

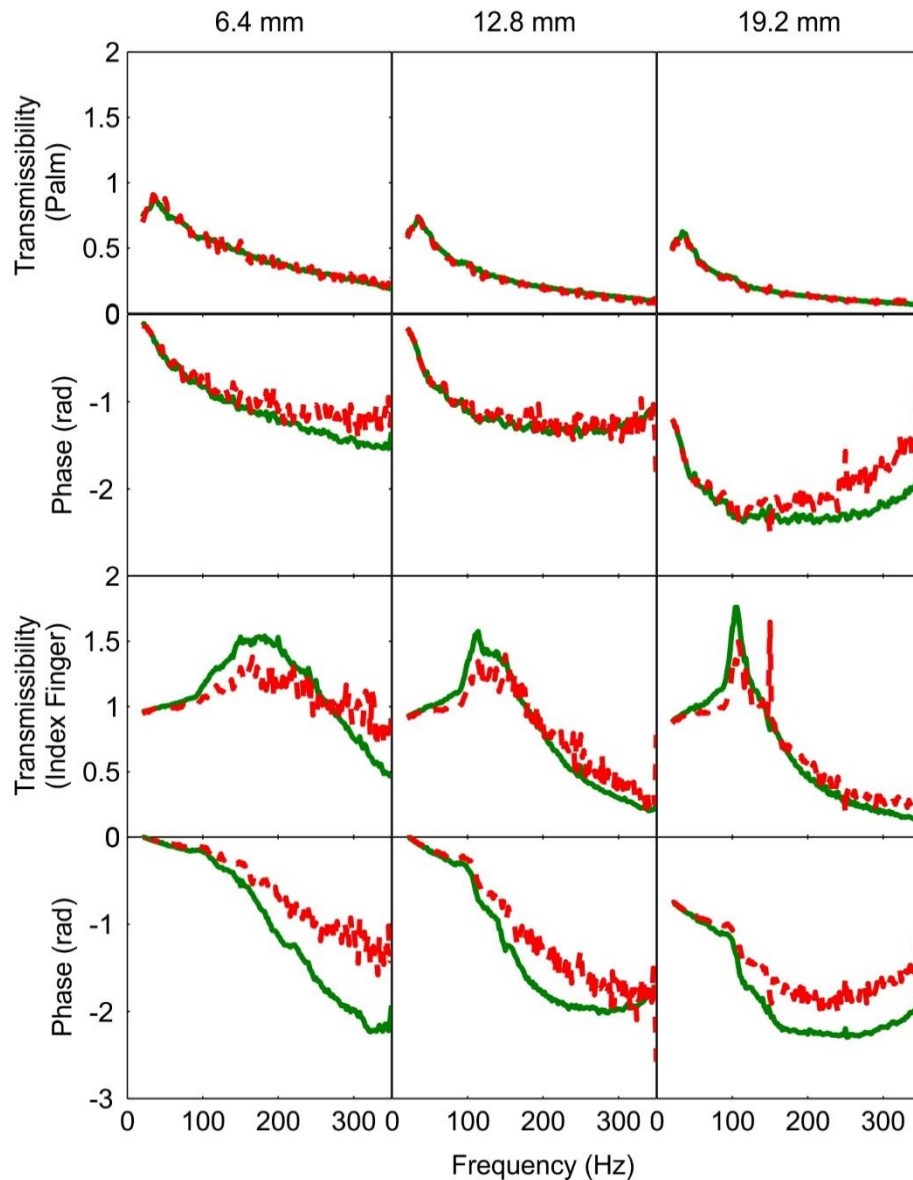


Figure 4-11 Comparison of predicted transmissibility to the palm (upper graphs) and to the index finger (lower graphs) with and without the wooden adapter: --- with adapter, — without adapter). Medians for 14 subjects.

The use of an adapter to measure vibration within a glove according to ISO 10819 (1996) and ISO 10819 (2013) may result in underestimation or overestimation of the transmissibility of a glove (Paddan and Griffin, 2001; Dong *et al.*, 2005). From the measures obtained in this study, it was possible to estimate the transmissibility of the material without the wooden adapter, by predicting the transmissibility with and without the mass of the wooden adapter included in the mass cancellation (see Chapter 3). The wooden adapter had little effect on the predicted transmissibility to the palm of the hand, but the transmissibility to the index finger was slightly affected (Figure 4-11). This is consistent with the finding of Mann and Griffin (1996) and Dong *et al.* (2005). It is to be expected that the effect of the adapter on the transmissibility will increase with increasing frequency of vibration, because the apparent mass of the index finger or the hand reduces with increasing frequencies whereas the apparent mass of the adapter is the same at all frequencies.

4.5 Conclusions

The difference between the apparent mass of the hand and the apparent mass of the finger has a large effect on the transmissibility of glove material to the palm and to the finger. Over much of the frequency range explored in this study (20 to 350 Hz), a glove material attenuated the transmission of vibration to the palm of the hand but amplified the transmission of vibration to the finger.

Varying the dynamic stiffness of a glove material (e.g., by changing the material thickness) can have a large effect on transmissibility to the palm of the hand and to the fingers. Reducing the dynamic stiffness may reduce transmissibility to the palm while increasing transmissibility to the finger.

The transmissibility of a glove material to the palm or a finger can be predicted from the dynamic stiffness of the material and the apparent mass measured at the palm or finger. It is also possible to predict the effect of different material properties (e.g., thickness).

The effects of gloves on the transmission of vibration to the fingers, where damage from exposure to hand-transmitted vibration is most commonly reported, will not be estimated in any useful way using the method of measuring glove transmissibility as specified in International Standard ISO 10819:2013.

Chapter 5: Transmission of vibration through gloves: Effects of area of contact with a glove

5.1 Introduction

There has been little study of how changes in the size of the contact area affect the biodynamic response of the hand. However, it has been reported that the driving-point mechanical impedance of the hand-arm system depends on the size of the contact area at frequencies greater than 100 Hz (Marcotte *et al.*, 2005), and that increasing the area of contact with a finger increases the apparent mass of the finger at frequencies greater than about 400 Hz (Mann and Griffin, 1996).

The stiffness and damping of materials used in gloves can also be expected to change if the size of the area of contact is changed. For a uniform material that behaves linearly, a doubling the area of contact can be expected to result in a doubling of both the stiffness and the damping of the material. However, for the materials used in gloves it is not reported how the stiffness and damping change with area, or how any change affects the transmission of vibration to the hand.

At high frequencies, the transmissibility of glove materials increases with increasing glove dynamic stiffness (O'Boyle and Griffin, 2004; Chapter 4) but decreases with increasing apparent mass of the hand (e.g., index finger or palm of the hand; Chapter 4). To understand the effect of contact area on glove transmissibility it is therefore necessary to understand how both the dynamic stiffness of the glove material and the dynamic response of the hand vary with area and with the frequency of vibration.

This study was designed to investigate how the size of the area of contact with the hand affects the dynamic response of the hand, the dynamic stiffness of glove materials, and the transmission of vibration to the hand. It was hypothesised that with increased area of contact, the apparent mass at the palm would increase at higher frequencies but be unchanged at lower frequencies. With increasing area, the stiffness and damping of the material were expected to increase. The transmission of vibration to the hand was expected to either increase or decrease with increasing area, depending on the relative changes in the material dynamic stiffness and the apparent mass of the hand.

5.2 Methods

5.2.1 Materials and contact area

Three materials, two foams and a gel (denoted as Foam A, Foam B and Gel A), with thicknesses of 6.4, 6.0, and 5.0 mm, respectively, were prepared with three contact areas having diameters of 12.5, 25.0, and 37.5 mm. The physical forms of the materials are summarized in Table 5-1.

Table 5-1 Physical characteristics of the materials used in the experiment.

Diameter (mm)	Weight (grams)			Area of contact (mm ²)	Relative area (%)
	Foam A	Foam B	Gel A		
12.5	<2	<2	<2	123	100
25.0	<2	<2	<2	491	400
37.5	<2	<2	4	1,105	900

5.2.2 Subjects

Ten male subjects participated in the experiment. Their characteristics are shown in Table 5-2. The experiment was approved by the Ethics Committee of the Faculty of Engineering and the Environment at the University of Southampton (reference number 8824).

Table 5-2 Characteristics of the subjects in the experiment.

Physical Forms	Range	Median
Age (years)	24 – 42	29
Stature (cm)	160 – 181	167
Weight (kg)	59 – 120	67
Hand circumference (mm)	165 – 230	200
Hand length (mm)	172 – 205	183

5.2.3 Measuring apparent mass at the palm and at the thenar eminence

The participants placed the palm of their hand, or their thenar eminence, on the circular wooden adapter (Figure 5-1). The arm was not otherwise supported. They pushed the circular wooden plate downward with a force of 10 N, as indicated on an oscilloscope (Figure 5-3). This force was applied for all measurements. The procedures were repeated with different contact area for metal plates (12.5-, 25.0- or 37.5-mm diameter and weighing 1, 12 or 20 grams, respectively) and wooden adapters (12.5-, 25.0- or 37.5-mm diameter and weighing less than 1, 3 or 5 grams). Please see Section 3.2 for the equipment setup used to measure the apparent mass of the hand.

A 10-s period of random vertical vibration (with an acceleration spectrum from 5 to 500 Hz as shown in Figure 5-2) was generated using MATLAB (R2011b) with the *HVLab* toolbox (version 1.0). The vibration was presented at a magnitude of 2.0 ms^{-2} r.m.s. (frequency-weighted using W_h according to ISO 5349-1:2001).



Figure 5-1 Posture of the hand for the measurement of the apparent mass at the thenar eminence.

5.2.4 Measuring the transmissibility of the material to the palm and to the thenar eminence

The procedures in Section 2.3 were repeated to measure the transmission of vibration to the palm and to the thenar eminence with each of the three materials and all three contact areas. The material samples were placed on top of a circular metal plate and below a wooden adapter of the same diameter (Figure 5-3).

The material transmissibility was measured using the same 10-s 2.0 ms^{-2} r.m.s. random vertical vibration used to measure the apparent mass of the hand.

The order of measuring apparent mass and material transmissibility of all three sizes and the three materials was randomised.

5.2.5 Determining the dynamic stiffness of the material

The dynamic stiffnesses of the three diameters of the three materials were measured using an indenter rig (see Section 3.4 for the equipment setup and procedures used to measure material dynamic stiffness). The preload force (i.e., 10 N) was applied on the material via an impedance head so as to measure the dynamic force during vibration. A 10-s period of random vertical vibration (with an acceleration spectrum from 5 to 500 Hz as shown in Figure 5-2) was generated using MATLAB (R2011b) with the *HVLab* toolbox (version 1.0). The vibration was presented at a magnitude of 0.75 ms^{-2} r.m.s. (frequency-weighted) using a Derritron VP4 vibrator. The vibration spectrum differed from that used to measure the apparent mass of the hand and the transmissibility of the material, due to the different dynamic conditions: the rigid indenter had impedance very different from that of the hand, so different acceleration was required to obtain easily measurable forces over the range 5 to 500 Hz.

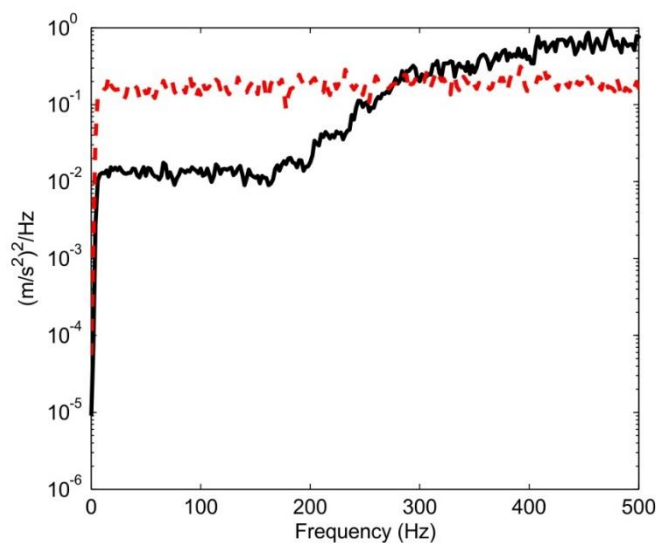


Figure 5-2 Acceleration power spectral densities of the stimuli: --- for the measurement of apparent mass and material transmissibility, — for the measurement of dynamic stiffness. Spectra with 2-Hz resolution.

5.2.6 Analysis

Constant bandwidth frequency analysis was performed with a resolution of 2 Hz and 84 degrees of freedom across the frequency range 10 to 300 Hz.

Procedures for the analysis of hand apparent mass, glove transmissibility to the hand and material dynamic stiffness can be found in Section 3.8.

The apparent mass of the hand was calculated with mass cancellation in time domain (see Section 3.8.2).

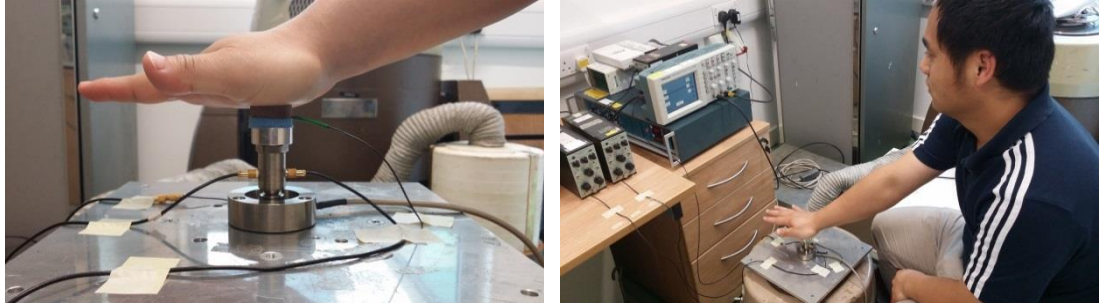


Figure 5-3 Left: posture of the hand for the measurement of the transmissibility of the material to the palm of the hand. Right: arrangement for the measurement of the apparent mass and the material transmissibility. The downward force is indicated on the oscilloscope.

The overall transmissibility of a glove material, T_o , was calculated from the ratio between the frequency-weighted r.m.s. acceleration measured on the wooden adapter, A_{wa} , to the frequency-weighted r.m.s. acceleration measured on the handle, A_{hm} .

$$T_o = \frac{A_{wa}}{A_{hm}} \quad (5.1)$$

The r.m.s. accelerations measured on the handle and on the wooden adapter for the calculation of overall transmissibility were low-pass filtered at 300 Hz using MATLAB (R2011b) with the *HVLab* toolbox (version 1.0).

5.2.7 Predicting the transmissibility of material to the palm and to the thenar eminence

The transmissibility of the material to the hand or finger, $T_h(f)$, was predicted using Equation 3.9.

The apparent mass of the hand, $M_h(f)$ was calculated with mass cancellation in time domain. For the calculation of the predicted transmissibilities, the mass of the wooden adapters were not included in the mass cancellation. The wooden adapters had masses of 1, 3, and 5 g for 12.5-, 25.0-, and 37.5-mm diameters of contact area, respectively, that added to the apparent mass of the hand and would have influenced the transmissibility of the material.

5.3 Results

The coherencies of all measurements of dynamic stiffness, apparent mass, and transmissibility were greater than 0.8 at all frequencies in the range 10 to 300 Hz.

5.3.1 Dynamic stiffnesses of the materials

The dynamic stiffness and the viscous damping of each of the three materials increased with increasing contact area (Figure 5-4). The viscous damping of the three materials decreased with increasing frequency of vibration. Foam B was the stiffest material and had the greatest damping, while Foam A was the softest material and had the least damping.

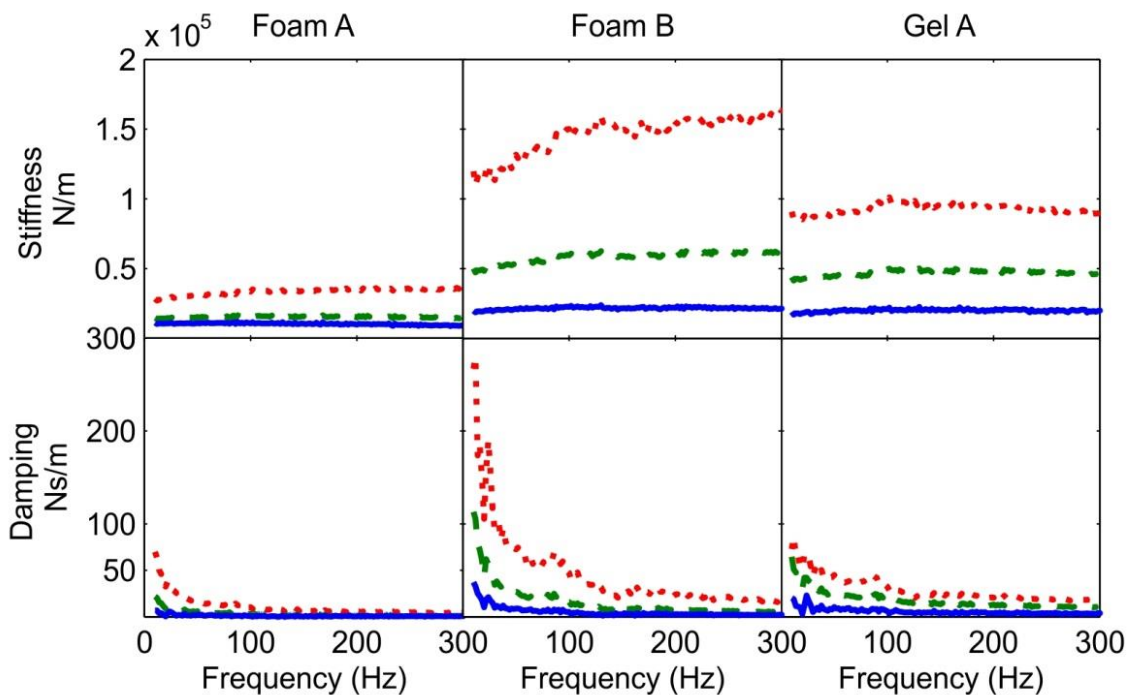


Figure 5-4 Stiffness and damping of the material according to the diameter of the contact area (— 12.5-mm, - - - 25.0-mm, ···· 37.5-mm; based on Kelvin Voigt viscoelastic model: see Section 3.8.3).

5.3.2 Apparent mass at the palm and at the thenar eminence

Inter-subject variability in the apparent mass measured at the palm and at the thenar eminence is shown in Figure 5-5.

The apparent mass measured at the palm of the hand decreased as the frequency of vibration increased (Figure 5-6). The first principle resonance frequency in the median apparent mass at the palm, around 14 Hz, did not change with a change in contact area ($p>0.277$; Friedman). The median apparent mass at the palm was independent of contact area at frequencies less than about 52 Hz ($p>0.061$; Friedman), but increased with increasing contact area at higher frequencies (Friedman $p<0.045$).

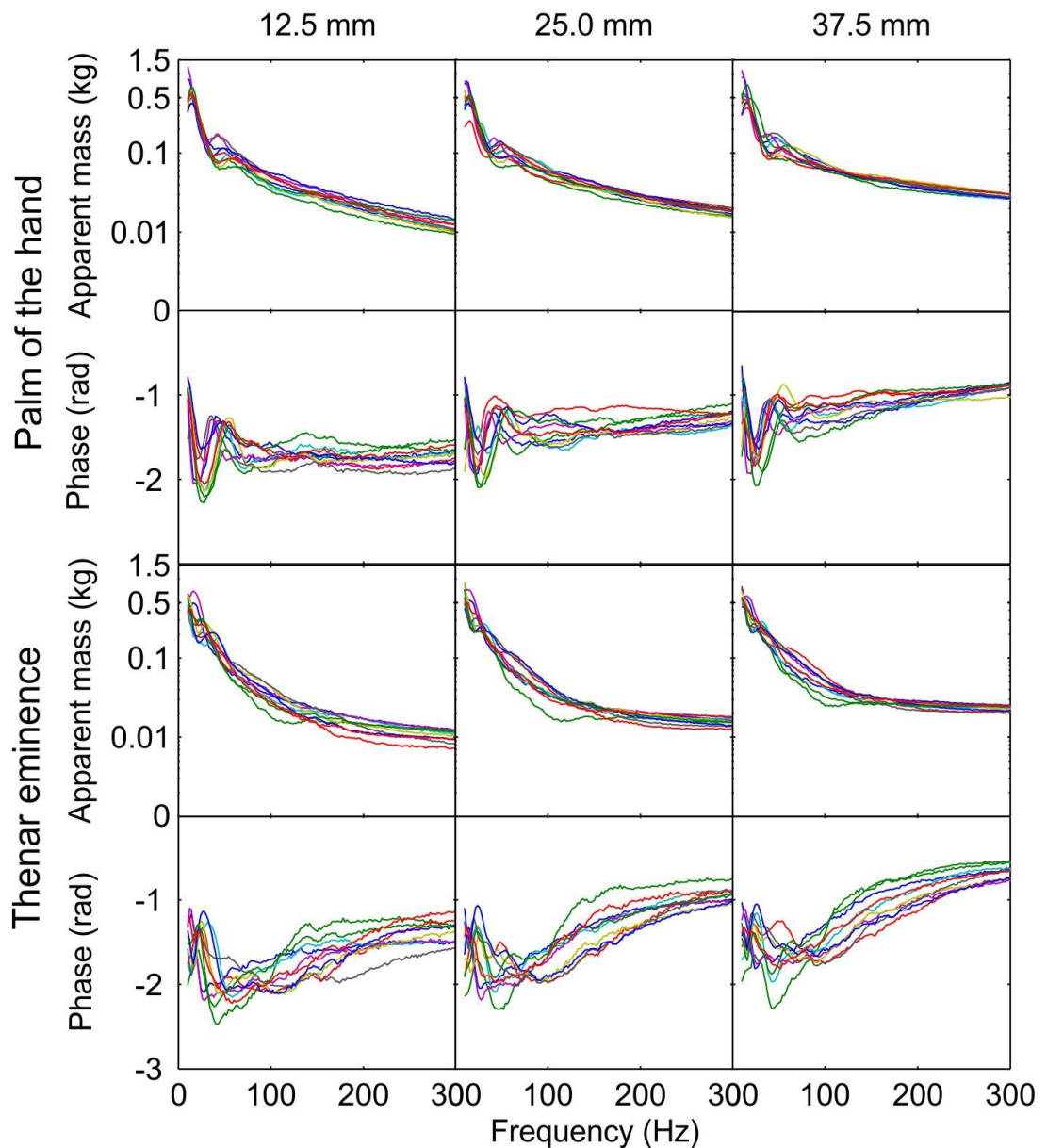


Figure 5-5 Individual apparent mass (modulus and phase) at the palm of the hand and at the thenar eminence according to its diameter of contact area. 10 Subjects.

With all three contact areas, the first principal resonance frequency in the median apparent mass at the thenar eminence, around 26 Hz, was unchanged with a change in contact area ($p>0.112$; Friedman). The median apparent mass at the thenar eminence

was independent of contact area at frequencies less than about 38 Hz ($p>0.061$; Friedman), but increased with increasing contact area at higher frequencies ($p<0.045$; Friedman).

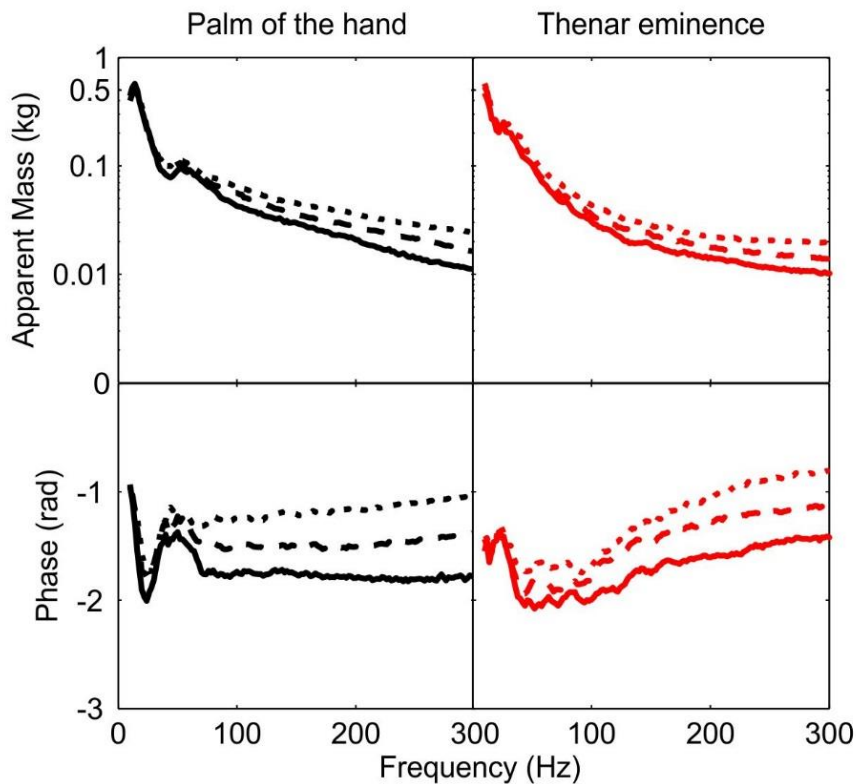


Figure 5-6 Apparent mass (modulus and phase) at the palm of the hand and at the thenar eminence according to the diameter of the contact area (— 12.5-mm, ---- 25.0-mm, 37.5-mm). Medians of 10 subjects.

The median apparent mass was greater at the palm than at the thenar eminence for all frequencies greater than about 60 Hz for the same material and same contact area ($p<0.001$; Friedman).

5.3.3 Transmissibility of glove materials to the palm and the thenar eminence

The effects of the area of contact on the median transmissibilities to the palm and to the thenar eminence are shown in Figure 5-7.

For Foam A, the median transmissibility to the palm of the hand was less than 1.0 at all frequencies of vibration (in the range 10 to 300 Hz) and for all three contact areas. At frequencies greater than 20 Hz, the transmissibilities to both the palm and the thenar eminence increased as the diameter of the contact area increased from 12.5 to 37.5 mm

(Figure 8; $p < 0.0136$ for palm, $p < 0.0247$ for thenar eminence; Friedman). However, at high frequencies, the transmissibility of Foam A to both the palm and the thenar eminence was similar for 12.5 and 25.0 mm diameter material ($p > 0.193$ for frequencies greater than 134 Hz at the palm, $p > 0.106$ for frequencies greater than 66 Hz at the thenar eminence; Wilcoxon).

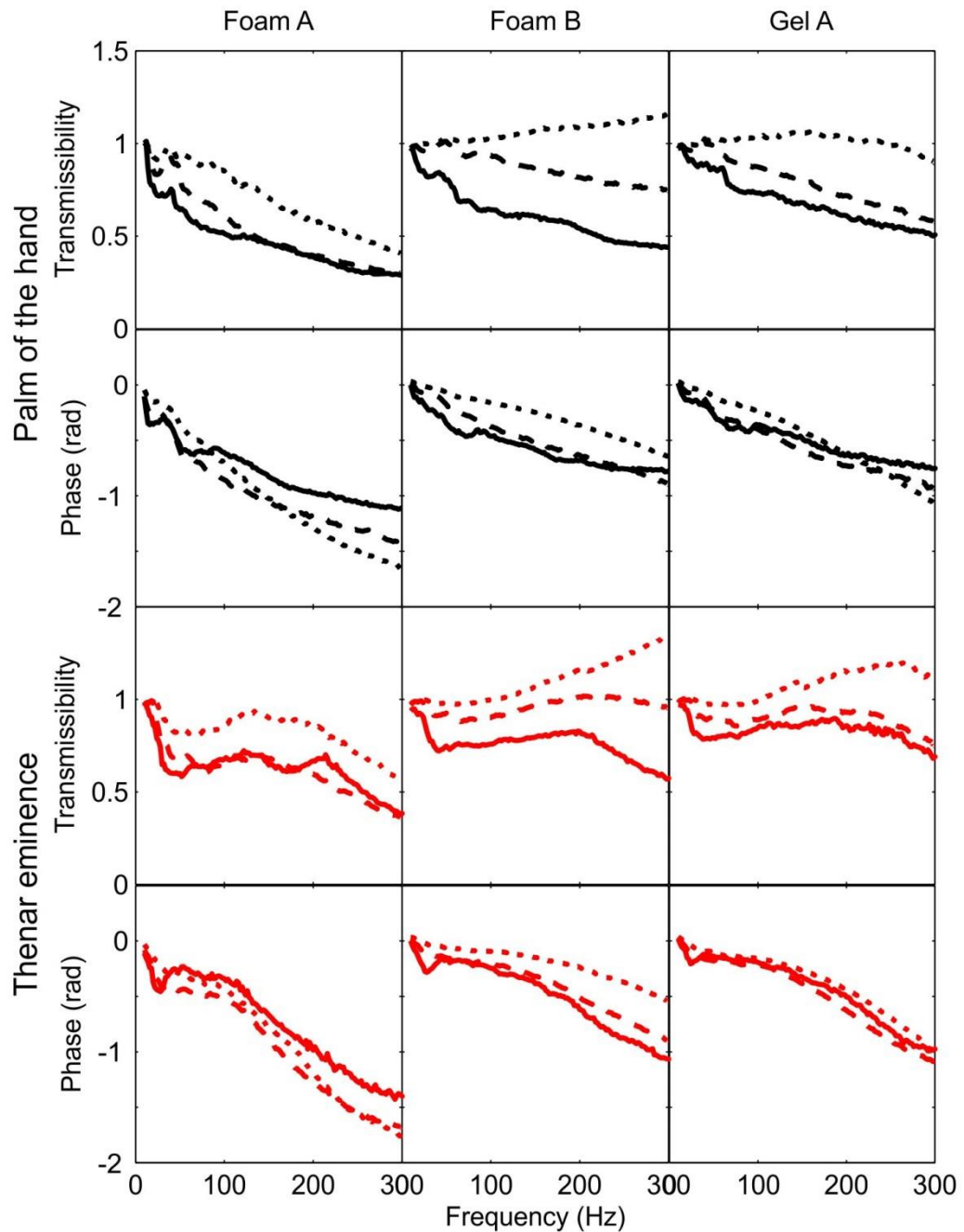


Figure 5-7 Median transmissibilities (modulus and phase) of the three materials to the palm and to the thenar eminence according to the diameter of the contact area (— 12.5 mm, ---- 25.0 mm, 37.5 mm). Median values from 10 subjects.

For Foam B, at very low frequencies the transmissibilities to the palm of the hand and to the thenar eminence were similar with all three contact areas. As the frequency increased to 300 Hz the transmissibilities to the palm and the thenar eminence were less with the smaller area and greater with the larger area (Figure 5-7; $p < 0.006$ for frequencies greater than 14 Hz for the palm of the hand, $p < 0.025$ for frequencies greater than 8 Hz for the thenar eminence; Friedman). There was a broadly similar trend with Gel A (Figure 5-7).

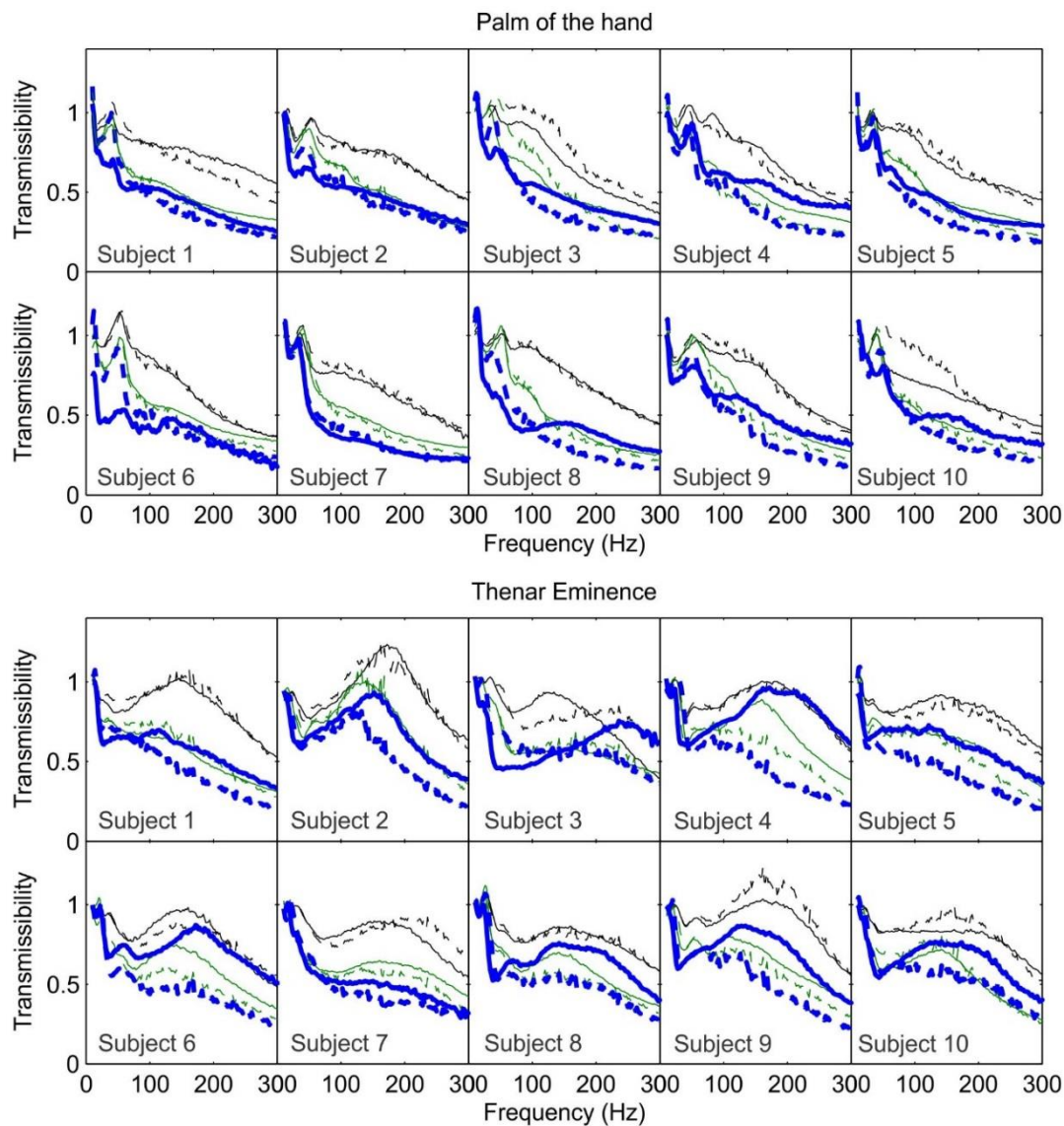


Figure 5-8 Individual transmissibilities (predicted and measured) for Foam A to the palm (upper figures) and to the thenar eminence (lower figures) according to the diameter of the contact area (— 12.5-mm, — 25.0-mm, — 37.5-mm; — measured, ---- predicted).

At high frequencies, for the same material and same contact area, the transmissibilities to the palm were lower than the transmissibilities to the thenar eminence ($p < 0.001$; Friedman).

The transmissibilities of the three glove materials to the palm and to the thenar eminence are shown for individual subjects in Figures 5-8, 5-9 and 5-10.

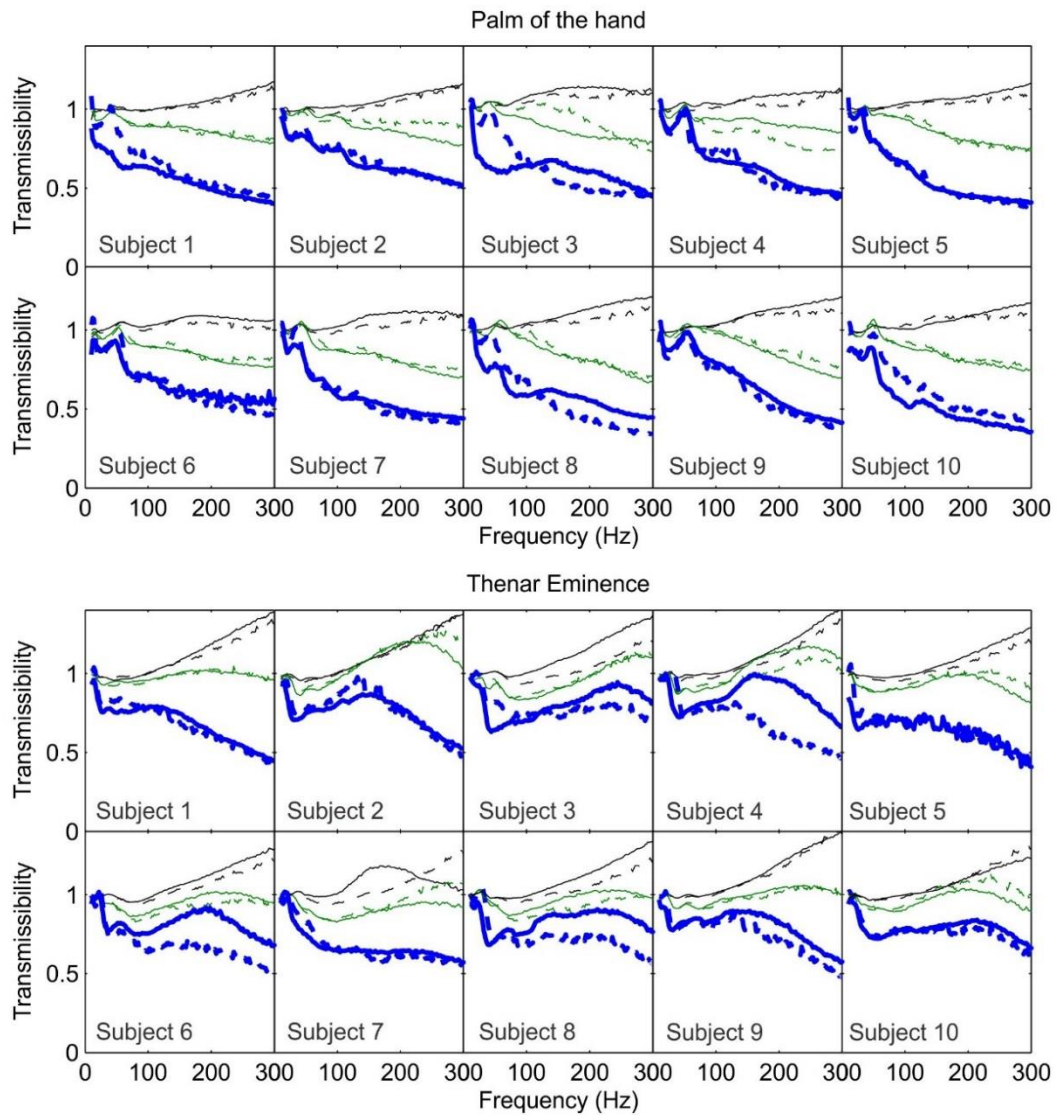


Figure 5-9 Individual transmissibility (predicted and measured) of Foam B to the palm (upper figures) and the thenar eminence (lower figures) according to the diameter of contact area (— 12.5-mm, — 25.0-mm, — 37.5-mm; — measured, ---- predicted).

The mean overall transmissibilities of the glove materials are shown in Table 5.3 (calculated using Equation 5.1). The mean overall transmissibilities of the glove materials

to both locations, palm and thenar eminence, reduced as the diameter of the contact area decreased from 37.5 to 12.5 mm.

Table 5-3 Overall transmissibility of the three glove materials to the hand. Means and standard deviations for 10 subjects.

Glove material	Diameter of contact area (mm)	Palm of the hand		Thenar eminence	
		Mean overall transmissibility	Standard deviation	Mean overall transmissibility	Standard deviation
Foam A	12.5	0.812	0.098	0.848	0.040
	25.0	0.896	0.025	0.887	0.027
	37.5	0.935	0.025	0.940	0.023
Foam B	12.5	0.857	0.048	0.873	0.050
	25.0	0.980	0.021	0.964	0.011
	37.5	0.994	0.014	0.998	0.010
Gel A	12.5	0.916	0.022	0.905	0.035
	25.0	0.976	0.022	0.962	0.023
	37.5	0.999	0.013	1.008	0.017

5.3.4 Predicted material transmissibilities to the palm and to the thenar eminence

The predicted transmissibilities are compared with the measured transmissibilities for individual subjects and Foam A, Foam B, and Gel A in Figures 5-8, 5-9 and 5-10, respectively.

For Foam A and Gel A, with the two larger contact areas the transmissibilities predicted for individual subjects are similar to the measured transmissibilities (Figures 5-8 and 5-

10). There are some discrepancies for both materials and both locations with the smaller contact area (12.5-mm diameter).

With Foam B, for all contact areas, the transmissibilities predicted for individual subjects can be seen to reflect how the measured transmissibility depends on individual variability in apparent mass and increasing dynamic stiffness with increasing contact area (Figure 5-9).

For all three materials, the predicted median transmissibilities to the palm of the hand and to the thenar eminence (predicted from the measured individual apparent masses at the palm and the thenar eminence and the measured dynamic stiffnesses of the materials) were similar to the measured median transmissibilities (Figure 5-11).

For the measured and the predicted transmissibilities to both locations, there is a progressive increase in glove transmissibility at higher frequencies as the contact area increased from 12.5 to 37.5 mm (Figure 5-11).

5.4 Discussion

5.4.1 Apparent mass at the palm and at the thenar eminence

The dynamic response of the soft tissue adjacent to the point of contact dominates the apparent mass of the hand at high frequencies (Dong *et al.*, 2005, Adewusi *et al.*, 2012), because high frequency vibration is not greatly transmitted to more distant locations. In the present study it was therefore hypothesised that increasing the contact area would increase the apparent mass at both the palm and the thenar eminence. At low frequencies, vibration is transmitted to the greater masses of the hand and arm, so the apparent mass of the soft tissue close to the point of contact has a smaller influence on the total apparent mass of the hand, and so changes in contact area have less effect on the apparent mass at low frequencies (see Figure 5-6).

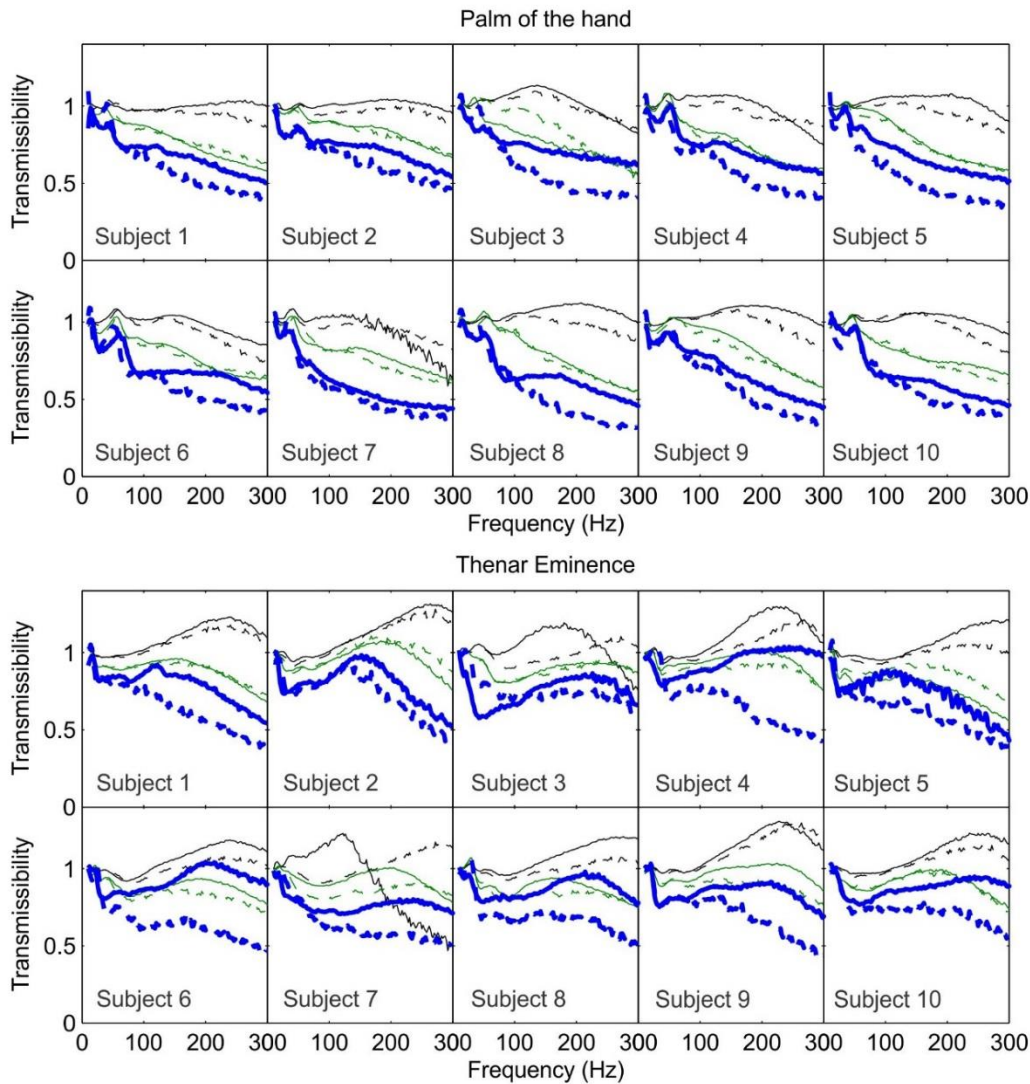


Figure 5-10 Individual transmissibility (predicted and measured) of Gel A to the palm (upper figures) and the thenar eminence (lower figures) according to the diameter of contact area (— 12.5-mm, — 25.0-mm, — 37.5-mm; — measured, ---- predicted).

The apparent mass measured at the palm of the hand in this study is similar to that reported for the palm in previous studies with similar conditions (i.e., similar contact area, contact force, direction of vibration excitation, and posture of the hand; Figure 5-12) but different subjects (Chapter 4). Even with the largest contact area, the apparent mass is less than the apparent mass measured in the horizontal axis of the hand gripping a handle (Dong *et al.*, 2005) and less than the horizontal axis apparent mass of the flat hand pushing down on a flat surface (Xu *et al.*, 2011) at frequencies up to 300 Hz. This is consistent with the combination of a greater contact area and a greater contact force

increasing the apparent mass, as well the direction of vibration excitation and posture having an influence.

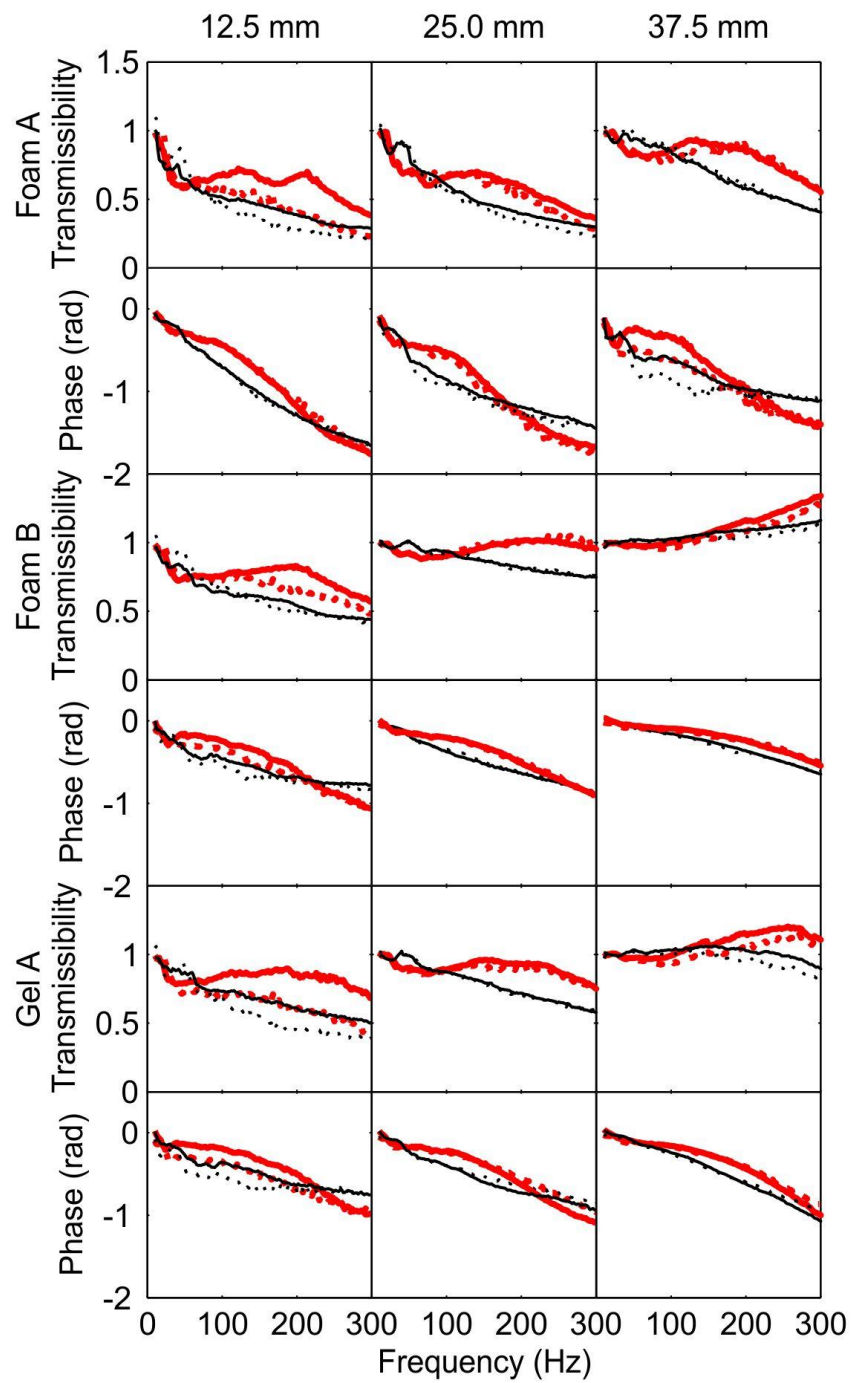


Figure 5-11 Median transmissibility (predicted and measured) with Foam A, Foam B, and Gel A to the palm and to the thenar eminence according to the diameter of the contact area (— measured thenar eminence, predicted thenar eminence, — measured palm, predicted palm). Median values from 10 subjects.

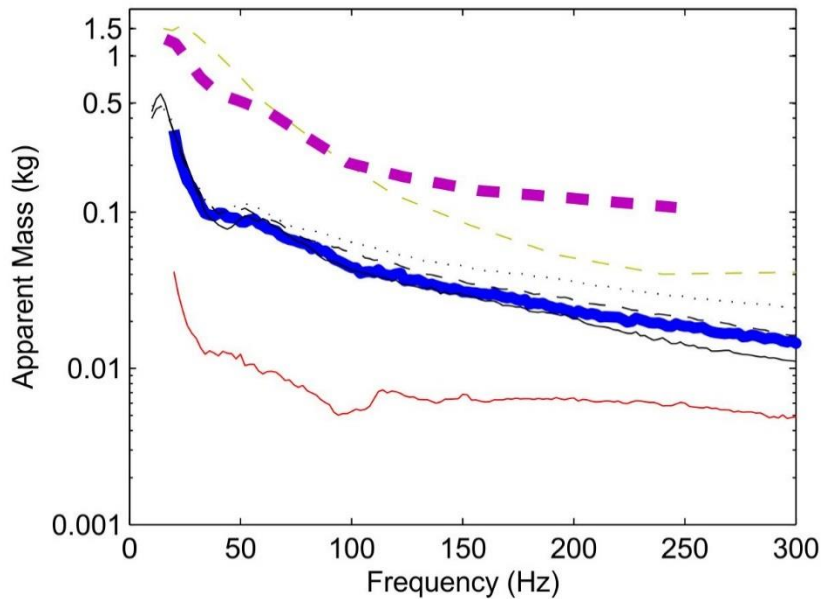


Figure 5-12 Median measured apparent mass at the palm of the hand with a force of 10 N, in the vertical direction. This study (— 12.5-mm, ---- 25.0-mm, 37.5-mm); — palm pushing a flat surface at 10 N on a 25-mm diameter plate, vertical direction, Rezali and Griffin (2014); — index finger pushing a flat surface at 10 N on a 25-mm diameter plate, vertical direction, Rezali and Griffin (2014); - - - palm pushing a cylindrical handle with adapter at 50 N, horizontal direction, Dong *et al.* (200); and - - - full-hand pushing on flat surface, horizontal direction, Xu *et al.* (2011).

5.4.2 Effect of apparent mass and dynamic stiffness on material transmissibility

Although both the hand and a material are complex dynamic systems, some simple approximations may provide useful indications of how transmissibility will depend on material dynamic stiffness and the apparent mass of the hand, and therefore the area of contact. At the higher frequencies, the transmissibility of a glove material will tend to increase if there is an increase in the material dynamic stiffness and decrease if there is an increase in the apparent mass of the hand. For all three materials in this study, the transmissibilities to the palm of the hand increased with increasing area of contact. This suggests that with increasing area of contact the increase in material dynamic stiffness had a greater effect on the transmissibility than the increase in apparent mass of the hand.

The softest material, from a glove that passed the test in ISO 10819:1996 (i.e., Foam A), had the least increase in stiffness and damping as the area of contact increased (see Figure 5-4). This resulted in the smallest increase in transmissibility as the area of contact increased (Figure 5-7).

The materials used in this study were solid, of uniform construction, and constant thickness. Increasing the thickness of a glove material can reduce its dynamic stiffness and reduce the transmissibility (see Chapter 4). Reducing the contact area of a material can also reduce its dynamic stiffness and reduce transmissibility. The area of a uniform material might be reduced or the area might be reduced by making the material non uniform (e.g., by the addition of holes or channels or using more than one material).

Since the area of contact can have a large influence on material transmissibility, there are implications for the design of materials used in gloves and the method of testing the transmissibility of gloves. Varying the area of material contacting the hand is a practical way of varying the dynamic response of a glove. To obtain reliable measures of the effectiveness of gloves in attenuating vibration, the area of contact must be well-defined and suitably controlled.

5.4.3 Predicting the effects of contact area on glove transmissibility

The impedance model can predict the effect of material thickness on the transmissibility of materials to the hand (see Chapter 4). This study shows that the model also predicts the effects of the size of the area contact on the transmissibility through materials to the hand.

In Figure 5-11, the measured transmissibilities of Foam A and Gel A to both locations with 12.5-mm diameter contact area are greater than the predicted transmissibility at high frequencies, especially for the thenar eminence. It is expected that because of the small size of the contact area, there is an overestimation of the measured apparent mass of the hand. The hand might not have been in a stable condition for some participants (i.e., without training) when they were asked to maintain a contact force on a small contact area during vibration exposure.

To better understand the relative importance of the dynamic stiffness of the material and the apparent mass of the hand, the transmissibility of Foam A to the palm of the hand was predicted for three cases: (i) the apparent mass varying with contact area but the dynamic stiffness fixed for a contact area of 12.5 mm, (ii) the dynamic stiffness varying with contact area but the apparent mass fixed for a contact area of 12.5, and (iii) both

apparent mass and dynamic stiffness varying with the area of contact area, as in this study (Figure 5-13).

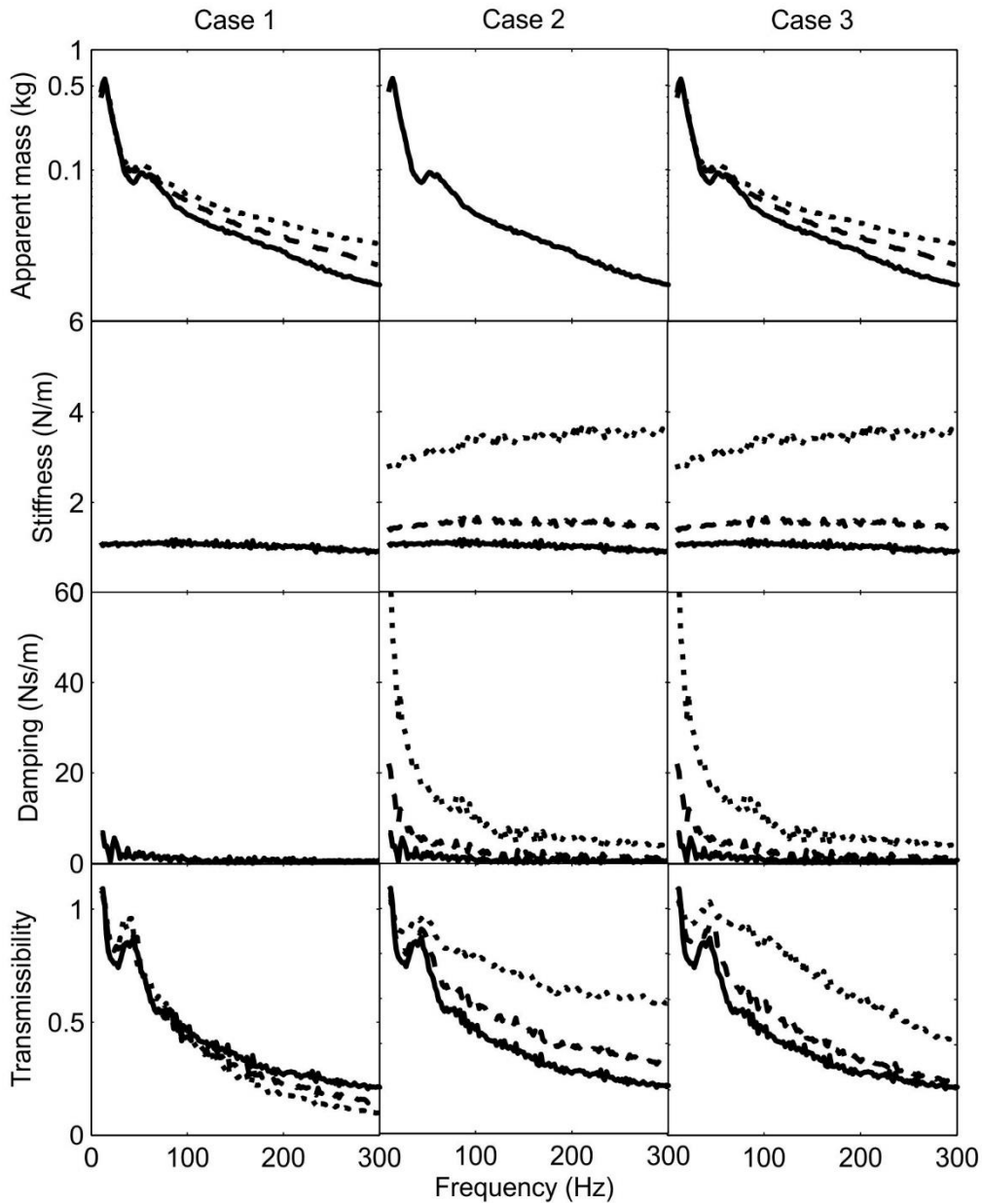


Figure 5-13 The predicted transmissibility (modulus and phase) of the three materials to the palm of the hand for three cases: (i) the dynamic stiffness unaffected by the area of contact, (ii) the apparent mass unaffected by the area of contact, (iii) both apparent mass and dynamic stiffness affected by the area of contact area, as in this study, Diameter of the contact area: — 12.5 mm, ---- 25.0 mm, 37.5 mm. Median values from 10 subjects.

For Case 1, the predicted transmissibility to the palm of the hand decreased at high frequencies as the contact area increased, although the decrease was relatively small.

For Case 2, the predicted transmissibility to the palm of the hand increased with increasing contact area. The increase was large and similar to that in the measured transmissibility (see Figure 5-7).

For Case 3 (i.e., the same as for the predicted transmissibilities in Figure 5-8), the predicted transmissibility to the palm increased with increasing contact area. For areas of contact with diameters of 25 mm and 37.5 mm, the transmissibilities predicted for Case 3 are slightly lower than those predicted for Case 2, due to the increasing apparent mass of the hand with increasing contact area.

5.4.4 Inter-subject variability

The material transmissibilities predicted for individuals from their individual apparent masses were similar to the measured individual transmissibilities (Figures 5-8, 5-9, and 5-10). This shows that, as expected, individual variability in the apparent mass at the palm and at the thenar eminence affect the transmission of vibration through gloves. This has implications for the design of materials used in gloves and the method of testing glove transmissibility. A glove that attenuates or amplifies vibration for one worker may, respectfully, attenuate or amplify vibration for another worker. It might even be possible to predict the effect of wearing a glove for an individual worker (see Chapter 4). To obtain useful measures of the effectiveness of a glove in attenuating vibration, the characteristics of the test subjects should be defined and controlled.

5.5 Conclusions

With increasing area of contact of a glove material with the hand, there are increases in both the dynamic stiffness of the glove material and the apparent mass of the hand (at the area of contact with the palm or the thenar eminence).

For the three materials used in this study, the transmissibility through the material to the hand increased at the higher frequencies when the area of contact increased. This increase in transmissibility is attributed to the increased dynamic stiffness of the material as the contact area increases.

Manipulating the area of contact is a means of modifying the transmissibility of a glove.

It is concluded that the area of contact must be defined and controlled when measuring and evaluating the vibration transmissibility of gloves.

Chapter 6: Transmission of vibration through gloves: Effects of contact force

6.1 Introduction

A glove is required to pass a test specified in International Standard 10819:2013 before it can be considered an 'anti-vibration glove'. In the test, subjects are required to push and grip a cylindrical handle with a push force of 50 N and a grip force of 30 N. In real world conditions, the push force and the grip force can be greater or less than that specified in the standard.

The transmissibility of a glove to the hand can be affected by the contact force (Laszlo and Griffin, 2011, Kuczyński, 2014). With increasing contact force, it has been reported that the transmissibility of a glove may increase (Laszlo and Griffin, 2011) although this is not always the case (O'Boyle and Griffin, 2004). The effects of force on glove transmissibility is expected to be complex, because the transmissibility depends on the dynamic stiffness of the glove material and the dynamic response of the hand, and both of these can vary with the applied force.

The resonance frequency in the apparent mass of the hand increases with increasing force (Burstrom, 1997; Riedel, 1995; O'Boyle and Griffin, 2004; Marcotte *et al.*, 2005; Xu *et al.*, 2011). The increase in the resonance frequency increases the apparent mass of the hand at frequencies greater than the resonance frequency. This increase in apparent mass can be expected to reduce glove transmissibility at frequencies greater than the resonance frequency, provided the dynamic stiffness of the material is not changed by the increase in force.

In practice, increasing the force applied to a glove can increase the dynamic stiffness of the glove material (e.g., O'Boyle and Griffin 2004). The increase can be small or large depending on the material properties. In the extreme, the contact force can be sufficient to cause the material to 'bottom out', so that the transmissibility is close to unity at all frequencies of interest. It has been shown that glove transmissibility tends to increase with increasing dynamic stiffness of the glove material (Rezali and Griffin 2014). The transmissibility of a glove may therefore be expected to increase when the applied force increases, due to an increase in glove dynamic stiffness.

This study investigated the effects of contact force on the dynamic response of the hand, the dynamic stiffness of glove materials, and the transmissibility of the glove materials to the hand. The measurements were made at two different locations: the centre of the

palm, and the tip of the index finger. It was hypothesised that at frequencies greater than the principal resonance the overall apparent mass of the hand at both locations (palm or index finger) would increase with increasing force. The dynamic stiffnesses of the glove materials were expected to increase at all frequencies as the force increased. Depending on the frequency of vibration, as the contact force increased, the transmissibilities of the glove materials to the hand were expected to increase or decrease in way that could be predicted from the measured changes in apparent mass and dynamic stiffness.

6.2 Methods

6.2.1 Glove materials

Three samples of materials, two foams and a gel (denoted as Foam A, Foam B and Gel A), with thicknesses of 6.4, 6, and 5 mm, respectively, were used.

6.2.2 Subjects

Ten subjects aged 24 to 42 years participated in the experiment. The characteristics of the subjects are shown in Table 6-1. The experiment was approved by the Ethics Committee of the Faculty of Engineering and the Environment at the University of Southampton (reference number 8824).

Table 6-1 Characteristics of the subjects in the experiment.

Physical Forms	Range	Median
Age (years)	24 – 42	29
Stature (cm)	160 – 181	167
Weight (kg)	59 – 120	67
Hand circumference (mm)	165 – 230	200
Hand length (mm)	172 – 205	183

6.2.3 Measuring the apparent mass of the hand and the material transmissibility to the hand

When measuring the apparent mass of the hand, subjects placed the palm or the tip of their index finger on the circular wooden adapter (25-mm diameter) and applied a downward push force of 10, 15 or 20 N. The arm was not otherwise supported. The same conditions were used when measuring material transmissibility, by placing the material between the metal plate and the wooden adapter. Please see Section 3.2 for the equipment setup used to measure the apparent mass of the hand.

A 10-s period of random vertical vibration (with an acceleration spectrum from 5 to 500 Hz) was generated using MATLAB (R2011b) with the *HVLab* toolbox (version 1.0). The vibration was presented at a magnitude of 2.0 ms^{-2} r.m.s. (frequency-weighted using W_h according to ISO 5349-1:2001; Figure 6-1).

The order of measuring either apparent mass or transmissibility was balanced, and the orders of presenting the three glove materials and the three forces were randomised.

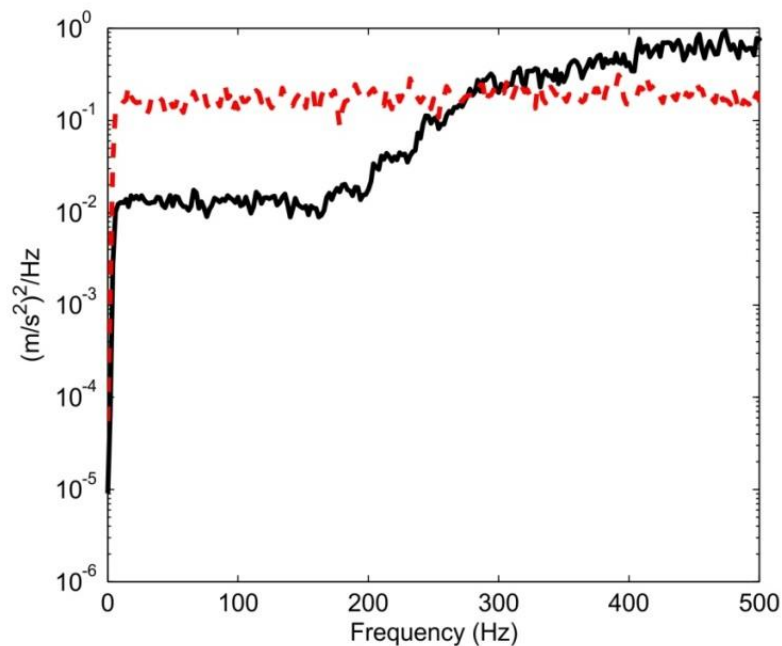


Figure 6-1 Acceleration power spectral densities of the stimuli: --- for the measurement of apparent mass and transmissibility, — for dynamic stiffness measurement. Spectra with 10-Hz resolution.

6.2.4 Measuring the material dynamic stiffness

Using the indenter rig, the dynamic stiffnesses of the glove materials were measured with three preload forces: 10, 15, and 20 N (see Section 3.4 for the equipment setup and procedures used to measure material dynamic stiffness).

A 10-s period of random vertical vibration (with an acceleration spectrum between 5 to 500 Hz as shown in Figure 6-1) was generated using MATLAB (R2011b) with the *HVLab* toolbox (version 1.0). The vibration was presented at a magnitude of 0.75 ms^{-2} r.m.s. (frequency-weighted). The vibration spectrum differed from that used to measure the apparent mass of the hand and the transmissibility of the material, due to the different dynamic conditions: the rigid indenter had impedance very different from that of the hand, so different acceleration was required to obtain easily measurable forces over the range 5 to 500 Hz.

6.2.5 Analysis

Constant bandwidth frequency analysis was performed across the frequency range 10 to 300 Hz with a frequency resolution of 2 Hz and 84 degrees of freedom.

Procedures for the analysis of hand apparent mass, glove transmissibility to the hand and material dynamic stiffness can be found in Section 3.8.

The apparent mass of the hand was calculated with mass cancellation in time domain (see Section 3.8.2).

6.2.6 Impedance model for predicting material transmissibility to the hand and finger

The transmissibility of the material to the hand or finger, $T_h(f)$, was predicted using Equation 3.9.

The apparent mass of the hand, $M_h(f)$ was calculated with mass cancellation in the time domain. For the calculation of the predicted transmissibilities, the mass of the wooden adapters were not included in the mass cancellation. The wooden adapters had a mass of 3g (i.e., 25.0-mm diameter contact area) that added to the apparent mass of the hand and would have influenced the transmissibility of the material.

6.3 Results

The coherencies of all measurements of dynamic stiffness, apparent mass, and transmissibility were greater than 0.8 at all frequencies from 10 to 300 Hz.

6.3.1 Dynamic stiffness and viscous damping of the glove material

The stiffness of all three materials (Foam A, Foam B and Gel A) increased with increasing contact force (Figure 6-2). The damping of Foam A and Foam B was independent of contact force, whereas the damping of Gel A increased with increasing contact force.

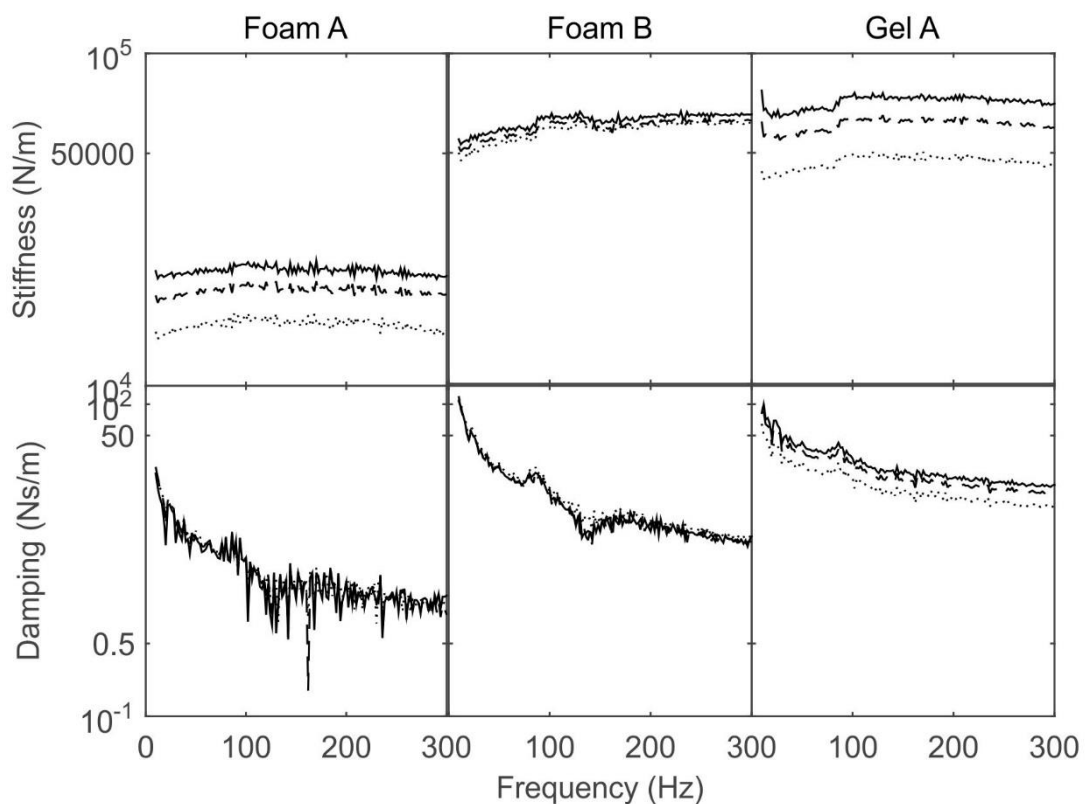


Figure 6-2 Stiffness and damping of the three materials as a function of the preload force in logarithmic scale (..... 10 N, ---- 15 N, ——— 20 N; based on Kelvin Voigt viscoelastic model: see Section 3.8.3).

The increase in the stiffness of Gel A from 10 to 20 N (about 47 to 75% increase) was greater than the increase in the stiffness of Foam A (about 32 to 55% increase) and Foam B (about 2 to 12% increase). With 10-N contact force, Foam B had the greatest stiffness, whereas with 20-N contact force, Gel A had the greatest stiffness. With all three forces, Gel A had the greatest damping.

6.3.2 Apparent mass at the palm and at the index finger

Figure 6-3 shows the inter-subject variability in the apparent mass measured at the palm and at the tip of the index finger.

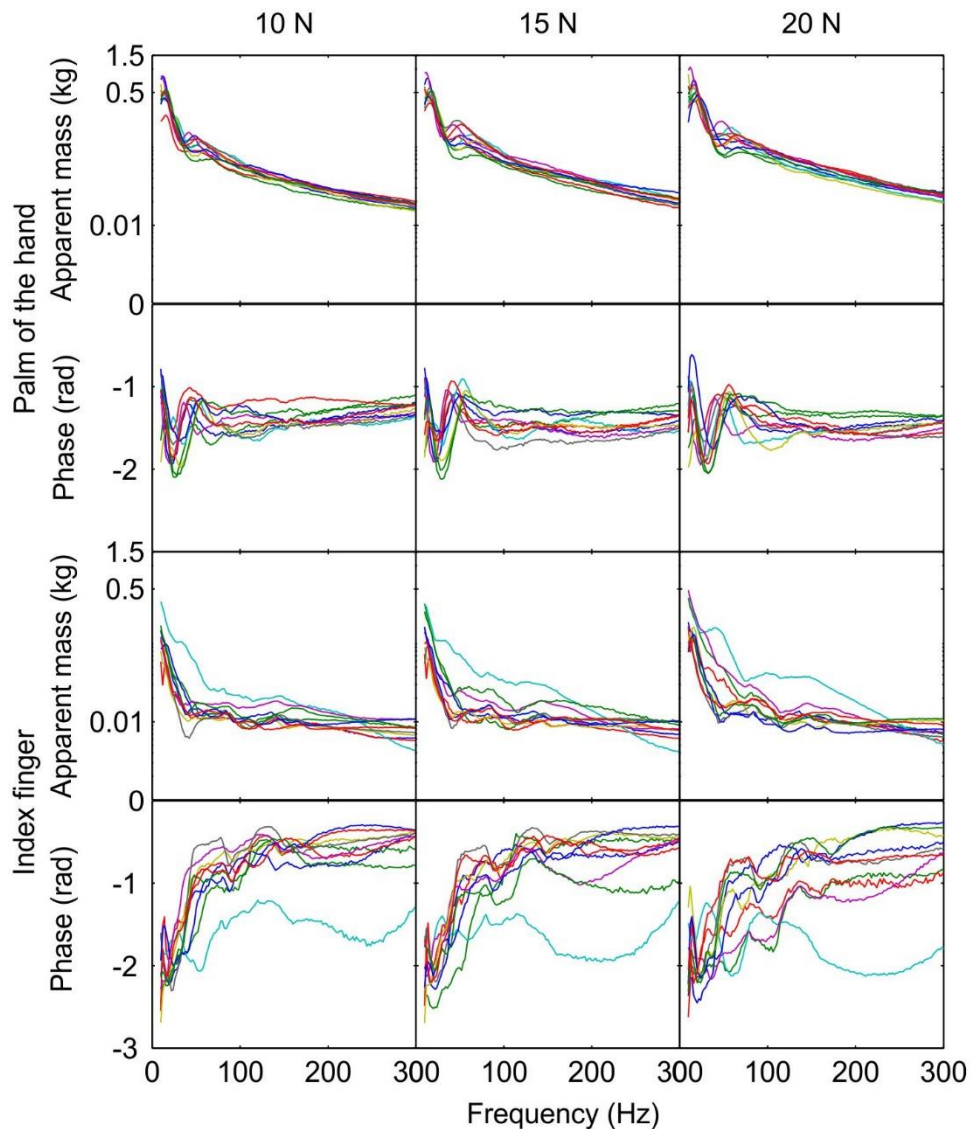


Figure 6-3 Apparent mass (modulus and phase; modulus in logarithmic scale) at the palm of the hand and at the tip of the index finger as a function of frequency and contact force. (Individual data for 10 subjects).

The median resonance frequency in the apparent mass at the palm of the hand increased from 14, to 16 and 18 Hz as the force increased from 10, to 15 and 20 N (Figure 6-4; Friedman $p=0.0004$). At frequencies greater than about 56 Hz, the apparent mass at the palm increased with increasing contact force (Figure 6-4; Friedman $p<0.007$).

At frequencies less than 50 Hz, the median apparent mass at the tip of the index finger increased as the force increased (Figure 6-4; Friedman $p < 0.05$). The apparent mass at the index finger was independent of contact force at frequencies greater than 50 Hz (Figure 6-4; Friedman $p > 0.05$) with the exception of frequencies between 60 to 70 Hz (Friedman $p < 0.045$).

At all frequencies and with all three forces, the apparent mass was greater at the palm than at the index finger.

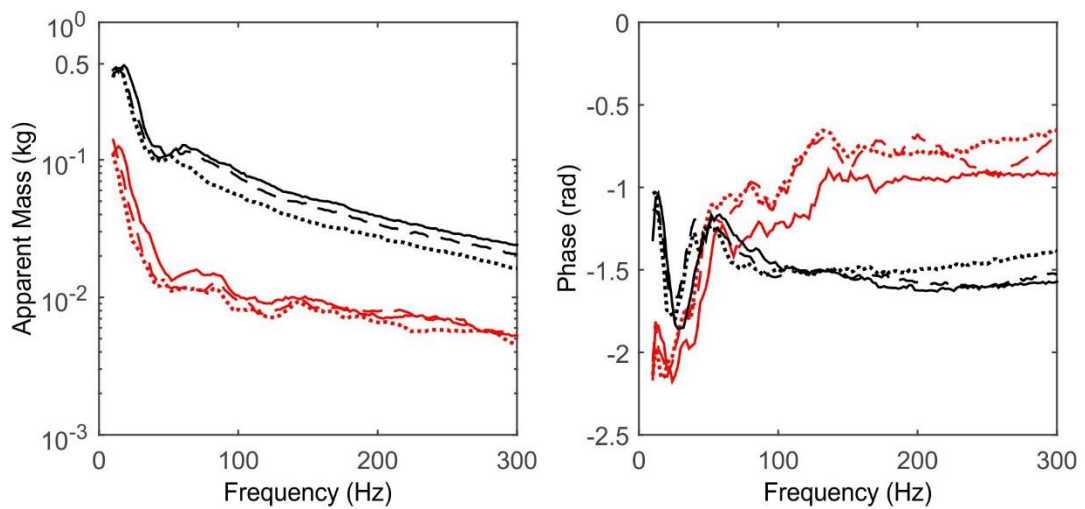


Figure 6-4 Apparent mass at the palm and at the index finger with contact force of 10, 15, and 20 N (—: Palm, —: Index finger, 10 N, ---- 15 N, — 20 N,).

6.3.3 Transmissibility of glove material to the palm and to the index finger

To the palm of the hand, Foam A had a lower median transmissibility than Foam B and Gel A with all three forces at frequencies greater than 60 Hz (Figure 6-5). The median transmissibilities of the three materials to the hand were less than 1.0 at all frequencies of vibration from 60 to 300 Hz. The transmissibility of Gel A was independent of contact force at all frequencies of vibration from 10 to 300 Hz (Friedman $p > 0.05$ for Gel A) with the exception of frequencies between 56 and 76 Hz (Friedman $p < 0.0273$). Similarly, the transmissibility of Foam A was not significantly affected by the change in contact force at any frequency from 10 to 300 Hz (Friedman $p > 0.05$), with exception of frequencies from 14 to 30 Hz, 50 to 74 Hz, and 138 to 170 Hz (Friedman $p < 0.05$). However, the transmissibility of Foam B to the palm of the hand reduced as the contact force increased at frequencies greater than 100 Hz (Figure 6-5; Friedman $p < 0.003$).

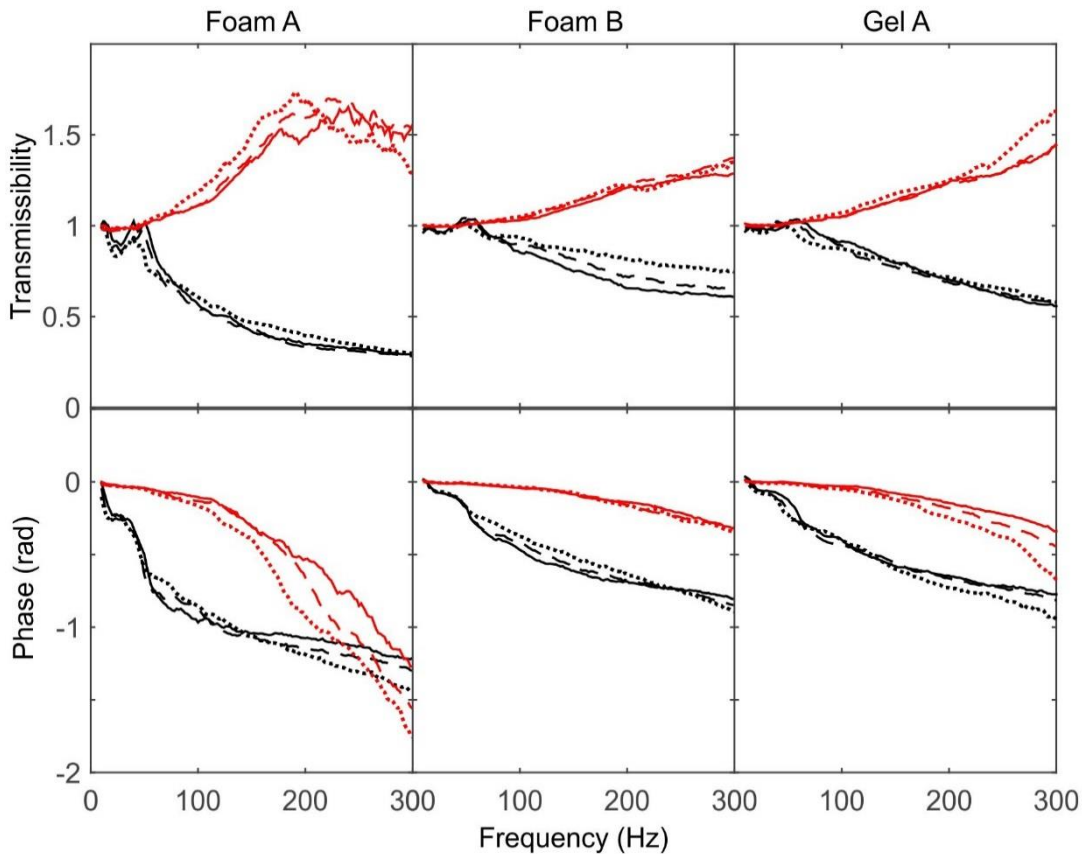


Figure 6-5 Transmissibilities of all materials to the palm and to the index finger (—: Palm, —: Index finger, 10 N, ---- 15 N, — 20 N,)

To the index finger, Foam A had a greater transmissibility than Foam B and Gel A with all three forces at all frequencies of vibration from 10 to 300 Hz (Figure 6-5). All three materials amplified the vibration to the finger at frequencies greater than 100 Hz. The first principal resonance frequency in the transmissibility of Foam A increased with increasing contact force (Friedman, $p=0.006$). For all three materials, the median transmissibility was unchanged at frequencies less than 40 Hz (Friedman, $p>0.06$). The median transmissibility of Gel A was unaffected by the increase in contact force at frequencies greater than 10 Hz (Friedman, $p>0.07$), with exception of frequencies between 100 and 120 Hz (Friedman, $p<0.05$). The median transmissibility of Foam B to the index finger was unchanged as the contact force increased at all frequencies from 10 to 300 Hz (Figure 6-5; Friedman, $p>0.07$), with the exception of frequencies between 40 and 70 Hz (Friedman, $p<0.02$), and 80 and 150 Hz (Friedman, $p<0.03$).

Figures 6-6, 6-7, and 6-8 show individual transmissibilities of glove materials to the palm and to the index finger.

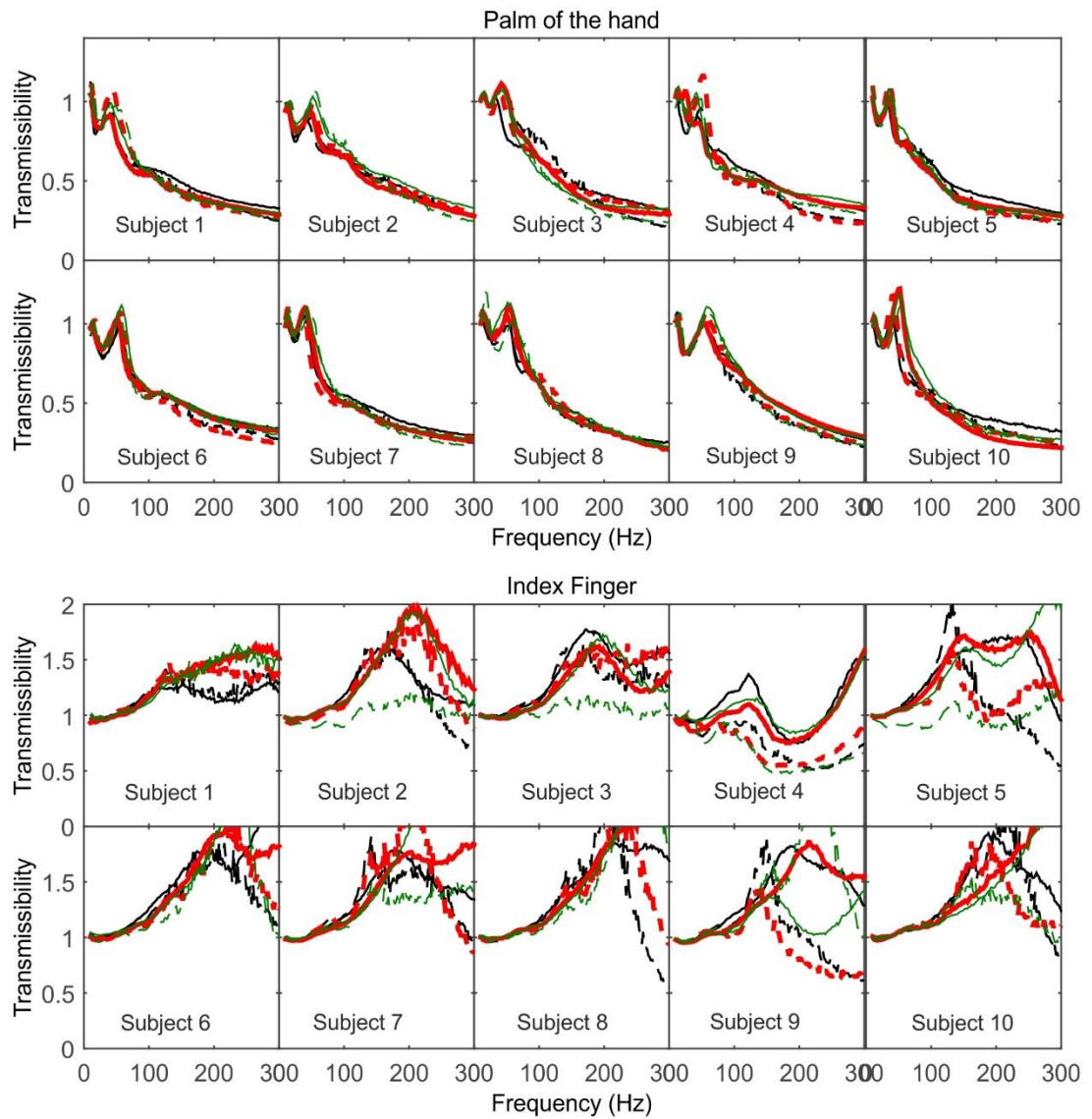


Figure 6-6 Individual transmissibility (predicted and measured) of Foam A to the palm and the index finger according to its contact force (— 10 N, — 15 N, — 20 N; — measured, ---- predicted).

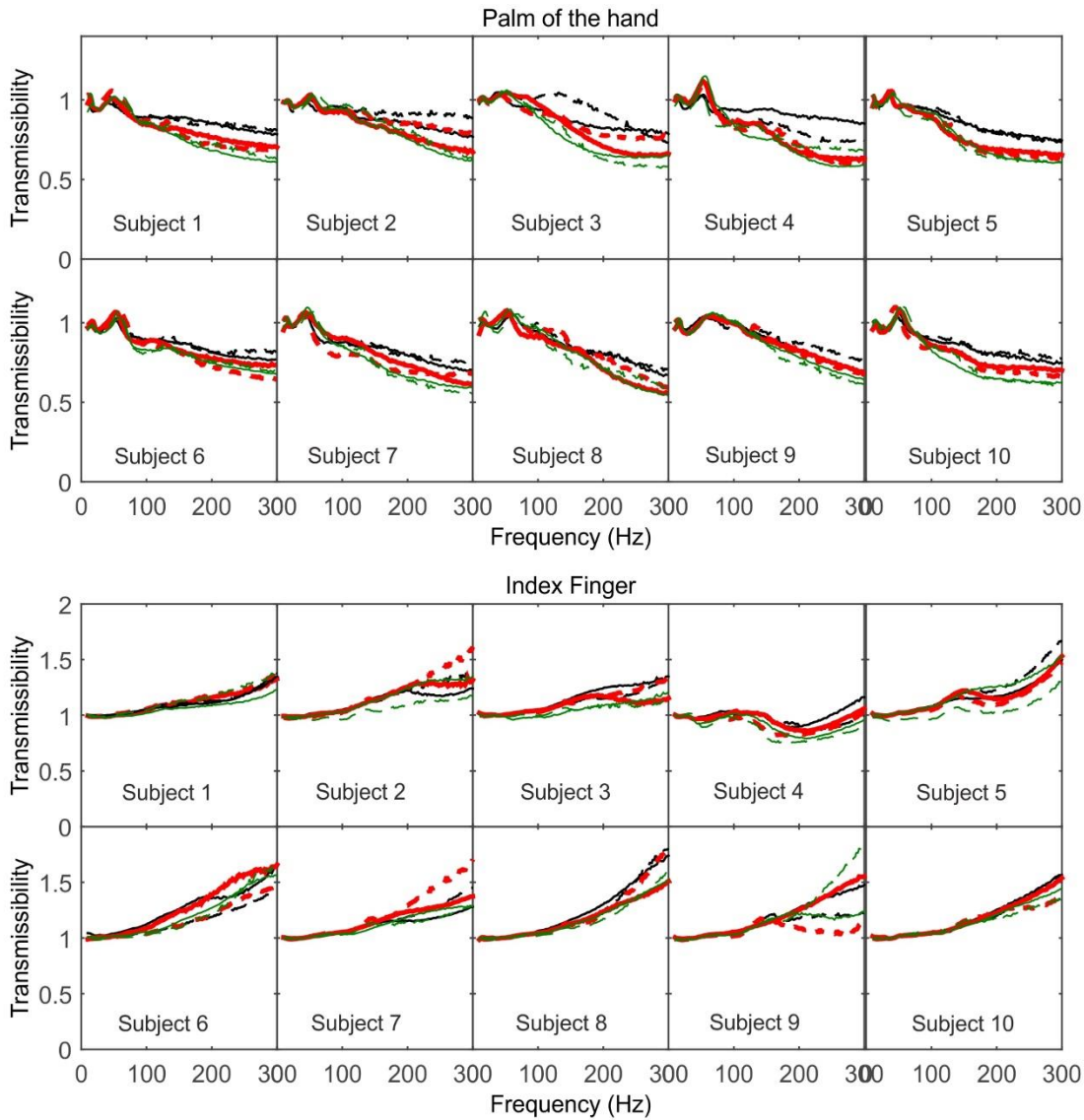


Figure 6-7 Individual transmissibility (predicted and measured) of Foam B to the palm and the index finger according to its contact force (— 10 N, — 15 N, — 20 N; — measured, ---- predicted).

6.3.4 Predicted transmissibility of the glove material to the palm and to the index finger

The measured and predicted transmissibilities are compared for both the median subject (Figure 6-9) and individual subjects (Figures 6-6, 6-7, and 6-8) with Foam A, Foam B and Gel A. The predicted transmissibilities were calculated from the measured dynamic stiffness of the material and the measured apparent mass of the hand or finger.

The predicted transmissibility of Foam A to the palm of the hand with all three contact conditions shows agreement with the measured transmissibility at frequencies less than

150 Hz (Friedman, $p>0.053$) but underestimated the measured transmissibility at frequencies greater than 150 Hz (Friedman, $p<0.05$) especially with a contact force of 10 N (Figure 6-9). The transmissibility of Foam B to the palm of the hand with all three contact conditions is similar with the measured transmissibility at all frequencies from 10 to 300 Hz (Friedman, $p>0.0533$). The predicted transmissibility of Gel A to the palm of the hand with all three contact conditions is similar to the transmissibility measured experimentally at all frequencies from 10 to 300 Hz (Friedman, $p>0.05$).

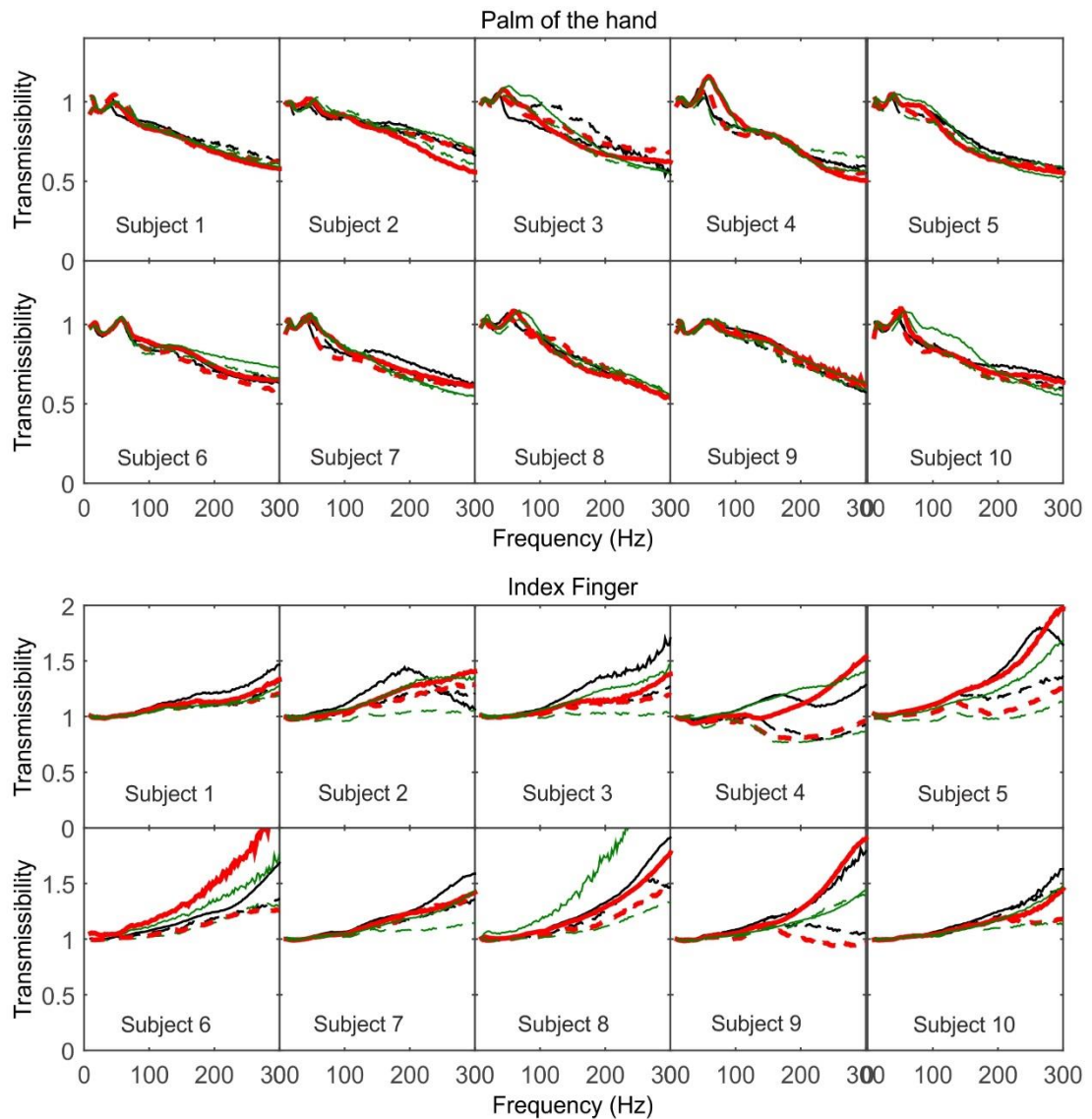


Figure 6-8 Individual transmissibility (predicted and measured) of Gel A to the palm and the index finger according to its contact force (— 10 N, — 15 N, — 20 N; — measured, ---- predicted).

The predicted transmissibilities to the index finger underestimated the measured transmissibilities with all three contact forces at frequencies greater than 90 Hz for Foam A (Friedman, $p < 0.031$) and at frequencies greater than 40 Hz for Gel A (Friedman, $p < 0.05$). However, the predicted transmissibility to the index finger for Foam B is similar to the measured transmissibilities with all three forces at all frequencies from 10 to 300 Hz (Friedman, $p > 0.05$), with exception of frequencies between 80 to 112 Hz (Friedman, $p < 0.02$).

6.4 Discussion

6.4.1 Dynamic stiffness of the glove materials

The effects of contact force on the dynamic stiffness of a material is complex and may require a measurement to predict the effect accurately. The area of contact used in this study was smaller than the area of contact specified in ISO 10819:2013. It is expected that the increase in the dynamic stiffness of glove materials with increasing contact force could be greater than measured in this study if the area of contact is larger than in this study.

In this study, as the contact force increased, Gel A had a greater change in stiffness and damping than the other materials. Foam B had the greatest stiffness with 10 N contact force but as the contact force increased, the material that had the greatest stiffness changed to Gel A. The changes in glove dynamic stiffness as the contact force increased indicated that the transmissibility of a glove could be affected by the contact force.

6.4.2 Apparent mass at the palm and at the finger

The apparent mass at the palm of the hand increased with increasing contact force at frequencies greater than 56 Hz. This trend is consistent with the findings of previous studies (O'Boyle and Griffin, 2004, Xu *et al.*, 2011) but occurred at a higher frequency (i.e., it may be due to the greater push force or wider range of push force that both studies employed). An increase in the contact force can be expected to increase the coupling of the arm, the hand, and the fingers with the driving point of the vibration. This resulted in an increase in the resonance frequency in the apparent mass at the palm, with an associated increase in apparent mass at higher frequencies, as the contact force increased (Figure 6-4).

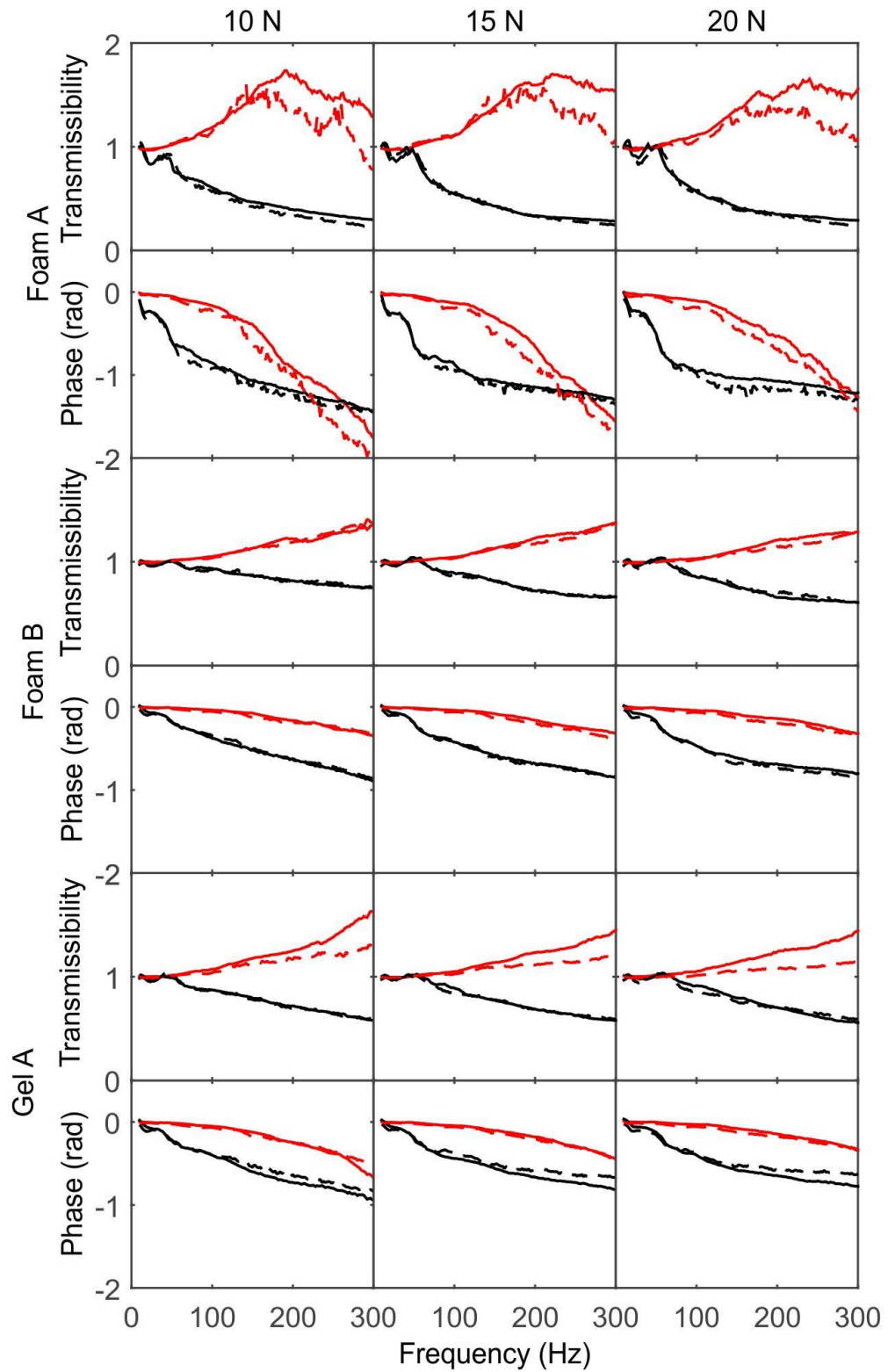


Figure 6-9 Transmissibility (predicted and measured) for Foam A, Foam B, and Gel A to the palm and to the index finger according to contact force (—: Palm, —: Index finger, ---- predicted, — measured) Median values from 10 subjects.

Similar to the palm of the hand, the coupling of the hand, the arm and the fingers increased with increasing contact force applied by the finger, so the apparent mass at the index finger increased with increasing contact force at frequencies greater than the resonance. However, the effect of contact force on the apparent mass at the index finger seemed to be less than at the palm and not statistically significant at frequencies greater than 70 Hz.

It can be concluded that the changes in apparent mass at the palm and at the fingers as the contact force increased indicated that the transmissibility of a glove could be affected by the contact force.

The apparent mass measured at the palm and at the index finger is compared with the apparent mass measured in previous studies (Figure 6-10). The apparent mass at the palm of the hand with 30-N contact force measured in this study is less than the apparent mass at the palm measured with 50-N contact force on a cylindrical handle at all frequencies of vibration (Dong *et al.*, 2005). The apparent mass at the palm and at the index finger in this study is similar to the apparent mass measured in previous studies that have similar contact conditions (i.e. similar contact force, contact area, and posture; O'Boyle and Griffin, 2004; Chapter 4; Chapter 5) but with different subjects.

6.4.3 Effect of contact force on the transmissibility of the glove materials to the palm and to the fingers

Similar to the trend reported in a previous study (O'Boyle and Griffin, 2004), increasing the contact force had little effect on the transmissibility of Foam A or Gel A to the palm of the hand. It seems that as the contact force increased the increase in the apparent mass at the palm and the increase in the dynamic stiffness (of Foam A and Gel A) resulted in little or no effect on glove transmissibility. However, the stiffness and damping of Foam B were not significantly affected by an increase in the contact force, and so the increase in apparent mass with increasing force reduced the transmissibility to the palm of the hand.

Previous chapters of this research have shown that increasing the dynamic stiffness of the glove material will increase the resonance frequency in the glove transmissibility (Chapter 4; Chapter 5). In this study, the contact force had little effect on the apparent mass of the index finger, so it was expected that the increase in the dynamic stiffness of glove materials with increasing force will tend to increase the resonance frequency and increase glove transmissibility to the index finger at frequencies greater than the

resonance. This was observed for Foam A. For Gel A and Foam B the resonance in the transmissibility to the index finger occurred at frequencies greater than 300 Hz and so the effect of contact force on the resonance frequency with either material could not be identified.

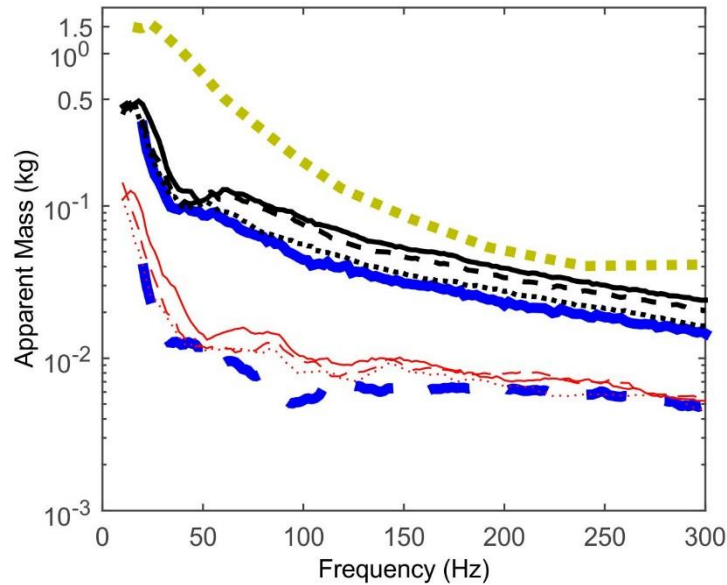


Figure 6-10 Median measured apparent mass at the palm of the hand, z direction, this study (— 20 N, ---- 15 N, 10 N); median measured apparent mass at the index finger, z direction, this study (— 20 N, ---- 15 N, 10 N), Palm pushing a flat surface at 10 N on a 25-mm diameter plate (—), z-direction, Rezali and Griffin (2014), Index Finger pushing a flat surface at 10N on a 25-mm diameter plate (—), z-direction, Rezali and Griffin (2014), and Palm pushing a cylindrical handle with adapter at 50 N (.....), x-direction, Dong et al (2005).

As the contact force increases, the increase in the dynamic stiffness of the material is expected to be greater with wider materials as mentioned previously. With wider materials, the effect of contact force will tend to predominantly be due to the increase in the glove dynamic stiffness rather than both the glove dynamic stiffness and apparent mass of the hand as seen in this study: increasing the contact force will tend to increase the glove transmissibility to the palm of the hand (Laszlo and Griffin, 2011).

6.4.4 Predicting the effects of contact force on glove transmissibility

Both the apparent mass of the hand and the dynamic stiffness of the glove materials were affected by an increase in the contact force. The transmissibilities of each of the three materials reflected the combined effect changes in the dynamic stiffness of the

material and changes in the dynamic response of the hand, but in different ways (see Section 6.4.3).

To better understand the importance of combined increases in the apparent mass and the dynamic stiffness on transmissibility as the contact force increases, the transmissibility of Foam A to the palm of the hand was predicted for three cases (Figure 6-11) : i. The dynamic stiffness varying with contact force but the apparent mass fixed at that measured with a contact force of 10 N; ii. The apparent mass varying with contact force but the dynamic stiffness fixed at that measured with a contact force of 10 N; iii. Both apparent mass and dynamic stiffness varying with contact force, as in this study.

For Case i, the predicted transmissibility to the palm of the hand reduced at high frequencies as the contact force increased. This is similar to the effect of contact force on the transmissibility of Foam B to the palm of the hand as measured in this study (Figure 6-5).

For Case ii, the predicted transmissibility to the palm of the hand at frequencies greater than the first resonance increased with increasing contact force. This trend is similar to the trend reported previously with various gloves (Laszlo and Griffin, 2011).

For Case iii (i.e. the same as for the predicted transmissibility of Foam A and Gel A in Figure 6-10), as the contact force increases the predicted transmissibility to the palm of the hand is unchanged at high frequencies. It may be concluded that the increase in the apparent mass cancelled the increase in the material dynamic stiffness, resulting in no effect of contact force as discussed in Section 6.4.3.

The contact force can have a large influence on transmissibility of a glove although this depends on the static and dynamic properties of the glove material. It would be useful to investigate the effects of contact force on area larger than in this study to understand better the performance of a glove in attenuating vibration to the hand. In this study, the range of force was chosen to be suitable for materials with small area of contact.

6.5 Conclusions

Increasing contact force increases the apparent mass of the hand at frequencies greater than the principal resonance due to increased coupling of the arm, the hand, and the fingers with the vibration driving point. The apparent mass of the fingers also increased with increasing contact force at frequencies less than 50 Hz. The effect of contact force on the apparent mass of the fingers is not significant at frequencies greater than 50 Hz.

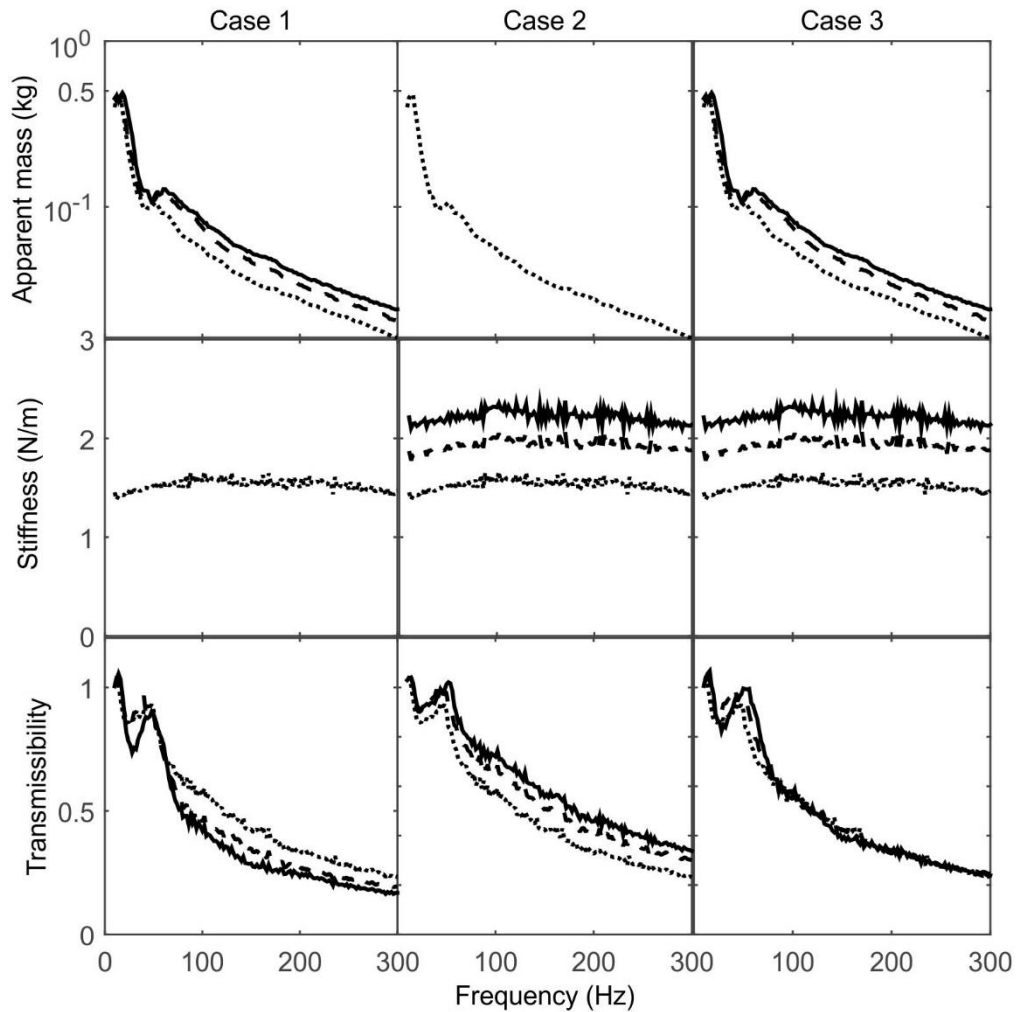


Figure 6-11 The predicted transmissibility (modulus) of Foam A to the palm of the hand for three cases: (case i) the dynamic stiffness unaffected by the contact force, (case ii) the apparent mass unaffected by the contact force, (case iii) both apparent mass and dynamic stiffness affected by the area of contact area, as in this study, according to the contact force conditions (..... 10 N, ---- 15 N, ——— 20 N). Median values from 10 subjects.

Increasing contact force will tend to increase the stiffness and damping of the glove material but any increase is likely to be non-linear and depend on material properties.

The resonance frequency in the transmissibility of a material to the hand is expected to either increase (due to the increase in the material dynamic stiffness) or decrease (due to the increase in the apparent mass of the hand) as the contact force increases. This tends to result in either a lower or a higher transmissibility, respectively, at frequencies greater than the resonance.

In this study, transmissibilities of Foam A and Gel A to the palm of the hand were little affected by increases in contact force. The transmissibility of Foam B to the palm of the hand reduced as the contact force increased at frequencies greater than 100 Hz. For all three materials, as the contact force increased the transmissibility to the index finger was not significantly affected at frequencies less than 40 Hz.

The measured and predicted performance of a glove in attenuating vibration has been shown to vary depending on the force applied to the glove. This study suggested that several combinations of push and grip force are required in order to assess the performance of a glove in attenuating vibration to the hand.

Chapter 7: Transmission of vibration through gloves: Effects of vibration magnitude and arm support

7.1 Introduction

At some frequencies, the vibration transmitted to the palm of the hand may be attenuated by a glove (Wu and Griffin, 1989; Dong et al., 2014). Before it can be considered an 'anti-vibration glove' the attenuation of vibration must be greater than 10% for a spectrum from 25 to 200 Hz and greater than 40% for a spectrum from 200 to 1250 Hz (International Standard ISO 10819:2013). The attenuation is measured with specific magnitudes of vibration and with the hand and arm in a specific posture. The input vibration is based on a flat velocity spectral density with a weighted r.m.s. acceleration of 4.82 m/s^2 . The arm is required to be in bent-arm position facing the vibrator horizontally. When exposed to the vibration from hand-held vibratory tools, both the vibration magnitude and the arm posture can be very different from that in the standardised test for anti-vibration gloves.

Two primary factors affect the transmissibility of a glove: the driving-point mechanical impedance of the hand and the dynamic stiffness of the glove material. To predict glove transmissibility, an understanding of the effects of arm support on the mechanical impedance of the hand, and the effects of vibration magnitude on material dynamic stiffness, mechanical impedance of the hand, and glove transmissibility is needed.

The dynamic response of the hand (e.g., mechanical impedance or apparent mass) can be affected by arm posture (Burström, 1997; Aldien et al., 2006; Adewusi et al., 2010). The apparent mass of the hand with extended arm posture was significantly greater than with a bent arm posture at frequencies less than 30 Hz (Aldien et al., 2006). At frequencies less than 20 Hz, the mechanical impedance of the hand decreases as the angle between the upper-arm and the shoulder decreases (i.e., the arm is bent; Burström, 1997). However, these studies only show the influence of the upper-arm on the mechanical impedance of the hand: it is not clearly evidenced whether the lower-arm also influences the impedance of the hand at those frequencies (i.e., less than 30 Hz).

If the dynamic response of a system (e.g., the apparent mass of the hand or the dynamic stiffness of a glove) is dependent on the magnitude of vibration, it is said to be nonlinear. If the transmissibility of glove is greatly dependent on the magnitude of vibration, standardised tests at one magnitude will not give reliable indications of the transmissibility at other magnitudes. The apparent mass of the human body tends to be

highly nonlinear: the resonance frequency in the vertical apparent mass of the body decreases as the magnitude of vibration increases (e.g., Fairley and Griffin, 1989). The effect of vibration magnitude on the dynamic response of the hand has received less attention. There is some evidence of nonlinearity in the apparent mass of the hand, although the nonlinearity may be small at frequencies greater than 100 Hz (e.g., Lundström *et al.*, 1989; Gurram *et al.*, 1995; Burström, 1997; Marcotte *et al.*, 2005).

If the dynamic response of the hand changes according to the magnitude of vibration or the posture of the arm, this will affect the vibration transmissibility of a glove worn on the hand. However, the effects of vibration magnitude and arm posture on glove transmissibility have received little attention. One study found the transmissibility of a glove decreased with increasing magnitude of vibration, but the effect was only apparent in one of four gloves tested (Laszlo and Griffin, 2011).

A mechanical impedance model of the apparent mass of the hand and the dynamic stiffness of glove materials can provide useful predictions of the vibration transmissibility of gloves worn on the hand (O'Boyle and Griffin, 2004; Chapters 4, 5, and 6). It might therefore be assumed that if any two of the three parameters (i.e., apparent mass, dynamic stiffness, or transmissibility) are known, the other parameter can be predicted. For example, the impedance model may be able to predict the apparent mass of the hand from the dynamic stiffness of the glove and the transmissibility of the glove worn on the hand. This could provide the apparent mass of the hand for the complex hand grips used on tools for which the measurement of apparent mass is difficult. When the apparent mass is known for such a posture, the dynamic stiffness of a material could be optimised to minimise the transmission of vibration to the hand in that posture.

This study investigated the effects of vibration magnitude and arm support on the transmissibility of glove materials to the palm of the hand. The transmissibility of the materials, the dynamic stiffness of the materials, and the apparent mass measured at the palm of the hand are presented and discussed. It was hypothesised that the resonance frequency in the apparent mass at the palm of the hand would decrease with increasing vibration magnitude. So, it was expected that at frequencies greater than the first major resonance, the transmissibility to the palm of the hand increases as the vibration magnitude increases (i.e., the resonance in the apparent mass of the hand was expected to decrease as the magnitude of vibration increased: this will also slightly reduce the apparent mass at frequencies greater than the resonance. The reduced apparent mass of the hand at frequencies greater than the resonance will increase glove transmissibility as discussed in Chapter 4). At frequencies less than about 30 Hz, the

apparent mass at the palm measured with arm support is expected to be less than the apparent mass at the palm measured without arm support. Consequently, glove transmissibility at frequencies less than 30 Hz is expected to be greater with arm support than without arm support.

7.2 Method

7.2.1 Glove materials

Three materials (two foams and a gel denoted as Foam A, Foam B, and Gel A), were used in this study. All materials had a diameter of 25 mm and weighed less than 2 grams.

7.2.2 Subjects

Twelve subjects aged 22 to 45 years participated in the experiment. The characteristics of the subjects are shown in Table 7-1. The experiment was approved by the Ethics Committee of the Faculty of Engineering and the Environment at the University of Southampton (reference number 12038).

Table 7-1 Characteristics of the subjects in the experiment.

Physical Forms	Range	Median
Age (years)	22-42	27.5
Stature (cm)	161-181	167
Weight (kg)	50-85	65
Hand circumference (mm)	166-238	206.5
Hand length (mm)	167-204	179.5

7.2.3 Measuring hand apparent mass and material transmissibility to the hand

During the measurement of hand apparent mass, subjects placed their palms on the wooden adapter (with a diameter of 25 mm) and pushed down until the preload force reached 20 N (as indicated on an oscilloscope) and then maintain this preload force

during vibration exposure. The arm was not otherwise supported. Please see Section 3.2 for the equipment setup used to measure the apparent mass of the hand.

A 10-s period of random vertical vibration (with an acceleration spectrum from 5 to 500 Hz as shown in Figure 7-1) was generated using MATLAB (R2011b) with the *HVLab* toolbox (version 1.0). The vibration was presented at a magnitude of 2.0 ms^{-2} r.m.s. (frequency-weighted using W_h according to ISO 5349-1:2001).

The procedures were repeated with lower and higher magnitudes of vibration (i.e., 1.0 and 4.0 ms^{-2} r.m.s.) and with arm support (with vibration magnitude of 2.0 ms^{-2} r.m.s.). The horizontal arm support was located about 15 cm from the centre of the wooden adapter, in-line with the surface of the wooden adapter. The support was 16.5 cm long and 5 cm wide.

Similar procedures were used to measure the transmissibility of the glove material to the palm of the hand. The glove materials were placed between the wooden adapter in the palm of the hand and the metal plate.

The order of measuring the apparent mass at the palm of the hand and glove transmissibility was balanced and the order of testing the three materials was randomised.

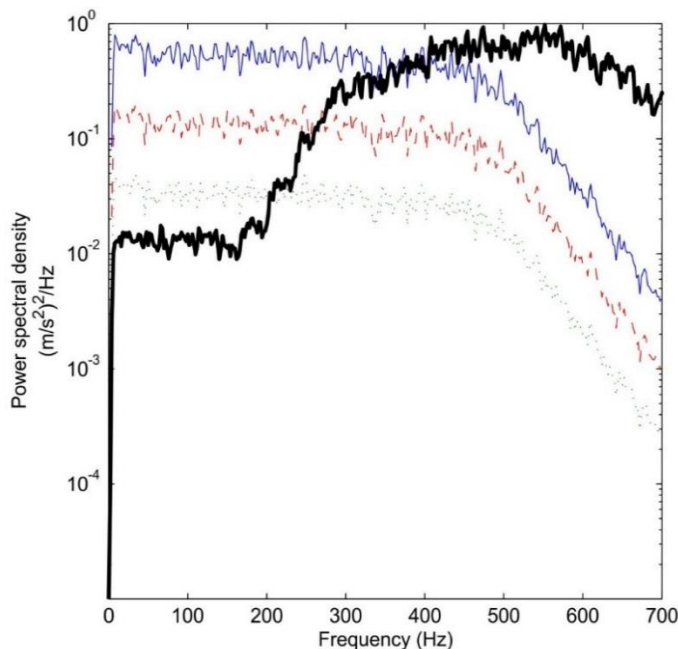


Figure 7-1 Acceleration power spectral densities of the stimuli: 1 ms^{-2} , ---- 2 ms^{-2} , ——— 4 ms^{-2} , for the measurement of apparent mass and transmissibility, ——— for dynamic stiffness measurement. Spectra with 2-Hz resolution.

7.2.4 Measuring the dynamic stiffnesses of the glove materials

The dynamic stiffnesses of the three diameters of the three materials were measured using an indenter rig (see Section 3.4 for the equipment setup and procedures used to measure material dynamic stiffness).

A 10-s period of random vertical vibration (with an acceleration spectrum from 5 to 500 Hz as shown in Figure 7-1) was generated using MATLAB (R2011b) with the *HVLab* toolbox (version 1.0). The vibration was presented at a magnitude of 0.75 ms⁻² r.m.s. (frequency-weighted) using a Derritron VP30 vibrator with a preload force of 20 N.

Glove transmissibility was measured with three vibration magnitudes: 1.0, 2.0 and to 4 m/s² r.m.s. (frequency weighted using W_h). At frequencies from 10 to 500 Hz, the deflection of the material by the vibration during the measurement of glove transmissibility with all three vibration magnitudes was similar to the deflection of the material by the vibration when measuring the dynamic stiffness of the material (i.e., although the magnitudes of vibration were different, at high frequencies, the difference in the deflection of the material by the vibration in both cases was small). In this study, the glove dynamic stiffness was assumed to be not affected by the vibration magnitude.

7.2.5 Analysis

Constant bandwidth frequency analysis was performed across the frequency range 10 to 300 Hz with a frequency resolution of 2 Hz and 84 degrees of freedom.

Procedures for the analysis of hand apparent mass, glove transmissibility to the hand and material dynamic stiffness can be found in Section 3.8.

The apparent mass of the hand was calculated with mass cancellation in time domain (see Section 3.8.2).

7.2.6 Predicting the apparent mass at the palm of the hand

The transmissibility of the material to the hand or finger, $T_h(f)$, was predicted using Equation 3.9.

By rearranging the Equation 3.9, the apparent mass at the palm of the hand can be predicted using the following equation:

$$M_{hw}(f) = \frac{S(f)(T(f)-1)}{\omega^2 T(f)} \quad (7.1)$$

7.3 Results

The coherencies of all measurements of dynamic stiffness, apparent mass, and transmissibility were greater than 0.8 at all frequencies from 10 to 300 Hz.

7.3.1 Dynamic stiffness of the glove materials

The dynamic stiffnesses of the glove materials are compared in Figure 7-2. Foam A was the softest material whilst Gel A was the stiffest material. Gel A had greater damping than the other two glove materials at frequencies greater than 20 Hz.

7.3.2 Apparent mass at the palm of hand

The inter-subject variability in the measurement of the apparent mass is shown in Figure 7-3.

In the frequency range 16 to 100 Hz, the apparent mass at the palm decreased as the vibration magnitude increased (Figure 7-4; Friedman $p < 0.0498$). There was no statistically significant effect of vibration magnitude on the apparent mass at frequencies outside this range (Friedman, $p > 0.05$).

The arm support reduced the apparent mass measured at the palm at frequencies less than the first resonance around 16 Hz (Figure 7-4; Friedman, $p < 0.012$). Although at higher frequencies the median apparent mass was less with the arm support than without the arm support as shown in Figure 7-4, the difference was not statistically significant (Friedman, $p > 0.058$) except at frequencies from 54 to 120 Hz (Freidman, $p < 0.0114$).

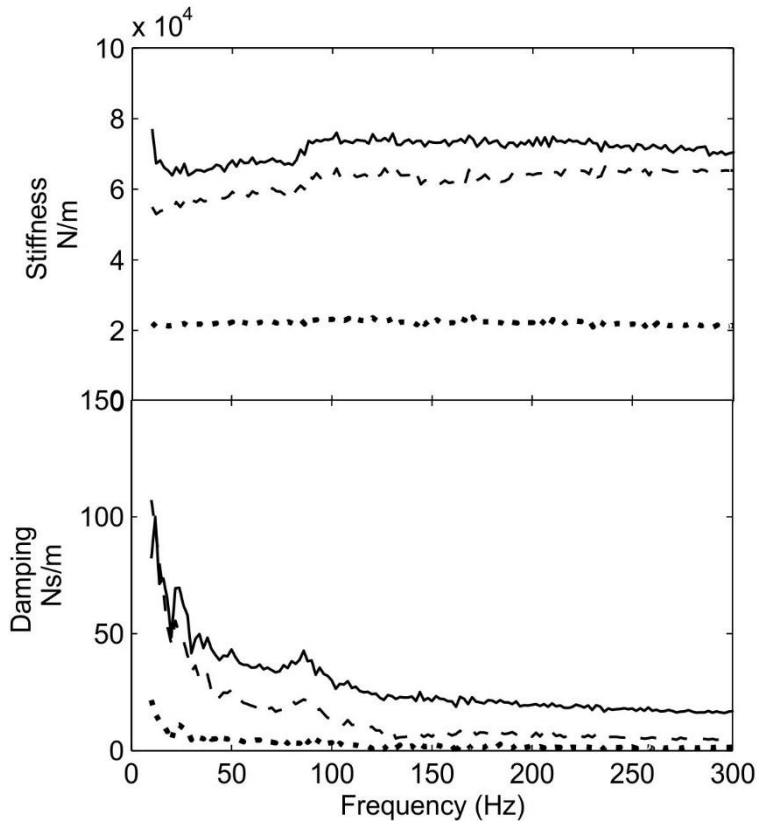


Figure 7-2 Dynamic stiffness of the glove materials (····· Foam A, ---- Foam B, ——— Gel A; based on Kelvin Voigt viscoelastic model: see Section 3.8.3).

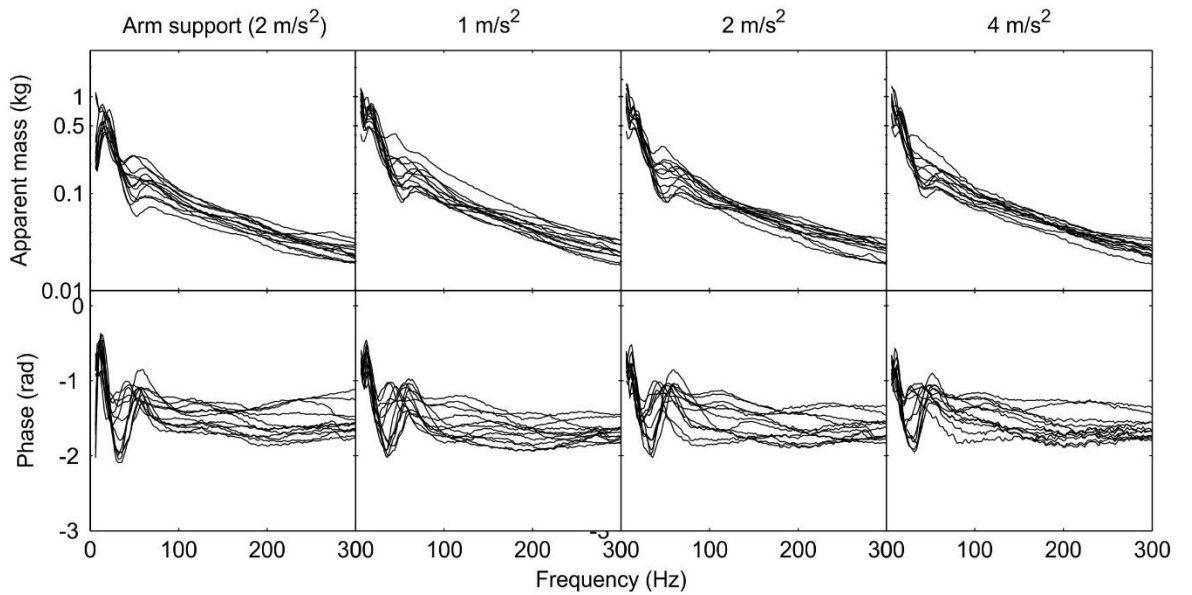


Figure 7-3 Individual apparent mass (modulus and phase) at the palm of the hand according to their vibration magnitude and arm condition. Median of 12 subjects.

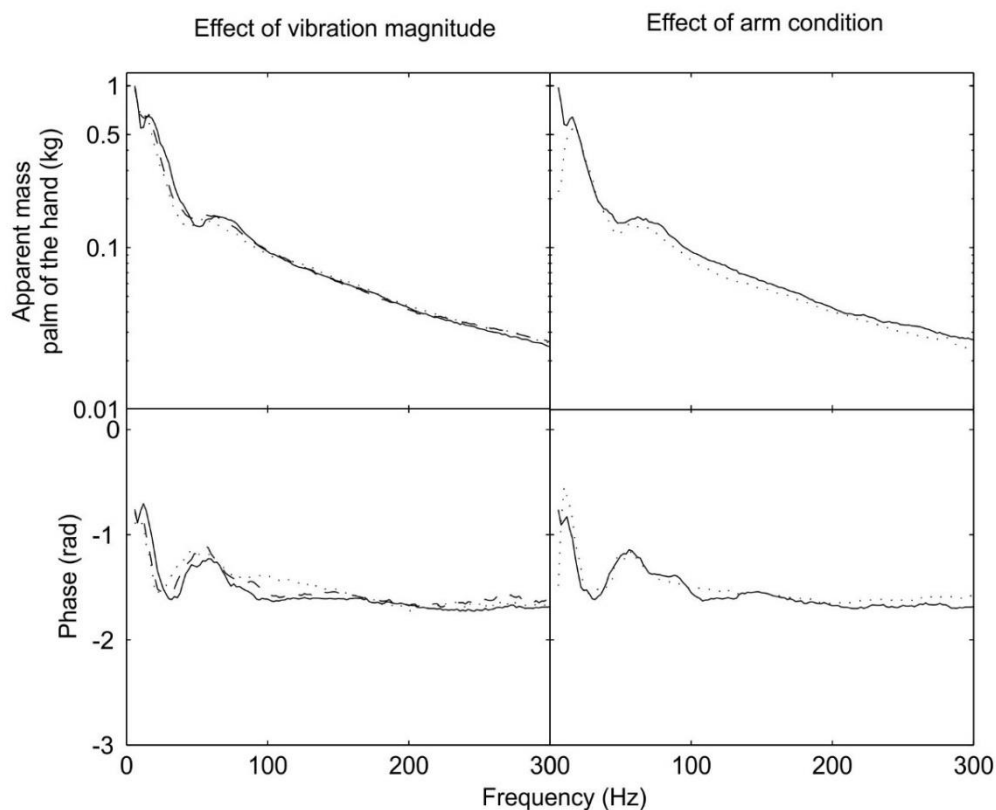


Figure 7-4 Apparent mass at the palm at the palm of the hand according to the vibration magnitude and arm condition (Left: —: 1 ms^{-2} , ---- 2 ms^{-2} , 4 ms^{-2} , Right: —: without arm support, with arm support). Median of 12 subjects.

7.3.3 Glove transmissibility to the palm of the hand

The inter-subject variability in the measurement of glove transmissibility for the effects of vibration magnitude and arm support are shown in Figure 7-5.

The transmissibilities of Foam A and Foam B to the palm of the hand were little affected by the change in the vibration magnitude at frequencies from 10 to 300 Hz (Figure 7-6; Friedman, $p > 0.05$ for Foam A, $p > 0.06$ for Foam B). However, the transmissibility of Gel A to the palm of the hand increased slightly as the vibration magnitude increased at frequencies between 80 and 220 Hz (Friedman, $p < 0.045$), with no significant differences at frequencies outside of this range (Friedman, $p > 0.061$)

The arm support had similar systematic effects on the transmissibilities of all three materials. The transmissibility of Gel A was similar with and without arm support at frequencies from 10 to 114 Hz (Friedman, $p > 0.058$) and from 128 to 300 Hz (Figure 7-7;

Friedman, $p>0.058$). At frequencies from 114 to 128 Hz, the median transmissibility without arm support was less than that with arm support (Friedman, $p<0.012$).

The transmissibility of Foam A to the palm of the hand without arm support was similar to the transmissibility with arm support at all frequencies (Figure 7-7; Friedman, $p>0.058$). A similar trend was found with Foam B (Friedman, $p>0.0578$).

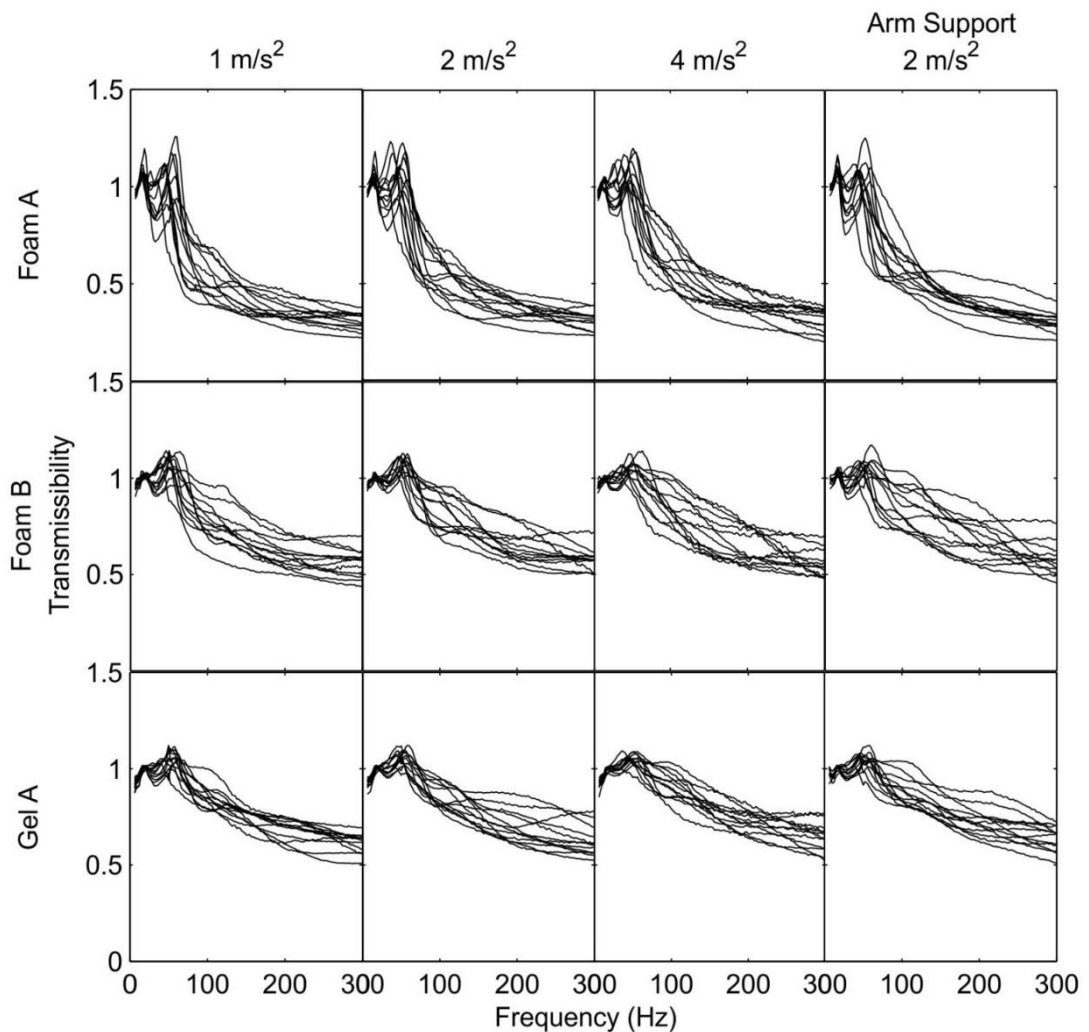


Figure 7-5 Individual transmissibility (modulus) of Foam A, Foam B, and Gel A to the palm of the hand according to their vibration magnitude and arm condition.

7.3.4 Predicting the transmissibility of material to the palm using an impedance model

The predicted and measured transmissibilities are compared in Figure 7-8.

With arm support, the predicted transmissibilities of Foam A and Gel A were similar to the transmissibilities measured experimentally at all frequencies from 10 to 300 Hz

(Figure 7-8; Friedman, $p>0.058$ for Foam A, $p>0.058$ for Gel A) except at frequencies less than 20 Hz (Friedman, $p<0.0114$ for Foam A, $p<0.0114$ for Gel A). For Foam B, the predicted transmissibility with arm support shows good agreement with the measured transmissibility at all frequencies from 10 to 300 Hz (Friedman, $p>0.0578$), with the exception of frequencies between 92 and 136 Hz (Friedman, $p<0.0114$) and frequencies less than 20 Hz (Friedman, $p<0.0114$).

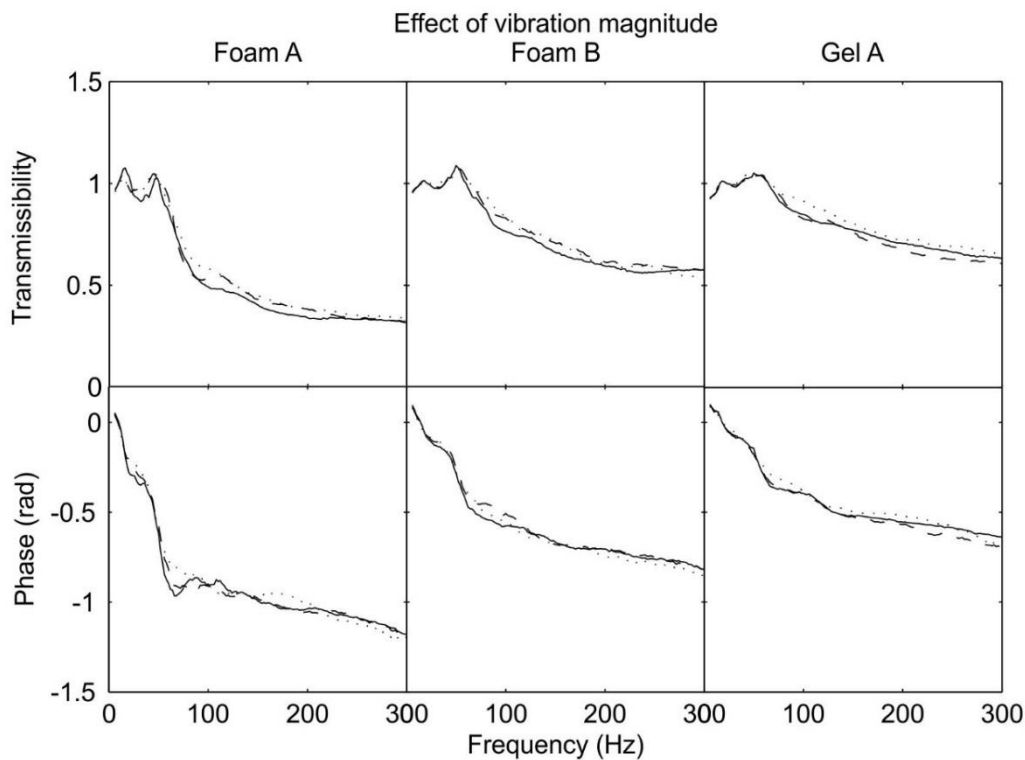


Figure 7-6 Transmissibilities of the materials to the palm of the hand according the glove materials (—: 1 ms^{-2} , ---- 2 ms^{-2} , 4 ms^{-2}). Median of 12 subjects.

With changing vibration magnitude, the predicted transmissibility of Foam A was similar to the transmissibility measured experimentally at frequencies from 20 to 140 Hz (Figure 7-8; Friedman, $p>0.0548$) but slightly less than the measured transmissibility at frequencies greater than 140 Hz (Friedman, $p<0.016$) and at frequencies less than 20 Hz (Friedman, $p<0.0114$). The predicted transmissibility of Foam B was similar at all frequencies measured in this study (Friedman, $p>0.0887$) but slightly less than the measured transmissibility at frequencies less than 20 Hz (Friedman, $p<0.0184$). The predicted transmissibility of Gel A slightly underestimated the measured transmissibility at frequencies less than 20 Hz (Friedman, $p<0.001$), and at frequencies greater than 158 Hz (Friedman, $p<0.049$) but similar to the measured transmissibility at frequencies outside of these ranges (Friedman, $p>0.05$).

The predicted transmissibility of Foam A to the palm of the hand with arm support was slightly greater than without the arm support at frequencies from 60 to 130 Hz (Figure 7-9; Friedman, $p < 0.0114$). The predicted transmissibility of Foam B and Gel A with arm support was similar to the transmissibility without arm support at all frequencies from 10 to 300 Hz (Friedman, $p > 0.0578$ for Foam B, $p > 0.0578$ for Gel A).

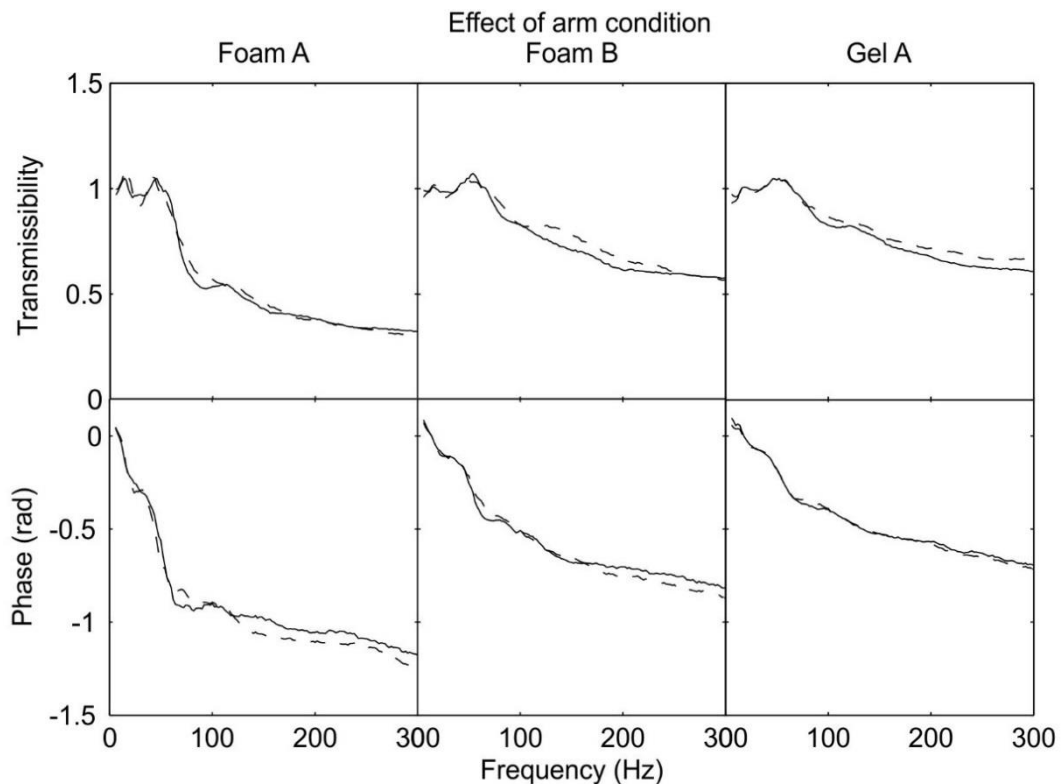


Figure 7-7 Transmissibilities of the materials to the palm of the hand according to the glove materials (—: without arm support, ----: with arm support). Median of 12 subjects.

The predicted transmissibility of Foam A was not affected by the increase in the vibration magnitude at any frequency from 10 to 300 Hz (Figure 7-9; Friedman, $p > 0.0578$), except at frequencies from 26 to 120 Hz (Friedman, $p < 0.0114$). At frequencies from 74 to 130 Hz, the transmissibility of Foam B slightly increased with increasing vibration magnitude (Friedman, $p < 0.0114$) but was unaffected by the increase in vibration magnitude at frequencies outside of this range (Friedman, $p > 0.0578$). Transmissibility of Gel A was unaffected by the increase in vibration magnitude at frequencies from 10 to 300 Hz (Friedman, $p > 0.0578$) but slightly increased at frequencies from 74 to 128 Hz (Friedman, $p < 0.0114$).

7.4 Discussions

7.4.1 Apparent mass at the palm of the hand

The apparent mass at the palm of the hand was not significantly affected by increases in vibration magnitude from 1.0 to 4.0 ms⁻² r.m.s., although there was a small decrease in the median apparent mass at frequencies from 16 to 100 Hz as the vibration magnitude increased. This is consistent with a trend found in previous studies (Burström, 1997, Aldien *et al.*, 2006).

Previous studies investigated the effects of arm posture by only changing the angle between the lower-arm and the upper-arm or between the upper-arm and the shoulder (Aldien *et al.*, 2006, Besa *et al.*, 2007, Adewusi *et al.*, 2010): this only signifies the effect of the upper-arm on the apparent mass of the hand. The influence of the lower-arm on the apparent mass at the palm is not clear. In this study, the arm support provided support to the forearm and the upper-arm, reducing their effects on the apparent mass measured at the palm and resulting in reduced apparent mass with arm support than without arm support at frequencies less than about 16 Hz. This indicates that both the lower-arm and the upper-arm predominantly affect apparent mass at the palm at frequencies less than 16 Hz. This also implies that the motion of the palm and the fingers predominantly influence vibration at frequencies greater than about 16 Hz.

The apparent mass measured with arm support was less than that measured without arm support at frequencies less than 16 Hz, lower than the 30 Hz found previously (Burström, 1997, Aldien *et al.*, 2006, ; Besa *et al.*, 2007, Adewusi *et al.*, 2010). Based on Chapter 6, increasing the contact force increases the resonance frequency around 16 Hz. It is expected that if the contact force in this study is similar to the previous study (e.g., Aldien *et al.*, 2006; 50 N push force instead of 20 N push in this study), the resonance frequency (i.e., at about 16 Hz in this study) would probably be increased (i.e., and be around 30 Hz) and the apparent mass with arm support would be less than without arm support at frequencies less than around 30 Hz as observed in the previous studies (i.e., assuming that both lower and upper-arm in those studies influence dynamic response of the hand at frequencies less than 30 Hz).

This study concluded that changing the posture of the arm will mainly affect the apparent mass of the hand at low frequencies rather than at high frequencies, as suggested in previous studies (Burström, 1997, Aldien *et al.*, 2006, Adewusi *et al.*, 2010) although that

the apparent mass of the hand at high frequencies is expected to be slightly reduced but not significant as suggested in Section 7.3.2.

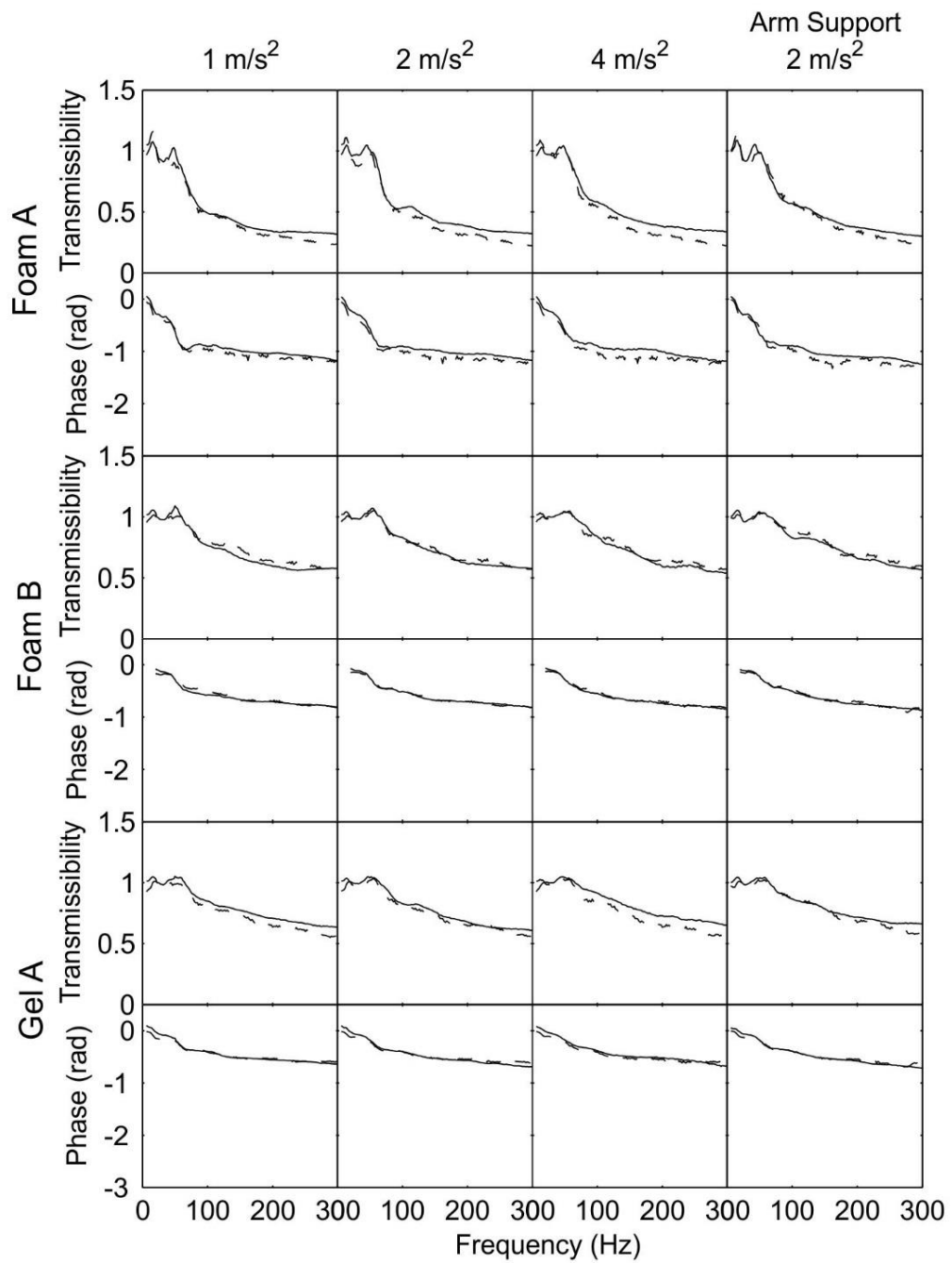


Figure 7-8 Predicted transmissibility of the glove materials to the palm of the hand (modulus and phase) according to the vibration magnitude and arm condition (—: measured, ---- predicted). Median of 12 subjects.

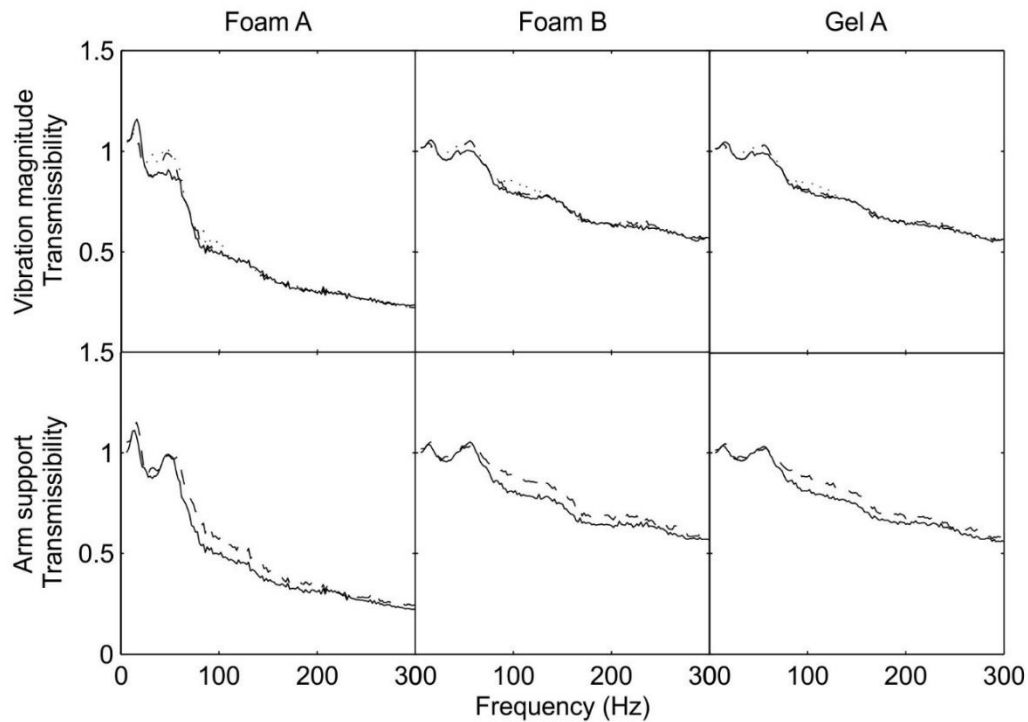


Figure 7-9 Predicted transmissibility of the glove materials to the palm of the hand (modulus) according to the vibration magnitude (top row; —: 1 ms^{-2} , ---- 2 ms^{-2} , 4 ms^{-2}) and arm condition (lower row; —: without arm support, ---- with arm support). Median of 12 subjects.

7.4.2 Effects of vibration magnitude and arm support on glove transmissibility

In this study, the apparent mass at the palm was measured and was found to be not significantly affected by changes in vibration magnitude from 1.0 to 4.0 ms^{-2} r.m.s. The material dynamic stiffnesses was assumed to be unaffected by vibration magnitude (see Section 7.2.4 for the explanation of the assumption made on the effects of vibration magnitude on glove dynamic stiffness). Since both the apparent mass and the dynamic stiffness were not expected to be affected by the vibration magnitude, it was expected that the transmissibilities of the glove materials to the palm would not be affected by a change in the vibration magnitude. As expected, the measured transmissibilities of the glove materials to the palm were not greatly affected by the changes in the vibration magnitude similar to the findings of a previous study (Laszlo and Griffin, 2011: the transmissibilities of three out of four gloves were not affected by increasing the vibration magnitude).

Increasing the apparent mass of the hand will tend to decrease the frequency of the principal resonance in the transmissibility of a glove, and tend to decrease the transmissibility to the hand at higher frequencies (see Chapters 4, 5, and 6). In this study, the median apparent mass at the palm from 10 to 300 Hz was generally less with the arm support than without the arm support (i.e., although it was not statically significant), suggesting that the transmissibility with arm support is expected to be greater than without arm support at frequencies greater than the resonance. The median measured and predicted glove transmissibility with and without arm support confirmed that is the case (i.e., the transmissibilities of the materials to the palm without arm support were slightly less than those with arm support) but they were not statistically significant (see Section 7.3.3).

It has been shown that changing the posture of the arm can dramatically change glove transmissibility (Wu and Griffin, 1989). This study indicates that an arm support will not have a large effect on glove transmissibility at frequencies from 10 to 300 Hz.

7.4.3 Predicting the apparent mass at the palm using the measured glove transmissibility

A mechanical impedance model has been shown to be capable of predicting glove transmissibility to the palm of the hand and to the index finger (O'Boyle and Griffin, 2004, Chapters 4, 5, and 6). The mechanical impedance model can also be used to predict the apparent mass at the palm of the hand using the measured glove transmissibility and the measured glove dynamic stiffness. The apparent masses predicted at the palm of the hand using Equation 7.2 for the three glove materials are shown in Figure 7-10.

The apparent mass predicted at the palm of the hand from the measured transmissibility of Foam A was slightly less than the apparent mass measured experimentally at all frequencies from 10 to 300 Hz.

The predicted apparent mass at the palm using the transmissibilities of Foam B and Gel A showed good agreement with the measured apparent mass at high frequencies but significantly less than the measured apparent mass at frequencies less than about 40 Hz. Foam B and Gel A had transmissibilities close to unity at low frequencies, so it is expected that the measurement of glove transmissibility at those frequencies (i.e., frequencies less than 40 Hz) were relatively insensitive to the apparent mass of the hand.

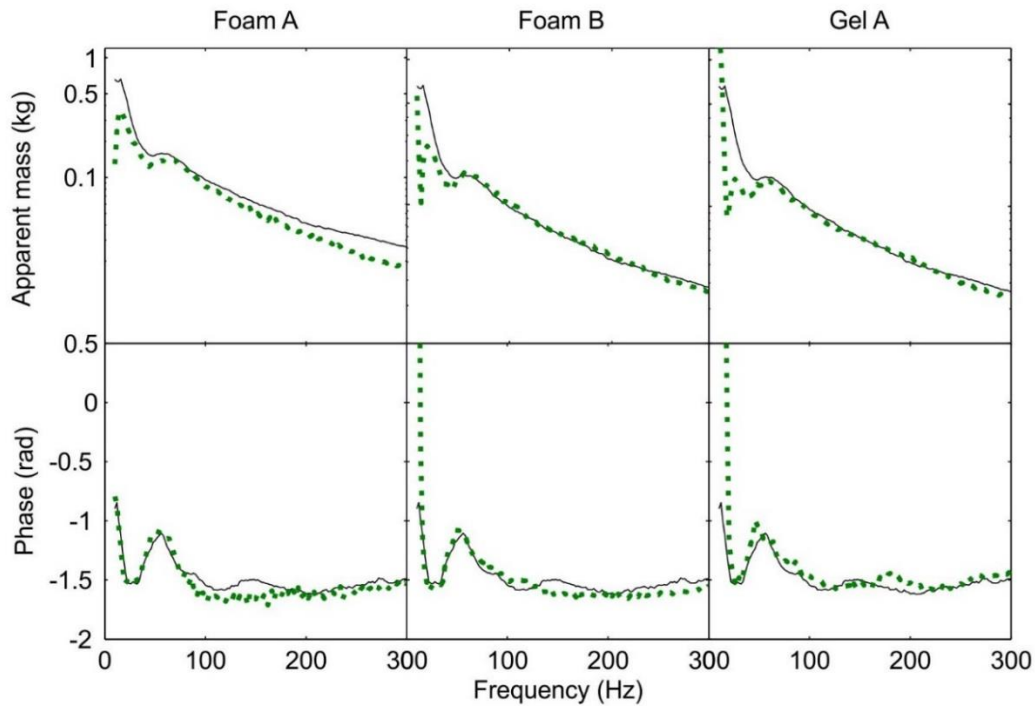


Figure 7-10 Predicted apparent mass at the palm (modulus and phase) without arm support using mechanical impedance model according to the glove materials (vibration magnitude 2m/s^2 ; —: measured, predicted). Median of 12 subjects.

7.5 Conclusions

The apparent mass at the palm of the hand, and the transmissibility of three glove materials to the palm of the hand, were not greatly affected by changes in vibration magnitude from 1.0 to 4.0 ms^{-2} r.m.s.

The apparent mass at the palm of the hand was significantly less with an arm support than without the arm support at frequencies less than 16 Hz .

Glove transmissibilities appeared slightly greater with the arm support than without the arm support, but the differences were not statistically significant.

Chapter 8: Low frequency measurement of the apparent mass at the palm of the hand

8.1 Introduction

A model of the hand and a model of the glove material are required to predict the transmissibility of a glove material to the hand. Predicting glove transmissibility using a lumped parameter model of the hand and a lumped parameter model of the glove may assist understanding of the mechanism affecting both the apparent mass of the hand and the transmissibility of the glove. The apparent mass at the palm and the dynamic stiffnesses of the glove materials have been measured previously (Chapters 6 and 7). The previous measurements were obtained at frequencies from 10 to 300 Hz with preload forces of 10, 15, and 20 N.

In Chapter 7, the apparent mass at the palm with and without arm support was measured from 10 to 300 Hz. It was observed that with the arm support, the apparent mass at the palm at frequencies less than 15 Hz was significantly lower than without the arm support. The lower arm and the upper arm could have influenced the apparent mass at low frequencies (i.e. less than 10 Hz), therefore, it is not possible to model the motion of the lower arm and upper arm without measurements at frequencies less than 10 Hz. Additional measurement at frequencies less than 10 Hz were required to better calibrate the model of the hand.

The effects of arm posture on the apparent mass at the palm have been investigated previously (Burström, 1997; Besa *et al.*, 2007). The impedance of the hand in an extended arm posture is greater than the impedance of the hand in a bent arm posture at frequencies less than 30 Hz (Besa *et al.*, 2007; Adewusi *et al.*, 2012). In both postures, the apparent mass of the hand increased with decreasing frequency of vibration at frequencies less than 30 Hz (Aldien *et al.*, 2006). Increasing the angle between the upper arm and the body increases the mechanical impedance of the hand at frequencies less than 20 Hz (Burström, 1997).

The objective of the experiment presented in this chapter was to investigate the apparent mass at the palm of the hand at frequencies less than 10 Hz. It was hypothesised that the apparent mass at the palm increased with decreasing frequency of vibration at frequencies less than 10 Hz. Two resonances were expected to be observed at frequencies less than 10 Hz, due to the motion of the lower-arm and the upper-arm. The

results of the experiment in this chapter provided data for the calibration of a lumped parameter model of the hand in the next chapter.

8.2 Method

8.2.1 Subjects

Twelve subjects aged 22 to 45 years participated in the experiment. The characteristics of the subjects are shown in Table 8.1. The subjects participating in this experiment were the same as the subjects who participated in the experiment in Chapter 7. The experiment was approved by the Ethics Committee of the Faculty of Engineering and the Environment at the University of Southampton (reference number 12038).

8.2.2 Measuring apparent mass at the palm of the hand

The method of measuring of the apparent mass at the palm was explained in Chapter 3. The measurements were obtained with a 25-mm diameter plate with a push force of 20 N. A 30-s period random vibration with magnitude 2.0 m/s² r.m.s. (frequency-weighted using W_h according to ISO 5349-1:2001; Figure 8.1) was generated with a frequency range from 2 to 50 Hz.

Table 8-1 Characteristics of the subjects in the experiment.

Physical Forms	Range	Median
Age (years)	22-42	27.5
Stature (cm)	161-181	167
Weight (kg)	50-85	65
Hand circumference (mm)	166-238	206.5
Hand length (mm)	167-204	179.5

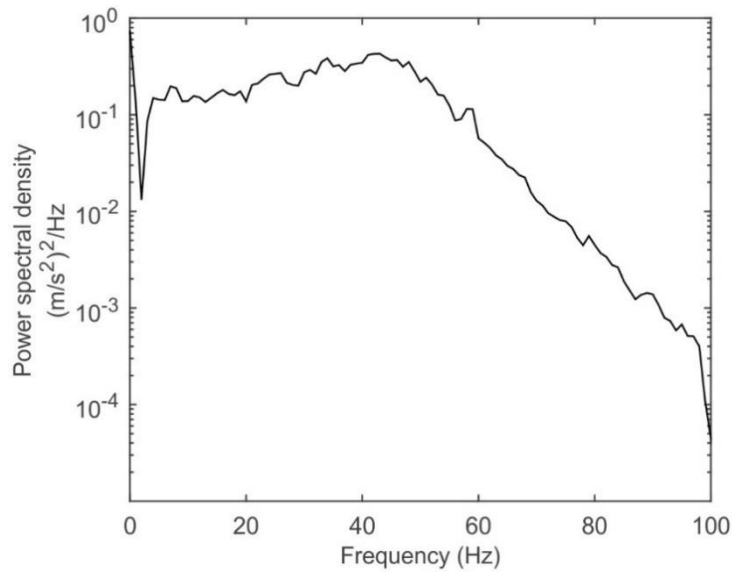


Figure 8-1 Acceleration power spectral density of the stimulus for measuring the apparent mass at the palm. Spectrum with 1-Hz frequency resolution.

8.2.3 Analysis

The data were acquired with a sampling rate of 2048 samples per second. Constant bandwidth frequency analysis was performed across the frequency range 2 to 50 Hz with a frequency resolution of 1 Hz and 124 degrees of freedom.

The method of analysis of the apparent mass at the palm with mass cancellation (i.e. in time domain) was explained in Chapter 3.

8.3 Results

The coherencies of all measurements of the apparent mass were greater than 0.8 at all frequencies from 2 to 50 Hz.

8.3.1 Apparent mass at the palm of the hand

The inter-subject variability in the measurement of the apparent mass is shown in Figure 8.2.

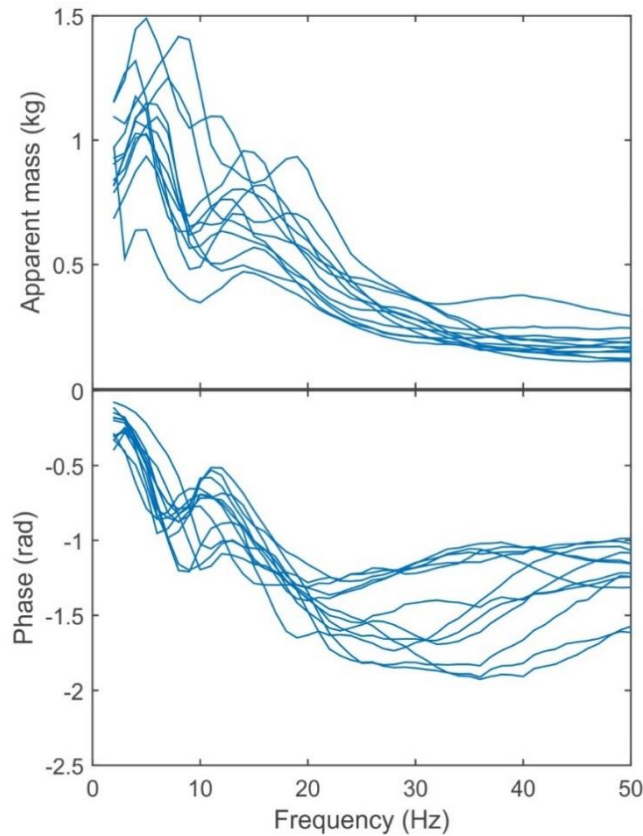


Figure 8-2 Inter-subject variability in apparent mass (modulus and phase) at the palm of the hand.

The apparent mass at the palm decreased with increasing frequency of vibration from 2 to 50 Hz (Figure 8-3). Two principle resonances were observed at about 5 and 15 Hz. All subjects showed two principle resonances, except subject 3 where one resonance was observed at about 7 Hz.

8.4 Discussion

The apparent mass measured in this chapter increased with decreasing frequency of vibration from 50 to 2 Hz, as hypothesised.

At frequencies less than about 15 Hz, the apparent mass at the palm is mainly due to the motion of the lower-arm and the upper-arm (see Chapter 7). Assuming the mass of the lower arm is about 0.95 kg and the mass of the upper arm is about 1.7 kg (i.e. calculated based on median data; Dempster and Gaughran, 1967), it was suspected that the resonance in the apparent mass at about 5 Hz could be due to the motion of the lower arm.

The modulus of the apparent mass at the palms of some subjects continued to increase with decreasing frequency of vibration at frequencies less than 3 Hz. This indicates there will be another resonance at frequencies less than 2 Hz.

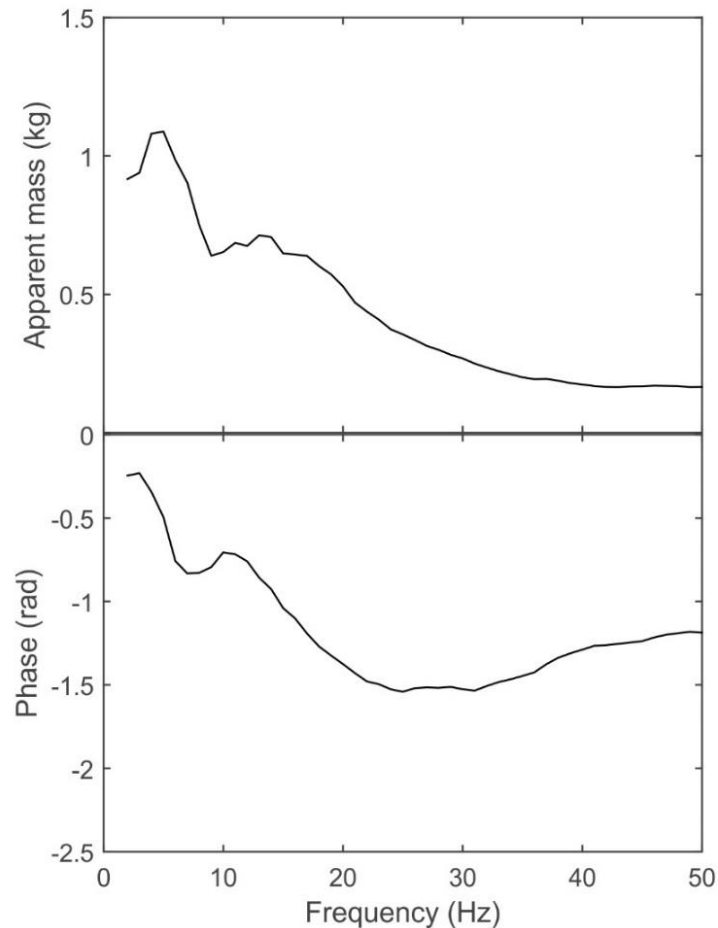


Figure 8-3 Apparent mass (modulus and phase) at the palm of the hand. Median of 12 subjects.

The apparent mass measured previously in the same condition and with the same subjects as in this chapter but a higher frequency range (see Chapter 7) is compared with the apparent mass measured in this chapter (Figure 8-4). The median apparent mass measured previously was slightly lower than the median apparent mass measured in this chapter. The resonance observed at about 15 Hz in this chapter was similar to the resonance in the measured apparent mass measured previously (Figure 8-4; see Chapter 7).

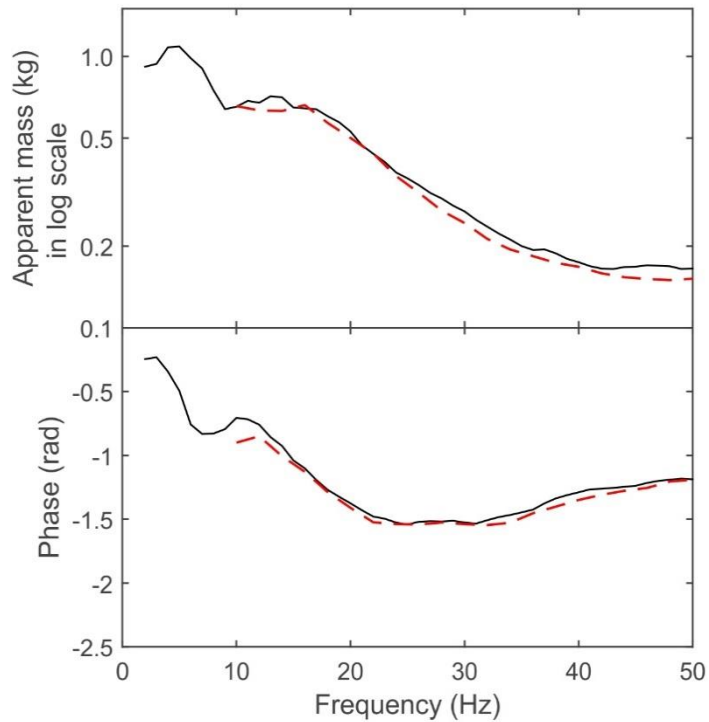


Figure 8-4 Apparent mass (modulus and phase) at the palm of the hand (— measured in this chapter, - - - measured in Chapter 7). Medians of 12 subjects.

8.5 Conclusions

The apparent mass at the palm increases with decreasing frequency of vibration at frequencies less than 10 Hz.

Two principle resonances were observed in the apparent mass measured in this chapter (at about 5 and 15 Hz). The resonance at about 5 Hz could be due to the motion of the lower arm.

The apparent mass continued to increase as the frequency of vibration decreased at frequencies less than 3 Hz in some subjects, which could indicate another resonance.

Chapter 9: Predicting the transmissibility of gloves to the hand using lumped parameter models of the hand

9.1 Introduction

A biodynamic model of the gloved hand could be developed to represent how vibration is transmitted to the hand and amplified or attenuated by glove material. The model may also be used to predict the effects of gloves on the transmission of vibration to the hand as studied in this research. The transmissibility of a glove to the hand depends on two primary factors: the dynamic response of the hand and the arm, and the dynamic stiffness of the glove material. A model that predicts or represents vibration transmission through a glove to the hand will have both components: they may be modelled as two separate components before they are combined to predict glove transmissibility. Several biodynamic models of the hand have been proposed for this purpose (International Standard ISO 10068:2012; Dong *et al.*, 2007, 2009; Adewusi *et al.*, 2012)

Simple lumped parameter models of the hand have been proposed and discussed (Gurram *et al.*, 1994; Rakheja *et al.*, 2002). Some of them are specified in International Standard ISO 10068:2012. These models were developed with the intention of representing the apparent mass of the hand. A two degree-of-freedom model proposed in International Standard ISO 10068:2012 offers a reasonable fit with the measured apparent mass of the hand but, in reality, this depends on many other factors such as the posture of the hand and arm, the direction of the vibration, the contact surface, the push force, and the frequency of the vibration. These models do not have much similarity with the parts of the hand and the arm and so it may not be possible to predict all the motion of the hand and the arm (i.e., they are limited to the prediction related to the parts of the hand or the arm that the models represent).

A seven degree-of-freedom lumped parameter model was developed to represent how vibration is transmitted to the hand through a glove (Dong *et al.*, 2009). The model has seven masses that consist of two main segments, hand segments (i.e., forearm, fingers, palm, fingers' tissues, palms' tissues) and material segments (material at the fingers interface, material at the palm interface). The model assumes the hand is in a grip condition (i.e., gripping a cylindrical handle) and the measurement used to fit the model was obtained with the arm in a bent posture. The model did not consider the posture of the upper arm (i.e., angle between the forearm and the upper arm) although it includes that mass of the upper arm. All the hand and the arm segments are connected by linear translational springs and dampers. The fitted glove transmissibility was similar to the

measured glove transmissibility at frequencies less than 100 Hz. The model underestimated the measured glove transmissibility at frequencies greater than 100 Hz (Dong *et al.*, 2009): it was not clear why the model underestimated the glove transmissibility at high frequencies. Without the material components, the model was also able to fit the measured apparent mass of the hand.

Two seven degree-of-freedom multi-body biodynamic models have been proposed to fit the measured impedance of the hand in two postures, bent-arm and extended arm (Adewusi *et al.*, 2012). These models were developed with the intention of representing the motion of the hand and the arm. Both models were developed with seven masses (i.e., forearm, upper arm, palm, fingers, trunk of the body) connected by several rotational and translational springs and dampers. In both models, the hand was assumed to be in a grip condition (i.e., gripping a cylindrical handle). Calibrated with combined impedance and transmissibility responses, the fitted impedance and transmissibility responses of the hand in both models show reasonable agreement with the impedance and transmissibility responses of the hand measured experimentally. Parameter sensitivity analysis suggested that in both models, the vibration at high frequencies was mainly influenced by the motion of the palm and the fingers whilst vibration at low frequencies was dominated by the motion of the lower-arm and upper-arm. It may be concluded that changing the posture of the arm will only affect the impedance of the hand at frequencies less than 30 Hz. Although these models are able to represent the motion of the hand and the arm, it may be difficult to observe some of the effects of factors studied in this research (e.g., area of contact, push force) on both the impedance of the hand and on the glove transmissibility.

There are two common materials used in anti-vibration gloves: gel and foam. Gels and foams usually possess viscoelastic properties that are difficult to predict without measurement. The viscoelastic property of a material is usually represented by three common lumped parameter models: i. Kelvin Voigt model, ii. Maxwell model, and iii. Standard Linear Solid model. The Kelvin Voigt model explains the creep behaviour of a material whilst the Maxwell model is used to represent the relaxation behaviour of a material. The Standard Linear Solid model explains both the creep and relaxation behaviour of a viscoelastic material during loading and unloading. Some studies have modelled glove materials as only a spring and a damper placed in parallel (i.e., Kelvin Voigt model; Dong *et al.*, 2009). A reasonable fit to glove transmissibility may be obtained with this method but understanding of the properties of the material and how the material affects glove transmissibility may be limited (i.e., the relaxation behaviour is not

included). The relaxation behaviour of a viscoelastic material may also be represented by adding hysteretic components to the Kelvin Voigt model (Tufano and Griffin, 2012).

The objective of this chapter was to develop models to predict the transmissibility of glove materials to the hand. The transmissibility of a glove to the hand was predicted using two models: a model of the hand and the arm, and a model of the glove material. The findings in previous chapters suggested the lower-arm and the upper-arm mainly contribute to the apparent mass at the palm at frequencies less than 15 Hz (see Chapter 7). It is expected that at frequencies greater than 15 Hz, the apparent mass at the palm of the hand is influenced by the motion of the palm and the fingers. A simple model consisting of the palm and the fingers was expected to provide acceptable predictions of glove transmissibility and predictions as good as a model with more degree-of-freedom at frequencies greater than 15 Hz.

9.2 Biodynamic models of the arm, the hand, and the fingers

In this study, two models of the hand were developed to be used to predict the transmissibility of a glove to the hand. The first model is a four degree-of-freedom model, and was assumed to represent four main body segments: the palm, the fingers, the lower-arm, and the upper-arm. The second model has two degree-of-freedom, a cut-off of the first model, consisting of two main body segments: the palm and the fingers.

9.2.1 Four degree-of-freedom multi-body biodynamic model of the hand (Model A)

9.2.1.1 Model description

Model A is a multi-body biodynamic model that consists of four segments corresponding to four main body segments of the hand and the arm (Figure 9-1).

The upper-arm was supported by a rotational joint attached to the trunk of the body (i.e., shoulder). The trunk of the body was assumed to be rigid and not moving (i.e., grounded). The upper-arm, the lower-arm, the palm, and the fingers were inter-connected by rotational springs and dampers.

The palm was assumed to be only moving in the vertical direction. The palm was connected to the palm tissues via a translational spring and damper. The palm tissues represent the tissues that are close to the driving-point of the vibration.

During the measurement of the apparent mass, the fingers were in a spread and stiff condition. The fingers could have moved together, so to reduce the complexity of the model, the fingers were assumed to be one body segment with the length and depth of the index finger, and the thumb excluded.

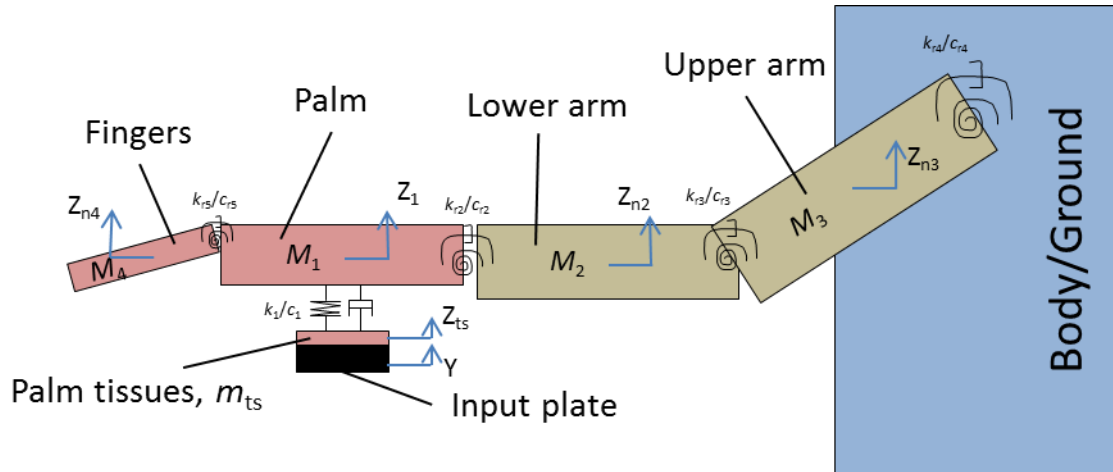


Figure 9-1 Multi-body biodynamic model of the hand and the arm, Model A

9.2.1.2 Geometry and inertial properties

All masses were assumed to be rigid and in the shape of a rectangular box. The dimensions of the hand and the arm were measured and are shown in Figure 9-2.

The masses of each segment of the hand and the arm were calculated as a percentage of total body mass (Table 9-1; Dempster and Gaughran, 1967). However, the mass of the fingers and the palm were only reported as one single mass: the mass of the hand. The mass of the palm was assumed to have three-quarters of the mass of the hand whilst the fingers were assumed to have one-quarter of the mass of the hand, based on Adewusi *et al.* (2012).

The angles of the fingers, the lower arm, and the upper arm are illustrated in Figure 9-3. It was assumed that the initial angle for the fingers and the forearm were inclined at 5 degrees whilst the forearm was at 30 degrees to the horizontal. The palm was assumed to be lying flat on the vibrating surface.

Table 9-1 Dimensions and masses of the body segments for Model A (Dempster and Gaughran, 1967; Adewusi *et al.*, 2012)

Mass	Mass (kg)	Length (m)	Depth (m)
Palm, m_1	$0.75 \cdot 0.006 \cdot M_t$	l_1	d_1

Fingers, m_4	$0.25 \cdot 0.006 \cdot M_t$	l_4	d_4
Lower arm, m_2	$0.015 \cdot M_t$	l_2	d_2
Upper arm, m_3	$0.026 \cdot M_t$	l_3	d_3

Where M_t is the total body mass of a subject.

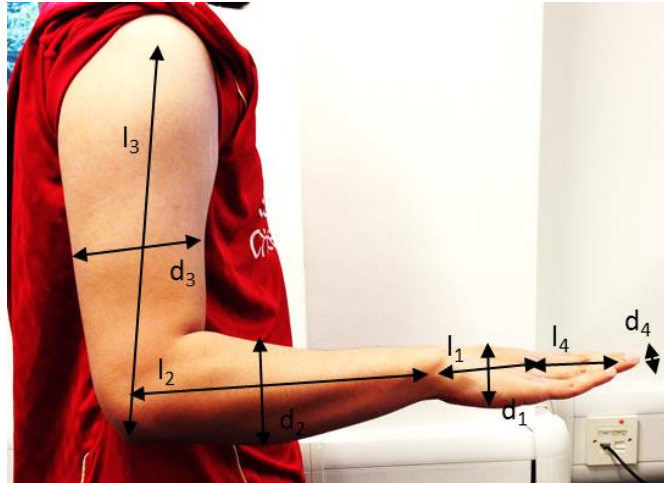


Figure 9-2 Locations of the measured dimensions of the fingers, the hand, the lower-arm, and the upper-arm.

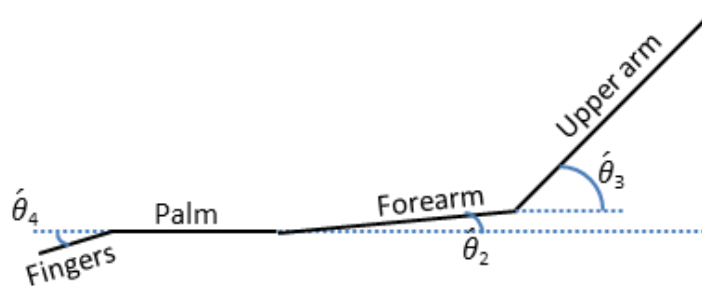


Figure 9-3 Angles of the fingers, the lower arm, and the upper arm.

9.2.1.3 Equations of motion

Model A is a four degree-of-freedom model with vertical displacement of the palm, z_1 , anti-clockwise rotational deflection of the fingers, $\hat{\theta}_4$, anti-clockwise rotational deflection of the forearm, $\hat{\theta}_2$, and anticlockwise rotational deflection of the upper arm, $\hat{\theta}_3$. All springs and dampers were assumed to be linear and the hand vibrated with small oscillations around the equilibrium position with a change of angle of less than 5 degrees. The equations of motion of Model A were derived from Lagrange formula (Thompson WT, 1981). The kinetic energy, T , potential energy, U and dissipation energy, D , of the system are:

$$T = \frac{1}{2}m_1(\dot{z}_{n1}^2 + \dot{x}_{n1}^2) + \frac{1}{2}m_2(\dot{z}_{n2}^2 + \dot{x}_{n2}^2) + \frac{1}{2}m_3(\dot{z}_{n3}^2 + \dot{x}_{n3}^2) + \frac{1}{2}m_4(\dot{z}_{n4}^2 + \dot{x}_{n4}^2) + \frac{1}{2}I_2\dot{\theta}_2^2 + \frac{1}{2}I_3\dot{\theta}_3^2 + \frac{1}{2}I_4\dot{\theta}_4^2 \quad (9.1)$$

$$U = \frac{1}{2}k_1(z_1 - y)^2 + \frac{1}{2}k_{r_2}(\theta_2)^2 + \frac{1}{2}k_{r_3}(\theta_3 - \theta_2)^2 + \frac{1}{2}k_{r_4}(-\theta_3)^2 + \frac{1}{2}k_{r_5}(\theta_4)^2 \quad (9.2)$$

$$D = \frac{1}{2}c_1(\dot{z}_1 - \dot{y})^2 + \frac{1}{2}c_{r_2}(\dot{\theta}_2)^2 + \frac{1}{2}c_{r_3}(\dot{\theta}_3 - \dot{\theta}_2)^2 + \frac{1}{2}c_{r_4}(-\dot{\theta}_3)^2 + \frac{1}{2}c_{r_5}(\dot{\theta}_4)^2 \quad (9.3)$$

The potential energy associated with gravity is ignored in the potential energy U in Equation 9.2. For each rotating rigid body, the position vectors of the centres of gravity are:

$$z_{n2} = z_1 + \frac{l_2}{2}\sin(\hat{\theta}_2)$$

$$x_{n2} = x_1 + \frac{l_2}{2}\cos(\hat{\theta}_2) + \frac{l_1}{2}$$

$$z_{n3} = z_1 + l_2\sin(\hat{\theta}_2) + \frac{l_3}{2}\sin(\hat{\theta}_3)$$

$$x_{n3} = x_1 + l_2\cos(\hat{\theta}_2) + \frac{l_3}{2}\cos(\hat{\theta}_3) + \frac{l_1}{2}$$

$$z_{n4} = z_1 - \frac{l_4}{2}\sin(\hat{\theta}_4)$$

$$x_{n4} = x_1 - \frac{l_4}{2}\cos(\hat{\theta}_4) - \frac{l_1}{2}$$

Where z_1 and x_1 are the change in the position vectors for m_1 , $\hat{\theta} = (\theta_0 + \theta)$ is the angle of inclination during vibration for each rotating rigid body, θ is the change in the angle of inclination of the rotating rigid bodies, and θ_0 is the initial inclination angle of the rotating rigid bodies. The nonlinearity in the geometry shown by the equations above was simplified (i.e., assuming that there was only small oscillation during vibration) using the trigonometry angle of transformation formulae:

$$\sin(\hat{\theta}) = \sin(\theta_0 + \theta) = \sin \theta_0 \cos \theta + \cos \theta_0 \sin \theta$$

$$\cos(\hat{\theta}) = \cos(\theta_0 + \theta) = \cos \theta_0 \cos \theta - \sin \theta_0 \sin \theta$$

As mentioned previously, the change of inclination angle, θ is $< 5^\circ$. So, $\sin(\theta) \approx \theta$ and $\cos(\theta) \approx 1$,

$$\sin(\hat{\theta}) = \sin(\theta_0 + \theta) = \sin \theta_0 + \cos \theta_0 \theta$$

$$\cos(\theta) = \cos(\theta_0 + \theta) = \cos \theta_0 - \sin \theta_0 \theta$$

The position vectors for each rotating rigid body were reproduced as follows:

$$z_{n2} = z_1 + \frac{l_2}{2} \sin \theta_{20} + \frac{l_2}{2} \cos \theta_{20} \theta_2$$

$$x_{n2} = x_1 + \frac{l_2}{2} \cos \theta_{20} - \frac{l_2}{2} \sin \theta_{20} \theta_2 + \frac{l_1}{2}$$

$$z_{n3} = z_1 + l_2 \sin \theta_{20} + l_2 \cos \theta_{20} \theta_2 + \frac{l_3}{2} \sin \theta_{30} + \frac{l_3}{2} \cos \theta_{30} \theta_3$$

$$x_{n3} = x_1 + l_2 \cos \theta_{20} - l_2 \sin \theta_{20} \theta_2 + \frac{l_3}{2} \cos \theta_{30} - \frac{l_3}{2} \sin \theta_{30} \theta_3 + \frac{l_1}{2}$$

$$z_{n4} = z_1 - \frac{l_4}{2} \sin \theta_{40} - \frac{l_4}{2} \cos \theta_{40} \theta_4$$

$$x_{n4} = x_1 - \frac{l_4}{2} \cos \theta_{40} + \frac{l_4}{2} \sin \theta_{40} \theta_4 - \frac{l_1}{2}$$

And $x_1 = 0$ (i.e., m_1 was assumed to be only moving in vertical direction); $\theta_{20}, \theta_{30}, \theta_{40}$ are initial angle for m_2, m_3 , and m_4 , respectively.

By applying the position vectors for each rotating rigid bodies in Equation 9.1, the equations of motion for Model A are:

$$m_1 \ddot{z}_1 + m_2 \left(\ddot{z}_1 + \frac{l_2}{2} \cos \theta_{20} \ddot{\theta}_2 \right) + m_3 \left(\ddot{z}_1 + l_2 \cos \theta_{20} \ddot{\theta}_2 + \frac{l_3}{2} \cos \theta_{30} \ddot{\theta}_3 \right) + m_4 \left(\ddot{z}_1 - \frac{l_4}{2} \cos \theta_{40} \ddot{\theta}_4 \right) + k_1(z_1 - y) + c_1(\dot{z}_1 - \dot{y}) = 0 \quad (9.4)$$

$$\begin{aligned} & \frac{l_2}{2} \cos \theta_{20} m_2 \left(\ddot{z}_1 + \frac{l_2}{2} \cos \theta_{20} \ddot{\theta}_2 \right) - \frac{l_2}{2} \sin \theta_{20} m_2 \left(-\frac{l_2}{2} \sin \theta_{20} \ddot{\theta}_2 \right) + l_2 \cos \theta_{20} m_3 \left(\ddot{z}_1 + \right. \\ & \left. l_2 \cos \theta_{20} \ddot{\theta}_2 + \frac{l_3}{2} \cos \theta_{30} \ddot{\theta}_3 \right) - l_2 \sin \theta_{20} m_3 \left(-\frac{l_3}{2} \sin \theta_{30} \ddot{\theta}_3 - l_2 \sin \theta_{20} \ddot{\theta}_2 \right) + I_2 \ddot{\theta}_2 + k_{r_2}(\theta_2) + \\ & k_{r_3}(\theta_2 - \theta_3) + c_{r_2}(\dot{\theta}_2) + c_{r_3}(\dot{\theta}_2 - \dot{\theta}_3) = 0 \end{aligned} \quad (9.5)$$

$$\begin{aligned} & \frac{l_3}{2} \cos \theta_{30} m_3 \left(\ddot{z}_1 + l_2 \cos \theta_{20} \ddot{\theta}_2 + \frac{l_3}{2} \cos \theta_{30} \ddot{\theta}_3 \right) - \frac{l_3}{2} \sin \theta_{30} m_3 \left(-\frac{l_3}{2} \sin \theta_{30} \ddot{\theta}_3 - l_2 \sin \theta_{20} \ddot{\theta}_2 \right) + \\ & I_3 \ddot{\theta}_3 + k_{r_3}(\theta_3 - \theta_2) + k_{r_4}(\theta_3) + c_{r_3}(\dot{\theta}_3 - \dot{\theta}_2) + c_{r_4}(\dot{\theta}_3) = 0 \end{aligned} \quad (9.6)$$

$$\begin{aligned} & -\frac{l_4}{2} \cos \theta_{40} m_4 \left(\ddot{z}_1 - \frac{l_4}{2} \cos \theta_{40} \ddot{\theta}_4 \right) + \frac{l_4}{2} \sin \theta_{40} m_4 \left(\frac{l_4}{2} \sin \theta_{40} \ddot{\theta}_4 \right) + I_4 \ddot{\theta}_4 + k_{r_5}(\theta_4) + c_{r_5}(\dot{\theta}_4) = \\ & 0 \end{aligned} \quad (9.7)$$

The apparent mass of the hand is the complex ratio of the resultant force to the acceleration on the input surface. The apparent mass at the palm of the hand, $m_{ap}(f)$ is given by:

$$m_{ap}(f) = m_{ts} + \left(\frac{(k_1 + i\omega c_1)(1 - \frac{z_1}{y})}{-\omega^2} \right) \quad (9.8)$$

Where m_{ts} is the mass of the palm tissues.

9.2.1.4 Measuring the apparent mass at the palm of the hand

The apparent mass at the palm of the hand was measured from 10 to 300 Hz with a magnitude of 2 m/s² r.m.s. (frequency-weighted using W_h according to ISO 5349-1:2001) with 20-N push force with 25-mm diameter contact area (see Chapter 7). In this chapter, this is called a high frequency measurement of the apparent mass at the palm.

Measurement as low as 2 Hz was required in order to better calibrate the models. The lower arm and the upper arm were expected to play a role in contributing to the apparent mass at the palm at frequencies less than 15 Hz, based on the measurement with arm support (see Chapter 7). Apparent mass at the palm was measured at frequencies from 2 to 50 Hz with a magnitude of vibration of 2 m/s² r.m.s. (frequency-weighted using W_h according to ISO 5349-1:2001) and with the same subjects as in the high frequency measurement. The apparent mass at the palm was measured with 20 N push force and on a 25-mm diameter of contact area. In this chapter, this is called a low frequency measurement. The details of this measurement are shown in Chapter 8.

9.2.1.5 Calibrating the model

The optimized parameters were obtained using the 'fmincon' function in MATLAB (version 2014b). The optimization function identified the model parameters by minimising the mean square errors between the computed and the measured vertical apparent mass at the palm of the hand for each of the subjects.

$$Error, E = \sum_{i=1}^N (Real(m_{ap}(i)) - Real(m_{am}(i)))^2 + \sum_{i=1}^N (imag(m_{ap}(i)) - imag(m_{am}(i)))^2 \quad (9.9)$$

Where m_{ap} is the calibrated apparent mass at the palm, m_{am} is the measured apparent mass at the palm. Both values are complex numbers.

It has been reported that the apparent mass at low frequencies is dominated by the motion of the upper-arm, the forearm, and the hand whilst vibration at higher frequencies

is dominated by vibration at the hand and the fingers (Adewusi *et al.*, 2012). This was similarly observed in Chapters 7 and 8: the effects of arm support were only seen at frequencies less than 15 Hz.

In this chapter, Model A was calibrated in two stages: 1. Low frequency calibration: Model A was calibrated with the apparent mass at the palm of the hand measured from 2 to 50 Hz, 2. High frequency calibration: Model A was calibrated with the apparent mass at the palm of the hand measured from 10 to 200 Hz.

In the first stage, all parameters with the exception of the mass of the palm, the fingers, the lower arm, and the upper arm, were acquired through optimization using 'fmincon'. The second stage was done only to acquire the optimized mass of the palm tissues, stiffness, k_1 , and k_2 , and damping, c_1 , and c_2 .

9.2.1.6 Identification of the model parameters

It can be difficult to set the upper and the lower boundary considering the number of variables that needed to be optimized. In this chapter, the upper boundary and the lower boundary were set based on results and discussions of the previous chapters (i.e., Chapter 5, 6, 7, and 8).

- I. The upper-arm and the lower-arm mainly contributed to the apparent mass at frequencies less than 15 Hz (see Chapter 7: the effects of arm support).
- II. The palm and the fingers significantly influenced the apparent mass of the hand at frequencies greater than 15 Hz (see Chapter 7).
- III. Three resonances were observed in the apparent mass at the palm. Resonances occurred in the measured apparent mass at about 5, 15, and 45 Hz (see Chapters 7 and 8). It was suggested that the resonance that occurred at about 5 Hz was expected to be primarily due to the motion of the forearm and the resonances at about 15 and 45 Hz were expected to be mainly due to the motions of the palm and the fingers, respectively.
- IV. It was suspected that the increase in the apparent mass at the palm as the contact area increased was due to the increase in the mass of the palm tissues close to the vibration driving-point: increasing the contact area only increased the apparent mass at the palm at frequencies greater than 70 Hz. Based on the median data, at 300 Hz, the apparent mass at the palm was roughly about 11, 16, and 25 grams for 12.5-, 25.0-, and 37.5-mm diameter of contact areas (see Chapter 5). The mass of the palm tissues close to the driving point of the vibration

can be calculated and was roughly about 6 to 7 grams for the 25-mm diameter of contact area.

The stiffnesses k_1 , and k_{r5} , and damping c_1 , and c_{r5} were set so that the palm and the fingers could contribute mainly at frequencies greater than 10 Hz. Resonance at about 15 Hz could be due to the motion of the palm based on the magnitude of the apparent mass at the palm (i.e., median mass of the palm is about 0.3 kg whilst median mass of the fingers is about 0.1 kg, the magnitude of apparent mass at the palm at this frequency was about 0.6 kg. See Chapters 7 or 8 for the magnitude of the apparent mass at the palm at 15 Hz). Since the mass of the palm is unchanged (i.e., fixed; see Section 9.2.1.2), the value of k_1 and c_1 were calibrated so that the resonance due to the motion of the palm occurred at about 15 Hz. The lower boundary and the upper boundary for stiffness k_1 was calculated roughly using $\omega^2=k/m$ (i.e., $10 \text{ Hz} > \omega^2=k/m > 20 \text{ Hz}$ using the median mass of the palm and these values were changed after several iterations).

Resonance at about 45 Hz could be due to the motion of the fingers (i.e., median mass of the palm is about 0.3 kg whilst median mass of the fingers is about 0.1 kg and the magnitude of the apparent mass at about 45 Hz was less than 0.3 kg: see Chapter 7 or 8 for the magnitude of the apparent mass at the palm at 45 Hz). Since the mass of the fingers is unchanged (i.e., fixed: see Section 9.2.1.2), the value of k_{r5} , and c_{r5} were calibrated so that the resonance due to the motion of the fingers occurred at frequencies less than 100 Hz (i.e., some of the subjects had resonance due to the motion of the fingers at frequencies around 50 to 70 Hz). The upper and the lower boundary for stiffness k_{r5} , and damping, c_{r5} , were set by running several iterations of the 'fmincon' function.

The upper and the lower boundary for both springs and dampers connected the upper-arm and the lower-arm, k_{r2} , k_{r3} , k_{r4} , and c_{r2} , c_{r3} , c_{r4} were set so that both of these segments would contribute to the apparent mass mainly at frequencies less than 15 Hz. The stiffnesses and damping connected to the lower-arm had a boundary set so that the resonance occurred at about 5 Hz: this is based on the magnitude of the apparent mass at the resonance (i.e., the median mass of the lower-arm was about 1.0 whilst the median mass of the upper-arm was about 1.7 kg and the magnitude of the measured apparent mass at about 5 Hz was less than 1.7 kg). The upper and the lower boundaries for the springs and dampers connecting the lower and the upper-arm (i.e., k_{r2} , k_{r3} , k_{r4} , c_{r2} , c_{r3} , c_{r4}) were set by running several iterations of the 'fmincon' function.

Based on the results in Chapter 5, the upper and the lower boundary for the mass of the palm tissues were set at 10 grams and 1 gram, respectively.

The same upper and lower boundaries were used in the first stage and in the second stage.

The median calculated mass and optimized parameters using 'fmincon' function in MATLAB (version 2014b) are shown in Table 9-2 (Please refer to Appendix B for the individual optimized parameters). The optimized values of the parameters produced local minima of the error (see Section 9.2.1.5 for the error function) between the fitted and the measured apparent mass that satisfied the constraints.

Table 9-2 Median optimized and calculated model parameters: Model A.

	Parameters	Upper boundary	Lower boundary	Optimized / Calculated	Initial Values
Springs(N/m)	k_1	10000	3000	3266	5500
	k_{r2}	100	0.1	0.10	5
	k_{r3}	100	0.1	22.04	5
	k_{r4}	100	0.1	14.48	5
	k_{r5}	40	5	6.77	5
Dampers (Ns/m)	c_1	80	0.01	52.93	30
	c_{r2}	5	0.01	0.01	0.05
	c_{r3}	5	0.01	0.09	0.01
	c_{r4}	5	0.01	0.68	0.28
	c_{r5}	5	0.001	0.005	4.8
Mass (kg)	m_1			0.3	
	m_2			1.0	
	m_3			1.7	

	m_4			0.1	
	Soft tissue	0.010	0.001	0.003	0.004

9.2.1.7 Comparison of fitted and measured apparent mass at the palm of the hand

Constant bandwidth frequency analysis was performed across the frequency range 2 to 50 Hz with a frequency resolution of 1 Hz for the low frequency calibration and across the frequency range 2 to 300 Hz with a frequency resolution of 2 Hz for the high frequency calibration.

For the low frequency calibration, the fitted apparent mass was not significantly different from the measured apparent mass at frequencies between 2 and 21 Hz (Wilcoxon, $p>0.052$) and at 40 and 50 Hz (Wilcoxon, $p>0.052$; Figure 9-4). The fitted apparent mass slightly overestimated the measured apparent mass at frequencies between 22 and 39 Hz (Wilcoxon, $p<0.035$).

The first median predicted median resonance frequency of the apparent mass at the palm occurred at 0.96 Hz. This was not visible in the apparent mass measured experimentally. The second median fitted resonance occurred at 6.7 Hz, slightly greater than the first median measured resonance frequency at about 5 Hz. The third fitted median resonance occurred at frequency 13.12 Hz, slightly lower than the median measured third resonance frequency at 14 Hz.

For the high frequency calibration, the fitted apparent mass at the palm was not significantly different from the measured apparent mass at frequencies from 10 to 24 Hz (Wilcoxon, $p>0.06$), from 46 to 66 Hz (Wilcoxon, $p>0.064$), and at frequencies greater than 84 Hz (Wilcoxon, $p>0.064$). The fitted apparent mass at the palm slightly overestimated the measured apparent mass at frequencies between 26 and 44 Hz (Wilcoxon, $p<0.012$), and slightly underestimated the measured apparent mass at frequencies between 68 and 82 Hz (Wilcoxon, $p<0.04$). Appendix C provides individual measured and fitted apparent masses.

The transmission of vibration to the hand, fingers, lower arm, and upper arm were not measured in this research. Comparisons between the predicted and the measured transmissibilities can still be made with data from a previous study (Concettoni and Griffin, 2009; Point 19-Condition 7 for the palm, Point 30-Condition 1 for the forearm, and

Point 7-Condition 7 for the fingers). The median predicted and measured transmissibilities are shown in Figure 9-5. There are differences between the predicted and the measured transmissibilities that might be explained by measured transmissibilities being obtained in somewhat different conditions. However, the predicted transmissibilities have similar characteristics to the measured transmissibilities (i.e., a similar number of resonances).

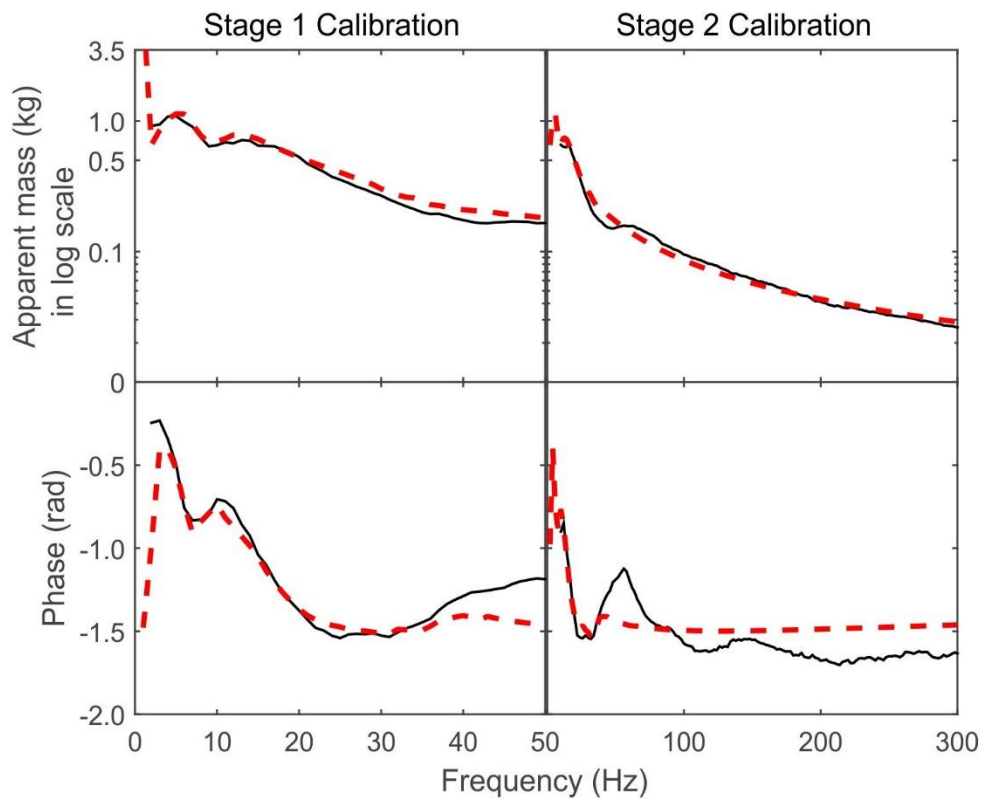


Figure 9-4 Fitted and measured apparent mass (modulus and phase) at the palm of the hand (--- fitted, — measured). Frequency resolution: Stage 1: 1 Hz Stage 2: 2 Hz). Median of 12 subjects.

9.2.1.8 Modal analysis

Modal analysis of the dynamic response of the arm was performed to study the vibration modes that contributed to the resonances observed during the resonance in the apparent mass at the palm. Using the matrix $M^{-1}K$ of the equation of motion of the models, the vibration modes can be determined by calculating the eigenvectors whilst the undamped natural frequencies can be determined by calculating the eigenvalues. Table 9-3 shows the median undamped natural frequencies and the modal vectors of Model A (Appendix B shows the undamped natural frequencies and modal vectors predicted for all subjects).

Table 9-3 Median undamped natural frequencies and mode shapes, Model A.

Mode		1	2	3	4
Natural frequency, Hz		0.96	6.53	12.62	38.11
Palm	Translational	0.000	0.004	0.010	0.005
Lower arm	Rotation	0.018	0.011	-0.058	-0.020
Upper arm	Rotation	0.013	-0.045	0.029	0.005
Fingers	Rotation	0.000	-0.003	-0.045	0.803

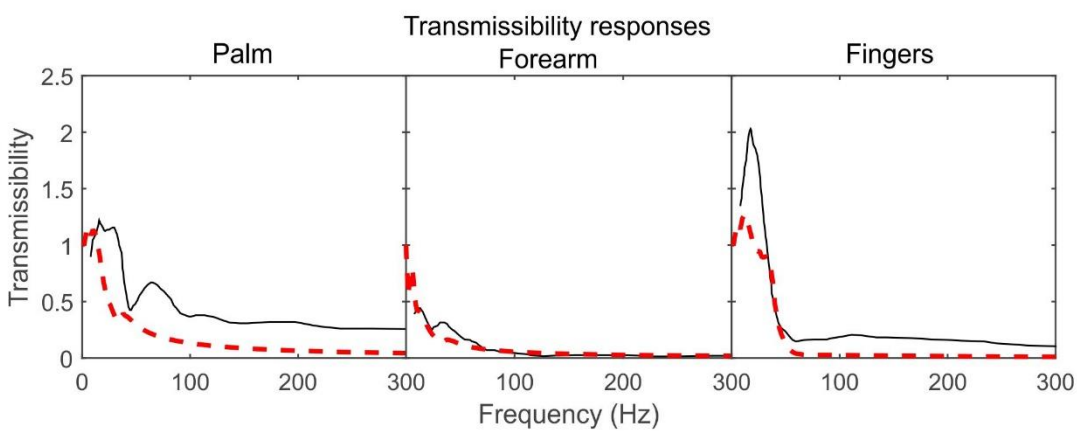


Figure 9-5 Transmissibility responses of the hand (— — — predicted, ——— measured). Frequency resolution: 2 Hz. Median of 12 subjects.

Figure 9-6 illustrated the mode shapes for Subject 12 in the initial condition of the hand and the arm and the predicted condition of the hand and the arm during the resonance. The first mode at 0.84 Hz is mainly due to the motion upper arm and the lower arm. The second mode occurred at 6.6 Hz mainly dominated by the motion of the forearm and the upper-arm. The motion of the palm, the fingers, and forearm mainly contributed to the third mode which occurred at 13.33 Hz. The fourth mode mainly contributed by the motion of the fingers occurred at 40.58 Hz.

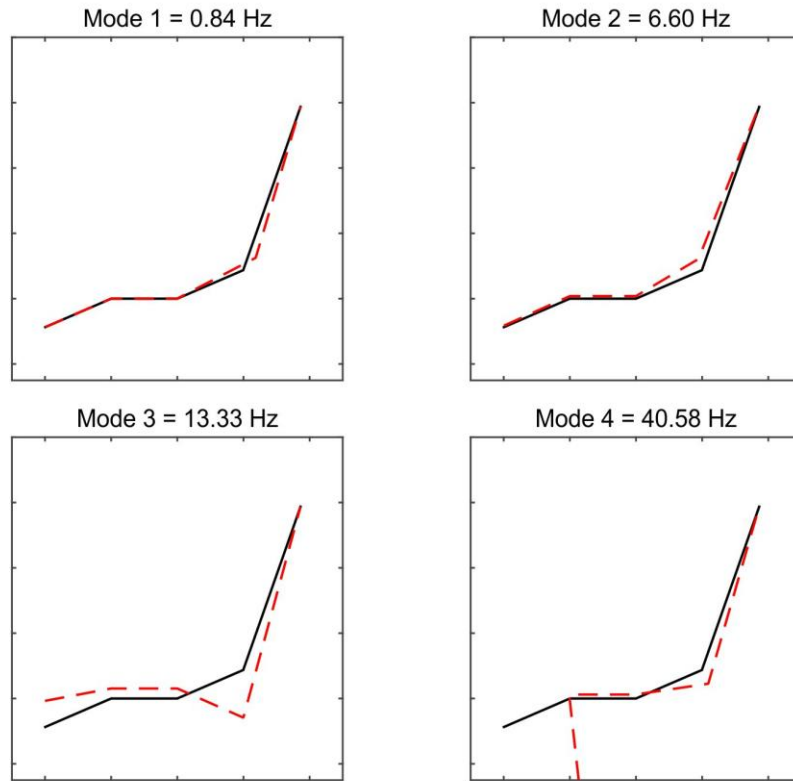


Figure 9-6 Illustration of the mode shapes for Model A (— initial condition of the hand and the arm, - - - predicted condition of the hand and the arm during resonance).

9.2.1.9 Parameter sensitivity

The parameter sensitivity matrix is given by (Ju *et al.*, 1987):

$$P_{ij} = \frac{\Delta R_i / R_i}{\Delta J / J} \quad (9.10)$$

Where J the parameters of the model, and R_i is the responses to be examined. In this study, six responses were examined: $i=1$ the predicted first natural frequency of the model, $i=2$ the predicted second natural frequency of the model, $i=3$ the predicted third natural frequency of the model, $i=4$ the predicted fourth natural frequency of the model, $i=5$ the modulus of the apparent mass at the palm at 300 Hz, $i=6$ the phase of the apparent mass at the palm at 300 Hz. ΔR_i is the difference of the responses between the nominal set and the new set of parameters calculated using perturbation factor, α , of 30%. If $\Delta J = \alpha J^{nominal}$ and $J^{new} = J^{nominal} + \Delta J$ is the new set of parameters, the new examined response, $R_i^{new} = R_i^{nominal} + \Delta R_i$. The greater the value of P_{ij} the greater the sensitivity of the response R_i to the parameter J .

The sensitivity matrix is based on three factors, P_m the mass of each body segment ($m_1, m_2, m_3, m_4, m_{ts}$) excluding mass of the soft tissues, P_{tr} translational stiffness and damping (k_1, c_1), P_{rt} rotational stiffness and damping ($k_{r2}, k_{r3}, k_{r4}, k_{r5}, c_{r2}, c_{r3}, c_{r4}, c_{r5}$). For the calculation of the parameter sensitivity, the apparent mass at the palm was calculated using optimized parameters for Subject 12.

$$P_{model A} = [P_{tr} P_{rt} P_m] \quad (9.11)$$

$$P_m = \begin{bmatrix} 0.000 & -0.045 & -0.379 & 0.000 & 0.000 \\ -0.013 & -0.136 & -0.291 & -0.004 & 0.000 \\ -0.175 & -0.159 & -0.047 & -0.076 & 0.000 \\ -0.026 & -0.025 & -0.002 & -0.356 & 0.000 \\ 0.000 & -0.000 & 0.000 & 0.000 & 0.001 \\ 0.036 & 0.035 & 0.003 & 0.004 & -0.017 \end{bmatrix} \quad (9.12)$$

$$P_{tr} = \begin{bmatrix} 0.006 & 0.000 \\ 0.077 & 0.000 \\ 0.368 & 0.000 \\ 0.007 & 0.000 \\ 0.033 & 0.962 \\ 0.081 & -0.135 \end{bmatrix} \quad (9.13)$$

$$P_{rt} = \begin{bmatrix} 0.006 & 0.073 & 0.353 & 0.000 & 0.000 & 0.000 & 0.000 & 0.000 \\ 0.000 & 0.267 & 0.094 & 0.000 & 0.000 & 0.000 & 0.000 & 0.000 \\ 0.000 & 0.107 & 0.006 & 0.005 & 0.000 & 0.000 & 0.000 & 0.000 \\ 0.000 & 0.001 & 0.000 & 0.461 & 0.000 & 0.000 & 0.000 & 0.000 \\ 0.000 & 0.000 & 0.000 & 0.000 & 0.000 & -0.001 & 0.000 & -0.001 \\ 0.000 & 0.000 & 0.000 & -0.002 & 0.000 & 0.000 & 0.000 & 0.000 \end{bmatrix} \quad (9.14)$$

The first resonance frequency is largely affected by the mass of the lower-arm, m_2 , and the upper-arm, m_3 and the rotational stiffness, k_{r2} , k_{r3} and k_{r4} .

The second resonance frequency is largely affected by mass of the lower-arm, m_2 and the upper-arm, m_3 , and rotational stiffness, k_{r3} and k_{r4} .

The third resonance frequency is largely affected by the mass of the lower arm, m_2 , and the palm, m_1 , as well as the translational stiffness k_1 .

The fourth resonance frequency is largely affected by the mass of the fingers, m_4 , and the rotational stiffness, k_{r5} .

At 300 Hz, the apparent mass at the palm increases with increasing mass of the palm tissues, m_{ts} , translational stiffness, k_1 , and translational damping, c_1 . Increasing the mass of the lower-arm, m_2 , and rotational damping c_{r3} and c_{r5} , will decrease the apparent mass at 300 Hz. The increase in the mass of the palm tissues, m_{ts} , and the translational damping, c_1 will decrease the phase.

9.2.2 Two degree-of-freedom multi-body biodynamic model of the hand

9.2.2.1 Model description

Model B is a cut-off of Model A (Figure 9-7). The palm was supported by two translational springs and dampers attached to the soft tissue and to a non-moving lower arm (i.e., the lower arm is now grounded). Similar to the previous Model A, the fingers were assumed as one body segment, attached to the palm via rotational spring and damper. The palm was assumed to be only moving vertically.

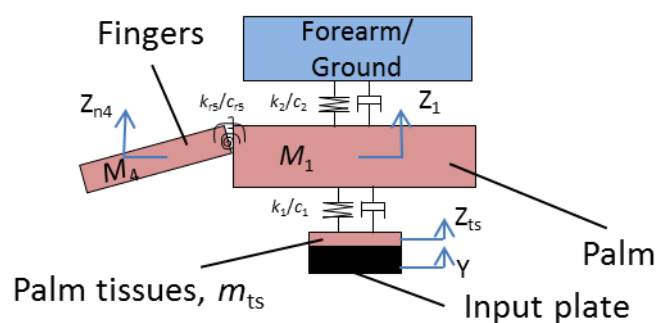


Figure 9-7 Simple biodynamic model of the hand, Model B

9.2.2.2 Geometry and inertial properties

Similar to the previous Model A, all body segments were assumed to be rigid and in the shape of a rectangular box. The dimensions of the palm and the fingers were measured (Figure 9-2) and are shown in Table 9-4.

Table 9-4 Dimension and mass of the hand segments, Model B

Mass	Mass (kg)	Length (m)	Depth (m)
Palm, m_1	$0.75 \cdot 0.006 \cdot M_t$	l_1	d_1
Fingers, m_4	$0.25 \cdot 0.006 \cdot M_t$	l_4	d_4

Where M_t is the total body mass of a subject.

9.2.2.3 Equations of motion

Model B is a two degree-of-freedom model with vertical displacement of the palm, z_1 and anti-clockwise rotational deflection of fingers, θ_4 . All springs and dampers were assumed to be linear. The palm and the fingers vibrated with small oscillation around the equilibrium position with a change of angle of less than 5 degrees. Using Lagrange formula, the equations of motion for Model B are given by

$$m_1 \ddot{z}_1 + m_4 \left(\ddot{z}_1 - \frac{l_4}{2} \cos \theta_{40} \ddot{\theta}_4 \right) + k_1(z_1 - y) + k_2(z_1) + c_1(z_1 - y) + c_2(z_1) = 0 \quad (9.15)$$

$$-\frac{l_4}{2} \cos \theta_{40} m_4 \left(\ddot{z}_1 - \frac{l_4}{2} \cos \theta_{40} \ddot{\theta}_4 \right) + \frac{l_4}{2} \sin \theta_{40} m_4 \left(\frac{l_4}{2} \sin \theta_{40} \ddot{\theta}_4 \right) + I_4 \ddot{\theta}_4 + k_{r_5}(\theta_4) + c_{r_5}(\dot{\theta}_4) = 0 \quad (9.16)$$

The apparent mass at the palm, $m_{ap}(f)$, was calculated using Equation 9.8.

9.2.2.4 Measuring the apparent mass at the palm

The apparent mass at the palm was measured previously at frequencies from 10 to 300 Hz with a magnitude of 2 m/s² r.m.s. (frequency-weighted using W_h according to ISO 5349-1:2001) with 20 N push force (see Chapter 7). Based on the parameter sensitivity analysis of Model A, the palm and the fingers influence the third resonance (i.e., about 15 Hz) and the fourth resonance (i.e., about 45 Hz). Hence, a two degree-of-freedom model consisting of the palm and the fingers is expected to be sufficient to fit the apparent mass at the palm at frequencies greater than 10 Hz.

9.2.2.5 Calibrating the model

The error function is shown in Equation 9.9. Model B was calibrated with the measured apparent mass at the palm at frequencies from 10 to 200 Hz.

9.2.2.6 Identification of the model parameters

Initial values, the upper boundaries, and the lower boundaries for the parameters for Model B were similar to the previous Model A but with several changes.

- i. The initial value for the translational spring, k_2 , was set to 10. The upper boundary for k_2 was set to 100 similar to the value of the upper boundary for k_{r2} of Model A.
- ii. The initial value for the translational damper, c_2 , was set to 0.1. The upper boundary for c_2 was set to 1, considering that the value of the optimized c_{r2} of Model A was less than 1.0 for all subjects (see Appendix B).
- iii. The lower boundaries for both k_2 and c_2 were set to 0, considering that the value of the optimized k_{r2} and c_{r2} of Model A was less than 1.0. This was also assuming that both k_2 and c_2 were soft and would not greatly influence the apparent mass at the palm at frequencies greater than 10 Hz.

The median calculated mass and optimized parameters using the 'fmincon' function in MATLAB (version 2014b) are shown in Table 9-5 (Appendix B shows individual optimized parameters). The optimized values of the parameters produced local minima of the error (see Section 9.2.2.5 for the error function) between the fitted and the measured apparent mass that satisfied the constraints.

Table 9-5 Optimized and calculated model parameters, Model B.

	Parameters	Upper boundary	Lower boundary	Optimized / Calculated	Initial Values
Springs (N/m)	k_1	10000	3000	3667	5500
	k_2	100	0	0.006	10
	k_{r5}	40	5	5	5
Dampers (Ns/m)	c_1	80	0.01	36.00	30
	c_2	1	0	1.00	0.1
	c_{r5}	5	0.001	0.008	0.01

Mass (kg)	m_1			0.30	
	m_4			0.10	
	Soft tissue	0.010	0.001	0.004	0.004

9.2.2.7 Fitted and measured apparent mass at the palm

Constant bandwidth frequency analysis was performed across the frequency range 10 to 300 Hz with a frequency resolution of 2 Hz.

The median measured and fitted apparent mass at the palm are compared in Figure 9-8.

The fitted apparent mass at the palm was similar to the apparent mass measured experimentally at frequencies less than 14 Hz (Wilcoxon, $p > 0.052$). The fitted apparent mass at the palm underestimated the measured apparent mass at frequencies greater than 16 Hz (Wilcoxon, $p < 0.045$). The first fitted undamped natural frequency occurred at 14.55 Hz, similar to the measured resonance frequency at about 14 Hz.

The predicted transmissibilities to the palm of the hand were compared with the measured transmissibilities to the palm and to the fingers (Concettoni and Griffin, 2009; palm point 19-Condition 7, fingers Point 7-Condition 7). The predicted transmissibilities to the palm and to the fingers were less than the measured transmissibilities (Figure 9-9; Concettoni and Griffin, 2009). On the other hand, the predicted transmissibilities have similar characteristics to the measured transmissibilities (i.e., a similar number of resonances).

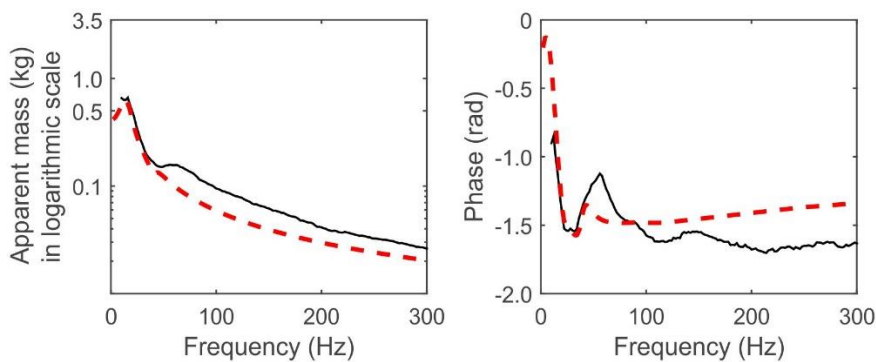


Figure 9-8 Measured and fitted apparent mass (modulus and phase) at the palm of the hand (— Fitted, — Measured) . Median of 12 subjects.

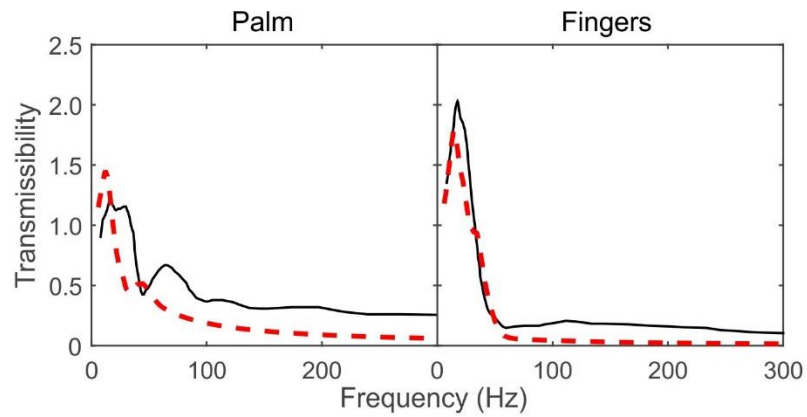


Figure 9-9 Transmission of vibration to the palm and to the fingers (Modulus). (--- predicted, — measured; Concettoni and Griffin, 2009) . Median of 12 subjects.

9.2.2.8 Modal analysis

The vibration modes for Model B were determined by calculating the eigenvectors and eigenvalues using the matrix $M^{-1}K$ of the equations of motion of the model. Table 9-6 shows the median undamped natural frequencies and modal vectors of Model B (Appendix B shows the undamped natural frequencies and modal vectors for each subject).

Table 9-6 Undamped natural frequencies and mode shapes, Model B.

Mode		1	2
Undamped Natural frequency, Hz		14.55	44.88
Palm	Translational	-0.015	0.010
Fingers	Rotation	0.094	1.022

Figure 9-10 illustrates the mode shapes for Subject 12 in the initial hand condition and during the predicted resonance. Both the first and the second mode involved motion of both body segments, the palm and the fingers.

In the first mode, the fingers rotated clockwise whilst the palm moves downward. This mode produced the greatest magnitude in the predicted apparent mass at the palm.

In the second mode, the fingers rotated clockwise and the palm moves upward. The predicted apparent mass was significantly less than in the first mode (i.e., the motion of the palm and the fingers may be out of phase).

9.2.2.9 Parameter sensitivity

The parameter sensitivity matrix is shown in Equation 9.10.

For Model B, four responses were examined: $i=1$ the predicted first undamped natural frequency of the model, $i=2$ the predicted second undamped natural frequency of the model, $i=3$ the modulus of the apparent mass at the palm at 300 Hz, $i=4$ the phase of the apparent mass at the palm at 300 Hz. The new set of parameters was calculated using perturbation factor of 30%.

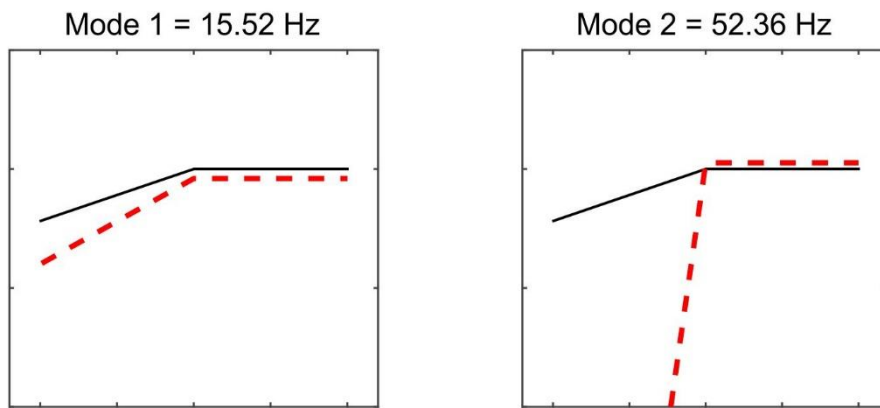


Figure 9-10 Illustration of the mode shapes for Model B (— initial condition of the hand and the arm, - - - predicted condition of the hand and the arm during resonance)

The sensitivity matrix is based on three factors, P_m the mass of each body segment (m_1, m_5, m_{ts}), P_{tr} translational stiffness and damping (k_1, k_2, c_1, c_2), P_{rt} rotational stiffness and damping (k_{r5}, c_{r5}). For the calculation of the parameter sensitivity, the apparent mass at the palm was calculated using optimized parameters for Subject 12.

$$P_{model B} = [P_{tr} \ P_{rt} \ P_m] \quad (9.18)$$

$$P_m = \begin{bmatrix} -0.305 & -0.143 & 0.000 \\ -0.115 & -0.280 & 0.000 \\ -0.008 & 0.002 & 0.008 \\ 0.104 & 0.002 & -0.058 \end{bmatrix} \quad (9.19)$$

$$P_{tr} = \begin{bmatrix} 0.446 & 0.000 & 0.000 & 0.000 \\ 0.019 & 0.000 & 0.000 & 0.000 \\ 0.063 & 0.000 & 0.931 & -0.001 \\ 0.124 & 0.000 & -0.175 & 0.000 \end{bmatrix} \quad (9.20)$$

$$P_{rt} = \begin{bmatrix} 0.014 & 0.000 \\ 0.452 & 0.000 \\ -0.003 & -0.006 \\ -0.016 & 0.001 \end{bmatrix} \quad (9.21)$$

The first resonance frequency is largely affected by the mass of the palm, m_1 , and the fingers, m_5 , as well as the stiffness, k_1 .

The second resonance frequency is largely affected by mass of the palm, m_1 , mass of the fingers, m_5 , and rotational stiffness, k_{r5} .

The apparent mass at the palm (modulus and phase) at 300 Hz is largely affected by the change in the mass of the palm tissues, m_{ts} , stiffnesses, k_1 , and damping, c_1 .

9.3 Lumped parameter model of glove material

9.3.1 Model description

The properties of a viscoelastic material can be observed from the material load deflection curve (i.e., indication of the material properties such as creep behaviour and relaxation behaviour), which could assist in the modelling of the glove dynamic stiffness. The load deflection curve for Foam A, Foam B, and Gel A and the procedures to measure it are shown in the Appendix D.

All three materials had a mass of less than 2 grams (i.e., for 25 mm diameter of contact area). In this chapter, the glove materials are assumed to be massless.

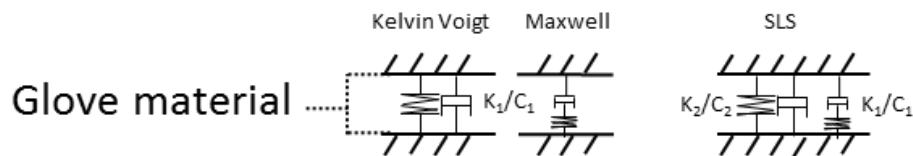


Figure 9-11 Viscoelastic models of the glove material (Jones, 2001).

The dynamic stiffness of the material for the Kelvin Voigt model is given by

$$d(f) = k_1 + ic_1w \quad (9.22)$$

The dynamic stiffness of the material for the Maxwell model is given by

$$d(f) = \frac{iwk_1c_1}{k_1+iwc_1} \quad (9.23)$$

The dynamic stiffness of the material for the Standard Linear Solid model is given by

$$d(f) = k_2 + ic_2\omega + \frac{i\omega k_1 c_1}{k_1 + i\omega c_1} \quad (9.24)$$

9.3.2 Measuring the material dynamic stiffness

The dynamic stiffnesses of the three materials, Foam A, Foam B and Gel A, were measured in a previous experiment (see Chapter 6) using an indenter rig. In this chapter, only the dynamic stiffnesses measured with a preload force of 20 N were used. The glove materials had a diameter of 25 mm with thicknesses of 6.4, 5.0, 6.0 mm for Foam A, Foam B, and Gel A, respectively.

9.3.3 Calibrating the model of the glove material

The error function is shown in Equation 9.25. All models of the glove materials were calibrated with the measured dynamic stiffness at frequencies from 10 to 60 Hz for Maxwell model, from 10 to 300 Hz for Kelvin Voigt model and from 10 to 200 Hz for the Standard Linear Solid Model (i.e., emphasis on lower frequency range).

$$Error, E = \sum_{i=1}^N (Real(d_p(i)) - Real(d_m(i)))^2 + \sum_{i=1}^N (Imag(d_p(i)) - Imag(d_m(i)))^2 \quad (9.25)$$

Where d_p is the calibrated dynamic stiffness in complex number, d_m is the measured dynamic stiffness in complex number.

9.3.4 Identification of the model parameters

Initial values for the parameters for all three models of viscoelastic material were mainly based on the median stiffness and median damping measured in the previous experiment (see Chapter 6).

For the Kelvin Voigt model and the Maxwell model, for all parameters, the upper boundaries were set to infinity whilst the lower boundaries were set to zero.

For the Standard Linear Solid model, the initial values for k_2 and c_2 (i.e., Kelvin Voigt components) were set to be the same as the optimized k_1 and c_1 in the Kelvin Voigt model. The upper and the lower boundaries for k_2 and c_2 were set to be $\pm 20\%$ of their initial values. The initial values of k_1 and c_1 (i.e., Maxwell components) were set to be the

same as the initial values of k_2 and c_2 , but with upper boundary of infinite and the lower boundary of zero.

The optimized parameters using 'fmincon' function in MATLAB (version 2014b) are shown in Table 9-7. The optimized values of the parameters were local minima of the error (see Section 9.3.3 for the error function) that satisfied the constraints.

9.3.5 Measured and fitted material dynamic stiffness

Constant bandwidth frequency analysis was performed across the frequency range 2 to 300 Hz with a frequency resolution of 2 Hz.

The measured and fitted dynamic stiffnesses of Foam A, Foam B, and Gel A are shown in Figure 9-12.

For Foam A, the best fit to the measured dynamic stiffness across all three models was the Standard Linear Solid model. The Kelvin Voigt model also produced a reasonable fit to the measured dynamic stiffness but discrepancies were seen at low frequencies especially in the phase.

Similarly, the dynamic stiffnesses of Foam B and Gel A calibrated using the Standard Linear Solid model were similar to the measured dynamic stiffness.

Table 9-7 Optimized model parameters for Foam A, Foam B, and Gel A.

Material	Model	Stiffness (N/m)		Damping (Ns/m)	
		k_1	k_2	c_1	c_2
Foam A	Kelvin Voigt	22152		1.53	
	Maxwell	21669		4503	
	Standard Linear Solid	2210	20529	11.30	1.35
Foam B	Kelvin Voigt	62301		6.61	
	Maxwell	56674		4766	
	Standard Linear Solid	13170	50818	57.20	5.28
Gel A	Kelvin Voigt	71470		19.33	
	Maxwell	67942		9070	
	Standard Linear Solid	12386	64152	26.65	17.80

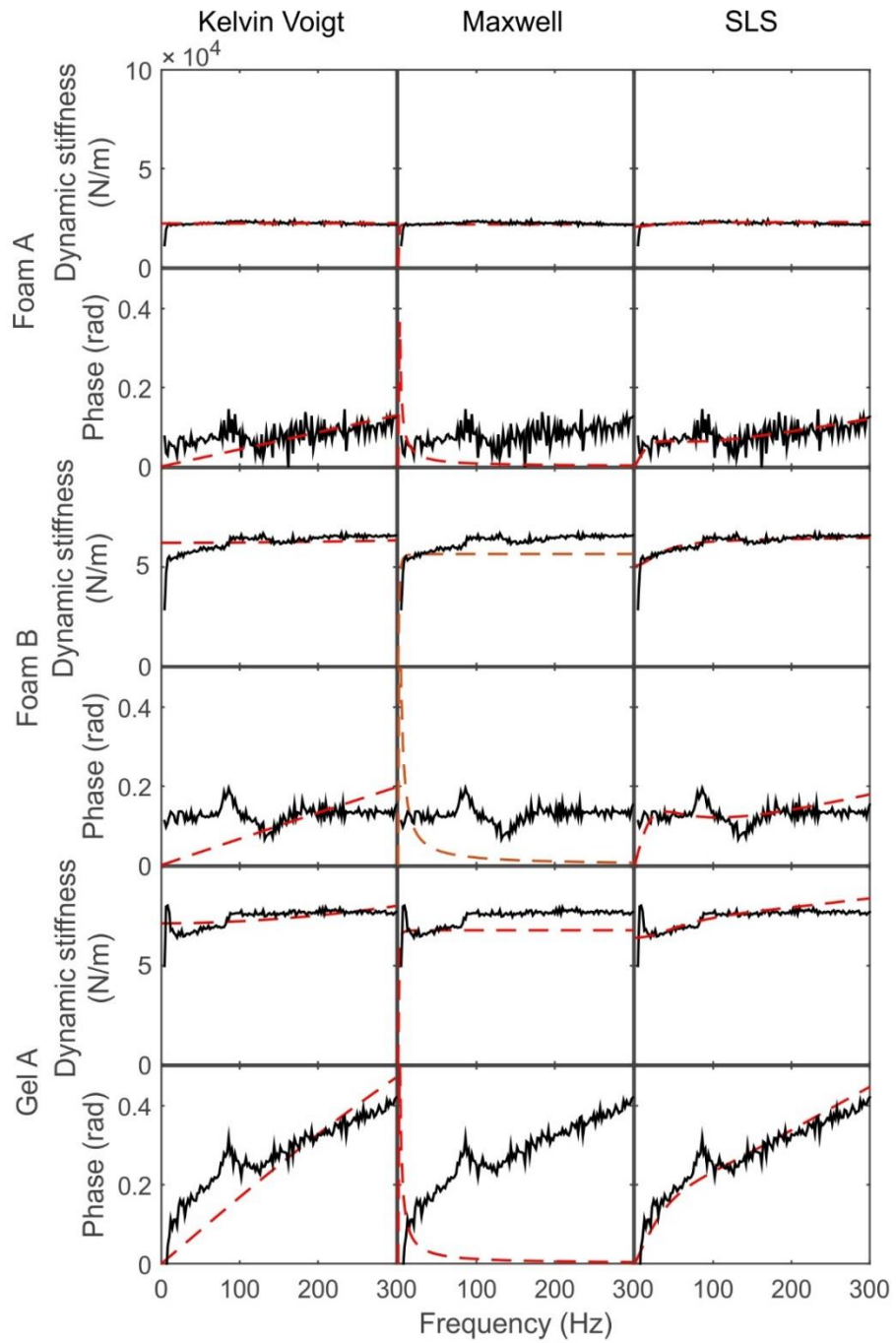


Figure 9-12 Measured and fitted dynamic stiffness (modulus and phase) of Foam A, Gel A, and Foam B (--- fitted, — measured)

9.4 Predicting the transmissibility of glove material to the palm of the hand

9.4.1 Model description

By combining both models, a model of the hand and a model of the glove material, a model that can predict the transmissibility of glove material to the palm of the hand is produced (Figure 9-13 for Model A, Figure 9-14 for Model B). Both Model A and Model B show reasonable agreement with the measured apparent mass at the palm although that they slightly underestimated the measured apparent mass at high frequencies. To reduce the complexity of this chapter, only the Standard Linear Solid model will be used as the model of the glove material.

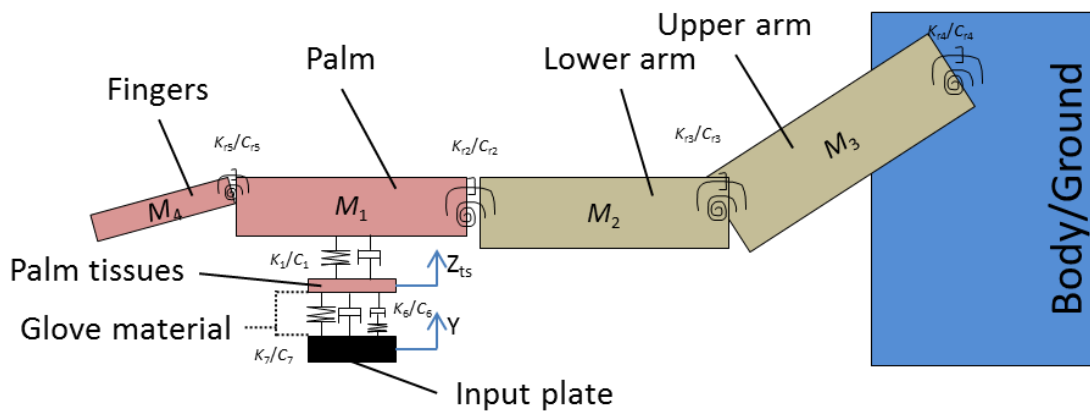


Figure 9-13 Model for predicting the transmissibility of a glove material to the palm of the hand: Model A.

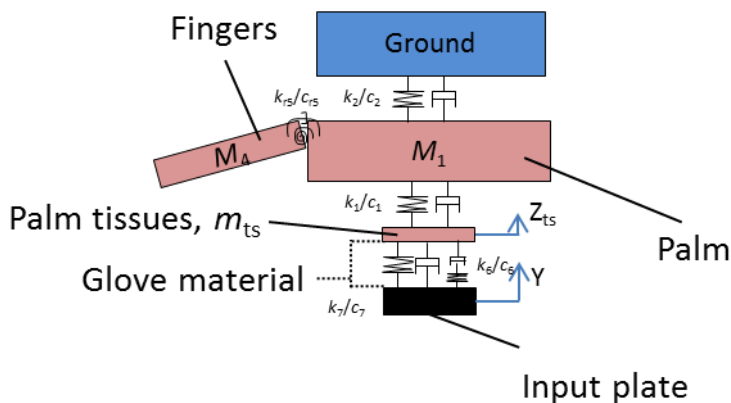


Figure 9-14 Model for predicting the transmissibility of a glove material to the palm of the hand: Model B.

It should be noted that there will be no parameter optimization in this section (i.e., Section 9.4) of this chapter. The dimensions, the mass of each segment of both models, and other model parameters were taken from the previously optimized and calculated model parameters.

Both models (i.e., Model A and Model B) assumed that the apparent mass at the palm was similar with and without the present of a glove material.

9.4.2 Equations of motion

Using Lagrange formula, the equations of motion for Model A are

$$m_1\ddot{z}_1 + m_2\left(\ddot{z}_1 + \frac{l_2}{2}\cos\theta_{20}\ddot{\theta}_2\right) + m_3\left(\ddot{z}_1 + l_2\cos\theta_{20}\ddot{\theta}_2 + \frac{l_3}{2}\cos\theta_{30}\ddot{\theta}_3\right) + m_4\left(\ddot{z}_1 - \frac{l_4}{2}\cos\theta_{40}\ddot{\theta}_4\right) + k_1(z_1 - z_{ts}) + c_1(\dot{z}_1 - \dot{z}_{ts}) = 0 \quad (9.25)$$

$$\begin{aligned} & \frac{l_2}{2}\cos\theta_{20}m_2\left(\ddot{z}_1 + \frac{l_2}{2}\cos\theta_{20}\ddot{\theta}_2\right) - \frac{l_2}{2}\sin\theta_{20}m_2\left(-\frac{l_2}{2}\sin\theta_{20}\ddot{\theta}_2\right) + l_2\cos\theta_{20}m_3\left(\ddot{z}_1 + \right. \\ & \left. l_2\cos\theta_{20}\ddot{\theta}_2 + \frac{l_3}{2}\cos\theta_{30}\ddot{\theta}_3\right) - l_2\sin\theta_{20}m_3\left(-\frac{l_3}{2}\sin\theta_{30}\ddot{\theta}_3 - l_2\sin\theta_{20}\ddot{\theta}_2\right) + I_2\ddot{\theta}_2 + k_{r_2}(\theta_2) + \\ & k_{r_3}(\theta_2 - \theta_3) + c_{r_2}(\dot{\theta}_2) + c_{r_3}(\dot{\theta}_2 - \dot{\theta}_3) = 0 \end{aligned} \quad (9.26)$$

$$\begin{aligned} & \frac{l_3}{2}\cos\theta_{30}m_3\left(\ddot{z}_1 + l_2\cos\theta_{20}\ddot{\theta}_2 + \frac{l_3}{2}\cos\theta_{30}\ddot{\theta}_3\right) - \frac{l_3}{2}\sin\theta_{30}m_3\left(-\frac{l_3}{2}\sin\theta_{30}\ddot{\theta}_3 - l_2\sin\theta_{20}\ddot{\theta}_2\right) + \\ & I_3\ddot{\theta}_3 + k_{r_3}(\theta_3 - \theta_2) + k_{r_4}(\theta_3) + c_{r_3}(\dot{\theta}_3 - \dot{\theta}_2) + c_{r_4}(\dot{\theta}_3) = 0 \end{aligned} \quad (9.27)$$

$$-\frac{l_4}{2}\cos\theta_{40}m_4\left(\ddot{z}_1 - \frac{l_4}{2}\cos\theta_{40}\ddot{\theta}_4\right) + \frac{l_4}{2}\sin\theta_{40}m_4\left(\frac{l_4}{2}\sin\theta_{40}\ddot{\theta}_4\right) + I_4\ddot{\theta}_4 + k_{r_5}(\theta_4) + c_{r_5}(\dot{\theta}_4) = 0 \quad (9.28)$$

$$m_{ts}\ddot{z}_{ts} + k_1(z_{ts} - z_1) + c_1(\dot{z}_{ts} - \dot{z}_1) + k_7(z_{ts} - y) + c_7(\dot{z}_{ts} - \dot{y}) + c_6(\dot{z}_{ts} - \dot{\varepsilon}) = 0 \quad (9.29)$$

$$k_6(\varepsilon - y) + c_6(\dot{\varepsilon} - \dot{z}_{ts}) = 0 \quad (9.30)$$

Where ε is displacement of the Maxwell component in the Standard Linear Solid model (Figure 9.15).

Maxwell component in SLS

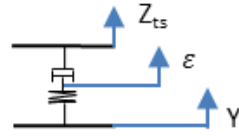


Figure 9-15 Maxwell component in Standard Linear Solid model.

The equations of motion for Model B are

$$m_1 \ddot{z}_1 + m_4 \left(\ddot{z}_1 - \frac{l_4}{2} \cos \theta_{40} \ddot{\theta}_4 \right) + k_1 (z_1 - z_{ts}) + k_2 (z_1) + c_1 (\dot{z}_1 - \dot{z}_{ts}) + c_2 (\dot{z}_1) = 0 \quad (9.31)$$

$$-\frac{l_4}{2} \cos \theta_{40} m_4 \left(\ddot{z}_1 - \frac{l_4}{2} \cos \theta_{40} \ddot{\theta}_4 \right) + \frac{l_4}{2} \sin \theta_{40} m_4 \left(\frac{l_4}{2} \sin \theta_{40} \ddot{\theta}_4 \right) + I_4 \ddot{\theta}_4 + k_{r_5} (\theta_4) + c_{r_5} (\dot{\theta}_4) = 0 \quad (9.32)$$

$$m_{ts} \ddot{z}_{ts} + k_1 (z_{ts} - z_1) + c_1 (\dot{z}_{ts} - \dot{z}_1) + k_7 (z_{ts} - y) + c_7 (\dot{z}_{ts} - \dot{y}) + c_6 (\dot{z}_{ts} - \dot{\varepsilon}) = 0 \quad (9.33)$$

$$k_6 (\varepsilon - y) + c_6 (\dot{\varepsilon} - \dot{z}_{ts}) = 0 \quad (9.34)$$

The transmissibility of the glove material to the palm of the hand is given by

$$\text{Transmissibility of the glove material to the palm, } TR = \frac{z_{ts}}{y} \quad (9.35)$$

During the measurement of glove transmissibility, a wooden adapter with embedded miniature accelerometer was used to measure vibration at the hand interface. The wooden adapter has a mass of about 1 gram (i.e., 25-mm diameter wooden adapter). The mass of the wooden adapter together with the accelerometer was assumed to be 2 grams. This mass was added to the apparent mass at the palm.

9.4.3 Measuring the material transmissibility to the palm of the hand

The transmissibility of the glove materials to the palm were measured in a previous experiment at frequencies from 10 to 300 Hz with a magnitude of 2 m/s² r.m.s. (frequency-weighted using W_h according to ISO 5349-1:2001) with 20 N push force. See Chapter 7 for details of this measurement.

9.4.4 Predicted and measured glove transmissibility

Constant bandwidth frequency analysis was performed across the frequency range 2 to 300 Hz with a frequency resolution of 2 Hz.

Figure 9-16 shows the predicted and the measured glove transmissibility to the palm of the hand.

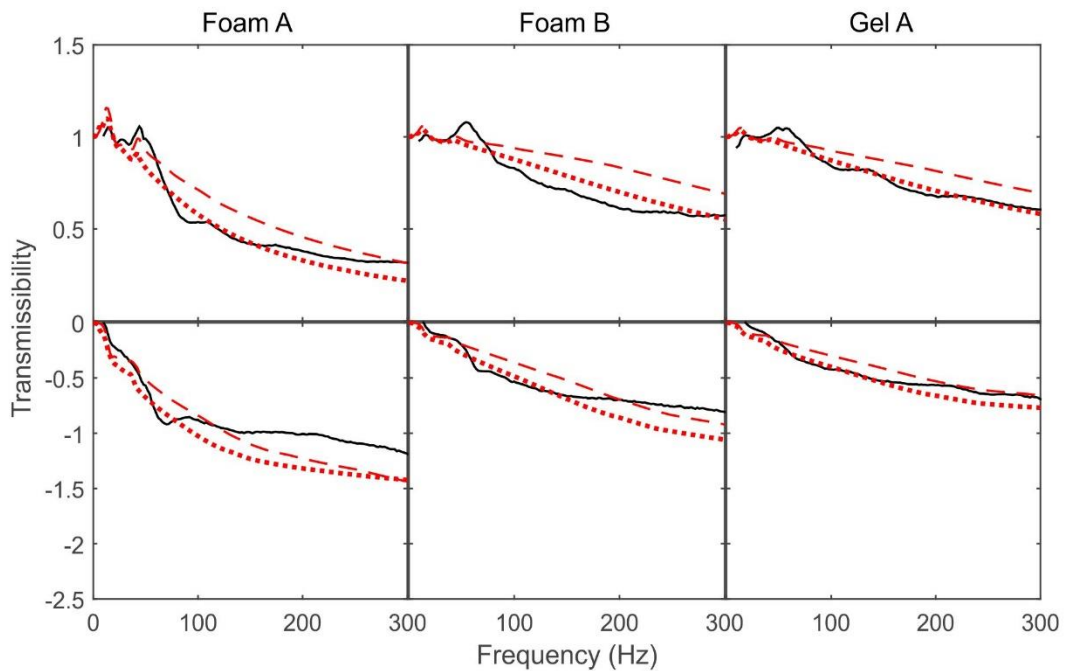


Figure 9-16 Predicted and measured transmissibility of glove materials to the palm of the hand (— measured, Model A, - - - Model B). Median of 12 subjects.

The predicted transmissibility of Foam A to the palm using Model A was not significantly different from the measured transmissibility at frequencies from 10 to 30 Hz (Wilcoxon, $p > 0.09$), 60 to 194 Hz (Wilcoxon, $p > 0.052$). The predicted transmissibility underestimated the measured transmissibility at frequencies from 32 to 58 Hz (Wilcoxon, $p < 0.035$) and at frequencies greater than 196 Hz (Wilcoxon, $p < 0.043$).

The predicted and the measured transmissibility of Foam B to the palm using Model A were not significantly different at frequencies less than 114 Hz (Wilcoxon, $p > 0.064$) and at frequencies greater than 208 Hz (Wilcoxon, $p > 0.064$). At frequencies between 116 and 206 Hz, the predicted transmissibility overestimated the measured transmissibility (Wilcoxon, $p < 0.043$).

The predicted transmissibility of Gel A to the palm using Model A was not significantly different from the transmissibility measured experimentally at any frequencies from 10 to 300 Hz (Wilcoxon, $p > 0.064$) except at frequencies between 34 and 72 Hz (Wilcoxon, $p < 0.043$).

The predicted transmissibility of Gel A to the palm using Model B was greater than the measured transmissibility at frequencies greater than 88 (Wilcoxon, $p < 0.043$) and at frequencies less than 18 Hz (Wilcoxon, $p < 0.007$) but slightly lower than the measured transmissibility at frequencies between 34 and 62 Hz (Wilcoxon, $p < 0.03$). The predicted transmissibility was similar at frequencies between 20 and 32 Hz (Wilcoxon, $p > 0.2$) and at frequencies between 64 and 86 (Wilcoxon, $p > 0.052$).

The predicted transmissibility of Foam A to the palm using Model B was not significantly different from the transmissibility measured experimentally at frequencies between 20 and 66 Hz (Wilcoxon, $p > 0.064$) and at frequencies greater than 234 Hz (Wilcoxon, $p > 0.052$). The predicted transmissibility overestimated the measured transmissibility at frequencies less than 18 Hz (Wilcoxon, $p < 0.02$), and at frequencies between 68 and 232 Hz (Wilcoxon, $p < 0.043$).

The predicted transmissibility of Foam B to the palm using Model B was similar at frequencies between 24 and 76 Hz (Wilcoxon, $p > 0.052$) but overestimated the measured transmissibility at frequencies less than 24 Hz (Wilcoxon, $p < 0.043$) and at frequencies greater than 78 Hz (Wilcoxon, $p < 0.01$).

At frequencies greater than about 70 Hz, transmissibility predicted by Model B provided poorer prediction than transmissibility predicted by Model A.

9.5 Discussion

9.5.1 Proposed model of biodynamic response of the hand and the arm

The tension in muscles and tissues that produces forces between the body segments was represented by stiffness and damping elements located below the palm, between the fingers and the palm, between the forearm and the palm, between the upper arm and the lower arm, and between the upper arm and the trunk of the body. These springs and dampers were assumed to be linear. The fitted apparent mass of the hand underestimated the apparent mass measured experimentally at high frequencies. It was not clear whether the discrepancies between the fitted and the measured apparent mass were influenced by the assumption made on the linearity of the springs and the dampers

connecting the body segments as evidenced in a previous study (i.e., Nawayseh and Griffin, 2004).

It has been reported previously that the posture of the arm can affect the biodynamic response of the hand at frequencies less than 30 Hz (Búrstrom, 1997; Adewusi *et al.*, 2012). It was also suggested that the dynamic response of the hand at high frequencies is mainly influenced by the motion of the hand and the fingers (e.g., Dong *et al.*, 2007). In this study, Model B was developed as a simplified version of Model A, to represent the apparent mass at the palm without considering the influence of the lower arm and the upper arm (i.e., to investigate whether the dynamic response of the hand can be represented using a simplified hand-fingers model). The fitted apparent mass of Model B underestimated the apparent mass measured experimentally at frequencies greater than 16 Hz, suggesting that a model of the hand without considering the influence of the arm (i.e., Model B) may not be able to represent the driving-point response of the hand similar to or better than the model of the hand and the arm (i.e., Model A). It should be noted that both models provided reasonably similar fitted apparent mass with the measured apparent mass at frequencies less than 14 Hz.

9.5.2 Parameter sensitivity, modal analysis, and effects of contact area and push force on the apparent mass at the palm

The parameter sensitivity analysis showed that increasing the overall mass of each segment of the hand reduces all four resonance frequencies in the apparent mass at the palm. In reality, these masses are unchanged, thus, the increase in the resonance frequencies in the apparent mass at the palm (i.e., at about 5, 15, and 45 Hz; see Chapter 8) is expected to be caused by the increase in the stiffness and damping elements connecting the palm, the fingers, and the arm (see Section 9.2.1.9). This is consistent with the previous model of the hand (Adewusi *et al.*, 2012) but the previous model was not able to clearly provide evidences (i.e., such as similar resonance frequencies in the measured and predicted apparent mass due to motion of the hand and the arm similar to this research).

Table 9-8 shows the predicted and the measured resonance frequencies of the apparent mass of the hand reported in this chapter, Chapters 7 and 8, and in three other studies. Resonances predicted by Model A and Model B, and resonances measured in Chapter 8 were closely similar to each other. The undamped natural frequencies predicted by both Model A and Model B are also similar to the resonance frequencies predicted by

the models of the hand and the arm (Dong *et al.*, 2007; Adewusi *et al.*, 2012), and resonance frequencies measured experimentally (Concettoni and Griffin, 2009).

Table 9-8 Predicted resonance frequencies of the apparent mass of the hand

Undamped natural frequency	Model A	Model B	Measured (Chapter 7 and 8)	Bent-arm model, Adewusi et al. (2012)	Bare hand model, Push, Dong et al., (2007)	Extended arm – Condition 7, Concettoni, and Griffin, 2009
1	0.96	-	-	4.17	-	-
2	6.5	-	5	10	-	-
3	12.6	14.6	14	18	13	22
4	38.1	44.9	45	69	30	46
5				64	222	
6				154		

The predicted mode shapes of Model A and Model B for the third and the fourth resonances had similar resemblance with the mode shape measured in a previous study (Figures 9-5 and 9-10; Concettoni and Griffin, 2009). At 22 Hz, the measured mode shape had fingers rotated downward with the palm moved downward similar to the third mode of Model B. At 46 Hz, the palm moved downward and the fingers rotated upward, contradictly in the fourth mode of Model A, the fingers were predicted to rotate in the anti-clockwise direction (i.e., downward) and the palm moved upward.

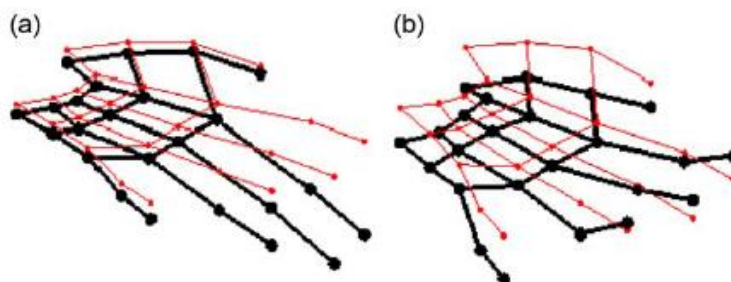


Figure 9-17 Operating deflection shapes in condition 7: a. 22 Hz, b. 46 Hz (—— deflection, - - - - initial condition; Concettoni and Griffin, 2009).

Increasing the area of contact increased the apparent mass at frequencies greater than about 70 Hz (see Chapter 5). In this study, the increase in the apparent mass at frequencies greater than 70 Hz without increasing the natural frequency in Model A and Model B can be observed by increasing the mass of the palm tissues, m_{ts} (i.e., mass close to the vibration driving-point), assuming that the masses of other body segments are unchanged. Although that this was suspected previously (i.e., Dong *et al.*, 2005, 2009), this study provided clearer evidence that this is the case.

The resonance frequency at about 15 Hz increases with increasing push force (see Chapter 6). The apparent mass of the hand at frequencies greater than the resonance also increases with increasing push force. The parameter sensitivity analyses of Model A and Model B in this study suggest that the third resonance frequency (i.e., at about 15 Hz) and the apparent mass at frequencies greater than the resonance increase with increasing the stiffness and damping elements (i.e., k_1 , c_1 ; assuming that the mass of the palm, the fingers, and the arm are unchanged) in the same manner when the contact force increases. This was expected previously (e.g., Marcotte *et al.*, 2005) but in this study, the evidence provided from previous chapters (i.e., effects of the motion of each body segments on apparent mass at the palm were identified) clearly suggest that the spring and damping elements between the palm and the palm tissues were the predominant reason for the increase in the resonance at about 15 Hz.

9.5.3 Predicting transmissibility of a glove material to the hand

Both models overestimated the measured transmissibility at high frequencies. It was observed previously that the transmissibility of a glove to the hand decreases at frequencies greater than the resonance when the apparent mass of the hand increases (see Chapter 4: transmissibility to the palm was less than the transmissibility to the index finger at frequencies greater than the resonance). In this study, the fitted apparent mass in both models was slightly less than the measured apparent mass at high frequencies. On the other hand, the fitted dynamic stiffness was reasonably similar to the dynamic stiffness measured experimentally. These suggest that the discrepancies between the predicted and the measured apparent mass (i.e., underestimation of apparent mass; see Section 9.2.1.7 and 9.2.2.7 for the predicted and measured apparent mass) at high frequencies in both models may be the primary reason the predicted transmissibility overestimated the measured transmissibility at high frequencies.

Model B provided inferior prediction of glove transmissibility compared to Model A at high frequencies. This may indicate that the exclusion of the dynamic response of the arm affects the ability of a model to accurately predict glove transmissibility.

Figure 9-18 shows the median predicted transmissibility based on the two biodynamic models of the hand and the impedance model (see Chapter 7). The median predicted transmissibilities of all three gloves using the impedance model showed better representation of the measured transmissibilities than either Model A or Model B, suggesting that the transmissibility to the palm is better predicted using impedance model than using lumped parameter models developed in this study

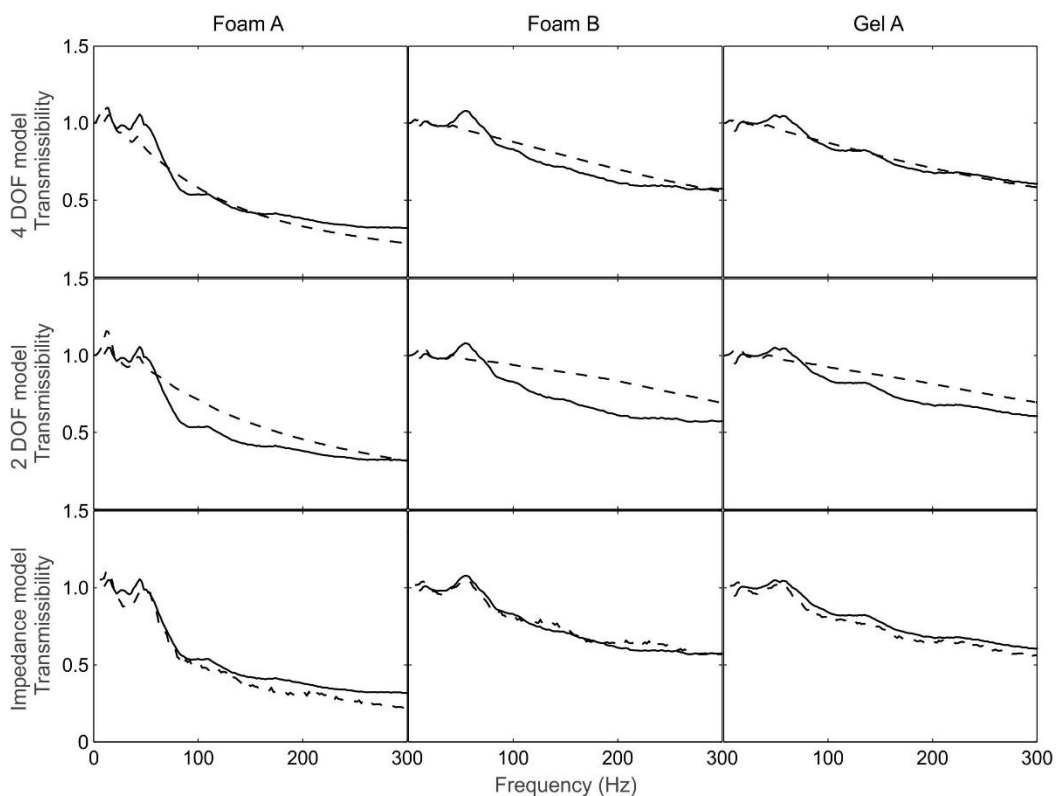


Figure 9-18 Predicted transmissibility for three prediction methods (— — — predicted, ——— measured).

9.6 Conclusions

Two models were developed to predict the transmissibility of a glove to the palm of the hand: a model of the hand and the arm (Model A) and a model of the hand (Model B).

The four degree-of-freedom model (Model A) was better in representing the measured apparent mass of the hand than the two degree-of-freedom model (Model B) although both models slightly underestimated the measured apparent mass at high frequencies.

Both models overestimated the measured transmissibilities of glove materials, especially the transmissibility of Foam B. Model B consistently provided poorer transmissibility prediction than Model A at all frequencies from about 70 to 300 Hz.

Both models provided poorer prediction of glove transmissibility to the palm than the mechanical impedance model.

Chapter 10: General discussions

10.1 Apparent mass of the hand

A summary of the measurements of apparent mass at the palm of the hand is shown in Figure 10-1.

Increasing the force applied to the vibrating surface increased the resonance frequency in the apparent mass at the palm around 15 Hz. This also resulted to an increase in the apparent mass at frequencies greater than the resonance. The trend of increasing resonance is similar to the trend found in previous studies (O'Boyle and Griffin, 2004; Marcotte *et al.*, 2005; Xu *et al.*, 2011). The increase in the resonance frequency around 15 Hz may be predominantly due to an increase in the stiffness and damping elements between the palm and the tissues in the palm, as suggested by the model of the hand (see Chapter 9).

Increasing the area of contact increases the apparent mass at the palm of the hand at frequencies greater than 70 Hz. This is consistent with the findings of the previous studies although the increase in the apparent mass in those studies occurred at a higher frequency of vibration (Mann and Griffin, 1996, Marcotte *et al.*, 2005). The model of the hand developed in this research suggests that increasing the mass of the palm tissues increases the modulus and decreases the phase of the apparent mass in the same manner as when the contact area is increased. This research suggests that increases in the apparent mass at the palm at high frequencies could be due to an increase in the mass of the palm tissues close to the vibration driving-point.

It has been reported that increasing the vibration magnitude increases the apparent mass of the hand at frequencies greater than 500 Hz (Lundström *et al.*, 1989). It has also been reported that the mechanical impedance of the hand increases with decreasing vibration magnitude at frequencies greater than 150 Hz (Burström, 1997) but a study performed recently suggested that the effects of vibration magnitude can be ignored at frequencies greater than 100 Hz (Marcotte *et al.*, 2005). In this study, an increase in the vibration magnitude had little to no effect on the apparent mass of the hand at any frequency of vibration from 10 to 300 Hz. It is not clear why the contradictory findings between this research and the other studies (i.e., it could be due to the different condition of the hand and the arm, different in terms of the frequency components of the vibration magnitude)

The apparent mass at the palm was little affected by the change in the arm condition (i.e. with and without arm support) at frequencies greater than 15 Hz (see Chapter 7). However, the apparent mass at the palm with arm support was significantly less than without arm support at frequencies less than 15 Hz. The mechanical impedance of the hand was also found to be affected at low frequencies when the arm posture was changed in the previous studies (i.e. at frequencies less than 30 Hz; Burström, 1997; Besa et al., 2007, Adewusi *et al.*, 2010, 2012), consistent with this research.

The apparent mass at the palm was affected by the change in the arm posture at frequencies less than 15 Hz (see Chapter 7). This indicates that the motion of the lower arm and the upper arm largely contributed to the apparent mass at the palm at frequencies less than 15 Hz. The resonance due to the motion of the lower arm was found to occur at about 5 Hz as suggested by the study in Chapter 8 and the study of lumped parameter model of the hand in Chapter 9. The resonance due to the motion of the upper arm is expected to occur at frequencies less than 2 Hz (see Chapter 9).

10.2 Dynamic characteristics of the glove materials

A summary of the measurements of the dynamic characteristics of Foam A is shown in Figure 10-1.

The stiffness and damping of Foam A were affected by contact area and contact force (see Chapter 5 and 6). This was similar with Gel A: the increase in the contact area and the contact force will increase the stiffness and damping of Gel A. However, the stiffness and damping of Foam B were only affected by the change in the contact area. These behaviours of the materials are expected because the stiffness and damping depend on the material characteristics such as the creep and the relaxation behaviour. However, it also implies and further proves that the characteristics of a glove material may not be possible to be predicted without a measurement.

10.3 Transmission of vibration through gloves to the hand

A summary of the measurements of the transmission of vibration through Foam A to the palm of the hand is shown in Figure 10-1. Increasing the area of contact was expected to increase the dynamic stiffness of the glove materials and therefore tend to increase glove transmissibility at frequencies greater than the resonance. However, with increasing contact area, the apparent mass at the palm was also expected to increase and tend to reduce glove transmissibility at frequencies greater than the resonance. In

this study, the increase in the dynamic response of the hand when the area of contact increased was small and may not be able to give a larger impact on glove transmissibility compared to the increase in the dynamic stiffness of the glove material (see Chapter 5). This research found that with increasing area of contact the transmissibility of the glove materials increased: it seems that when the area of contact varied, the effects on glove transmissibility predominantly depended on the material dynamic stiffness rather than the dynamic response of the hand.

Previous study has shown that increasing the contact force increases glove transmissibility to the palm of the hand (Laszlo and Griffin, 2011). This is not always the case, the glove transmissibility seemed to be relatively unaffected by increases in contact force in another study (i.e. there was an increase in the glove transmissibility but the increase is too small; O'Boyle and Griffin, 2004). In this study, the increased apparent mass of the hand offset the increase in the dynamic stiffness of Foam A and Gel A, resulting to little change in glove transmissibility. The increase in the dynamic stiffness of Foam B was small, and the transmissibility of Foam B to the palm decreased with increasing contact force. This is consistent with the underlying theory that glove transmissibility depends on both the apparent mass of the hand and the glove dynamic stiffness. It may be concluded that the assessment of the performance of a glove in reducing vibration will be insufficient without measurements with varying contact force.

In this research, glove transmissibility to the palm of the hand was little affected by changes in the magnitude of vibration. It is suggested that if there is a systematic effect on glove transmissibility due to the change in the magnitude of vibration (e.g. Laszlo and Griffin, 2011), it may be due to the changes in the dynamic stiffness of the glove material rather than the apparent mass of the hand because the apparent mass of the hand was little affected by changes in the magnitude of vibration, especially at high frequencies (Chapter 7, Marcotte *et al.*, 2005).

At frequencies greater than 15 Hz, glove transmissibility was little affected by the arm condition (i.e., with and without arm support). This was expected because the apparent mass at the palm was little affected by the arm condition at frequencies greater than 15 Hz. However, a study investigating the effects of arm angle previously has found that the resonance in glove transmissibility increased and decreased as the angle of the arm increased (Wu and Griffin, 1989) but the measurements were obtained at the knuckle.

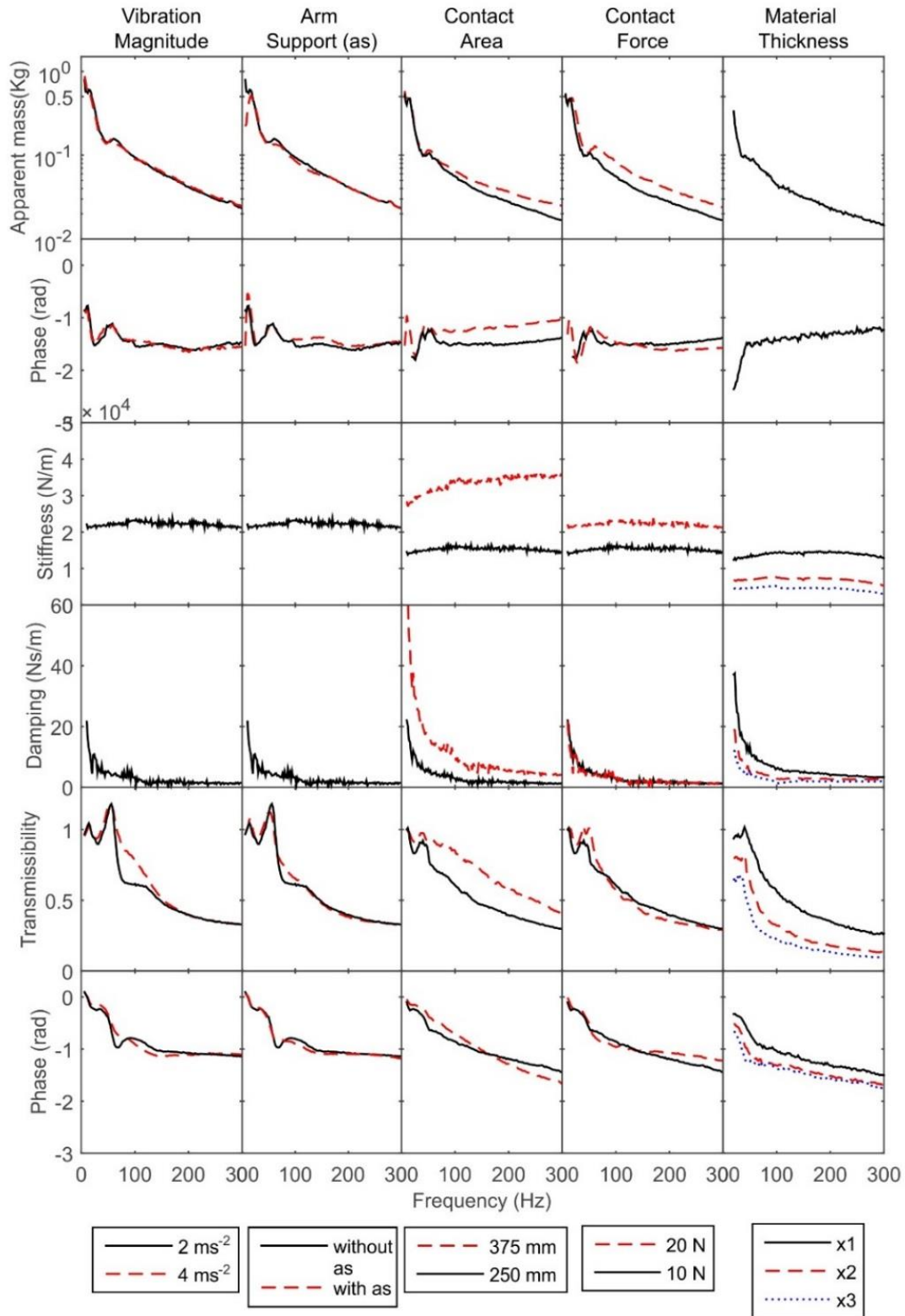


Figure 10-1 The effects of vibration magnitude, arm support, contact area, contact force and material thickness on the apparent mass at the palm, the dynamic stiffness of Foam A, and the transmissibility of Foam A to the palm. Median data.

10.4 Repeatability and reproducibility of the measurement in this research

In the first experiment investigating the effects of material thickness, the apparent mass at the palm of the hand was measured with a contact force of 10 N and a 20-mm diameter contact area. In the second experiment investigating the effects of contact area and contact force, the apparent mass at the palm was measured in the same conditions but with different subjects. Figure 10-2 compares the apparent masses measured in both experiments with those reported previously (O'Boyle and Griffin, 2004). The median apparent mass at the palm measured in the first experiment was similar to the median apparent mass measured in the second experiment and in the previous study (i.e. O'Boyle and Griffin, 2004). This suggests measurements of apparent mass of the hand between groups of human subjects can be similar if the conditions are similar.

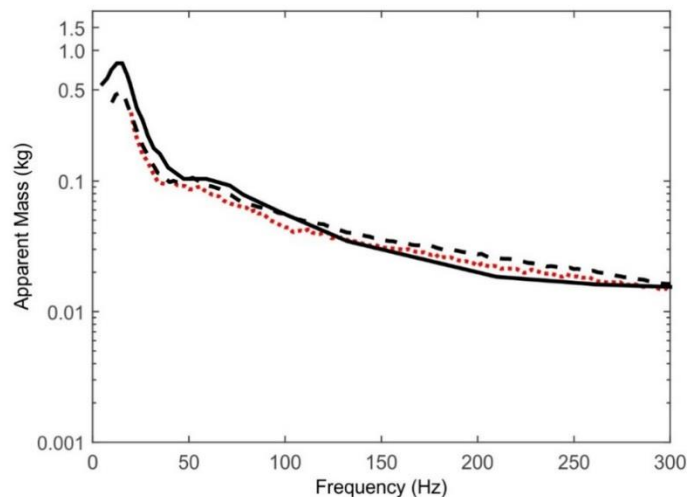


Figure 10-2 Apparent mass at the palm measured in similar conditions but with different sets of subjects (— Boyle and Griffin, 2004, - - - Experiment 2, Experiment 1).

10.5 Predicting glove transmissibility using a mechanical impedance model of the hand and the glove

An impedance model of the hand and glove was used to predict the transmissibility of the glove materials to palm of the hand and to the finger. It was first used as a method to predict seat transmissibility (Fairley and Griffin, 1986) but later adapted to be used to predict glove transmissibility to the hand (O'Boyle and Griffin, 2004). In all experiments, the transmissibilities of the glove materials to the hand predicted using the mechanical

impedance model were in reasonable agreement with the transmissibilities measured experimentally. The impedance model reflected the effects of variations in conditions (contact area, material thickness, and applied force) and variations between subjects. In Chapters 5 and 6, the mechanical impedance model was used to understand better the relative importance of the dynamic stiffness of glove material and the apparent mass of the hand on glove transmissibility.

The mechanical impedance model however, has several limitations.

- In this research, the application of the mechanical impedance method was limited to frequencies less than 350 Hz (in the second experiment, this was reduced to 300 Hz) due to a resonance around 480 Hz found in the indenter rig. Although that this may be improved in a new indenter rig, it may be difficult to eliminate all resonances below 1000 Hz (the upper frequency often assumed when evaluating hand-transmitted vibration).
- The samples of glove materials in this study were obtained from the inside of gloves. Gloves can have several layers of materials and so a method of measuring the dynamic response of several layers of materials may need to be developed.
- It is not known whether this method is able to predict glove transmissibility to the hand in the condition similar to the one specified in the ISO 10819:2013.
- Measuring apparent mass of the hand at high frequencies can be difficult because the mass of the hand at frequencies greater than 300 Hz could be less than 10 grams for the measurement at the palm or less than about 5 grams for the measurement at the index finger.

10.6 Transmissibility of Foam A to the palm of the hand assessed according to ISO 10819:2013

It is expected that there will be differences between the transmissibility measured in this research and the transmissibility measured according to the ISO 10819:2013 (e.g. different in the area of contact, contact force, vibration direction). Comparison between the measurement of glove transmissibility in this research and in the ISO 10819:2013 was done to show the difference between both measurements. The transmissibility of the glove from which one of the foam materials (Foam A) was extracted was measured using the procedure defined in ISO 10819:2013, with the addition of a broadband random spectrum (acceleration spectrum over the frequency range 25 to 1250 Hz). The thickness of the foam inside the glove was about 6.4 mm. When measuring with the full glove, the

subject stood upright, forearm directed in the axis of vibration (horizontal vibration) with the angle of the elbow approximately 90°. The measurement was done in two conditions:

1. The grip force and feed force were maintained at about 30 N and 50 N, respectively,
2. Only the feed force was applied to the handle and maintained at about 25 N. The transmissibility of the glove measured at the palm of the hand is shown in Figure 10-3 together with transmissibility of the 37.5-mm diameter sample of foam (with a thickness of 6.4 mm and push force of 10 N; see Chapter 5). The glove transmissibilities were measured on the same subject (i.e., Subject 1 of Chapter 5). The transmissibilities are dissimilar.

The differences between the two transmissibilities may have arisen from:

- A difference in contact area. The glove contact area in the ISO 10819:2013 (i.e. the area of the wooden adapter; about $2.0 \times 10^{-3} \text{ m}^2$) is greater than the area of the 37.5-mm diameter disc (about $1.1 \times 10^{-3} \text{ m}^2$) measured in this research.
- A difference in contact force. The contact force used in the measurement specified in the standard was greater than measured in this research (see Figure 10-3 for the difference in the push force).
- A difference in vibration direction. In this research, the vibration was vertical compared to horizontal in the standard.
- A difference in hand posture. The apparent mass of the hand was measured on a cylindrical surface compared to a flat surface in this research. The hand was in grip condition in the standard whilst the hand was lying flat of the vibration surface in this research.
- The palm adapter used for measurements according to ISO 10819:2013 has a mass greater than the adapter used in this research (i.e., 7.33 grams for the ISO 10819:2013 compared to 5 grams for the 37.5-mm diameter contact area). Increased mass of the adapter will reduce the resonance frequency and reduce transmissibility at higher frequencies.

10.7 Improving methods of assessing glove transmissibility to the palm of the hand

This research suggests several methods to improve the way a glove is assessed before it can be considered as anti-vibration glove (i.e. ISO 10819:2013, ISO 13753:2008).

10.7.1 Effects of contact area and contact force on the glove transmissibility

It has been shown that contact area and contact force are predominantly influencing glove transmissibility to the hand (see Chapters 5 and 6). The transmissibility of a glove to the hand can increase or decrease with increasing contact area or increasing contact force.

If the handle (i.e., contact area) used by a powered tool is larger than the one specified in this standard, the transmissibility of a glove to the hand could be larger with the powered tool than with the standard. Hence, a glove should be assessed using several sizes of handle and be rated according to the size of the handle that it can provide reasonable vibration attenuation. The lower the transmissibility with the largest handle, the better the performance of the glove in reducing vibration to the hand. In addition, the glove should also provide reasonable vibration attenuation with the smallest handle because with the small contact area, it may be easy to cause the glove material to bottom-out.

Some powered tools require the operator to hold it with a larger grip force than the one specified in the standard. This research has shown that the push force can increase or decrease the glove transmissibility to the hand. A glove may provide reasonable vibration attenuation when assessed according to the standard but when the glove is used with a larger grip force, the glove may provide poorer attenuation. To consider this in the standard, the glove should be assessed with several sets of grip or feed force. The glove can be rated by the maximum push or grip force that it can be subjected before it provides unreasonable vibration attenuation.

10.7.2 Measuring glove transmissibility to the fingers

The apparent mass at the index finger is a lot less than the apparent mass at the palm of the hand (see Chapter 4). With the same material dynamic stiffness, the resonance frequency in glove transmissibility to the index finger is greater than the resonance frequency in glove transmissibility to the palm of the hand. At frequencies from 20 to 100 Hz, the transmissibility of Foam A to the index finger increased with increasing frequency but the transmissibility of Foam A to the palm decreased with increasing frequency (see Chapter 4). The results in this study indicate that measurements of the transmission of vibration to the palm of the hand (as in ISO 10819:2013) will not provide

a useful indication of the vibration transmitted to a finger. A method to assess vibration at the finger needs to be developed.

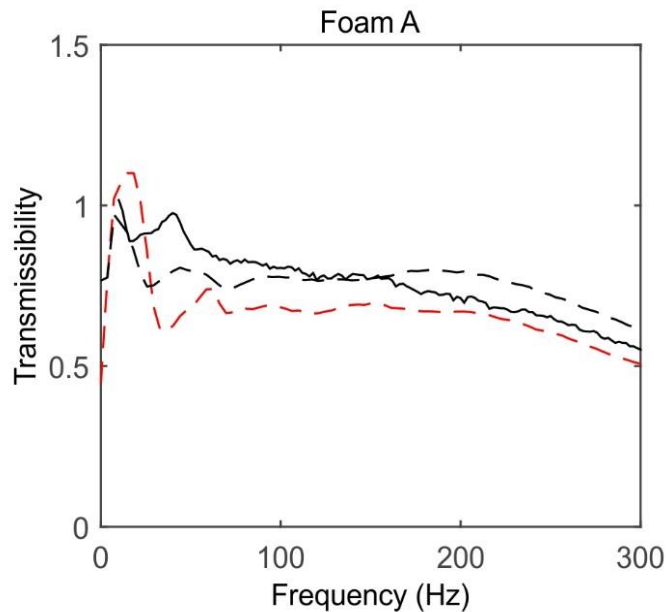


Figure 10-3 Transmissibility of Foam A to the palm of the hand. (— measured on a 37.5-mm diameter flat plate at 10 N push force in Chapter 5, --- ISO 10819:2013 Condition 1 The grip force and feed force were maintained at about 30 N and 50 N, respectively, ---- ISO 10819:2013 Condition 2 Only the feed force was applied to the handle and maintained at about 25 N). Subject 1 of Chapter 5.

10.7.3 Rank ordering gloves in terms of effectiveness in reducing vibration

The currently standardised method of measuring the transmissibility of a glove to the palm of the hand (ISO 10819:2013) may not indicate the actual performance of a glove when it is used in different conditions (e.g., different arm support, contact area, contact force, vibration direction). If the tests as suggested in the section previously are included in the standard, it would increase the time taken for a glove test and increase the number of test performed on human subjects.

The mechanical impedance model of the hand has been shown to reflect the relative importance of the biodynamic response of the hand and the dynamic characteristics of glove material. Transmissibilities predicted using the model show reasonable agreement with transmissibilities measured experimentally. It seems that if the biodynamic response of the hand is known and the dynamic stiffnesses of gloves are measured, the transmissibilities of the gloves can be predicted without requiring tests with subjects. The

mechanical impedance method is similar to the method specified in the ISO 13753:2008 except the standard does not consider the various factors that can affect glove transmissibility (e.g., contact area, contact force).

This research proposes that the effectiveness of a glove in reducing vibration should be assessed based on its dynamic stiffness similar to the ISO 13753:2008. Using measures of the biodynamic response of the hand and fingers and the measured glove dynamic stiffness, the transmissibility of the glove can be predicted using the mechanical impedance model. This could reduce the number of tests performed on human subjects, improve the repeatability and reliability of glove assessments, and reduce the time to assess gloves in various conditions (e.g., different contact areas, contact forces, arm conditions, vibration directions).

Chapter 11: Conclusions and recommendations

11.1 Conclusions

The following conclusions are based on findings from the studies carried out during this research. The conclusions address the research objectives set up in Section 2.8.5.

Over much of the frequency range studied in this research (20 to 350 Hz), glove materials attenuated the transmission of vibration to the palm of the hand but amplified the transmission of vibration to the finger. This is due to the difference in the apparent mass of the hand and the apparent mass of the finger (the apparent mass of the hand was greater than the apparent mass of the finger at all frequencies considered in this research).

Increasing or decreasing the dynamic stiffness of a glove material (e.g., by changing the material thickness, contact area, contact force) can have large effects on transmissibility to the palm of the hand and to the fingers. Reducing the dynamic stiffness of glove material tends to reduce transmissibility to the palm but may increase transmissibility to the finger.

The transmissibility of a glove material to the palm or the finger can be predicted from the dynamic stiffness of the glove material and the apparent mass measured at the palm or finger (i.e., a mechanical impedance model). It is also possible to predict the effect of different material properties (e.g., thickness, contact area, contact force). Alternatively, the apparent mass at the palm can be predicted from the dynamic stiffness of a glove material and the transmissibility of the glove material to the palm (i.e., rearranging the equation of the mechanical impedance model).

Glove transmissibility to the palm of the hand is predominantly affected by the area of contact. Increasing the area of contact of a glove material with the hand increases both the dynamic stiffness of the glove material and the apparent mass of the hand. When the area of contact increased, for the three materials used in this study, the transmissibility through the material to the hand increased at frequencies greater than the resonance frequency. This increase in transmissibility was mostly attributed to the increased dynamic stiffness of the material as the contact area increases rather than a change in the dynamic response of the hand.

The other predominant factor that affects glove transmissibility is the force applied to the glove material. Increasing the contact force increases the frequency of the principal

resonance in the apparent mass of the hand (at about 15 Hz), due to increased coupling of the arm, the hand, and the fingers with the driving-point of the vibration: the apparent mass at frequencies greater than the resonance increases with increasing resonance frequency of the apparent mass of the hand. Increasing the contact force also increases the stiffness and damping of the glove. As contact force increases, these changes either increase the resonance frequency in the transmissibility of the glove to the hand (due to increased material dynamic stiffness) or decrease the resonance frequency in the transmissibility of the glove to the hand (due to increased apparent mass of the hand), resulting in either reduced or increased transmissibility at frequencies greater than the resonance frequency.

Changes in vibration magnitude (from 1 to 4 ms⁻² r.m.s.) had little effect on either the apparent mass at the palm of the hand or the transmissibility of the glove materials to the palm of the hand.

This research indicates that the changes in the posture of the forearm and the upper-arm will not give a significant impact on the apparent mass of the hand or the glove transmissibility at frequencies greater than the first principal resonance (i.e., at about 15 Hz).

Three principal resonances were observed in the measured apparent mass of the hand in the frequency range 2 to 300 Hz: around 5, 15, and 44 Hz. The resonance at about 5 Hz appears to be associated with the motion of the lower-arm. The resonances at about 15 and 44 Hz seems to be associated with motion of the palm of the hand and the fingers, respectively.

A four degree-of-freedom model (representing the motion of the palm, the fingers, the lower-arm, and the upper-arm, Model A) was better in representing the measured apparent mass than a two degree-of-freedom model (representing the motion of only the palm and the fingers, Model B). The fitted apparent mass of Model A slightly underestimated the measured apparent mass at frequencies between 68 and 82 Hz but was similar to the measured apparent mass at frequencies greater than 84 Hz. The fitted apparent mass of Model B underestimated the measured apparent mass at frequencies greater than 16 Hz. Both models overestimated the measured transmissibilities of the glove materials at high frequencies: this was suspected to be due to the underestimation of the fitted apparent mass of both models at high frequencies (i.e., the fitted dynamic stiffness of the glove materials were similar to the dynamic stiffness measured experimentally). Model B showed a poorer transmissibility prediction than Model A at all frequencies from 70 to 300 Hz, suggesting the exclusion of the arm in the model affects

the model prediction. Both models suggest that increasing the mass of the palm tissues close the driving-point of the vibration represents the increases in apparent mass at the palm at high frequencies when the area of contact increases (see Chapter 5). Both models also suggest that increasing the stiffness of the spring between the palm and the palm tissues represents the increase in the third resonance frequency when the push force increases (see Chapter 6).

The research suggests that in order to assess the performance of a glove in attenuating vibration, the relevant standards (e.g., ISO 10819:2013 and ISO 13753:2008) should require tests with a range of contact areas and a range of contact forces, since both factors have prominent effects on glove transmissibility to the hand. The effects of contact force and contact area on glove transmissibility to the hand can be difficult to predict, as shown in this research (glove transmissibility can either increase or decrease depending on the dynamic response of the hand and the dynamic stiffness of the glove material, see Chapters 5 and 6). The assessment of the performance of a glove should also include measurement of vibration transmitted to the fingers, as this can be very different from the transmission of vibration through gloves to the palm of the hand. Alternatively, this research shows that a simple mechanical impedance model can be used to predict glove transmissibility to the palm (instead of measuring glove transmissibility) using procedures similar to those in ISO 13753:2008.

11.2 Recommendations

The transmissibilities of glove materials to the hand as measured and predicted in this research may differ from glove transmissibilities in working environments. This is because the controlled conditions employed in this research differed from working conditions (e.g., Pinto *et al.*, 2001). This research suggests more systematic study (i.e., measuring the apparent mass of the hand, glove dynamic stiffness, and glove transmissibility) of the effects of gloves on the transmission of vibration to the hand is needed, performed in a condition similar to the working environments.

In this research, it has been shown that the predominant motion of the lower and the upper-arm occurred at frequencies less than 15 Hz. At 5 Hz, a resonance was observed and was expected to be due to the motion of the lower-arm based on the magnitude of apparent mass. The apparent mass continues to increase as the frequency of vibration decreases at frequencies less than 3 Hz in some subjects which could indicate another resonance (i.e., resonance due to the motion of the upper-arm). A measurement at frequencies less than 3 Hz is required to investigate the resonance.

Contradictory findings were found when investigating the effects of vibration magnitude. This research suggests that the effects of vibration magnitude on the apparent mass of the hand and on the glove transmissibility to the hand can be ignored at all frequencies from 10 to 300 Hz but some previous studies found a significant impact of increasing vibration magnitude on the apparent mass of the hand (e.g., Lundström *et al.*, 1989, Burström, 1997): if the change in the apparent mass due to the increase in the vibration magnitude is greater than in this research, it could affect glove transmissibility. A systematic study that investigates the effects of vibration magnitude on glove transmissibility using vibration magnitudes greater than in this research, or at frequencies outside the range of frequency in this research, is needed.

Two lumped parameter models of the hand were able to provide reasonable predictions of glove transmissibility to the hand at low frequencies. However, both models overestimated glove transmissibility at high frequencies. The discrepancies in the predicted glove transmissibility at high frequencies was suspected to be due to the underestimation of fitted apparent mass of the hand (i.e., the fitted apparent mass of the hand of both models underestimated the apparent mass measured experimentally whilst the fitted dynamic stiffnesses of the glove materials were similar to the dynamic stiffness measured experimentally, see Chapter 9). This research recommends that if a better prediction of glove transmissibility is needed, the model should include other factors such as the motion of the body (i.e., the body has a large mass that could affect apparent mass of the hand at all frequencies of vibration), or vibration in different directions (e.g., shear vibration). This requires further investigation of the effects of other factors (e.g., the motion of the body) on the glove transmissibility to the hand.

The apparent mass of the hand or the fingers was acquired in a condition where the index finger or the palm of the hand was lying on a flat surface. This was performed to control unknown effects of factors such as shear vibration. If the effects of other factors, such as shear vibration, on the apparent mass of the hand are small, at high frequencies, the dynamic response of the hand or the fingers when holding a handle (e.g., according to the ISO 10819:2013) would be similar to the dynamic response in the postures used in this research. The effects of factors investigated in this research are therefore expected to be similar to when holding a handle. This is because at high frequencies, the apparent mass of the hand or the fingers mainly depends on the dynamic response of the body close to the vibration driving-point. However, it is not clear at what frequencies the dynamic response of the hand or the fingers in this research is similar to the dynamic response in the posture of holding a handle. This requires further investigation.

Appendices

Appendix A: Procedures to calibrate transducers

Procedures in calibrating accelerometers using calibrator

1. Accelerometer was attached on a calibrated B&K 4294 (i.e., calibrator; acceleration generated by the calibrator was 10.07 m/s^2) using double-sided tape.
2. Magnitude of the signal from the accelerometer without vibration was recorded.
3. Sinusoidal vibration was generated by the calibrator at frequency of 159.2 Hz at 10.07 m/s^2 r.m.s.. Magnitude of the signal from the accelerometer with the sinusoidal vibration was recorded.
4. Sensitivity of the accelerometer was then calculated.
5. Vibration was again generated by the calibrator to determine whether the acceleration measured by the calibrated accelerometer was similar to the target acceleration generated by the calibrator. The tolerance for the accelerometer calibration was set to be less than $\pm 5\%$.

Procedures in calibrating piezo-resistive force transducer using static mass.

1. Magnitude of the signal from the force transducer without a mass placed on-top was recorded.
2. A 2 kg rigid mass was placed on top of the force transducer. Magnitude of the signal from the force transducer with the mass was recorded.
3. Sensitivity of the force transducer was then calculated.
4. The 2 kg rigid mass was again placed on top of the force transducer to remeasure the amount of force acquired by the force transducer with the new sensitivity to determine the accuracy of the force transducer. The tolerance for the force transducer calibration was set to be less than $\pm 5\%$.

Procedures in calibrating a piezo-electric force transducer dynamically.

1. The force transducer and a calibrated accelerometer (i.e., impedance head, B&K 8001) were attached on a table of a vibrator (VP30).
2. A sinusoidal vibration was generated by the vibrator. The frequency of the sinusoidal vibration was about 100 Hz.
3. The magnitude of the signal from the force transducer was recorded. The magnitude of the acceleration measured by the accelerometer was also recorded.
4. A 12 gram rigid mass was placed on top of the force transducer.
5. Step 1 to 3 were repeated.

6. Sensitivity of the force transducer was then calculated.
7. The 12 grams rigid mass was again placed on top of the force transducer and a sinusoidal vibration was generated. The force acquired by the force transducer with the new calculated sensitivity was compared to the target force expected to be produced by the 12 gram mass. The tolerance for the force transducer calibration was set to be less than 5%.

Appendix B: Individual calculated and optimized parameters for Model A and Model B, individual predicted resonance frequency for Model A and Model B, and individual modal analysis for Model A and Model B.

Predicted resonance frequency of Model A – individual

	S1	S2	S3	S4	S5	S6	S7	S8	S9	S10	S11	S12	median
f_1	0.84	1.15	0.96	1.00	1.00	0.90	1.00	1.03	0.66	0.97	0.73	0.84	0.96
f_2	5.97	7.44	6.00	7.30	6.98	6.43	8.20	6.48	4.90	7.03	5.07	6.58	6.53
f_3	10.92	13.97	10.97	14.06	12.67	12.33	15.71	12.58	11.49	12.72	11.54	13.33	12.62
f_4	25.41	34.22	38.89	42.32	38.16	35.23	34.99	37.28	25.44	30.45	25.99	40.58	35.11

*S1 = Subject 1

Calculated/optimized parameters of Model A - individual

	S1	S2	S3	S4	S5	S6	S7	S8	S9	S10	S11	S12	median
m_1	0.39	0.23	0.34	0.29	0.31	0.26	0.33	0.30	0.35	0.30	0.30	0.28	0.30
m_2	1.30	0.77	1.13	0.98	1.04	0.86	1.10	1.00	1.18	1.00	1.00	0.92	1.00
m_3	2.24	1.32	1.95	1.69	1.80	1.48	1.90	1.72	2.03	1.72	1.72	1.58	1.72
m_4	0.13	0.08	0.11	0.10	0.10	0.09	0.11	0.10	0.12	0.10	0.10	0.09	0.10
m_{ts}	0.00	0.01	0.01	0.01	0.00	0.00	0.00	0.01	0.00	0.01	0.00	0.00	0.00
k_1	3000	3000	3000	3000	3455	3010	4379	3557	4073	3000	3539	3876	3233
k_{r2}	0.10	1.31	0.10	0.10	0.10	0.10	0.10	3.58	0.10	0.10	0.10	0.10	0.10
k_{r3}	36.91	21.80	18.02	41.70	30.64	16.58	61.37	18.49	15.35	33.94	10.23	22.27	22.04
k_{r4}	19.84	12.86	18.27	14.60	20.70	12.41	16.22	11.53	11.31	16.70	14.36	12.61	14.48

k_{r5}	6.37	5.00	8.37	8.55	11.78	5.00	8.70	7.18	5.00	5.00	5.00	10.91	6.77
c_1	61.80	52.72	49.92	46.41	57.55	52.18	54.89	50.33	71.50	53.13	53.68	47.61	52.93
c_{r2}	0.01	0.01	0.01	0.01	0.01	0.01	0.01	0.01	0.20	0.01	0.01	0.01	0.01
c_{r3}	0.01	0.01	0.59	0.15	0.02	0.09	0.38	0.01	0.64	0.05	0.08	0.09	0.09
c_{r4}	1.59	0.74	0.51	0.73	1.01	0.49	0.68	0.67	0.13	0.81	0.43	0.68	0.68
c_{r5}	0.01	0.01	0.00	0.00	0.00	0.00	0.01	0.00	0.01	0.01	0.01	0.00	0.01

Modal analysis of Model A - individual

	S1	S2	S3	S4	S5	S6	S7	S8	S9	S10	S11	S12	median
mode 1													
Z_1	0.000	0.000	0.000	0.000	0.000	0.000	0.000	0.000	0.000	0.000	0.000	0.000	0.000
O_2	0.014	0.023	0.019	0.018	0.017	0.020	0.017	0.019	0.016	0.018	0.018	0.018	0.018
O_3	0.011	0.017	0.012	0.015	0.012	0.014	0.015	0.014	0.011	0.013	0.009	0.013	0.013
O_4	0.000	0.000	0.000	0.000	0.000	0.000	0.000	0.000	0.000	0.000	0.000	0.000	0.000
mode 2													
Z_1	0.005	0.005	0.004	0.006	0.004	0.004	0.006	0.003	0.002	0.006	0.002	0.003	0.004
O_2	0.004	0.011	0.012	-0.001	0.008	0.016	0.000	0.015	0.019	0.003	0.020	0.017	0.011
O_3	-0.035	-0.055	-0.047	-0.040	-0.044	-0.056	-0.038	-0.054	-0.044	-0.043	-0.052	-0.051	-0.045
O_4	-0.006	-0.006	-0.002	-0.005	-0.003	-0.003	-0.008	-0.003	-0.001	-0.008	-0.001	-0.002	-0.003
mode 3													
Z_1	0.009	0.012	0.010	0.010	0.011	0.012	0.009	0.011	0.010	0.010	0.011	0.012	0.010
O_2	-0.047	-0.077	-0.060	-0.066	-0.056	-0.063	-0.059	-0.061	-0.045	-0.058	-0.047	-0.056	-0.058

O_3	0.026	0.038	0.028	0.039	0.030	0.029	0.036	0.029	0.016	0.035	0.018	0.025	0.029
O_4	-0.044	-0.061	-0.023	-0.032	-0.027	-0.045	-0.054	-0.036	-0.062	-0.055	-0.061	-0.031	-0.045
	mode 4												
Z_1	0.004	0.005	0.004	0.004	0.004	0.005	0.005	0.004	0.005	0.005	0.005	0.005	0.005
O_2	-0.017	-0.028	-0.019	-0.021	-0.019	-0.022	-0.022	-0.021	-0.019	-0.021	-0.020	-0.019	-0.020
O_3	0.005	0.007	0.004	0.005	0.005	0.006	0.006	0.005	0.005	0.006	0.005	0.005	0.005
O_4	0.624	0.950	0.840	0.904	0.694	0.981	0.735	0.868	0.701	0.845	0.717	0.766	0.803

Predicted resonance frequency of Model B – individual

	S1	S2	S3	S4	S5	S6	S7	S8	S9	S10	S11	S12	median
f_1	13.035	15.798	12.793	13.955	16.496	15.663	14.370	16.463	14.282	13.494	14.731	15.517	14.551
f_2	29.788	44.162	49.100	50.095	49.059	45.588	34.747	48.656	33.295	39.206	34.015	52.363	44.875

Calculated/optimized parameters of Model B – individual

	S1	S2	S3	S4	S5	S6	S7	S8	S9	S10	S11	S12	median
m_1	0.39	0.23	0.34	0.29	0.31	0.26	0.33	0.30	0.35	0.30	0.30	0.28	0.30
m_2	0.13	0.08	0.11	0.10	0.10	0.09	0.11	0.10	0.12	0.10	0.10	0.09	0.10
m_{ts}	0.00	0.01	0.00	0.01	0.01	0.00	0.00	0.01	0.00	0.00	0.00	0.00	0.00
k_1	3825	3178	3000	3000	4678	3482	3883	4426	4138	3000	3725	3609	3667
k_2	0.01	0.01	0.00	99.97	0.04	0.01	0.01	30.52	0.00	0.00	0.01	0.00	0.01
k_{r5}	5.00	5.00	8.09	7.26	11.65	5.00	5.00	7.27	5.00	5.00	5.00	10.99	5.00

c_1	50.23	42.44	34.20	35.20	37.40	34.81	34.91	32.19	44.18	46.29	36.79	29.27	36.00
c_2	1.00	1.00	1.00	1.00	1.00	1.00	1.00	1.00	1.00	1.00	1.00	1.00	1.00
c_{r5}	0.01	0.01	0.00	0.00	0.01	0.01	0.02	0.00	0.01	0.01	0.01	0.00	0.01

Modal analysis of Model B – individual

	S1	S2	S3	S4	S5	S6	S7	S8	S9	S10	S11	S12	median
	mode 1												
Z_1	-0.013	-0.017	-0.014	-0.016	-0.015	-0.016	-0.014	-0.015	-0.013	-0.015	-0.014	-0.016	-0.015
O_4	0.121	0.108	0.046	0.057	0.068	0.101	0.121	0.086	0.128	0.087	0.134	0.056	0.094
	mode 2												
Z_1	0.010	0.012	0.009	0.010	0.010	0.011	0.011	0.010	0.010	0.010	0.011	0.010	0.010
O_4	0.790	1.204	1.070	1.150	0.880	1.247	0.931	1.105	0.887	1.072	0.904	0.974	1.022

Subjects' characteristics for Model A and Model B

No	Age	Height (cm)	Weight (kg)	Hand circumference (cm)	Hand length (cm)	Upper arm circumference (cm)	Upper arm length (cm)	Forearm circumference (cm)	Forearm length (cm)	Palm circumference (cm)	Palm length (cm)	Index finger length (cm)	Index finger circumference (cm)
1	27	181	85	23	20	31	37	26	30	23	13	8	8
2	30	166	50	16.6	16.7	23.4	31.5	20.6	24	16.6	9.6	6.9	5.1

3	25	165	74	22	17.5	28	32	29	25	22	10	6.4	5.4
4	29	170	64	19.5	17.1	26	33	24	25.3	19.5	10	6.4	5.5
5	42	172	68	23.8	19.9	26.5	34	26	28.5	23.8	11.6	8.1	6.4
6	27	161	56	19.8	16.8	20.74	32	22	27	19.8	9.8	6.3	5.34
7	31	168	72	21.5	18.1	27	33	27	26	21.5	10.1	7.4	6.5
8	28	163	65	19.2	17.6	26	30	23.7	26	19.2	10.1	6.6	6.2
9	26	181	77	19.5	20.4	31	36	24.5	30	19.5	12.2	7.5	6.2
10	27	163	65	19.8	17.8	30.8	33	25.8	28	19.8	10	6.8	5
11	22	177	65	22.8	19.3	26.5	34	23.5	31	22.8	11	8	6
12	38	162	60	22	19.7	29	34	24.3	29	22	11.6	7.8	6.4

Appendix C: Individual calibrated apparent mass at the palm for Model A and Model B, and individual predicted glove transmissibilities for Model A and Model B

Individual calibrated apparent mass at the palm, individual predicted glove transmissibilities

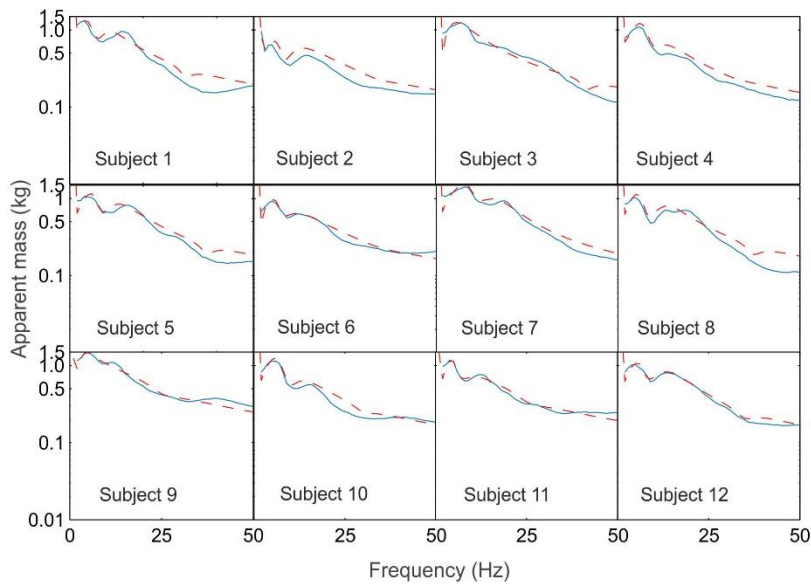


Figure C 1 Individual measured and calibrated apparent mass (modulus and phase) at the palm of the hand (--- Calibrated, — Measured). Stage 1: Model A

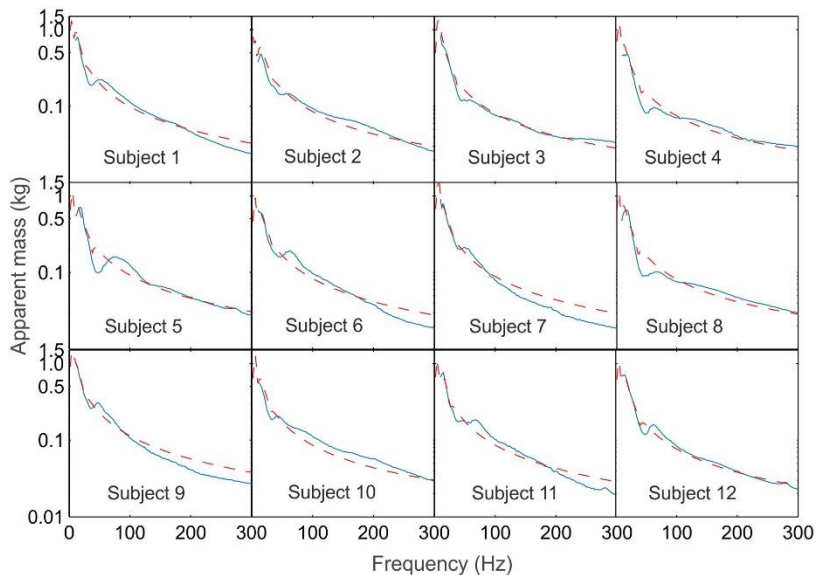


Figure C 2 Individual measured and calibrated apparent mass (modulus and phase) at the palm of the hand (--- Calibrated, — Measured). Stage 2: Model A

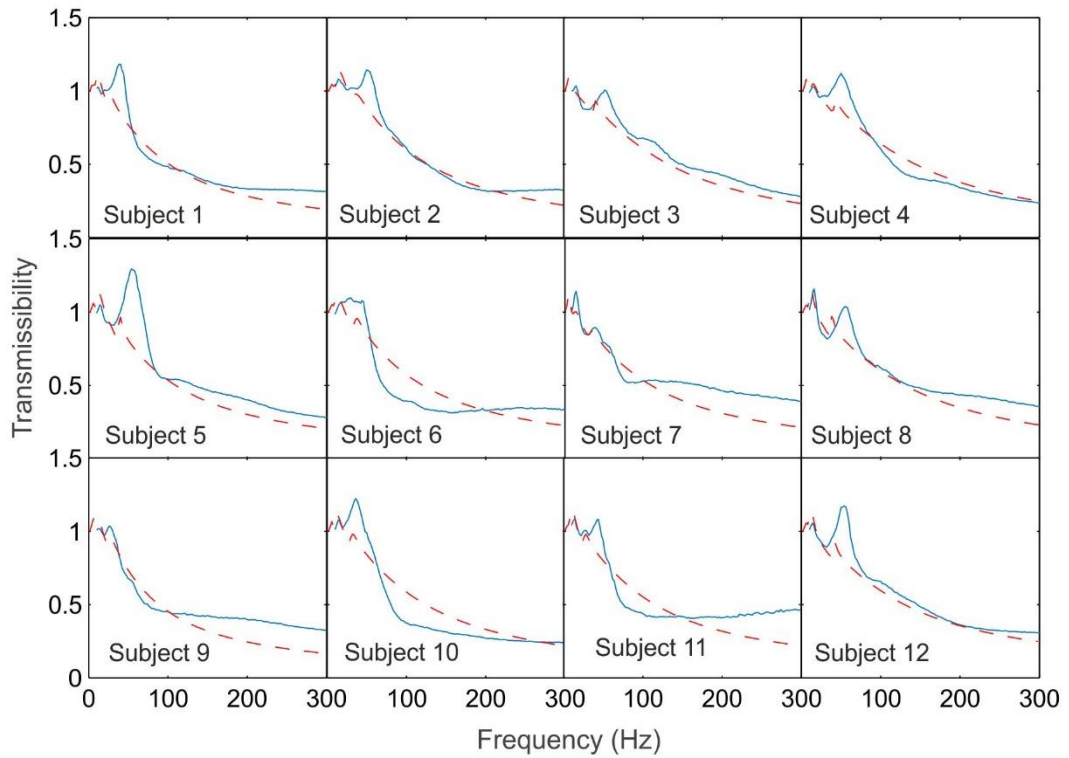


Figure C 3 Individual measured and predicted transmissibility (modulus and phase) of Foam A to the palm of the hand (--- Predicted, — Measured). Model A.

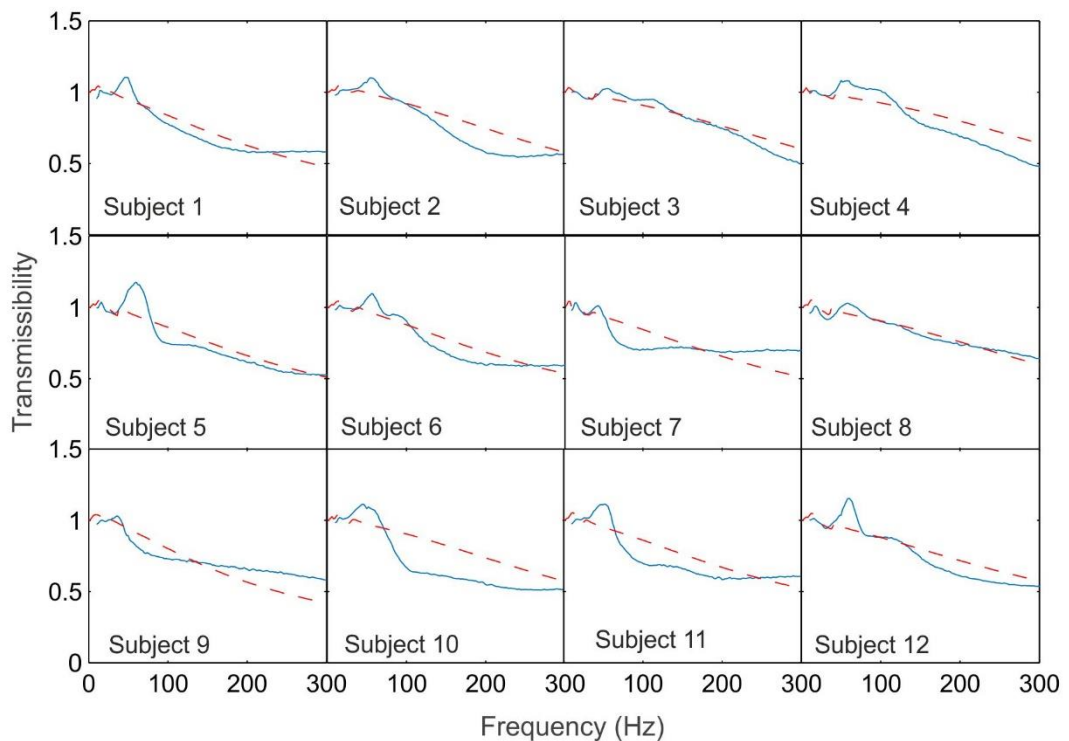


Figure C 4 Individual measured and predicted transmissibility (modulus and phase) of Foam B to the palm of the hand (--- Predicted, — Measured). Model A.

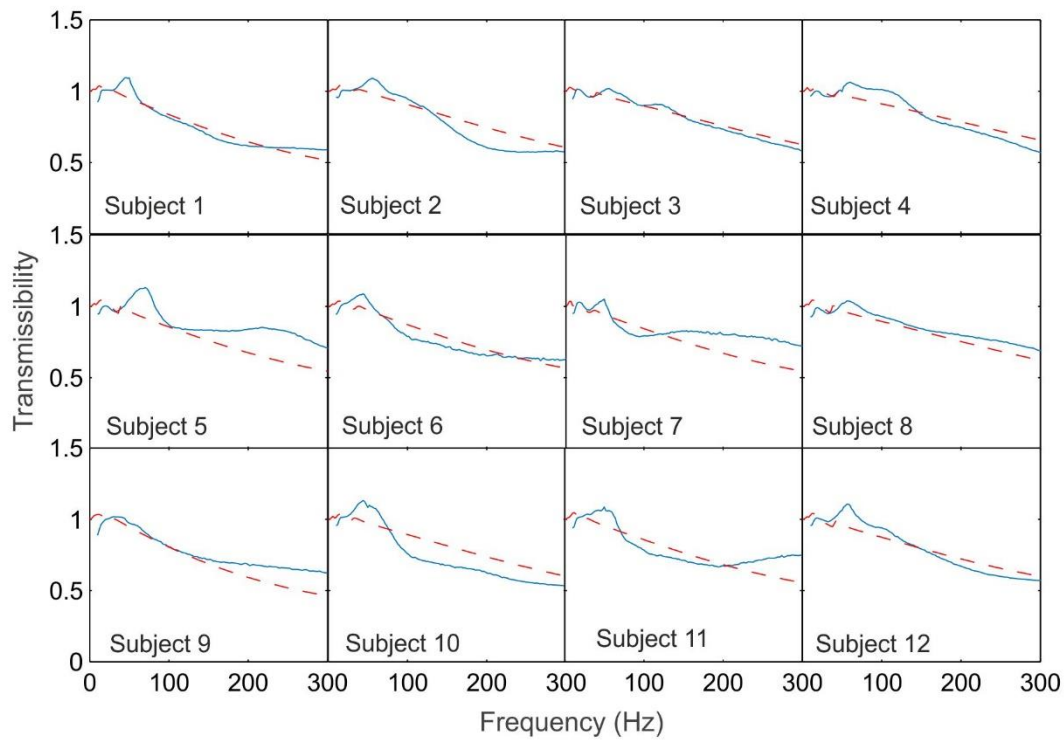


Figure C 5 Individual measured and predicted transmissibility (modulus and phase) of Gel A to the palm of the hand (--- Predicted, — Measured). Model A.

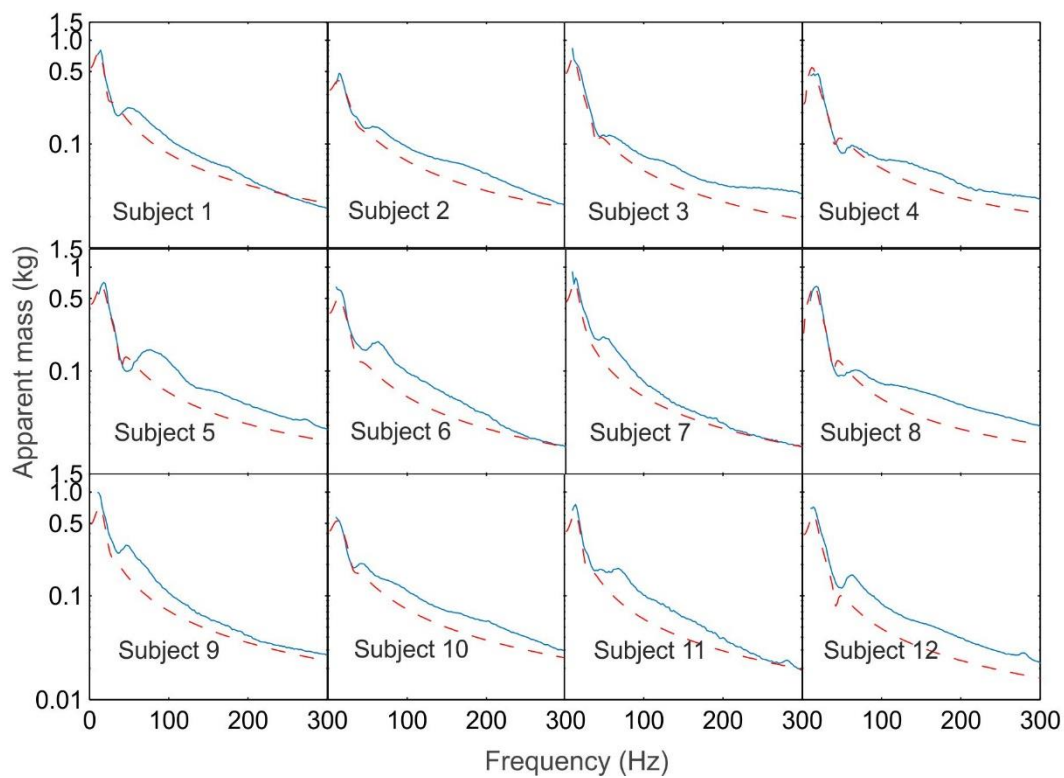


Figure C 6 Individual measured and calibrated apparent mass (modulus and phase) at the palm of the hand (--- Calibrated, — Measured). Model B.

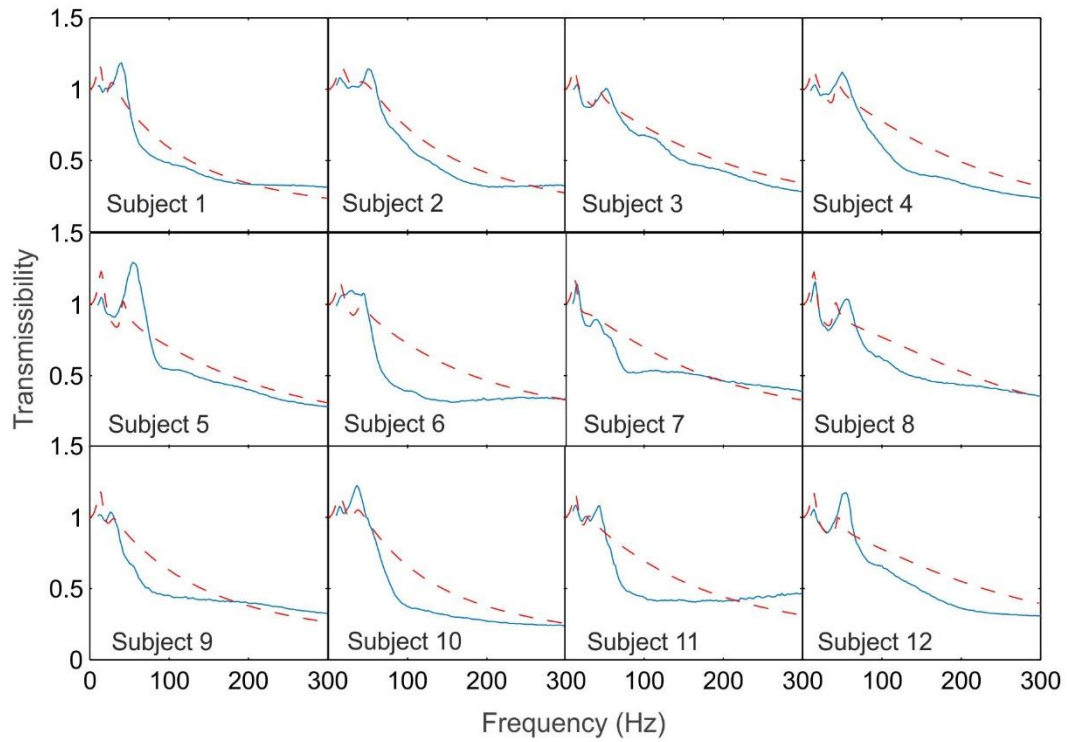


Figure C 7 Individual measured and predicted transmissibility (modulus and phase) of Foam A to the palm of the hand (--- Predicted, — Measured). Model B.

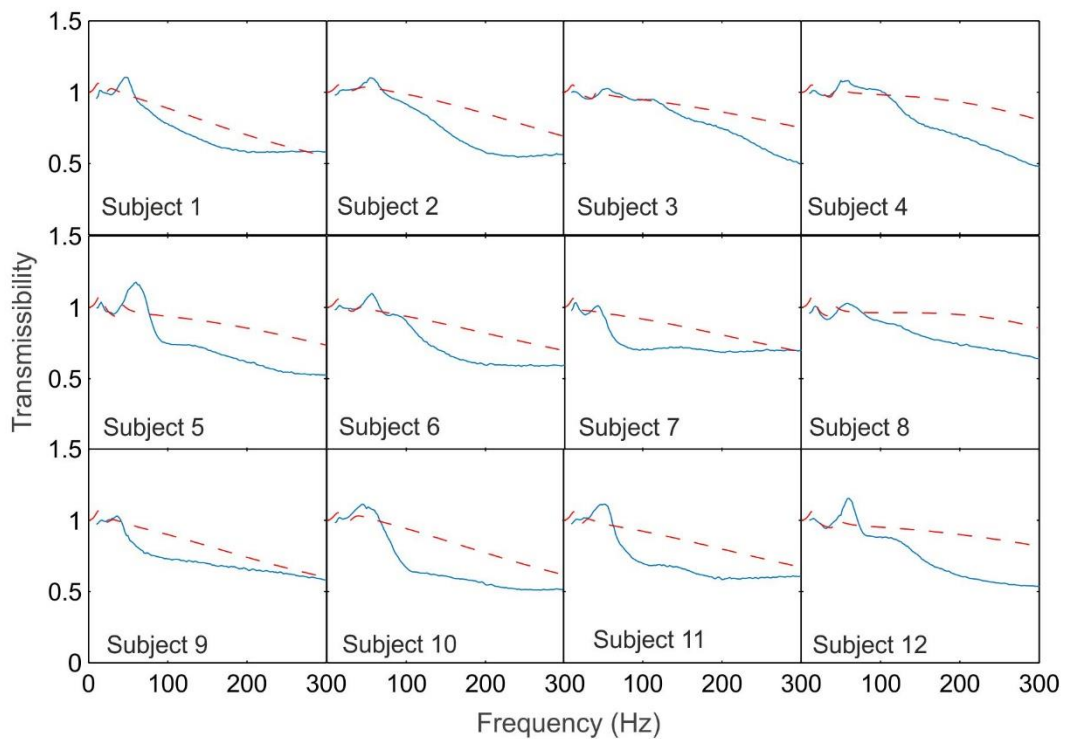


Figure C 8 Individual measured and predicted transmissibility (modulus and phase) of Foam B to the palm of the hand (--- Predicted, — Measured). Model B.

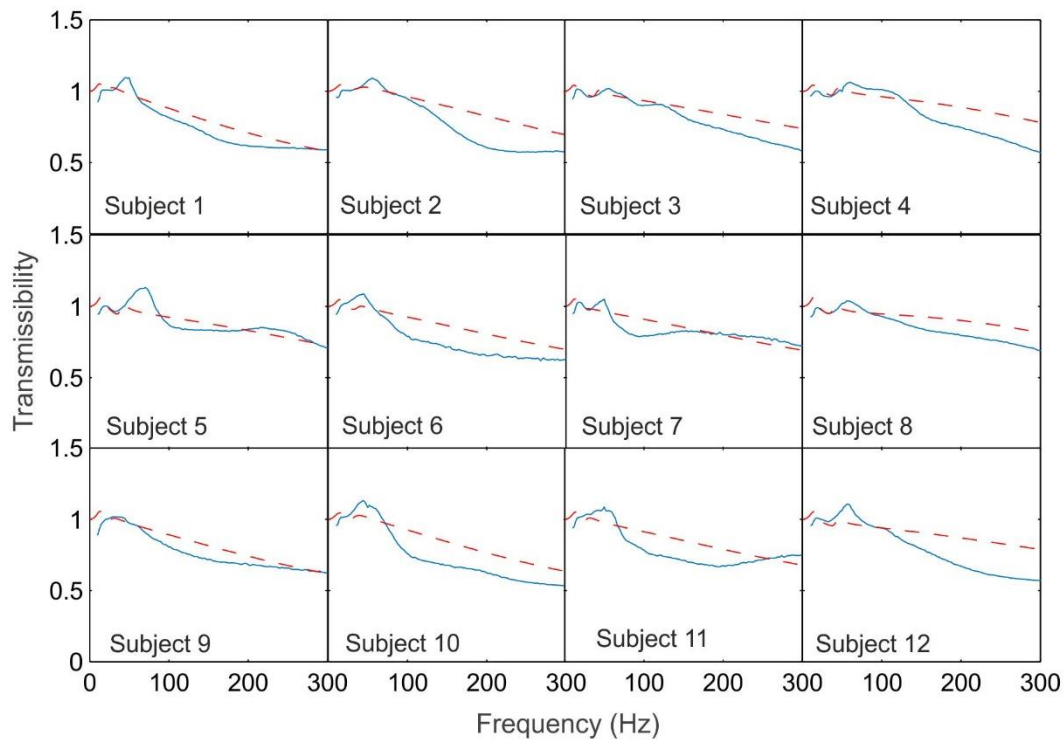


Figure C 9 Individual measured and predicted transmissibility (modulus and phase) of Gel A to the palm of the hand (— — — Predicted, ——— Measured). Model B.

Appendix D: Load deflection curves of the glove materials

Measuring the load deflection curve of the glove materials

To understand the behaviour of the materials during loading and unloading, load deflection curves of the three materials were measured using equipment as shown in Figure D1. Two transducers, a force transducer (Kistler 4567A) used to measure the loading force, and a linear-voltage-displacement transducer (LVDT) used to measure displacement, were attached to a plate that secured to a bearing suspended to a frame. Material was placed between two metal plates that have similar diameter as the material. The load was subjected to the material with a rate of change of 0.07 mm/s. When it reached to the peak travelled displacement (i.e., about 4 mm), the material was subjected to no displacement for about 5 seconds before the unloading sequence (Figure D2).

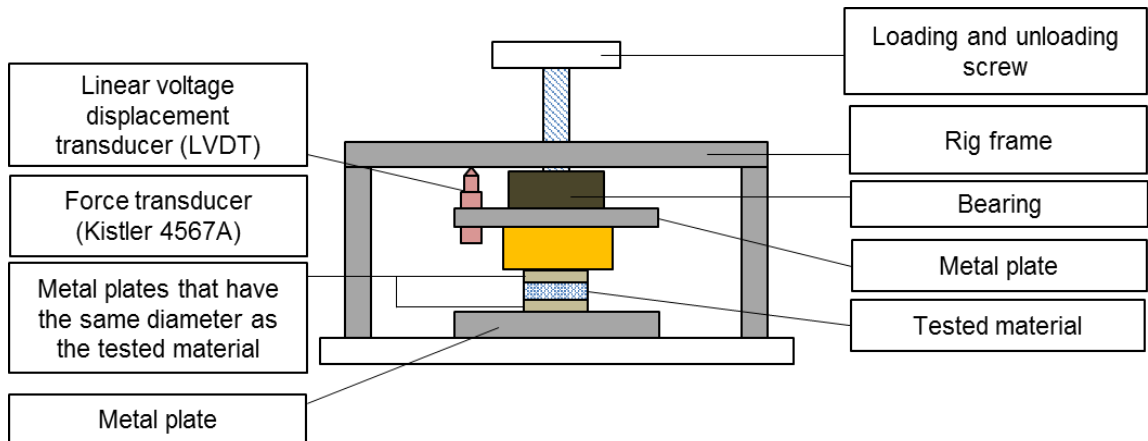


Figure D 1 Equipment setup used to measure load deflection curve of glove materials.



Figure D 2 Load-deflection curve loading and unloading sequence.

The load deflection curves of the three materials are shown in Figure 9-30.

All three materials showed hysteretic behaviour. Gel A showed large energy loss (dissipation) compared to the other two materials. All three materials also showed

relaxation behaviour. Foam A showed little relaxation behaviour compared to the other two materials. Gel A had the greatest stiffness compared to Foam A and Foam B.

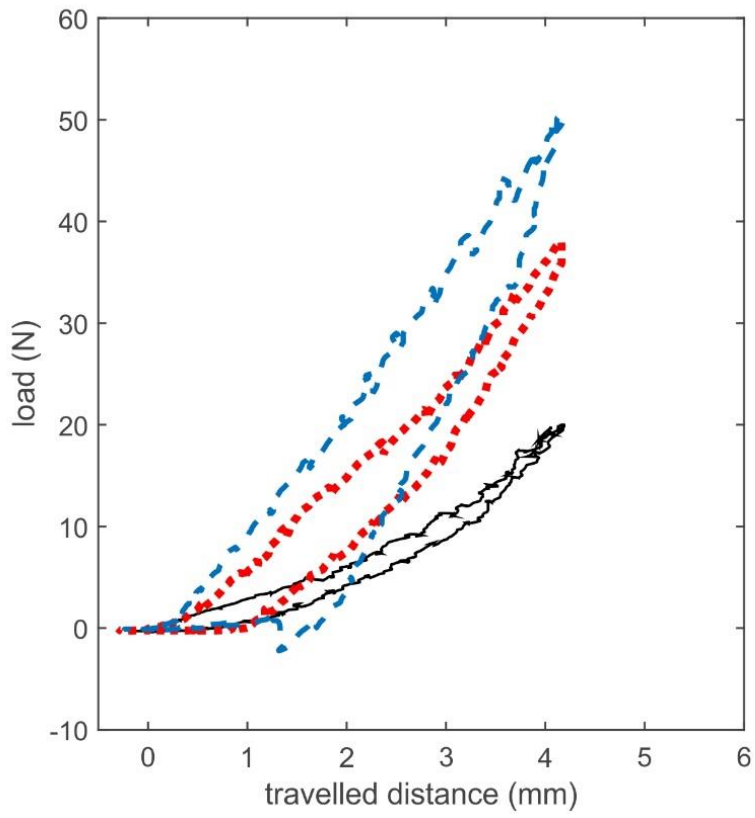


Figure D 3 Load-deflection curve of the three materials (— Foam A, --- Gel A, Foam B).

List of References

- Adeyemi SA, Rakheja S, Marcotte P, Boutin J, (2010). Vibration transmissibility characteristics of the human hand–arm system under different postures, hand forces and excitation levels. *Journal of Sound and Vibration* 329(14): 2953-2971.
- Adeyemi SA, Rakheja S, Marcotte P, (2012). Biomechanical models of the human hand-arm to simulate distributed biodynamic responses for different postures. *International Journal of Industrial Ergonomics* 42 249-260.
- Aldien Y, Welcome D, Rakheja S, Dong R, Boileau PE (2005) Contact pressure distribution at hand-handle interface: role of hand forces and handle size. *International Journal of Industrial Ergonomics*. 267-286.
- Aldien Y, Marcotte P, Rakheja S, and Boileau PE (2006), Influence of hand-arm posture on biodynamic response of the human hand-arm exposed to z_h -axis vibration, *International Journal of Industrial Ergonomics* 36. 45-59.
- Besa AJ, Valero FJ, Suner JL, Carballeira J (2007) Characterisation of the mechanical impedance of the human hand-arm system: the influence of vibration direction, hand-arm posture and muscle tension. *International Journal of Industrial Ergonomics* 37. 225-231
- Boileau PE, Rakheja S, Boutin J (2001) An interlaboratory evaluation of the vibration transmissibility of gloves following the ISO 10819 test method. *Canadian Acoustics* Vol 29.
- Burström L (1997), The influence of biodynamic factors on the mechanical impedance of the hand and arm, *International Archives of Occupational Environmental Health* 69 (1997) 437–446.
- Burström L, Lundström R, Hagberg M, and Nilsson T (1998). Comparison of different measures for hand-arm vibration exposure. *Safety Science* (28), pp 3-14
- Bovenzi M (1990). Medical aspects of the hand arm vibration syndrome. *International Journal of Industrial Ergonomics* 6: 61-73.
- Chang CS, Wang MJJ, Lin SC (1999) Evaluating the effects of wearing gloves and wrist support on hand-arm response while operating an in-line pneumatic screwdriver. *International Journal of Industrial Ergonomics* 24. 473-481

Cherian T, Rakheja S, Bhat RB (1995) An analytical investigation of an energy flow divider to attenuate hand-transmitted vibration. *International Journal of Industrial Ergonomics* 17. pp 455-467.

Chetter IC, Kent PJ, et al. (1997). The hand arm vibration syndrome: a review. *Cardiovascular Surgery* 6: 1-9.

Concettoni E and Griffin MJ (2009). The apparent mass and mechanical impedance of the hand and the transmission of vibration to the fingers, hand, and arm. *Journal of Sound and Vibration* 325(3): 664-678.

Dempster WT and Gaughran GRL (1967) Properties of Body Segments Based on Size and Weight, *AM Journal of Anatomy* (120), 33-54

Directive, E. (2002). Directive 2002/44/EC of the European Parliament and of the Council. On the minimum health and safety requirements regarding the exposure of workers to risks arising from physical agents (vibration)

Dong RG, Welcome DE, McDowell TW, and Wu JZ (2004) Biodynamic response of human fingers in a power grip subjected to a random vibration. *Journal of Biomechanical Engineering* Vol 126

Dong RG, Rakheja S, McDowell TW, Welcome DE, Wu JZ, Warren C, Barkley J, Washington B, Schopper AW, (2005a). A method for assessing the effectiveness of anti-vibration gloves using biodynamic responses of the hand–arm system. *Journal of Sound and Vibration* 282(3-5): 1101-1118.

Dong RG, McDowell TW, Welcome DE, Smutz WP (2005b) Correlations between biodynamic characteristics of human hand-arm system and the isolation effectiveness of anti-vibration gloves. *International Journal of Industrial Ergonomics* (35) 205-216

Dong RG, Dong JH, Wu JZ and Rakheja S. (2007) Modeling of biodynamic responses distributed at the fingers and the palm of the human hand-arm system. *Journal of Biomechanics*, 40, 2335-40.

Dong RG, McDowell TW, et al. (2009). Analysis of anti-vibration gloves mechanism and evaluation methods. *Journal of Sound and Vibration* 321(1-2): 435-453.

Dong RG, Welcome DE, McDowell TW, Wu JZ, (2009b) Methods for deriving a representative biodynamic response of the hand-arm system to vibration. *Journal of Sound and Vibration* 325, 1047-1061.

Dong RG, Welcome DE, et al. (2012). Modeling of the mechanical impedances distributed at the fingers and palm of the hand in three orthogonal directions. 4th American Conference on Human Vibration, Hilton Hartford, Hartford, Connecticut, USA.

Fairley TE and Griffin MJ (1986). A test method for the prediction of seat transmissibility. Society of Automotive Engineers International Congress and Exposition, Detroit, USA.

Fairley TE and Griffin MJ (1989) The apparent mass of the seated human body: vertical vibration. *Journal of Biomechanics* 22 (2), 81–94.

Griffin MJ, Howarth HVC, Pitts PM, Fischer S, Kaulbars U, Donati, PM, Bereton PF (2006) EU Good Practice Guide HAV V7.7

Griffin MJ (1990). *Handbook of Human Vibration*, Elsevier Academic Press.

Griffin MJ (1997). Measurement, evaluation, and assessment of occupational exposures to hand-transmitted vibration. *Occupational and Environmental Medicine* 54: 73-89.

Griffin MJ (1998). Evaluating the effectiveness of gloves in reducing the hazards of hand-transmitted vibration. *Occupational and Environmental Medicine* 55: 340-348.

Griffin MJ (2004). Minimum health and safety requirements for workers exposed to hand-transmitted vibration and whole-body vibration in the European Union; a review. *Occupational and Environmental Medicine* 61(5): 387-397.

Griffin MJ, Pitts PM, Fischer S, Kaulbars U, Donati PM, Bereton PF (2006) Guide to good practice on hand-arm vibration. EU Good Practice Guide HAV V7.7

Grounds MD (1964). Raynauds phenomenon in the users of chainsaws. *Medical Journal of Australia*: 270–272.

Gurram RS, Rakheja S, Gouw GJ (1994). Vibration transmission characteristics of the human hand-arm and gloves. *International Journal of Industrial Ergonomics* 13: 217-234.

Hamilton A (1918). A study of spastic anaemia in the hands of stone cutters. *Bulletin* 236: US Bureau of Labour Statistics, : 53-66.

Hewitt S (1998). Assessing the performance of anti-vibration gloves: A possible alternative to ISO10819, 1996. *Annals of Occupational Hygiene* 42: 245-252.

Hunter D, McLaughlin, et al. (1945). Clinical effects of the use of vibrating tools. *British Journal of Industrial Medicine*: 10–16.

International Organization for Standardization, G., Switzerland. (1996). EN ISO10819:1996 Mechanical vibration and shock - Hand-arm vibration - Method for the measurement and evaluation of the vibration transmissibility of gloves at the palm of the hand.

International Organization for Standardization, G., Switzerland. (2013). EN ISO10819:2013 Mechanical vibration and shock - Hand-arm vibration - Method for the measurement and evaluation of the vibration transmissibility of gloves at the palm of the hand.

International Organization for Standardization, G., Switzerland. (2001). EN ISO 5349-1:2001 Mechanical vibration - Measurement of human exposure to hand-transmitted vibration Part 1: General requirements.

International Organization for Standardization, G., Switzerland. (2002). EN ISO 5349-2:2001 Mechanical vibration - Measurement of human exposure to hand-transmitted vibration Part 2: Practical guidance for measurement at the workplace.

International Organization for Standardization, G., Switzerland. (2008). EN ISO13753 Mechanical vibration and shock - Hand-arm vibration - Method for measuring the vibration transmissibility of resilient materials when loaded by the hand-arm system (ISO13753:1998).

International Organization for Standardization, G., Switzerland. (2012). EN ISO10068 Mechanical vibration and shock – Mechanical impedance of the human hand-arm system at the driving point (ISO 10068:2012).

Jones DIG, (2001) Handbook of viscoelastic vibration damping, Wiley.

Ju JW, Simo JC, Pister KS, Taylor RL, (1987) A parameter estimation algorithm for inelastic material model, Constitutive Laws for Engineering Materials: Theory and Applications, pp. 1233-1240

Koton J, Kowalski P, Szopa J (1998) An attempt to construct anti-vibration gloves on the basis of information of the vibration transmissibility of materials. 8th International Conference on Hand-Arm Vibration, 9-12 June 1998, Umea, Sweden.

Kuczyński J (2014) Improved methods of assessment of vibration risks. 49th UK Conference on Human Responses to Vibration, Health and Safety Laboratory, Buxton.

Laszlo HE and Griffin MJ (2011). The transmission of vibration through gloves: effects of push force, vibration magnitude and inter-subject variability. *Ergonomics* 54(5): 488-496.

Lundstrom R, Burstrom L, Mechanical impedance of the human hand–arm system, *International Journal of Industrial Ergonomics* 3 (1989) 235–242.

Mann NAJ and Griffin MJ (1996). Effect of contact conditions on the mechanical impedance of the finger. *Cent. Eur. Journal of public health* (4), 46-49

Marcotte P, Aldien Y, Boileau PE, Rakheja S, and Boutin J (2005), Effect of handle size and hand-handle contact force on the biodynamic response of the hand-arm system under z-h-axis vibration, *Journal of Sound and Vibration* 283 1071-1091

Miwa T (1964a). Studies in hand protectors for portable vibrating tools. 1. Measurement of attenuation effect of porous elastic materials. *Industrial Health* 2: 95-105.

Miwa T (1964b). Studies in hand protectors for portable vibrating tools. 2. Simulations of porous elastic materials and their applications to hand protectors. *Industrial Health* 2: 106-123.

Nataletti P, Paone N, Scalise L (2005) Measurement of hand-vibration transmissibility by non-contact measurement techniques. *Environmental Health Risk*

Nawayseh N and Griffin MJ (2004) Tri-axial forces at the seat and backrest during whole-body vertical vibration. *Journal of Sound and Vibration* 277 (1-2) 309-326

O'Boyle M and Griffin MJ (2001). Inter-subject variability in the measurement of the vibration transmissibility of gloves according to current standards. *International Conference on Hand-Arm Vibration*. N. (F).

O'Boyle M and Griffin MJ (2004). Predicting the effects of push force on the transmission of vibration through glove materials to the palm of the hand. *International Conference on Hand-Arm Vibration*, Las Vegas, Nevada, USA.

O'Boyle M, and Griffin MJ (2005) Effect of vibration magnitude on glove material transmissibility. In: 40th United Kingdom conference on human responses to vibration, 13–15 September 2005. Liverpool, UK: Health and Safety Executive, 7 pp.

Paddan GS and Griffin MJ (1999). Standard test for the vibration transmissibility of gloves, Institute of Sound and Vibration Research, University of Southampton.

Pinto I, Stacchini N, Bovenzi M, Paddan GS, Griffin MJ (2001). Protection effectiveness of anti-vibration gloves: Field evaluation and laboratory performance assessment. International Conference on Hand-Arm Vibration. N. (F).

Rakheja S, Wu JZ, Dong RG, Schopper AW (2002a) A comparison of biodynamic models of the human hand-arm system for applications to hand-held power tools, Journal of Sound and Vibration 249(1), 55-82

Rakheja S, Dong R, Welcome D, Schopper AW (2002b) Estimation of tool-specific isolation performance of anti-vibration gloves. International Journal of Industrial Ergonomics 30. 71-87.

Reidel S, Consideration of grip and push forces for the assessment of vibration exposure, Central European Journal of Public Health 3 (1995) 139–141.

Reynolds DD and Keith RH (1977). Hand-arm vibration, Part 1: Analytical model of the vibration response characteristics of the hand. 1977 51: 237-253.

Reynolds DD and Angevine EN Hand-arm vibration (1977), Part 2: Vibration transmission characteristics of the hand and arm. 1977 51: 255-265.

Reynolds DD and Wolf E (2005) Evaluation of anti-vibration glove test protocols associated with the revision of ISO 10819. Industrial Health (43) 556-565.

Rossi GL and Tomasini EP (1995) Hand-arm vibration measurement by a laser scanning vibrometer. Measurement 16. Pp 113-124

Shibata N and Maeda S (2008) Vibration-isolating performance of cotton work gloves based on newly issued JIS T8114. Industrial Health (46) 477-483

Seyring M. (1930). Erkrankungen durch arbeit mit pressluftwerkzeugen. Arch Gewerbepath Gewerbehug.

Starck J, Pyykko I, et al. (1994). Vibration exposure and prevention in Finland. Nagoya Journal of Medical Science: 203-210.

Takamatsu, M., M. Futatsuka, et al. (1984). "A study of the extent and scope of local vibration hazards in Japan : M. Takamatsu, M. Futatsuka, T. Sakurai, T. Matoba, M. Gotoh, H. Aoyama, J. Osaki, K. Ishida, Y. Nasu, S. Watanabe, M. Hosokawa, H. Iwata, S. Yamada, T. Matsumoto, K. Kaneda, A. Okada, S. Nohara, T. Miura, T. Miwa, T. Uehata, K. Yamazaki, H. Suzuki, S. Usutani, H. Honma, H. Koshichi and K. Wakaba

1982 *Industrial Health* 20, 177–190 (14 pages, 1 figure, 6 tables, 21 references)." *Journal of Sound and Vibration* 95(4): 583.

Tufano S and Griffin MJ (2013) Nonlinearity in the vertical transmissibility of seating: the role of the human body apparent mass and seat dynamic stiffness, *Vehicle System Dynamics*, 51(1), 122-138

Wasserman DE (1994). Vibration exposure and prevention in the United States. *Nagoya Journal of Medical Science*: 211-218.

Wei L and Griffin MJ (1998a) Mathematical models for the apparent mass of the seated human body exposed to vertical vibration. *Journal of Sound and Vibration* 212. 855-874.

Wei L and Griffin MJ (1998b) The prediction of seat transmissibility from measures of seat impedance. *Journal of Sound and Vibration* 214, 121-137

Welcome D, Rakheja S, Dong R, Wu JZ, Schopper AW (2004) An investigation of the relationship between grip, push, and contact forces applied to a tool handle. *International Journal of Industrial Ergonomics*. 507-518

Welcome DE, Dong RG, Xu XS, Warren C, McDowell TW (2012). Effectiveness of anti-vibration gloves for reducing finger vibration. 4th American Conference on Human Vibration, Hilton Hartford, Hartford, Connecticut, USA.

Welcome DE, Dong RG, Xu XS, Warren C, McDowell TW. (2012). An evaluation of the proposed revision of the anti-vibration glove test method defined in ISO10819:1996. *International Journal of Industrial Ergonomics* 42(1): 143-155.

Welcome DE, Dong RG, Xu XS, Warren C, McDowell, TW, Wu JZ (2015) An examination of the vibration transmissibility of the hand-arm system in three orthogonal directions. *International Journal of Industrial Ergonomics* Pages 21-34.

Welcome DE, Dong RG, Xu XS, Warren C, McDowell TW (2014) The effects of vibration reducing gloves on finger vibration. *International Journal of Industrial Ergonomics* pp. 45-59

Wu GL and Griffin MJ (1989). Experimental investigation of the dynamic properties of some prototype anti-vibration gloves. ISVR Technical Memorandum 693, Institute of Sound and Vibration Research, University of Southampton.

Xueyan XS, Welcome DE, et al. (2011). The vibration transmissibility and driving-point biodynamic response of the hand exposed to vibration normal to the palm. *International Journal of Industrial Ergonomics* 41(5): 418-427.

Ye Y. and Griffin MJ (2014) Relation between vibrotactile perception thresholds and reductions in finger blood flow induced by vibration of the hand at frequencies in the range 8-250 Hz. *European Journal of Applied Physiology*

Zheng G and Griffin MJ (2011) An analytic model of the in-line and cross-axis apparent mass of the seated human body exposed to vertical vibration with and without a backrest. *Journal of Sound and Vibration* (330) 6509-6525

Zheng G (2012) Biodynamics of the seated human body with dual-axis excitation: Nonlinearity and cross-axis coupling, Thesis for the degree of Doctor Philosophy, University of Southampton